

**Cerebral blood flow measurements
with arterial spin labelling in a
tri-ethnic population cohort:
associations of cardiovascular risk
factors and MR imaging markers of
brain ageing**

Lorna A. Smith

A thesis submitted to University College London for
the degree of Doctor of Philosophy

Department of Population Science and Experimental
Medicine

UCL Institute of Cardiovascular Sciences

2019

Declaration statement

I, Lorna Smith confirm that the work presented in this thesis is my own. Where information has been derived from other sources, I confirm that this has been indicated in the thesis.

Lorna A. Smith

Date: 14th July 2019

Acknowledgements

First thanks must go to the participants of the Southall and Brent Revisited (SABRE) study who gave their time to attend the research clinic and have provided all the data for this thesis. Thanks also to the SABRE clinic team who performed the cardiovascular measurements, to Therese Tillin for collating much of the data, and to the MRI radiographers of UCLH for their support.

Special thanks and much gratitude to my supervisors for their patience and guidance throughout this project: Rolf Jäger and Alun Hughes.

Acknowledgement and thanks to the CMIC team for processing the MRI data: Jorge Cardoso for brain segmentation and parcellation, Andrew Melbourne and David Owen for processing ASL and Carole Sudre for quantifying white matter hyperintensities. Many thanks are also due to Nish Chaturvedi, Shonit Punwani, Frederick Barkhof, David Atkinson, Anna Barnes, Magda Sokolska and Siana Jones who helped to show the way.

Heartfelt thanks to my husband Michael who travelled on this journey with me, and to my Mum - who couldn't stay to see this finished, but always taught me anything was possible.

Funding

The Southall and Brent Revisited (SABRE) study has received funding from the British Heart Foundation, Diabetes UK, the Medical Research Council and the Wellcome Trust. The work included in this thesis from SABRE (visit 3) was funded by the British Heart Foundation.

Abstract

Differences in cerebral blood flow (CBF) have been identified between older individuals in good cognitive health and those experiencing cognitive decline and dementia. Previous studies have shown that the aetiology of dementia includes a substantial vascular component and there is evidence that CBF decline in old age may be linked to cardiovascular disease. Although the incidence, prevalence and impact of vascular risk varies by ethnicity and gender, many previous studies have focused on participants of white European origin or have pooled ethnically diverse samples, while differences between sexes have been under-investigated.

This thesis used arterial spin labelling (ASL) to measure cortical CBF in an elderly tri-ethnic population cohort and examined its relationship with vascular risk and the brain ageing markers of cortical volume and white matter hyperintensity (WMH) volume from magnetic resonance imaging (MRI). Chapter 4 showed that use of the currently recommended mean haematocrit (Hct) value in equations that calculate CBF from ASL underestimated CBF in women and non-European ethnicities. The alternative method of substituting individually measured Hct into the equation was implemented in the following chapters. Results from Chapter 5 indicated that increased vascular risk factors were associated with lower CBF, but these relationships varied by ethnicity and sex. Ethnicity and sex also modified the strength of associations of increased vascular risk with decreased cortical tissue volume and increased volume of WMHs examined in Chapter 6. However, there was no evidence of any association of CBF with the MRI markers of brain ageing.

Impact statement

Interventions that ameliorate poor physical and cognitive outcomes in old age are of major importance in the promotion of healthy and prosperous societies with expanding ageing populations. The failure to develop effective pharmacological treatment for dementia has led to a research focus on the early identification of disease and the promotion of lifestyle interventions aimed at reducing risk and slowing disease progression. CBF measured using the non-invasive MRI technique of ASL has potential as a biomarker for the early diagnosis of dementia and cognitive impairment. Chapter 4 of this thesis investigated CBF measured by ASL in an elderly multi-ethnic sample. It found that the current recommended method for estimating CBF includes a population mean parameter of haematocrit which is not representative of non-European ethnicities or women. Results indicated that adoption of individualised measurements of haematocrit, or a mean calculated from the population stratified by ethnicity and sex, would increase the accuracy of CBF estimations thus improving the utility of CBF as a biomarker to assess individuals in a clinical context and to compare groups in research studies.

Many studies support the association of cardiovascular disease with cognitive decline in old age. Although there is previous evidence that the outcomes of cardiovascular risk are modified by sex and ethnicity, previous work has under-reported stratified results. Results from Chapter 5 of this thesis showed that systolic blood pressure, HDL cholesterol, diabetes and Framingham risk score were associated with CBF. However, these relationships were modified by sex and ethnicity. These results suggest that the adverse outcomes of cardiovascular disease may be expressed earlier in the life course and the severity of cardiovascular risk may vary by sex and ethnic group. Results from chapter 6 that suggested vascular risk is associated with decreases in cortical volume and increases in white matter intensities were also modified by sex and ethnicity, although CBF did not appear to mediate any of these relationships.

Evidence of variation by sex and ethnicity in the relationships of vascular risk with CBF and brain ageing supports the need for inclusion of ethnically diverse and gender balanced samples in future studies, and emphasizes the importance of conducting analyses with consideration for effect modification by group. Such research informs management of cardiovascular risk that optimizes individual clinical outcomes and is crucial to the development of public health recommendations that effectively avert cognitive decline and reduce health inequalities in the elderly.

Statement of Contribution

Prior to commencement of data collection for SABRE visit 3, I developed and optimised the MRI protocol via a pilot study, in collaboration with David Atkinson, Magdalena Sokolska and Rolf Jager. During the data collection phase I collected the participants from the SABRE clinic and escorted them to the MRI scanner at UCLH. I performed the majority (~90%) of MRI scans used in this thesis. I wrote a Standard Operating Procedure for the MRI radiographers and trained them to deliver the protocol without deviation on those occasions I was unable to attend the scanner. I collected, anonymised and archived all MR data to ensure secure storage, management of incidental findings and to facilitate access by other researchers. I supplied the MR data in appropriate formats for post-processing by CMIC. I performed QA checks on all raw and processed MR data. Cardiovascular data was collected by the SABRE clinic team and collated by Therese Tillin. I conceived and planned all work included in this thesis. I planned and executed all statistical analyses with advice from Therese Tillin and Alun Hughes. I authored the manuscript and designed the tables and figures for all chapters in this thesis including the paper on which I am first author (any exceptions are acknowledged in figure captions). In the two papers on which I am second author I collected and provided the MRI data as stated above and proof-read and corrected the manuscripts.

Publications associated with this thesis

Smith L.A, Melbourne A, Owen D, Cardoso MJ, Sudre CH, Tillin T, Sokolska M, Atkinson D, Chaturvedi N, Ourselin S, Hughes AD, Barkhof F, Jäger HR. (2019). *Cortical cerebral blood flow in ageing: effects of haematocrit, sex, ethnicity and diabetes*. Eur Radiol <https://doi.org/10.1007/s00330-019-06096-w> (also presented prior to publication as an electronic poster at ISMRM 2018).

Leeuwis AE, Smith LA, Melbourne A, Hughes AD, Richards M, Prins ND, Sokolsaka M, Atkinson D, Tillin, T, Jäger HR, Chaturvedi N, van der Flier WM, Barkhof F. (2018) *Cerebral Blood Flow and Cognitive Functioning in a Community-Based, Multi-Ethnic Cohort: The SABRE Study*. Front Aging Neurosci 10:279-279

Sudre CH, Smith LA, Atkinson D, Chaturvedi N, Ourselin S, Barkhof F, Hughes AD, Jäger HR, Cardoso MJ, (2018) *Cardiovascular Risk Factors and White Matter Hyperintensities: Difference in Susceptibility in South Asians Compared With Europeans*. J Am Heart Assoc 7:e010533

Table of Contents

Title page	1
Declaration statement	2
Acknowledgements	3
Abstract	4
Impact statement.....	5
Statement of Contribution.....	6
Publications associated with this thesis.....	7
Table of Contents	8
List of Figures	13
List of Tables	24
Abbreviations.....	36
1 . Background and Literature Review	40
1.1 Introduction.....	40
1.2 Cerebral blood supply	40
1.2.1 Cerebral macrovasculature	40
1.2.2 Cerebral microvasculature	42
1.2.3 Regulation of cerebral blood flow.....	43
1.3 MR imaging of the ageing brain.....	47
1.3.1 Imaging of dementia	47
1.3.2 Arterial spin labelling.....	48
1.3.3 Brain volume.....	53
1.3.4 White matter hyperintensities.....	54
1.4 Cognitive decline and dementia	57
1.4.1 Causes of cognitive decline and dementia.....	58

1.4.2 Cognitive decline and cerebral blood flow.....	60
1.5 Vascular risk factors	61
1.5.1 Hypertension.....	61
1.5.2 Diabetes.....	62
1.5.3 Serum cholesterol and lipoproteins.....	62
1.5.4 Smoking.....	64
1.5.5 Multifactorial vascular risk.....	65
1.6 Previous studies: evidence of associations of vascular risk with cognitive decline and the MR markers of brain ageing.....	66
1.6.1 Vascular risk and dementia.....	66
1.6.2 Vascular risk and the MR markers of brain ageing	67
1.6.3 Hypertension, cerebral blood flow and the MR markers of brain ageing.....	67
1.6.4 Diabetes, cerebral blood flow and the MR markers of brain ageing..	70
1.6.5 Lipoproteins, cerebral blood flow and the MR markers of brain ageing	72
1.6.6 Smoking, cerebral blood flow and the MR markers of brain ageing..	73
1.6.7 Multifactorial vascular risk, cerebral blood flow and the MR markers of brain ageing	74
1.6.8 Associations of cerebral blood flow with brain atrophy and white matter hyperintensities.....	75
1.7 Limitations of previous studies	76
1.8 Conclusion.....	77
2 . Research questions.....	78
2.1 Aims	78
2.2 Hypotheses	79
3 . General methods.....	81
3.1 Study sample.....	81

3.2 MRI methods	84
3.2.1 MRI acquisition	84
3.2.2 MRI processing	91
3.2.3 Cerebral blood flow quantification	95
3.3 Cardiovascular risk measurements	97
3.3.1 Anthropometrics.....	97
3.3.2 Blood pressure and heart rate	97
3.3.3 Haematocrit	97
3.3.4 Blood analyses	97
3.3.5 Diabetes mellitus	98
3.3.6 Demographic information.....	98
3.3.7 Smoking.....	98
3.3.8 Medications.....	98
3.3.9 Framingham risk score	99
3.4 Statistical methodology.....	101
4 . Cortical cerebral blood flow in ageing: effects of haematocrit, sex, ethnicity and diabetes	102
4.1 Abstract	102
4.2 Introduction.....	103
4.3 Materials and methods	104
4.3.1 Statistical analysis.....	104
4.4 Results	105
4.4.1 Participant characteristics	105
4.4.2 Haematocrit	107
4.4.3 Cerebral blood flow	109
4.4.4 Diabetes.....	117
4.5 Discussion	118

4.6 Conclusion.....	121
5 . Associations of cardiovascular risk with cerebral blood flow in a tri-ethnic elderly population cohort.	122
5.1 Abstract	122
5.2 Introduction.....	124
5.3 Materials and methods	125
5.3.1 Statistical analysis.....	125
5.4 Results	130
5.4.1 Demographic characteristics.....	130
5.4.2 Cardiovascular characteristics	131
5.4.3 Framingham risk score	134
5.4.4 Characteristics of cerebral blood flow	142
5.4.5 Associations of cardiovascular risk factors with cerebral blood flow	147
5.4.6 Associations of cerebral blood flow with Framingham risk score	170
5.5 Discussion	196
5.5.1 Study findings	196
5.5.2 Study strengths	202
5.5.3 Study limitations.....	203
5.5.4 Summary	204
6 . Associations of Framingham risk score and cerebral blood flow with cortical volume and white matter hyperintensity volumes	205
6.1 Abstract	205
6.2 Introduction.....	206
6.3 Methods.....	206
6.3.1 Statistical Analysis	206
6.4 .Results	214

6.4.1 Brain characteristics.....	214
6.4.2 Independent variable: Framingham risk score	233
6.4.3 Independent variable: cerebral blood flow	257
6.4.4 SEM mediation analysis.....	275
6.5 Discussion	304
6.5.1 Main Findings	304
6.5.2 Study Strengths and Limitations	311
6.5.3 Future studies	312
6.5.4 Summary	313
7 . Summary of results and future directions	314
7.1 Review of hypotheses and results.....	314
7.1.1 Chapter 4	314
7.1.2 Chapter 5	315
7.1.3 Chapter 6	317
7.2 Strengths and Limitations	318
7.3 Future Directions	320
References.....	322
8 . Appendices.....	344

List of Figures

Figure 1-1. Maximum intensity projections from MRA 3D Circle of Willis, transverse view showing major arteries. Image is from the SABRE (v3) study.	41
Figure 1-2. Components of the neurovascular unit. Figure adapted from (10) and (11).	43
Figure 1-3. CBF autoregulatory plateau and vessel diameter in hypotensive, normotensive and hypertensive conditions. Dotted lines denote the lower and upper limits of the normal autoregulatory plateau. (Figure adapted from (19)).	46
Figure 1-4. Brain parcellation image showing precuneus and posterior cingulate areas. Image is from the SABRE (v3) study.	47
Figure 1-5. A perfusion image is created from the subtraction of the RF labelled image, acquired after 2s delay, from a control image. (Images are from SABRE v3 study).	50
Figure 1-6. FLAIR images illustrating severe WMHs (Images are from SABRE v3 study).	56
Figure 1-7. The '2 Hit' vascular model for Alzheimer's disease (adapted from (7, 8)). 'Hit 1' (vascular pathway) is shown in red, 'Hit 2' (amyloid β pathway) is shown in green, outcomes are in black.	60
Figure 3-1. Consort diagram, showing sample from the SABRE Study. (figure adapted from (175))	83
Figure 3-2. MRI survey showing example of SMARTEXAM automated planning. (Dotted red line shows alignment of slices through anterior/posterior commissure line and perpendicular to this line on coronal and transverse planes). (Images are from the SABRE v3 study).	85

Figure 3-3. MRI planning of PCASL on T1w sagittal (left) and fast PC-MRI (right) showing slice acquisition and RF labelling planes. (Images are from the SABRE v3 study).	85
Figure 3-4. Perfusion weighted ASL image in transverse plane illustrating movement artefact (Image is from the SABRE v3 study).	86
Figure 3-5. T1w sagittal and subtracted ASL images in transverse plane illustrating susceptibility artefact from dental work (white arrow) causing loss of signal in right hemisphere (Images are from the SABRE v3 study).	87
Figure 3-6 T1w transverse and subtracted ASL image in transverse plane illustrating hypointense perfusion deficit resulting from extensive mature damage in right cerebral hemisphere secondary to ischaemic stroke (Images are from the SABRE v3 study).	87
Figure 3-7. Subtracted ASL images in transverse plane illustrating hyperintense signal in vessels due to arterial transit artefacts (ATAs) as a result of delayed perfusion in the posterior circulation which is more marked on the right. (Images are from the SABRE v3 study).	88
Figure 3-8: Example of regional brain parcellation (image is from the SABRE study).	92
Figure 3-9 Geodesic information flow flowchart showing propagation steps and iterative process. Figure from (180)	93
Figure 3-10: FLAIR images illustrating WMH segmentation with lobe and zone allocations. WMHs are highlighted in green (left column), lobular segmentation (middle column), and zonal distribution (1-4), zone 1 is periventricular shown here in purple, zone 4 is sub-cortical shown here in pink (right column) (186) .	95

Figure 4-1. Boxplot showing median, interquartile range, upper and lower adjacent values and outside values for Hct by sex and ethnicity. ** = P<0.01 by 2-way analysis of variance followed by Fisher's LSD test.	107
Figure 4-2. Scatterplot with line-fit and Pearson's correlation coefficient (r) showing correlation of age and Hct, by sex	108
Figure 4-3. Boxplot showing median, interquartile range, upper and lower adjacent values and outside values for CBF without correction for individual haematocrit (CBF _{fixed}) and CBF with correction for individual haematocrit (CBF _{Hct}), by sex and ethnicity. * = P <0.05, **=P <0.01 by 2 way analysis of variance followed by Fisher's LSD test	109
Figure 4-4. Scatterplot with line-fit and Pearson's r showing correlation of age (years) and CBF (mL/100g/min) by sex.	110
Figure 4-5. Scatterplots showing the effect of correction for individual Hct on the correlation between Hct and cortical CBF in men and women. Top figure shows CBF _{fixed} , bottom figure shows CBF _{Hct}	114
Figure 4-6. Kernel density (kdensity) plots of CBF without correction for individual Hct (CBF _{fixed}) and CBF with correction for individual Hct (CBF _{Hct}) by sex and ethnicity.	115
Figure 4-7. CBF maps overlaid on segmented T1w without and with adjustment for measured Hct. The subject was a white European woman with an Hct of 37.3%.....	116
Figure 4-8. Boxplot showing median, interquartile range, upper and lower adjacent values and outside values for CBF without correction for individual Hct (CBF _{fixed}) and CBF with correction for individual Hct (CBF _{Hct}) by diabetes status. . * = P <0.05, ** = P <0.01 by Student's t-test.....	117

Figure 5-1. Pie chart of distribution of sample by ethnic group (% of sample).	130
Figure 5-2. Histogram with normal density overlay, showing distribution of FRS, pooled sample.	131
Figure 5-3. Histogram with normal density overlay, showing distribution of age, pooled sample.	132
Figure 5-4. Histogram with normal density overlay, showing distribution of systolic BP, pooled sample.	132
Figure 5-5. Histogram with normal density overlay, showing distribution of HDL cholesterol, pooled sample	133
Figure 5-6. Histogram with normal density overlay, showing distribution of total cholesterol pooled sample.	133
Figure 5-7. Boxplot showing FRS by sex and ethnicity. Data show median (solid white line), IQR (solid blue block), upper and lower adjacent values, (i.e. 1.5 x nearest IQR range), (whiskers), and outliers (dots).	135
Figure 5-8. Histogram with normal density overlay, showing distribution of CBF, pooled sample.	142
Figure 5-9 Histogram with normal density overlay, showing distribution of CBF,(men).	143
Figure 5-10. Histogram with normal density overlay, showing distribution of CBF, (women).	143
Figure 5-11. Boxplot showing CBF by sex and ethnicity. *P<.05, ** P<.001.	144
Figure 5-12. Boxplot showing CBF by sex and diabetes status. * P<.05, **P<.001.	145
Figure 5-13. Predictive margins plot showing CBF by age, pooled sample	148

Figure 5-14. Mean linear predictions of CBF by ethnicity and diabetes status (all participants) with 95% CIs adjusted for all covariates (see model 4a(i), Table 5-14).	153
Figure 5-15. Predictive margins plot showing CBF by age, (men)	158
Figure 5-16. Predictive margins plot showing CBF by age, (women)	158
Figure 5-17 Mean linear predictions of CBF by ethnicity and diabetes status (men) with 95% CIs, adjusted for all covariates (see model 4b(i) Table 5-19.)	164
Figure 5-18. Mean linear predictions of CBF by ethnicity and diabetes status (women) with 95% CIs, adjusted for all covariates (see model 4c(i) Table 5-19).	164
Figure 5-19. Scatterplot with line fit showing associations of CBF and FRS by ethnicity	171
Figure 5-20. Scatter diagrams with line fit and 95% CIs showing associations of CBF and FRS in Europeans (top), South Asians (middle) and African Caribbeans (bottom).	172
Figure 5-21. Predictive margins plot showing CBF by FRS by ethnicity (all participants), model 6a, Table 5-26	175
Figure 5-22. Scatterplot showing associations of CBF and FRS by sex	176
Figure 5-23 Scatterplot showing associations of CBF and FRS by ethnicity, (men).	178
Figure 5-24 Scatterplot showing associations of CBF and FRS by ethnicity, (women)	178
Figure 5-25 Predictive margins plots showing CBF for FRS by ethnicity (men) model 5b.	180

Figure 5-26: Predictive margins showing CBF by FRS by ethnicity (women), model 5c.	180
Figure 5-27. Predictive margins plots showing CBF by FRS by ethnicity in groups stratified by diabetes status, all participants, (models 6d and 6e). Top figure shows sample with diabetes, bottom figure shows sample without diabetes..	187
Figure 5-28. Predictive margins plots showing CBF by FRS, by ethnicity (men). Top figure shows sample with diabetes, bottom figure shows sample without diabetes (Table 5-32.	190
Figure 5-29 Predictive margins plots showing CBF by FRS, by ethnicity (women). Top figure shows sample with diabetes, bottom figure shows sample without diabetes (Table 5-34).....	191
Figure 6-1 Histogram with normal density overlay, distribution of total WMHs.	209
Figure 6-2. Histogram with normal density overlay, distribution of log total WMHs.	209
Figure 6-3. Histogram with normal density overlay, distribution of WMHs zones 1 & 2.	210
Figure 6-4. Histogram with normal density overlay, distribution of log WMHs zones 1 & 2.	210
Figure 6-5. Histogram with normal density overlay, distribution of WMHs zones 3 & 4.	211
Figure 6-6 Histogram with normal density overlay, distribution of log WMHs zones 3 & 4.	211

Figure 6-7. Predictive margins plot showing cortical volume by age, (whole sample).....	218
Figure 6-8. Cortical volume by sex and ethnicity, adjusted for age and TIV...	218
Figure 6-9. Predictive margins plot showing total WMHs by age in men.....	223
Figure 6-10. Predictive margins plot showing total WMHs by age in women.	223
Figure 6-11. Predictive margins plot showing cortical volume and FRS, by ethnicity (all participants), adjusted for TIV.	233
Figure 6-12. Predictive margins plot showing cortical volume and FRS by ethnicity (men), adjusted for TIV.	236
Figure 6-13 Predictive margins plot showing cortical volume and FRS, by ethnicity (women), adjusted for TIV.....	236
Figure 6-14 Predictive margins plot showing total WMHs and FRS, by ethnicity (all participants), adjusted for TIV.	239
Figure 6-15 Predictive margins plot showing total WMHs and FRS, by ethnicity (men), adjusted for TIV.	242
Figure 6-16. Predictive margins plot showing total WMHs and FRS, by ethnicity (women), adjusted for TIV.....	242
Figure 6-17 Predictive margins plot showing total WMHs zones 1 & 2 and FRS, by ethnicity (all participants), adjusted for TIV.	245
Figure 6-18 Predictive margins plot showing total WMHs in zones 1 & 2 and FRS, by ethnicity (men), adjusted for TIV.	248
Figure 6-19. Predictive margins plot showing total WMHs in zones 1 & 2 and FRS, by ethnicity (women), adjusted for TIV.....	248

Figure 6-20 Predictive margins plot showing total WMHs zones 3 & 4 and FRS, by ethnicity (all participants), adjusted for TIV	251
Figure 6-21 Predictive margins plot showing total WMHs in zones 3 & 4 and FRS, by ethnicity (men), adjusted for TIV.	254
Figure 6-22. Predictive margins plot showing total WMHs in zones 3 & 4 and FRS, by ethnicity (women), adjusted for TIV.....	254
Figure 6-23. SEM diagram examining the role of CBF as a mediator between FRS and cortical volume; Europeans. Connectors show standardised beta coefficients, (95% CIs) and P-values.	280
Figure 6-24. SEM diagram examining the role of CBF as a mediator between FRS and cortical volume; South Asians. Connectors show standardised beta coefficients, (95% CIs) and P-values.	281
Figure 6-25. SEM diagram examining the role of CBF as a mediator between FRS and cortical volume; African Caribbeans. Connectors show standardised beta coefficients, (95% CIs) and P-values	282
Figure 6-26. SEM diagram examining the role of CBF as a mediator between FRS and cortical volume; Europeans vs South Asians. Connectors show unstandardised beta coefficients, (95% CIs) and P-values.....	283
Figure 6-27. SEM diagram examining the role of CBF as a mediator between FRS and cortical volume; Europeans vs African Caribbeans. Connectors show unstandardised beta coefficients, (95% CIs) and P-values.....	284
Figure 6-28. SEM diagram examining the role of CBF as a mediator between FRS and cortical volume; South Asians vs African Caribbeans. Connectors show unstandardised beta coefficients, (95% CIs) and P-values.....	285

Figure 6-29. SEM diagram examining the role of CBF as a mediator between FRS and log total WMHs; Europeans. Connectors show standardised beta coefficients, (95% CIs) and P-values	286
Figure 6-30. SEM diagram examining the role of CBF as a mediator between FRS and log total WMHs; South Asians. Connectors show standardised beta coefficients, (95% CIs) and P-values.	287
Figure 6-31. SEM diagram examining the role of CBF as a mediator between FRS and log total WMHs; African Caribbeans. Connectors show standardised beta coefficients, (95% CIs) and P-values.	288
Figure 6-32. SEM diagram examining the role of CBF as a mediator between FRS and log total WMHs; Europeans vs South Asians. Connectors show unstandardised beta coefficients, (95% CIs) and P-values.....	289
Figure 6-33. SEM diagram examining the role of CBF as a mediator between FRS and log total WMHs; Europeans vs African Caribbeans. Connectors show unstandardised beta coefficients, (95% CIs) and P-values.....	290
Figure 6-34. SEM diagram examining the role of CBF as a mediator between FRS and log total WMHs; South Asians vs African Caribbeans. Connectors show unstandardised beta coefficients, (95% CIs) and P-values	291
Figure 6-35. SEM diagram examining the role of CBF as a mediator between FRS and log WMHs in zones 1 & 2; Europeans. Connectors show standardised beta coefficients, (95% CIs) and P-values.	292
Figure 6-36. SEM diagram examining the role of CBF as a mediator between FRS and log WMHs in zones 1 & 2; South Asians. Connectors show standardised beta coefficients, (95% CIs) and P-values.....	293

Figure 6-37. SEM diagram examining the role of CBF as a mediator between FRS and log WMHs in zones 1 & 2; African Caribbeans. Connectors show standardised beta coefficients, (95% CIs) and P-values.....	294
Figure 6-38. SEM diagram examining the role of CBF as a mediator between FRS and log WMHs in zones 1 & 2; Europeans vs South Asians. Connectors show unstandardised beta coefficients, (95% CIs) and P-values.....	295
Figure 6-39. SEM diagram examining the role of CBF as a mediator between FRS and log WMHs in zones 1 & 2; Europeans vs African Caribbeans. Connectors show unstandardised beta coefficients, (95% CIs) and P-values.	296
Figure 6-40. SEM diagram examining the role of CBF as a mediator between FRS and log WMHs in zones 1 & 2; South Asians vs African Caribbeans. Connectors show unstandardised beta coefficients, (95% CIs) and P-values.	297
Figure 6-41. SEM diagram examining the role of CBF as a mediator between FRS and log WMHs in zones 3 & 4; Europeans. Connectors show standardised beta coefficients, (95% CIs) and P-values.	298
Figure 6-42. SEM diagram examining the role of CBF as a mediator between FRS and log WMHs in zones 3 & 4; South Asians. Connectors show standardised beta coefficients, (95% CIs) and P-values.....	299
Figure 6-43. SEM diagram examining the role of CBF as a mediator between FRS and log WMHs in zones 3 & 4; African Caribbeans. Connectors show standardised beta coefficients, (95% CIs) and P-values.....	300
Figure 6-44. SEM diagram examining the role of CBF as a mediator between FRS and log WMHs in zones 3 & 4; Europeans vs South Asians. Connectors show unstandardised beta coefficients, (95% CIs) and P-values.....	301

Figure 6-45. SEM diagram examining the role of CBF as a mediator between FRS and log WMHs in zones 3 & 4 Europeans vs African Caribbeans.

Connectors show unstandardised beta coefficients, (95% CIs) and P-values.302

Figure 6-46 SEM diagram examining the role of CBF as a mediator between FRS and log WMHs in zones 3 & 4; South Asians vs African Caribbeans.

Connectors show unstandardised beta coefficients, (95% CIs) and P-values.303

Figure 8-1. Scatter plots showing the correlation of systolic BP and age.....344

Figure 8-2. Scatter plots showing the correlation of pulse pressure and age.

.....3443

List of Tables

Table 1-1. Prevalence of vascular risk factors, by sex and age (England).	65
Table 3-1. MRI protocol for SABRE v3 study.....	89
Table 3-2. Beta coefficients for Framingham risk score algorithm (199).....	100
Table 4-1. Participant characteristics; data are mean \pm SD or number of observations (n) (%). *P<0.05, **P<0.01 compared to reference (male/Europeans) by Fisher's LSD test after 2-way analysis of variance (ANOVA).....	106
Table 4-2. Multiple linear regression analyses of associations of demographic and cardiovascular risk factors. Hct is dependent variable, model 1 independent variables are age, sex and ethnicity, model 2 is model 1 + independent variables LDL Cholesterol, HDL Cholesterol, mean arterial pressure, HbA1c and BMI.	112
Table 4-3. Comparison of CBF without correction for individual haematocrit (CBF_fixed) and CBF with correction for individual Hct (CBF_Hct) by sex, ethnicity and diabetes diagnosis. Data are mean \pm SD, except difference (95% CIs), mean difference (%). P values were calculated using a Student's t-test. Effect size is Cohen's d.....	113
Table 5-1. Key to multiple linear regression models using vascular risk factors as predictor variables, * and ** denote interaction models.....	128
Table 5-2. Key to multiple linear regression models using FRS as predictor variable.	129

Table 5-3: Demographic and cardiovascular characteristics for categorical variables by ethnicity. Data are number of observations and (%). Tests for significance use Chi square or *Fisher's exact, **uses chi square goodness of fit. P <0.05 shown in bold..... 136

Table 5-4. Demographic and cardiovascular characteristics for continuous variables by ethnicity, pooled sample. Data are mean \pm SD. Tests for significance are compared to reference (white Europeans) by post hoc Fisher's LSD test after ANOVA. P <0.05 shown in bold 137

Table 5-5. Demographic and cardiovascular characteristics for categorical variables by ethnicity (men), Data are number of observations and (%). Tests for significance use Chi square or *Fisher's exact, **uses chi square goodness of fit. P <0.05 shown in bold..... 138

Table 5-6. Demographic and cardiovascular characteristics for continuous variables by ethnicity, (men). Data are mean \pm SD. Tests for significance are compared to reference (Europeans) by post hoc Fisher's LSD test after one-way ANOVA. P <0.05 shown in bold..... 139

Table 5-7. Demographic and cardiovascular characteristics for categorical variables by ethnicity, (women). Data are number of observations and (%). Tests for significance use Chi square or *Fisher's exact, **uses chi square goodness of fit. P <0.05 shown in bold. 140

Table 5-8. Demographic and cardiovascular characteristics for continuous variables by ethnicity, (women). Data are mean \pm SD. Tests for significance are compared to reference (white Europeans) by post hoc Fisher's LSD test after one-way ANOVA. P <0.05 shown in bold..... 141

Table 5-9. CBF by sex. Data are mean \pm SD. Tests for significance are compared to reference (Europeans) by post hoc Fisher's LSD test after one-way ANOVA, $P < 0.05$ shown in bold..... 146

Table 5-10. CBF by diabetes status. Data are mean \pm SD. Tests for significance use 2 sample unpaired Student's t-test, $P < 0.05$ shown in bold..... 146

Table 5-11: Bivariate analysis, correlations of CBF and continuous cardiovascular risk factors in all participants and stratified by sex, $P < 0.05$ shown in bold. 147

Table 5-12 .Multiple linear regression models for dependent variable cortical CBF, demographic independent variables(all participants): shows unstandardized beta coefficients and η^2 , $P < 0.05$ in bold. 149

Table 5-13. Multiple linear regression models using single cardiovascular risk factors (all participants): shows unstandardized beta coefficients and η^2 , $P < 0.05$ in bold..... 151

Table 5-14. Multiple linear regression models for dependent variable cortical CBF, single cardiovascular risk factors and diabetes/ethnicity interaction terms (all participants): shows unstandardized beta coefficients and η^2 , $P < 0.05$ in bold. 152

Table 5-15. Multiple linear regression model for dependent variable cortical CBF, single cardiovascular risk factors and diabetes/ethnicity and age/ethnicity interaction terms (all participants): shows unstandardized beta coefficients and η^2 , $P < 0.05$ in bold..... 154

Table 5-16. Multiple linear regression models for dependent variable cortical CBF and demographic independent variables (men): shows unstandardized beta coefficients and η^2 , $P < 0.05$ in bold..... 156

Table 5-17. Multiple linear regression models for dependent variable cortical CBF and demographic independent variables (women): shows unstandardized beta coefficients and η^2 , $P < 0.05$ in bold. 157

Table 5-18. Multiple linear regression models stratified by sex using single cardiovascular risk factors, (men and women) unstandardised beta coefficients and η^2 , $P < 0.05$ in bold..... 160

Table 5-19. Multiple linear regression models stratified by sex using single cardiovascular risk factors with interaction term diabetes*ethnicity, unstandardized beta coefficients and η^2 , $P < 0.05$ in bold. 162

Table 5-20. Marginal means for cortical CBF according to diabetes status by sex and ethnicity data derived from Table 5-14 and Table 5-19. 163

Table 5-21. Multiple linear regression model for dependent variable cortical CBF, single cardiovascular risk factors and diabetes/ethnicity and age/ethnicity interaction terms (men): shows unstandardized beta coefficients and η^2 , $P < 0.05$ in bold 165

Table 5-22. Multiple linear regression model for dependent variable cortical CBF, single cardiovascular risk factors and diabetes/ethnicity and age/ethnicity interaction terms (women): shows unstandardized beta coefficients and η^2 , $P < 0.05$ in bold 166

Table 5-23. Multiple linear regression models for dependent variable cortical CBF, using demographic covariates. shows unstandardised beta coefficients and η^2 . Groups stratified by diabetes status, $P < 0.05$ in bold..... 168

Table 5-24. Multiple linear regression models for dependent variable cortical CBF using single cardiovascular risk factors (all participants), showing

unstandardised beta coefficients and η^2 . Groups stratified by diabetes status.
P<0.05 in bold..... 169

Table 5-25. Pearson’s correlation coefficient of FRS with CBF by sex and ethnic groups, P<0.05 in bold..... 170

Table 5-26. Multiple linear regression models (all participants) showing associations of CBF with FRS and ethnicity showing unstandardised beta coefficients and η^2 , P<0.05 in bold..... 174

Table 5-27 Multiple linear regression models showing associations of CBF with FRS and ethnicity, (men), showing unstandardised beta coefficients and η^2 , P<0.05 in bold..... 181

Table 5-28. Multiple linear regression models showing associations of CBF with FRS and ethnicity, (women). showing unstandardised beta coefficients and η^2 , P<0.05 in bold..... 182

Table 5-29 Multiple linear regression using samples grouped by diabetes status showing unstandardised and η^2 , P<0.05 in bold. 184

Table 5-30 Multiple linear regression including ethnicity/FRS interaction terms, samples grouped by diabetes status, showing unstandardised beta coefficients and η^2 , P<0.05 in bold..... 186

Table 5-31. Multiple linear regression using samples grouped by diabetes status (men), showing unstandardised beta coefficients and η^2 , P<0.05 in bold. 192

Table 5-32: Multiple linear regression including ethnicity/FRS interaction terms using samples grouped by diabetes status (men), showing unstandardised beta coefficients and η^2 , P<0.05 in bold..... 193

Table 5-33. Multiple linear regression using samples grouped by diabetes status (women), showing unstandardised beta coefficients and η^2 , $P < 0.05$ in bold.	194
Table 5-34. Multiple linear regression including ethnicity/FRS interaction terms using samples grouped by diabetes status (women), showing unstandardised beta coefficients and η^2 , $P < 0.05$ in bold.....	195
Table 6-1. Key to naming of generalized linear regression models using demographic variables and FRS as predictor variables.....	212
Table 6-2. Key to naming of generalized linear regression models using demographic variables and CBF as predictor variables.....	213
Table 6-3. Brain characteristics by sex: data are mean \pm SD, percentage of TIV or *median (IQR), tests for significance are calculated by Student's unpaired t-tests, except ^{MW} which denotes P value by rank sum Mann-Whitney test.	215
Table 6-4. Brain characteristics by ethnicity: data are mean \pm SD, percentage of TIV or median (IQR).....	216
Table 6-5. Multiple linear regression models 1a, 2a, (all participants), cortical tissue volume is dependent variable. Models are adjusted for TIV, beta coefficients are unstandardised, $P < .05$ shown in bold.	219
Table 6-6. Multiple linear regression models 1b, 2b, (men), cortical tissue volume is dependent variable. Models are adjusted for TIV, beta coefficients are unstandardised, $P < .05$ shown in bold.	220
Table 6-7. Multiple linear regression models 1c, 2c (women), dependent variable is cortical tissue volume. Models are adjusted for TIV, beta coefficients are unstandardised, $P < .05$ shown in bold.	221

Table 6-8. Generalized linear models 1d, 2d (all participants), dependent variable is total WMH volume. Models are adjusted for TIV, exponentiated beta coefficients, P <.05 shown in bold.....224

Table 6-9. Generalized linear models 1e, 2e (men), dependent variable is total WMH volume. Models are adjusted for TIV, exponentiated beta coefficients, P <.05 shown in bold.....225

Table 6-10. Generalized linear models 1f, 2f (women), dependent variable is total WMH volume. Models are adjusted for TIV, exponentiated beta coefficients, P <.05 shown in bold.....226

Table 6-11. Generalized linear models 1g, 2g (all participants), dependent variable is WMH zones 1 & 2 volume. Models are adjusted for TIV, exponentiated beta coefficients, P <.05 shown in bold.227

Table 6-12. Generalized linear models 1h, 2h (men), dependent variable is WMH zones 1 & 2 volume. Models are adjusted for TIV, exponentiated beta coefficients, P <.05 shown in bold.....228

Table 6-13. Generalized linear models 1i, 2i (women), dependent variable is WMH zones 1 & 2 volume. Models are adjusted for TIV, exponentiated beta coefficients, P <.05 shown in bold.....229

Table 6-14. Generalized linear models 1j, 2j (all participants), dependent variable is WMH zones 3 & 4 volume. Models are adjusted for TIV, exponentiated beta coefficients, P <.05 shown in bold.230

Table 6-15. Generalized linear models 1k, 2k (men), dependent variable is WMH zones 3 & 4 volume. Models are adjusted for TIV, exponentiated beta coefficients, P <.05 shown in bold.....231

Table 6-16. Generalized linear models 1I, 2I (women), dependent variable is WMH zones 3 & 4 volume. Models are adjusted for TIV, exponentiated beta coefficients, P <.05 shown in bold.....232

Table 6-17. Multiple linear regression models 3a, 4a,5a, (all participants), cortical tissue volume is dependent variable. Models are adjusted for TIV, unstandardised beta coefficients, P <.05 shown in bold.234

Table 6-18. Multiple linear regression models 3b, 4b,5b, (men), cortical tissue volume is dependent variable. Models are adjusted for TIV, unstandardised beta coefficients, P <.05 shown in bold.....237

Table 6-19 Multiple linear regression models 3c, 4c,5c, (women), cortical tissue volume is dependent variable. Models are adjusted for TIV, unstandardised beta coefficients, P <.05 shown in bold.....238

Table 6-20 Generalized linear models 3d, 4d, 5d (all participants), dependent variable is total WMH volume. Models are adjusted for TIV, exponentiated beta coefficients, P <.05 shown in bold.....240

Table 6-21. Generalized linear models 3e, 4e, 5e (men), dependent variable is total WMH volume. Models are adjusted for TIV, exponentiated beta coefficients, P <.05 shown in bold.....243

Table 6-22. Generalized linear models 3f, 4f, 5f (women), dependent variable is total WMH volume. Models are adjusted for TIV, exponentiated beta coefficients, P <.05 shown in bold.....244

Table 6-23. Generalized linear models 3g, 4g, 5g (all participants), dependent variable is WMH volume zones 1 & 2. Models are adjusted for TIV, exponentiated beta coefficients, P <.05 shown in bold.246

Table 6-24. Generalized linear models 3h, 4h, 5h (men), dependent variable is WMH volume in zones 1 & 2. Models are adjusted for TIV, exponentiated beta coefficients, P <.05 shown in bold.....249

Table 6-25. Generalized linear models 3i, 4i, 5i (women), dependent variable is WMH volume zones 1 & 2. Models are adjusted for TIV, exponentiated beta coefficients, P <.05 shown in bold.....250

Table 6-26. Generalized linear models 3j, 4j, 5j (all participants), dependent variable is WMH volume zones 3 & 4. Models are adjusted for TIV, exponentiated beta coefficients, P <.05 shown in bold.252

Table 6-27. Generalized linear models 3k, 4k, 5k (men), dependent variable is WMH volume zones 3 & 4. Models are adjusted for TIV, exponentiated beta coefficients, P <.05 shown in bold.....255

Table 6-28. Generalized linear models 3l, 4l, 5l (women), dependent variable is WMH volume zones 3 & 4. Models are adjusted for TIV, exponentiated beta coefficients, P <.05 shown in bold.....256

Table 6-29. . Generalized linear model 6a, dependent variable is cortical tissue volume (all participants), Model is adjusted for TIV, unstandardised beta coefficients, P <.05 shown in bold.....258

Table 6-30.. Generalized linear models 7a, 8a, dependent variable is cortical tissue volume (all participants). Models are adjusted for TIV, unstandardised beta coefficients, P <.05 shown in bold.....259

Table 6-31. Generalized linear models 7b, 8b, dependent variable is cortical tissue volume (men). Models are adjusted for TIV, unstandardised beta coefficients, P <.05 shown in bold.....260

Table 6-32. Generalized linear models 7c, 8c, dependent variable is cortical tissue volume (women). Models are adjusted for TIV, unstandardised beta coefficients, P <.05 shown in bold.....	261
Table 6-33. Generalized linear model 6d (all participants), dependent variable is total WMH volume. Models are adjusted for TIV, exponentiated beta coefficients, P <.05 shown in bold.....	263
Table 6-34. Generalized linear models 7d, 8d (all participants), dependent variable is total WMH volume. Models are adjusted for TIV, exponentiated beta coefficients, P <.05 shown in bold.....	264
Table 6-35. Generalized linear models 7e, 8e (men), dependent variable is total WMH volume. Models are adjusted for TIV, exponentiated beta coefficients, P <.05 shown in bold.....	265
Table 6-36. Generalized linear models 7f, 8f (women), dependent variable is total WMH volume. Models are adjusted for TIV, exponentiated beta coefficients, P <.05 shown in bold.....	266
Table 6-37. Generalized linear model 6g (all participants), dependent variable is WMH volume zones 1 & 2. Models are adjusted for TIV, exponentiated beta coefficients, P <.05 shown in bold.....	267
Table 6-38. Generalized linear models 7g, 8g (all participants), dependent variable is WMH volume in zones 1 & 2. Models are adjusted for TIV, exponentiated beta coefficients, P <.05 shown in bold	268
Table 6-39. Generalized linear models 7h, 8h (men), dependent variable is WMH volume in zones 1 & 2. Models are adjusted for TIV, exponentiated beta coefficients, P <.05 shown in bold.....	269

Table 6-40 Generalized linear models 7i, 8i (women), dependent variable is WMH volume in zones 1 & 2. Models are adjusted for TIV, exponentiated beta coefficients, P <.05 shown in bold.....270

Table 6-41. Generalized linear model 6j (all participants), dependent variable is WMH volume in zones 3 & 4. Models are adjusted for TIV, exponentiated beta coefficients, P <.05 shown in bold.....271

Table 6-42. Generalized linear models 7j, 8j (all participants), dependent variable is WMH volume in zones 3 & 4. Models are adjusted for TIV, exponentiated beta coefficients, P <.05 shown in bold.272

Table 6-43. Generalized linear models 7k, 8kj (men), dependent variable is WMH volume in zones 3 & 4. Models are adjusted for TIV, exponentiated beta coefficients, P <.05 shown in bold.....273

Table 6-44. Generalized linear models 7l, 8l (women), dependent variable is WMH volume in zones 3 & 4. Models are adjusted for TIV, exponentiated beta coefficients, P <.05 shown in bold.....274

Table 6-45. Direct, indirect and total effects of FRS mediated by CBF on cortical volume estimated from SEMs, standardised beta coefficients, P<.05 in bold. 276

Table 6-46. Wald tests for invariance of parameters across ethnic groups for SEMs including cortical volume using multi group option, P<.05 in bold.276

Table 6-47. Direct, indirect and total effects of FRS mediated by CBF on log total WMHs volume estimated from SEMs, standardised beta coefficients P<.05 in bold.277

Table 6-48. Wald tests for invariance of parameters across ethnic groups for SEMs including log total WMH volume using multi group option, P<.05 in bold.277

Table 6-49. Direct, indirect and total effects of FRS mediated by CBF on log WMHs zones 1 & 2 volume estimated from SEMs, standardised beta coefficients, P<.05 in bold.	278
Table 6-50. Wald tests for invariance of parameters across ethnic groups for SEMs including log WMH zones 1 & 2 volume using multi group option, P<.05 in bold.	278
Table 6-51. Direct, indirect and total effects of FRS mediated by CBF on log WMHs zones 3 & 4 volume estimated from SEMs, standardised beta coefficients, P<.05 in bold.	279
Table 6-52. Wald tests for invariance of parameters across ethnic groups for SEMs including log WMH zones 3 & 4 volume using multi group option, P<.05 in bold.	279
Table 8-1. Dependent variable: total white matter hyperintensities volume (all participants). Models are adjusted for TIV exponentiated beta coefficients, P <.05 shown in bold.	345

Abbreviations

A β	amyloid beta
AD	Alzheimer's disease
ADNI	Alzheimer's Disease Neuroimaging Initiative
AGE	advanced glycation end product
ANOVA	analysis of variance
APOE4	apolipoprotein E4
APP	amyloid precursor protein
ASL	arterial spin labelling
ATA	arterial transit artefact
ATT	arterial transit time
BaMoS	Bayesian Model Selection
BBB	blood brain barrier
BMI	body mass index
BP	blood pressure
CASL	continuous arterial spin labelling
CBF	cerebral blood flow
CBV	cerebral blood volume
CGM	cortical grey matter
CMIC	Centre for Medical Image Computing
CoW	circle of Willis
CSF	cerebro-spinal fluid
CT	computed tomography
DTI	diffusion tensor imaging

DWM	deep white matter
DWMH	deep white matter hyperintensities
EPI	echo planar imaging
FA	fractional anisotropy
FDG-PET	¹⁸ F-fluoro-deoxyglucose positron emission tomography
FLAIR	Fluid attenuated inversion recovery
FRS	Framingham risk score
GIF	geodesic information flow
GLM	generalized linear model
GSEM	generalized structural equation model
HbA1c	haemoglobin A1c (glycated haemoglobin)
Hct	haematocrit
HDL	high density lipoprotein cholesterol
ICA	internal carotid artery
IR	insulin resistance
ISMRM	International Society for Magnetic Resonance in Medicine
LDL	low density lipoprotein cholesterol
LR	likelihood ratio test
MAP	mean arterial pressure
MCI	mild cognitive impairment
MD	mean diffusivity
MetS	metabolic syndrome
MRA	magnetic resonance angiography
MRI	magnetic resonance imaging

MT	magnetization transfer
NICE	National Institute for Clinical Excellence
NO	nitric oxide
eNOS	endothelial nitric oxide synthase
NVU	neurovascular unit
OEF	oxygen extraction fraction
PASL	pulsed arterial spin labelling
PC-MR	phase contrast angiography
PCASL	pseudo-continuous arterial spin labelling
PDw	proton density weighted
PET	positron emission tomography
PLD	post labelling delay
PP	pulse pressure
PV	periventricular
PVC	partial volume correction
RF	radio frequency
ROI	region of interest
ROS	reactive oxygen species
SABRE	Southall and Brent Revisited study
SAR	specific absorption rate
SEM	structural equation model
SD	standard deviation
SI	signal intensity
SNR	signal to noise ratio

SPECT	single photon emission computed tomography
SVID	small vessel ischaemic disease
T1w	T1 weighted
T2w	T2 weighted
T2DM	type 2 diabetes mellitus
TFE	turbo field echo
TIA	transient ischaemic attack
TIV	total intracranial volume
TSE	turbo spin echo
VaD	vascular dementia
VBM	voxel based statistical parametric mapping
VRF	vascular risk factor
WM	white matter
WMHs	white matter hyperintensities
WMHZ12	white matter hyperintensities in brain zones 1 & 2
WMHZ34	white matter hyperintensities in brain zones 3 & 4
WHO	World Health Organization

1 . Background and Literature Review

1.1 Introduction

This thesis examines the relationship of CBF to vascular risk and the appearances of brain ageing shown by MRI in a tri-ethnic population cohort. The first chapter describes the context of this thesis. It presents the background of cerebral blood supply and vascular risk factors, and describes the hypothesised relationship of CBF to vascular risk. A description of the MRI markers of brain ageing and MRI techniques employed in this thesis follows. Previous work investigating the relationships of vascular risk to CBF, brain atrophy and WMH volume is reviewed.

1.2 Cerebral blood supply

The brain is an organ of high metabolic demand but has little access to stored energy. Regional activation of neurons and clearance of toxic waste products require rapid response of blood flow to specific areas of tissue. A continuous and dynamic blood supply is therefore essential for the maintenance of healthy cognitive function (1).

1.2.1 Cerebral macrovasculature

Blood is supplied to the brain via two pairs of arteries. The left and right internal carotid arteries (ICAs) mainly supply the anterior circulation, and the vertebral arteries, which converge to form the basilar artery, supply the posterior circulation. The ICAs, basilar artery and communicating arteries form the circle of Willis (CoW) which is an anastomotic ring (**Figure 1-1**). Anastomoses provide connections between circulations although there are a number of common variants and the CoW is complete in only 40% of the population (2).

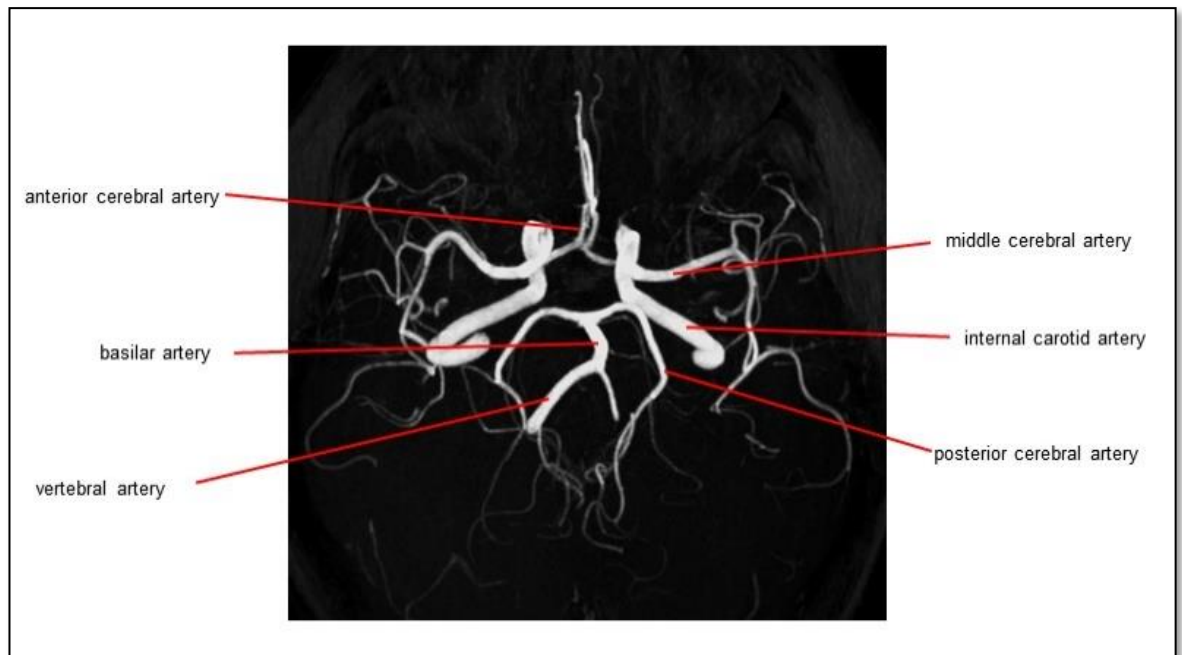


Figure 1-1. Maximum intensity projections from MRA 3D Circle of Willis, transverse view showing major arteries. Image is from the SABRE (v3) study.

The anterior, middle and posterior cerebral arteries arise from the CoW, and divide into a system of cortical arteries. There are 6 variants of microvascular supply to the cerebrum, some of which protect areas of tissue from hypoperfusion via anastomotic flow. Other areas of tissue are vulnerable to interruption of the blood supply as they are supplied by a single source vessel, potentially resulting in stroke and small vessel ischaemic disease (SVID) (3). 'Watershed' areas comprising border zones where tissue lies at the confluence of the major cerebral arteries are particularly vulnerable to cortical microinfarcts and stroke in circumstances of decreased and interrupted blood flow (4). Such cortical microinfarcts in the locale of border zones are also associated with Alzheimer's disease (AD) (5).

Pial vessels branch along the surface of the cortex and smaller perpendicular parenchymal arterioles penetrate the cortical tissue. Long medullary arteries reach white matter (WM) with little collateral flow to protect blood supply. The

cortex benefits from a rich leptomeningeal collateral network of short pial branches. Arterioles finally give way to the capillary network.

1.2.2 Cerebral microvasculature

Cerebral perfusion is provided by capillary beds which transport oxygen, nutrients and glucose to tissue (2). It is measured by CBF which is the delivery of blood to an area of brain tissue over a defined period of time, i.e. mL/100g/min (6). Almost every neuron is fed by a separate capillary, with the network comprising ~600km of densely packed vessels, each with a diameter of ~ 7 μ m (1). Capillary vessels comprise an inner basement membrane encased by an outer sleeve of endothelium with associated pericytes. In the cerebral circulation, the outer sleeve is enveloped by astrocytic endfeet. The neurovascular unit (NVU) is formed of neurons, glial cells (including astrocytes, microglia and oligodendroglia), the endothelial layer, pericytes and vascular smooth muscle cells (**Figure 1-2**). The NVU co-ordinates vessels and neurons to adjust blood flow in accordance with neuronal demand through the mechanism of neurovascular coupling. (7-9). Early studies inspecting post-mortem histological specimens of the brain concluded there were substantial changes in the microvasculature associated with ageing (3). These changes included increased vessel tortuosity, increased periventricular venous collagenosis, basement membrane thickening, hypoxia, decline in angiogenesis, reduction in capillary density and string vessel formation (4).

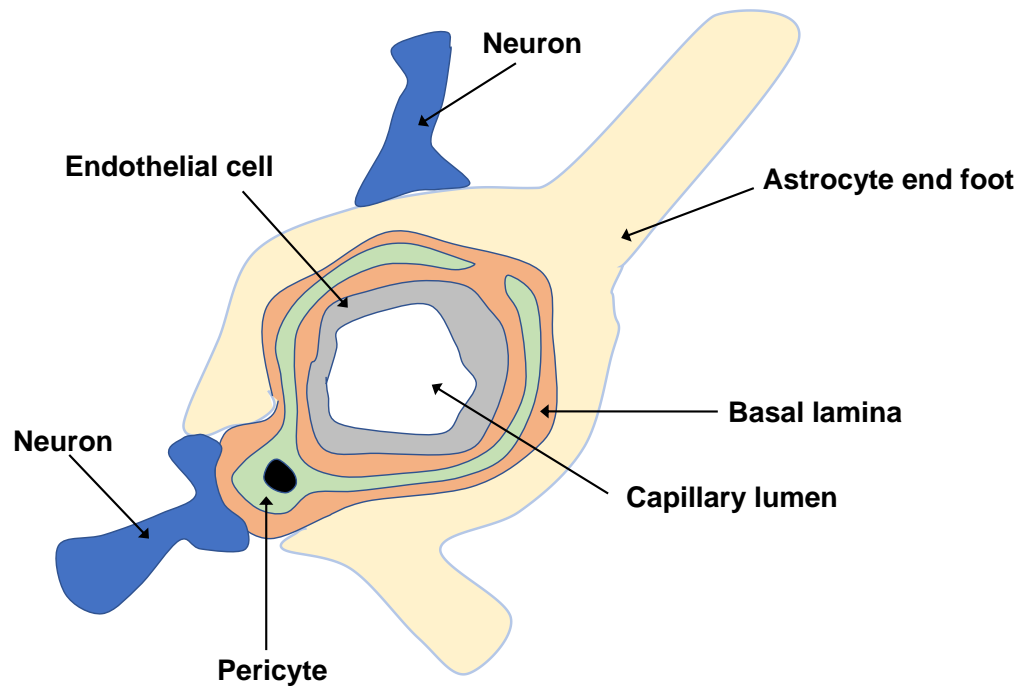


Figure 1-2. Components of the neurovascular unit. Figure adapted from (10) and (11).

1.2.3 Regulation of cerebral blood flow

Modification of cerebrovascular resistance to maintain adequate blood flow and facilitate the redistribution of blood to regionally activated areas of the brain (functional hyperaemia) is achieved through several mechanisms. These are cerebral autoregulation, neurovascular coupling which involves complex cellular signalling to the vasculature via the NVU, and endothelial influence on vascular tone (12). Failure of functional hyperaemia results, not only in reduced capillary flow, but in suboptimal flow distribution in the capillary bed leading to inefficient oxygen extraction fraction (OEF) (13).

1.2.3.1 Cerebral autoregulation

Cerebral autoregulation enables the brain to maintain nearly constant perfusion despite fluctuating cerebral perfusion pressure. It also contributes to the matching of blood flow and metabolic demand. (14). Cerebral autoregulation is

achieved through appropriate vasodilatation or vasoconstriction, boosting of OEF, and control of blood volume (15).

Myogenic, neurogenic and metabolic processes have been hypothesised as factors that influence cerebral autoregulation. The intrinsic myogenic response of cerebral arteries, whereby smooth muscle cells respond to intravascular pressure in order to moderate vascular resistance through constriction and dilatation of vascular walls, is an important factor for maintaining constant perfusion pressure despite fluctuations in blood pressure (BP), particularly in the context of rapid changes in perfusion pressure (16). This mechanism minimises high pressure damage to the vulnerable downstream cerebral microvasculature and guarantees sufficient blood flow to prevent hypoxia through hypotension within the autoregulatory range. Metabolic and neural factors also contribute to autoregulation. Vasoactive substances such as the neurotransmitters acetylcholine, GABA, catecholamines, neuropeptides and glutamate, as well as ions (K^+ , H^+) are secreted in association with synaptic activation and may influence blood vessel tone. Metabolic pathways include the increase in neuronal ATP activity leading to adenosine release which is a strong vasodilator and may contribute to coupling between energy utilization and blood delivery (17). Vascular risk factors can cause disruption to the mechanisms of cerebral autoregulation. For example, chronic hypertension may result in vascular remodelling thus increasing vascular resistance, vessel rarefaction and endothelial dysfunction (18, 19).

1.2.3.1 Neurovascular coupling

Components of the NVU act in concert in response to increased neuronal energy demand through numerous complex cellular processes. One of these is the 'feed-forward' response. This initially involves release of extracellular ions as a result of synaptic activity causing hyperpolarization which is conducted through endothelial cells to produce retrograde vasodilation (20). In addition, a 'feed-back' mechanism adjusts vascular dilatation in response to hypoxic conditions through high levels of adenosine and lactate released as a result of energy metabolism (20). In addition, the decrease in arterial O_2 that

accompanies neural activity may increase the deformability of red blood cells thus reducing blood viscosity and increasing capillary flow (20).

1.2.3.2 Endothelial function

The endothelial layer regulates arterial and arteriole vascular dilatation through a number of mechanisms including the release of nitric oxide (NO) through the activity of NO synthase (eNOS) and the release of other vasoactive factors (eicosanoids, endothelin). The endothelial cell layer also functions to maintain the blood brain barrier (BBB) via coupled adherens and tight-junctions allowing free diffusion of CO₂, O₂ and lipophilic agents but limiting or excluding the egress of other molecules. It governs the transport of nutrients, metabolites, amino acids and peptides from capillary blood into the brain by controlling the permeability of the BBB and prevents transmission of potentially toxic substances such as plasma proteins into the brain. It also clears toxic metabolic brain by-products, thus controlling a delicate homeostasis (21).

Damaged or dysfunctional endothelium fails to adequately control flow in the capillary vasculature and encourages the release of neurotoxins and multiple inflammatory factors (22). Dynamic contrast enhanced MRI has shown the brain to have regionally increased permeability in elderly individuals with cognitive impairment and dementia suggesting damage to the BBB (23). In addition to healthy endothelium, intact pericytes are crucial for the control of capillary calibre via neuronal feedback (24). Consequences of a compromised BBB include decreased nutrient delivery leading to neuronal death, increased cerebral toxicity and inhibition of the autoregulation of cerebral blood supply.

Under normotensive conditions cerebral autoregulation can maintain a mostly flat CBF plateau in the range 60 -150mmHg mean arterial pressure (MAP). CBF is initially maintained by vasodilatation accompanied by an increase in cerebral blood volume (CBV). When dilatatory capacity reaches its maximum, further decreases in perfusion pressure result in a drop in CBF and OEF increases to compensate. However, once OEF reaches its maximum level,

functional consequences of low CBF occur (15). Prolonged high pressure promotes adaptive changes to the vasculature via remodelling of vessel walls and reduction of lumen size in arteries and arterioles (16). These alterations are associated with a change in the autoregulatory response shifting the lower and upper boundaries of the plateau up to higher values of perfusion pressure (**Figure 1-3**). This upwards shift leaves brain tissue vulnerable to hypoperfusion and ischaemia during episodes of low BP as autoregulatory mechanisms are unable to recruit sufficient vasodilatation to preserve CBF.

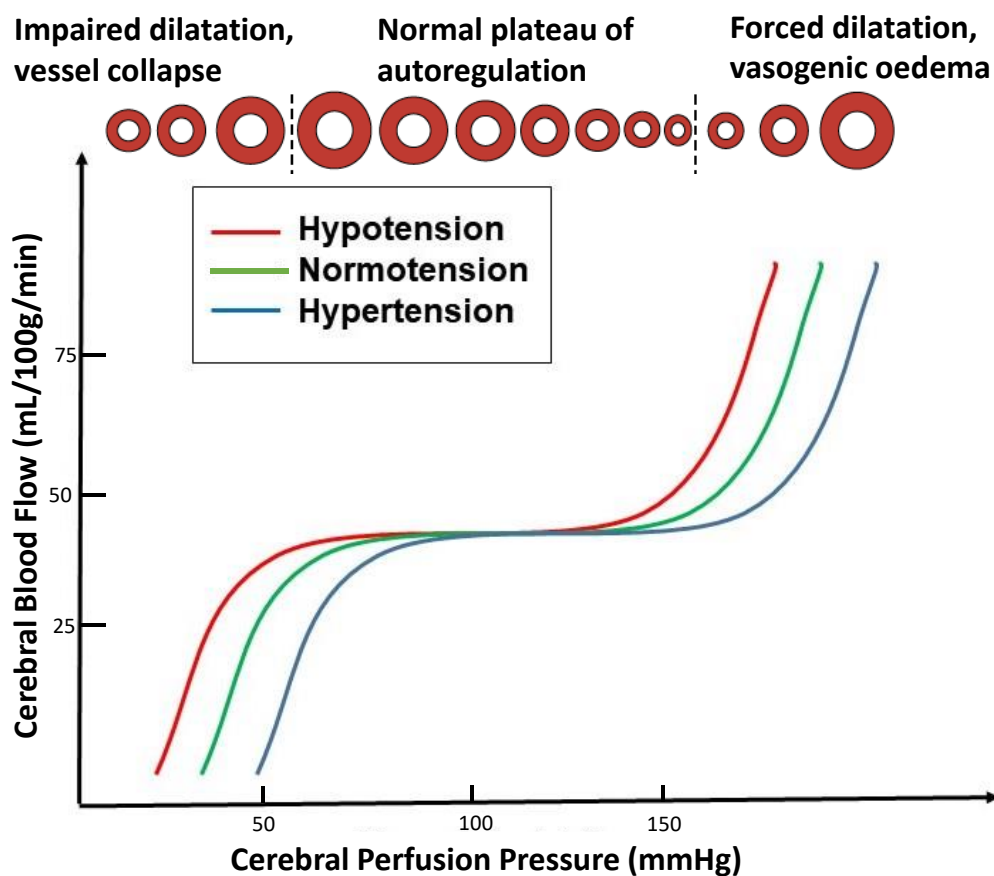


Figure 1-3. CBF autoregulatory plateau and vessel diameter in hypotensive, normotensive and hypertensive conditions. Dotted lines denote the lower and upper limits of the normal autoregulatory plateau. (Figure adapted from (19)).

1.3 MR imaging of the ageing brain

1.3.1 Imaging of dementia

Studies that diagnose or assess dementia by cognitive testing or clinical evaluation capture the disease at a late stage in a degenerative process that may span decades. Five imaging biomarkers have been identified with potential to detect AD at earlier stages of its development (25):

1. The earliest biomarker in this scheme is the detection of amyloid beta ($A\beta$) plaques in the precuneus/posterior cingulate regions of the brain using positron emission tomography (PET) imaging. 2. ^{18}F -fluoro-deoxyglucose (FDG) PET was originally used to detect glucose uptake as a surrogate marker of amyloid, but novel radio-tracers such as Pittsburgh compound-B (PIB) (26) and florbetapir (^{18}F) (27) have enabled direct imaging of $A\beta$ plaques. 3. The spread of $A\beta$ plaques to the parietal, lateral temporal and frontal lobes can be detected at the next stage of disease. 4. Further disease progression is revealed on structural MRI showing regional brain volume loss in the temporal, lateral temporal and eventually in the frontal lobes. 5. In the later stages of AD, memory dysfunction and other clinical symptoms are measurable by cognitive testing (25).

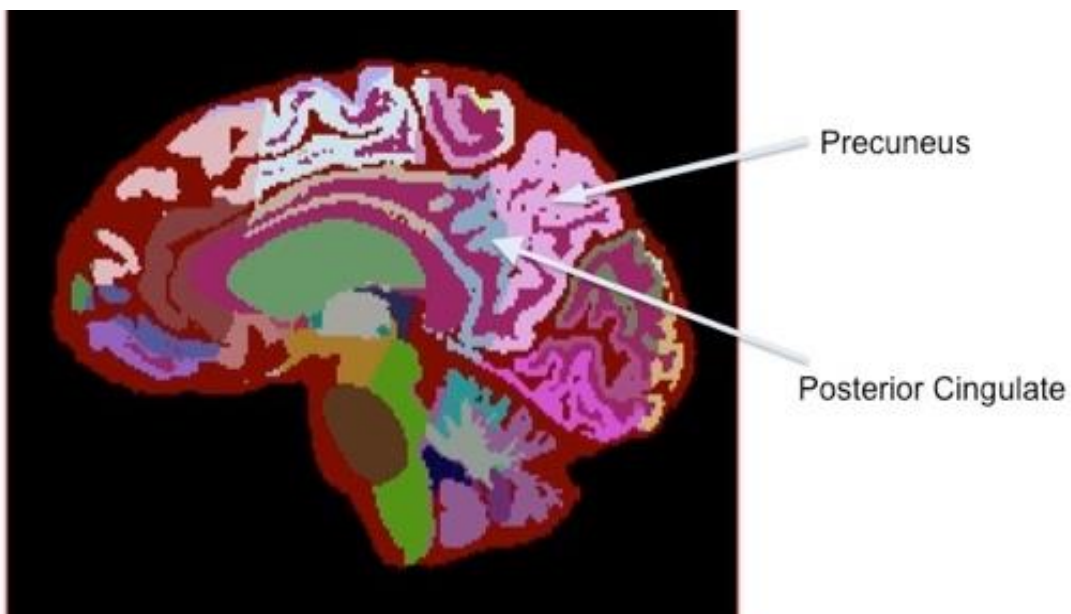


Figure 1-4. Brain parcellation image showing precuneus and posterior cingulate areas. Image is from the SABRE (v3) study.

Phenomena such as hippocampal atrophy and cortical thinning imaged using structural MRI become evident only when cognitive symptoms such as memory loss are imminent. Even the earliest of these 5 biomarkers captures AD at a relatively late stage when A β plaques are already prevalent. Failure to make progress with dementia drug treatment may be an indication that identifying AD in these stages is too late to implement effective interventions.

1.3.2 Arterial spin labelling

1.3.2.1 Role of arterial spin labelling as a biomarker of cognitive decline

Changes in glucose metabolism appear to precede cerebral volume loss according to the model of AD biomarkers discussed earlier (25). Early studies using FDG PET identified regional glucose hypo-metabolism in mild cognitive impairment (MCI) and AD (28, 29). These studies were costly and invasive due to the use of injected tracer and as a result were limited to small samples. However, the close coupling of CBF to brain metabolism (30) means the development of MRI techniques that measure CBF, initially phase contrast angiography (PC -MR) and more recently ASL, can be used as relatively inexpensive and non-invasive functional measures of brain health. CBF calculated from ASL has been correlated with FDG PET derived measurements in a number of studies (31, 32). The association of decreased CBF with hypometabolism, whether as a consequence of reduced metabolic demand or as a precursor to neuronal injury, indicates that ASL could be used as a non-invasive alternative to PET imaging as an early biomarker of AD. A study investigating the mechanisms of late-onset AD in the large Alzheimer's Disease Neuroimaging Initiative (ADNI) trial analysed abnormal biomarkers denoting multiple mechanisms associated with progressive cognitive decline (33). These imaging biomarkers were: (a) vascular dysregulation imaged using ASL, (b) amyloid deposition using Florbetapir PET, (c) glucose metabolism dysregulation using FDG PET, (d) functional impairment using functional MRI, (e) grey matter (GM) atrophy imaged with structural MRI, plus plasma and cerebro-spinal fluid (CSF) biomarkers. This study identified vascular dysregulation measured by

ASL as the earliest and strongest indicator of the factors associated with cognitive decline.

ASL as a means of measuring CBF fulfils the requirements set out in the “Molecular and Biochemical Markers of Alzheimer’s Disease” report: (a) able to detect a fundamental feature of Alzheimer’s neuropathology; (b) validated in neuro-pathologically confirmed AD cases; (c) precise (able to detect AD early in its course and distinguish it from other dementias); (d) reliable; non-invasive; (e) simple to perform and (f) inexpensive (34). The rate of blood flow and consequently the delivery of oxygen and nutrients is an indicator of cellular health and viability of tissue in terms of its functionality, rarefaction and ability to repair. Decreases in blood flow may indicate early pathological changes. Accurate assessment of brain perfusion therefore has potential to become a useful diagnostic and prognostic tool in the detection and classification of early stage neurodegenerative diseases. Quantifiable CBF measurement could indicate early signs of vascular damage, brain atrophy, prodromal dementia and functional deterioration.

1.3.2.2 Arterial spin labelling techniques

One of the earliest successful experiments to quantify cerebral perfusion was performed using the nitrous-oxide technique (35). This method involved inhalation of nitrous oxide (N_2O), a freely diffusible tracer, for 10 minutes while arterial and venous blood samples were extracted in order to measure the presence of N_2O in each sample. In accordance with the Fick principle, the difference in N_2O between arterial and venous samples can be accounted for by the consumption of the substance by the organ of interest (in this case the brain). Less invasive techniques such as computed tomography (CT) with xenon gas detection, single-photon emission computed tomography (SPECT) and PET with radionuclide tracers emerged to measure perfusion, but all required the injection of exogenous tracers and the use of radiation.

ASL is based on the principle that blood and tissue behave differently in an MRI scanner in terms of relaxation times. Radio-frequency (RF) labelling of arterial blood water upstream of the brain tissue creates a tracer. Images of the brain acquired without the tracer and images of the same tissue with the arterial blood water label present are subtracted. The subtracted image constitutes the perfusion signal as the label in the perfused brain creates a proportional change in tissue MR signal (36) (**Figure 1-5**). Although the perfusion image is a grey scale depiction of relative MRI signal intensities for visual inspection, CBF can be quantified from the MR signal by using pharmacokinetic models (36, 37). The ASL method has a number of advantages over other perfusion measurements. It has superior spatial resolution, it is quantifiable, it is minimally invasive as the labelled blood water acts as an endogenous contrast agent and, as MRI does not use ionising radiation, ASL provides improvements in safety, repeatability and patient acceptability over previous methods. However, disadvantages include low signal to noise ratio (SNR), arterial transit time artefacts (ATAs) caused by slow or collateral flow, and incomplete labelling of spins (6).

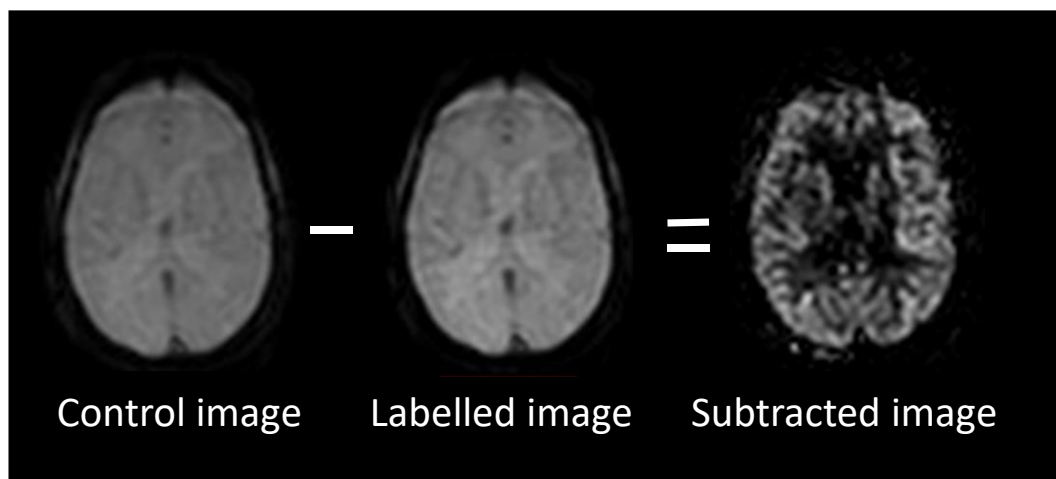


Figure 1-5. A perfusion image is created from the subtraction of the RF labelled image, acquired after 2s delay, from a control image. (Images are from SABRE v3 study).

1.3.2.3 Implementations of arterial spin labelling

Continuous ASL

A number of strategies have been developed for the acquisition of ASL. Continuous arterial spin labelling (CASL) was initially described in the rat brain using long continuous RF and gradient pulses to label the flowing arterial blood water (38, 39). Detre et al imaged the brain using a T1w spin echo sequence after application of an adiabatic saturation pulse in a slice in a selected area of the neck for the label images, and a saturation pulse outside the area of interest for the control images (40). The additional saturation pulse in the control images was intended to compensate for the effect of the saturation of macromolecules in the brain (magnetization transfer effects) caused by the prolonged labelling pulse. CASL was later refined through the use of a flow driven adiabatic inversion pulse for labelling, and image acquisition became faster with the use of echo-planar imaging (EPI) (41).

Disadvantages of the CASL method in humans included difficulties producing a continuous pulse with standard clinical MRI hardware, magnetization transfer effects (MT) producing inaccurate signal intensities that are not possible to correct in multi-slice acquisitions, inefficiency of blood water labelling producing low SNR, the large power deposition of a continuous pulse creating high specific absorption rates (SAR) in the subject, and over-sensitivity to arterial transit times (ATTs) (i.e. the duration of the transit of blood spins between labelling and arrival at the tissue of interest) (42).

Pulsed ASL

Pulsed ASL (PASL) was developed to address some of these problems, particularly MT effects and the susceptibility of CASL to inaccuracies introduced by transit time artefacts. The echo-planar imaging and signal targeting with alternating radio frequency (EPSTAR) method (41) used EPI for fast acquisition with a labelling design of short rapid inversion pulses on a thick selected slab adjacent to the perfused tissue to reduce transit time artefacts. Subsequently, flow-sensitive alternating inversion recovery (FAIR) (43) and quantitative

imaging of perfusion using a single subtraction, second version (QUIPSS II) (44) provided refinements by increasing the amount of successfully labelled blood and improving the accuracy of the labelling pulse respectively. Despite these improvements PASL suffers from poor SNR that is approximately half that of CASL and does not entirely eliminate MT and ATT sensitivity.

Pseudo-Continuous ASL

Pseudo-continuous ASL (PCASL) is currently the recommended sequence for clinical implementation of ASL (42). The labelling strategy is designed to emulate the CASL scheme of flow driven adiabatic inversion of blood water spins but uses repeated 1–2 second duration trains of pulsed RF and gradients (45). Commercial 3T MRI scanners with standard clinical specification are capable of running the PCASL sequence as it does not demand the continuous application of RF and gradients. It avoids the MT asymmetry effects of CASL enabling multi-slice acquisitions, produces acceptable levels of SAR, achieves a higher labelling efficiency than amplitude modulated CASL and has superior SNR to PASL (46). It is therefore possible to acquire relatively artefact free ASL coverage of the whole cerebrum with acceptable resolution within a reasonable acquisition time.

1.3.2.4 Partial volume correction

Partial volume correction (PVC) is used to adjust the intensity value of a voxel when the presence of more than one tissue type produces a mixed signal. The greater the tissue heterogeneity within the voxel the greater the error in CBF estimation is likely to be due to partial volume effects (47). Cortical atrophy commonly found in old age exacerbates partial volume effects when aiming to segment GM tissue due to the thinness of the cortical ribbon. ASL is particularly susceptible to partial volume effects as resolution is sacrificed to increase acquisition speed, and the single difference image is composed of two acquisitions, control and label, which increases the likelihood of movement artefact.

The ASL sequence used in this study has a voxel size of 3.75mm x 3.75mm x 5mm. An area of this size in the brain could contain GM, WM and CSF. In PVC methods using only binary masking generated from structural segmentation, a voxel is classified as belonging entirely to one tissue type -the type deemed to be dominant within the voxel. Asllani et al calculate that if a voxel in a thin cortical region classified as GM through simple masking or thresholding methods actually contains only 80% GM and 20% CSF, this would result in ~24% underestimation of CBF (48). The method used in this thesis is based on that developed by Asllani et al. with the aim of minimising such errors. The fractional volume of a tissue type within a voxel is computed from a regression kernel employing segmented posterior probability images from hi-resolution T1w scans. Weighting coefficients are then allocated according to tissue fraction estimation to calculate the sum of CBF in a voxel (48).

1.3.3 Brain volume

Although some individuals successfully age without discernible alterations in brain structure, it is more typical for GM and WM tissue loss to be present in the elderly with concomitant minor changes to cognitive functioning. Most atrophy in old age is attributable to neuronal loss with some tissue decrease due to absorption of necrotic tissue, loss of glial cells and myelin, and inflammatory changes (49).

High resolution volumetric magnetisation prepared gradient echo T1w such as MP-RAGE sequences (50) are most commonly used to assess brain volumes due to the excellent structural contrast between GM, WM and CSF (51) and good SNR facilitating automated segmentation.

Longitudinal studies provide direct evidence of brain atrophy in old age. Cross-sectional studies measure brain volume as a surrogate for tissue loss. A longitudinal MRI study with 4 year follow-up of 92 healthy elderly participants (age range 59 -85 years) found a mean (SD) decrease of 5.4 (\pm 0.3) cm³/year for total brain tissue, and 2.4 (\pm 0.4) cm³/year for GM volume (52). Other

longitudinal MR imaging studies have estimated the rate of whole brain atrophy to be 0.3-0.5 % per year between ages 70-80 (53) (52) (54) with another study suggesting the rate of volume loss accelerates after the age of 70 (55).

Accelerated rates of loss and areas of exaggerated regional tissue loss have been found in demented individuals compared to controls (53). Participants with AD have been found to have accelerated rates of global atrophy of mean (SD) 2.4% (± 1.4) compared to 0.4% (± 0.7) per year in healthy controls (56). In addition to generalised brain atrophy there is mixed evidence of regionally heterogeneous volume loss with many AD studies finding the greatest age-related loss in the hippocampi, entorhinal cortex and pre-frontal cortex (57) (58). Histopathological changes detectable using MRI provide evidence that the corollary of memory impairment is substantial damage to the hippocampi in terms of gliosis and destruction of nerve cells (59).

1.3.4 White matter hyperintensities

The wasting of WM in post-mortem brains was initially described by Binswanger in 1894. In 1898 Alois Alzheimer described similar findings in a condition where the cortex was relatively preserved but WM appeared 'narrow', 'grey' and 'studded with patches'; he wrote that in some cases 'the entire WM of a cerebral lobe appears to have completely wasted away' (60). The condition was found in association with fatty vascular degeneration and was accompanied by clinical symptoms of mental decline and specific physical weakening (61). WMHs have become a common *in vivo* finding on examination of the ageing brain using CT and MRI. Regions of increased signal intensity in WM are highly prevalent on T2w FLAIR MR images of participants from early old age. Only 5% of participants' brains in the Rotterdam Study (n = 1077, age range 60-90) were found to be entirely free from WMHs (62). There was an increasing prevalence of 0.2% for deep white matter hyperintensities (DWMHs) and 0.4% for periventricular (PV) hyperintensities per year of age. This study also found women to have more severe WM disease than men after adjusting for age.

WMHs are generally considered to be indicative of SVID. However, the mechanisms of WMH formation are not entirely understood and there is evidence that not all WMHs have identical aetiology. Inflammation, BBB breakdown, glial pathology and amyloid deposition as well as ischaemia have all been implicated as determinants of WMHs (63). It has been argued that WMHs are not the 'tombstone markers' of an ischaemic event but are evidence of a dynamic pathological process (64). WMHs in the PV region may be related to damage to the ependymal lining of the ventricles and CSF leakage. Additionally, inflammatory change and glial cell damage may cause myelin destruction and axonal atrophy (64).

Many studies have indicated WMHs are the result of hypoxia resulting from vascular dysfunction (65). The blood supply of WM by long singular medullary arterioles located in watershed areas is considered to leave WM at high risk of lacunar infarction in circumstances of severe ischaemia, and diffuse WM damage in the event of chronic hypoperfusion may be due to atherosclerosis or stenosis of the supplying vessel (66).

WMHs occurring in subcortical or deep WM areas can be sub-divided into confluent and punctate types (67). These types are associated with different causes, rates of progression and clinical consequences. In the Austrian Stroke Prevention Study the punctate type was identified as less harmful to cognitive function and less likely to progress. The subcortical confluent type was associated with vascular disease, was more progressive, and had greater impact on cognition (68). These important distinctions may explain why there has been a lack of conclusive support for clear associations between WMHs and cardiovascular risk factors. Furthermore, there is evidence that extensive WM damage extends into the penumbra surrounding the WMHs visible on FLAIR, encroaching into otherwise normal appearing WM as demonstrated on diffusion tensor imaging (DTI) images (69).

1.3.4.1 MRI visualisation of white matter hyperintensities

3D inversion recovery TSE with SPIR, (FLAIR) is the MRI sequence most commonly used to detect WMHs due to its sensitivity to differences in the molecular structure of myelin and fluid. Areas of CSF appear as hypo-intense signal due to the echo time coinciding with the recovery of the 'free' water signal eliciting a null signal thus facilitating the identification of hyperintense areas adjacent to ventricles, whereas the low frequency tumbling of water bound to larger molecules of damaged myelin elicits rapid T2 decay and a hyper-intense appearance (**Figure 1-6**).

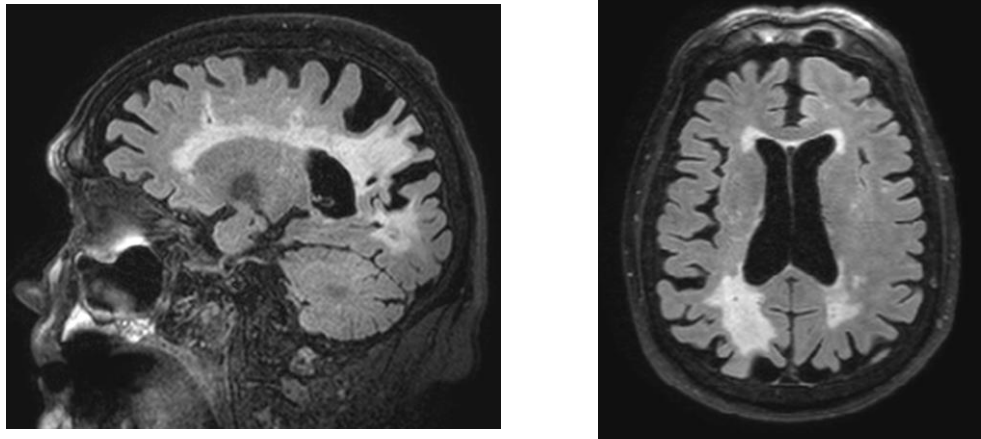


Figure 1-6. FLAIR images illustrating severe WMHs (Images are from SABRE v3 study).

However, the interpretation of WMHs on the MR image is not straightforward. The MR signal is a representation of anatomy which may contain a number of constituents within a single voxel. In addition to tissue cells, which may be of different types, there are interstitial spaces and microvasculature. It can therefore be challenging to compare pathologies depicted on an MR image with post-mortem histological findings. MR appearances are non-specific. For example, hyper-intense signal on FLAIR images may be due to increased water content from ventricular leakage or tissue damage such as severe demyelination. Comparisons between MR studies of WMHs are complicated by the variation in sensitivity of MRI sequences to WMH visualization and by

qualitative and quantitative processing heterogeneity. Historically there have been a range of manual, semi-automated and automated methodologies utilised for the quantification of hyperintensities and statistical modelling can be complex due to the large variance and skewness of WMH data within samples.

1.4 Cognitive decline and dementia

The high prevalence of severe cognitive impairment and dementia is in large part a result of expanding populations and increases in longevity. In addition to major social and human costs, dementia has the potential to create a massive economic burden due to the impact on communities and rising healthcare demands. Worldwide prevalence of dementia in 2015 was estimated to be 47 million. This figure is likely to increase to 131.5 million by 2050, with 2 million estimated dementia cases in the UK by 2051 (70).

Minor cognitive changes experienced by many older individuals are typical of normal ageing in late life and are often noticed as alterations in perceived memory function or cognitive slowing (71). More serious conditions range from MCI, defined by the DSM-5 as 'modest impairment' in one or more cognitive domains, to severe dementias that impair the individual's ability to live independently. AD is the most common subtype of dementia (62%) (70). AD constitutes a substantial progressive decline from a previous level of performance in at least two cognitive domains, one of which is memory impairment (72)^a. Other major neurocognitive disorders of old age display various patterns of cognitive deficit and include vascular dementia (VaD) (17%), mixed dementia (10%), and less commonly fronto-temporal dementia, dementia with Lewy bodies and Parkinson's disease (70). There is increasing evidence that the causes of AD have a significant vascular component and that cerebrovascular disease and AD frequently co-exist (73).

^a Although the DSM 5 has updated the use of the term 'dementia' to 'mild' and 'major neuro-cognitive disorder', this thesis will continue to use the term 'dementia' as it remains in common use in the UK.

A study investigating the incidence of dementia diagnosis in the UK by ethnic group discovered that Asian women were 18%, and Asian men were 12% less likely than their white counterparts to receive a dementia diagnosis, whereas black women were 25% and black men were 28% more likely to receive such a diagnosis (74). The authors considered the reported incidence of dementia in the minority ethnic population to be underestimated due to lower rates of diagnosis as a result of cultural attitudes to mental health and barriers accessing the health service.

1.4.1 Causes of cognitive decline and dementia

The causes of dementia are complex and, although there have been major advances in understanding the cellular pathway of AD, effective pharmacological treatment has not significantly progressed. Recent efforts have focused on prevention as there is increasing evidence that vascular disease contributes to the causal pathway of dementia and cognitive decline. The Lancet International Commission on Dementia and Care (2017) listed interventions for reducing dementia risk derived from evidence-based guidelines in the U.S and U.K (75). The life course model identified hypertension and obesity commencing in mid-life as modifiable risk factors for dementia. This model supposes dementia to be a disease with a long latent period involving extensive silent progression prior to late-stage symptomatic and terminal cognitive expression. Accordingly, successful reduction of risk requires early intervention or treatment. Targets for modifiable risk include control of BP and blood lipids, prevention and control of diabetes, protection of cardiac function, and improvements in lean muscle and body fat composition. Lifestyle changes including smoking cessation, preservation of social engagement, education and mental activity to protect and promote cognitive reserve, management of hearing loss and depression, and maintenance of exercise have been suggested as further preventative interventions.

1.4.1.1 The ‘cascade’ hypothesis

Over 25 years ago the ‘cascade’ hypothesis of AD proposed abnormal processing of amyloid precursor protein (APP) as the initiator of disease. Overproduction and reduced clearance of $A\beta$ leads to amyloid plaques and subsequently to neurofibrillary tangles of hyperphosphorylated tau in the cortex of the brain. Loss of synapses, neuronal cell dysfunction and cell death are consequent on these processes and are ultimately responsible for the late clinical symptoms of AD (76).

1.4.1.2 The ‘two-hit’ hypothesis

The ‘two-hit’ vascular hypothesis was a development of the ‘cascade’ theory and proposed that vascular risk factors (VRFs) such as hypertension, atherosclerosis, cardiac disease, diabetes, and hyper-homocysteinemia were antecedents of AD (7, 8). ‘Hit 1’ proceeds from a combination of genetic and vascular factors. Systemic vascular disease leads to the development of neurovascular disease as a consequence of BBB breakdown, capillary endothelial dysfunction and cerebral hypoperfusion leading to chronic hypoxia. Increased toxicity in the brain, failure to clear $A\beta$ and increased expression of APP promote ‘Hit 2’ (**Figure 1-7**). The increased burden of $A\beta$ and hyperphosphorylated neurofibrillary tau tangles accelerate the symptomatic phase of dementia involving neuronal death and cognitive decline as identified in the ‘cascade’ hypothesis. The increased deposition and reduced clearance of beta amyloid typical of AD and cerebrovascular disease may work synergistically to accelerate neurovascular damage and exacerbate dementia symptoms (77).

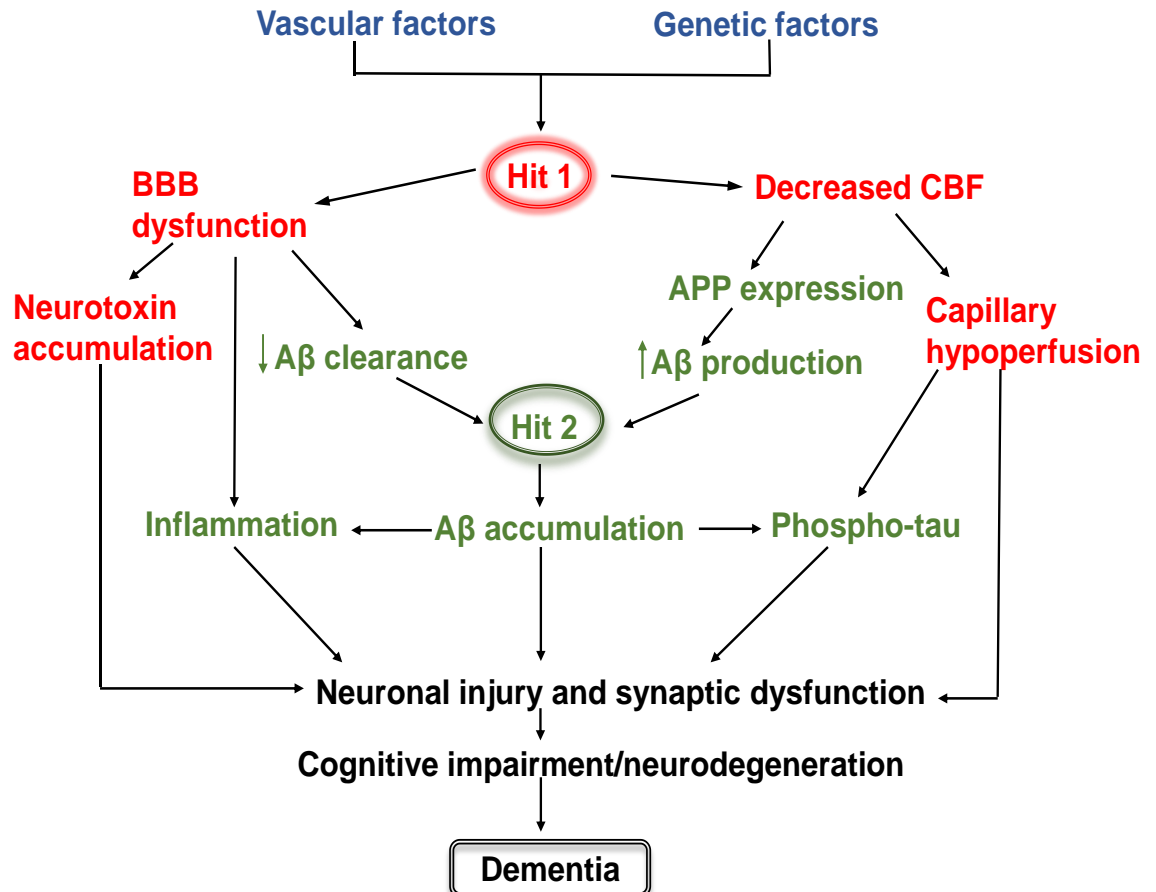


Figure 1-7. The ‘2 Hit’ vascular model for Alzheimer’s disease (adapted from (7, 8)). ‘Hit 1’ (vascular pathway) is shown in red, ‘Hit 2’ (amyloid β pathway) is shown in green, outcomes are in black.

1.4.2 Cognitive decline and cerebral blood flow

Studies of participants with cognitive decline ranging from mild memory complaints to those with diagnoses of MCI and AD have consistently found associations between lower CBF and increasing severity of cognitive impairment (78-84) and accelerated rates of cognitive decline (85). These results are congruent with both the vascular ‘two hit’ hypothesis which suggests chronic oligoemia is an antecedent of symptomatic dementia (7), and with evidence from the ADNI study that found vascular dysregulation to be one of the earliest biomarkers of AD (33).

1.5 Vascular risk factors

Cardiovascular disease is the leading cause of morbidity and mortality in developed countries. Statistics from 2016 provided by the British Heart Foundation attributed 26.7% of male deaths in the UK to cardiovascular disease, including 14% from coronary heart disease, 5% stroke; 24.4% of female deaths were attributed to cardiovascular disease, including 9% from coronary heart disease and 7% from stroke <https://www.bhf.org.uk/what-we-do/our-research/heart-statistics/heart-statistics-publications/cardiovascular-disease-statistics-2018>. VRFs increase the likelihood of developing vascular disease and are associated with increasing disease severity. Some key modifiable VRFs relevant to this study are described in the following part of this chapter, and previous studies investigating their relationship with CBF and the ageing brain are discussed.

1.5.1 Hypertension

Hypertension is defined by the National Institute for Health and Care Excellence (NICE) as a clinic systolic BP >140mmHg or a diastolic BP > 90mmHg (86). Prevalence is estimated at 24% of the UK population (87) and increases with age (

Table 1-1).

Vasoconstriction and longer term vascular remodelling are considered to be adaptive responses to chronic high BP which protect the vulnerable downstream cerebral microvasculature (19). However, as illustrated in **Figure 1-3**, chronic hypertension shifts the cerebral autoregulation curve resulting in increased risk of hypoperfusion with potential consequences of neuronal compromise, cognitive impairment and dementia. Reduction in the Windkessel effect due to loss of vascular wall elasticity in old age increases systolic BP and pulse pressure (PP), and may result in increased pulsatile energy transmission into the cerebral microcirculation with concomitant tissue damage and cognitive repercussions (88). The impact on the delicate microvasculature may also include BBB breakdown, microhaemorrhages and capillary damage (73)

1.5.2 Diabetes

Diabetes is a metabolic disease with the potential to cause severe end organ damage through macrovascular and microvascular complications. Type 2 diabetes mellitus (T2DM) accounts for 90 -95% of diabetes prevalence and is due to insulin resistance (IR) and the inability to secrete enough compensatory insulin. A diagnosis of T2DM in adults is confirmed with a serum Haemoglobin A1c (HbA1c) $\geq 48\text{mmol/mol}$ (concentration $\geq 6.5\%$)

<https://cks.nice.org.uk/diabetes-type-2#!diagnosisSub> (86). The prevalence of diagnosed diabetes in the UK is 3.8 million, with an estimated additional 1 million who have diabetes but have not been diagnosed

<https://www.diabetes.org.uk/professionals/position-statements-reports/statistics/diabetes-prevalence-2018> (89).

Prevalence increases with age and varies by ethnicity and sex (

Table 1-1). The Health Survey for England (2004) estimated that diagnosed diabetes was 2.5 -5 times greater in South Asians than the white population in the UK <https://digital.nhs.uk/data-and-information/publications/statistical/health-survey-for-england/health-survey-for-england-2004-health-of-ethnic-minorities-headline-results> (90) while the prevalence of African Caribbeans in the UK is three times higher than Europeans (91).

Mechanisms linking T2DM to deleterious effects on the brain are considered to result largely from the effects of endothelial dysfunction. Prolonged hyperglycemia results in the formation of advanced glycation end products (AGES) leading to increased production of reactive oxygen species (ROS), oxidative stress and a state of chronic inflammation that damages cell functionality and causes cell death. Effects include reduction of endothelial capacity to effect vasodilation (92).

1.5.3 Serum cholesterol and lipoproteins

Cholesterol is a molecule essential in the manufacture of cell membranes, hormones and production of some vitamins. Serum cholesterol is carried in

plasma by lipoproteins (very low density lipoprotein, low density lipoprotein (LDL) and high density lipoprotein (HDL)). Lipoproteins also contain other lipids, such as triglycerides and phospholipids. Total cholesterol is measured from lipoproteins and chylomicrons from (fasting) blood samples. LDL is stated in concentration of mmol/L and is usually calculated using the Friedewald formula:

$$\text{LDL} = (\text{Total Cholesterol}) - (\text{triglycerides} / 2.19) - (\text{HDL})$$

<https://www.heartuk.org.uk/downloads/health-professionals/factsheets/calulating-cholesterol.pdf>

NICE no longer provide cut-off thresholds for categorisation of dyslipidaemia

<https://www.nice.org.uk/guidance/cg181/chapter/1-Recommendations>.

Optimum levels suggested by the American Heart Association (AHA) are a total cholesterol concentration of 3.8mmol/L and LDL of 2.6mmol/L (93).

High blood levels of LDL cholesterol are associated with atherosclerosis in large to medium size arteries causing degenerative vascular disease such as blocked or stenosed arteries and thromboses. High levels of HDL cholesterol are generally considered to be protective, although the evidence is less certain that this association is causal (94). Increased glycation of LDL to which individuals with diabetes are more liable appears to increase atherosclerotic complications (95).

Cholesterol concentration increases with age until around 55 years then declines in old age (

Table 1-1). This late life decrease may be the result of survival bias or a decline in ability to synthesise LDL (96). Metabolic factors such as obesity and T2DM as well as lifestyle factors influence cholesterol levels. Exercise increases HDL and reduces triglycerides, while a diet high in saturated and trans fats may increase LDL. The association of dyslipidaemia with stroke and heart disease has led to widespread use of lipid modifying drugs such as statins

for the prevention of cardiovascular events. Current NICE recommendations are to offer lipid-modification therapy to all people older than 85 years, people under 85 years who have a QRISK2 score of >10%, and to all people with T2DM <https://cks.nice.org.uk/lipid-modification-cvd-prevention>.

A study investigating HDL cholesterol and brain volumes found that HDL was positively associated with GM volume and better cognitive outcomes (97).

1.5.4 Smoking

Over 40 years ago smoking was recognised as a cause of excess death rates from heart and vascular disease (98, 99). Effects of the toxic chemicals from smoking affecting the vasculature include reduction of nitric oxide (NO) bioavailability, increased expression of adhesion molecules and promotion of chronic inflammation. These mechanisms result in damage to the endothelium, increased atherosclerosis and a pro-coagulatory environment (100).

Recognition of cessation of smoking as an effective modifiable risk factor has led to successful public health intervention efforts. Smoking prevalence has decreased since the 1940's (https://www.cancerresearchuk.org/health-professional/cancer-statistics/risk/tobacco?_ga=2.220561041.827573618.1554296280-1619266932.1542106998#heading-Three). 2013 data from Cancer Research UK cite a prevalence of smoking in the UK of 19.5% for men and 10.3% for women at age 50-64, falling to 10.3% and 9.4% respectively at age > 65.

https://www.cancerresearchuk.org/health-professional/cancer-statistics/risk/tobacco?_ga=2.220561041.827573618.1554296280-1619266932.1542106998#heading-Two

	Age range (years)		
	55-64	65-74	75+
Hypertension, (%)^a			
<i>Men</i>	51	65	79
<i>Women</i>	47	63	79
Diabetes, (%)^b			
<i>Men</i>	11.1	15.2	15.9
<i>Women</i>	8.0	12.2	13.2
High total cholesterol, (%)^c			
<i>Men</i>	70	53	39
<i>Women</i>	83	75	66

Table 1-1. Prevalence of vascular risk factors, by sex and age (England).

^a systolic BP >140mmHg or diastolic >90mmHg or medicated for high BP, ^b self-report of diabetes diagnosed by doctor, ^c total cholesterol >5mmol/L. (Data drawn from Coronary Heart Disease Statistics, British Heart Foundation, (101).

1.5.5 Multifactorial vascular risk

Composite vascular risk scores aim to predict the cumulative effect of multiple VRFs on cardiovascular events. Clustered VRFs may behave synergistically to have a greater impact than individual or purely additive effects of single VRFs. Various methods to calculate composite scores have been validated in community-based populations including the Framingham risk score (FRS), QRISK2, QRISK3, ASSIGN, and by metabolic syndrome (MetS) categorisation. MetS is commonly used as a dichotomous variable, whereby individuals are characterised as having MetS if they reach cut-off points in 3 of 5 inter-related vascular risk factors, namely: abdominal obesity, hypertension, hyperglycaemia, hypertriglyceridemia and high LDL cholesterol levels (102). Simple bespoke additive point systems have also been utilised in previous studies (103-105).

1.6 Previous studies: evidence of associations of vascular risk with cognitive decline and the MR markers of brain ageing.

1.6.1 Vascular risk and dementia

There is a substantial body of evidence to support the theory of a causal relationship between vascular disease and risk of dementia. A systematic review of studies (106) investigating VRFs and cognitive function in old age concluded that, although not all studies were in agreement, T2DM and hypertension were most consistently associated with worse cognitive results. Mixed evidence supported associations of cognition with obesity and dyslipidaemia. The authors suggested that the lack of strong consensus may be due to the small to moderate effect size of VRFs on cognition, and they criticised some studies for using insufficient sample sizes. Furthermore, many studies omitted interactions between risk factors and/or age that other studies found to be highly influential.

Another review of VRFs (107) and dementia found that T2DM was consistently associated with dementia risk measured in either mid-life or old age, whereas hypertension, dyslipidaemia and obesity were only strongly associated with dementia in longitudinal studies that took baseline measurements in mid-life. One explanation may be the greater prevalence of T2DM in old age, or the effects of late developing hyperglycaemic brain damage could have a severe and rapid additive effect on existing chronic vascular disease.

Other results have suggested that VRFs normally considered detrimental to health are associated with better cognitive outcomes in older individuals. For example, high BP, high BMI and adverse cholesterol levels have been associated with a lower risk of dementia, particularly in studies with short follow up times in older-aged people (108, 109). These associations may be non-linear, and there is speculation that cerebral hyperperfusion may be a temporary compensatory response to inflammation and neuronal damage which

is most often observed in younger participants prior to onset of symptomatic dementia (83, 110). Findings could also be confounded by the association of factors such as low BMI and hypotension with the later stages of dementia and poor mental health. Studies in old age are susceptible to survivor bias. In this instance individuals with worse cardiovascular risk profiles from mid-life have higher mortality rates and are less likely to reach old age when dementia is more prevalent.

1.6.2 Vascular risk and the MR markers of brain ageing

Large population cohort studies such as the Second Manifestations of Arterial Disease - Magnetic Resonance Study (SMART) (111-113) the PROspective Study of Pravastatin in the Elderly at Risk (PROSPER) trial (114, 115) and the Rotterdam Scan Study (116, 117) have investigated correlations of VRFs and CBF with age-related changes of the brain identified on MRI scans. There is a broad consensus that decreased CBF is associated with vascular disease and that both of these factors are associated with reduced brain volume and increased volume of WMHs in old age. However, some results differ possibly due to differences in sample size, type of cohort, (e.g. community-based cohorts, clinical populations) and as a consequence of differing methodologies.

1.6.3 Hypertension, cerebral blood flow and the MR markers of brain ageing

Hypertension has been associated with decreased CBF and cerebrovascular disease in numerous studies. However, there is evidence this relationship is moderated by age, duration of hypertension, age of onset, use of BP lowering medication, time variant patterns of hypertension/hypotension and genetic factors (103, 118, 119). There are also suggestions that the association is not linear as low BP may result in cerebral hypoperfusion in older persons.

An early study using the ¹³³Xenon inhalation technique in 101 patients (120) discovered that cerebral perfusion was lower in untreated hypertensive patients compared to healthy controls, and those who were successfully treated for

hypertension had higher levels of global perfusion than participants with untreated hypertension. A study using ^{15}O -PET to measure CBF, found longer duration of hypertension was associated with lower CBF (121). Results from a large sample from the SMART study broadly agreed with these findings (119). Longitudinal analysis of this cohort over 4 years showed that CBF declined in untreated and poorly controlled hypertensive participants as well as in those with high BP in comparison to successfully treated hypertensive participants. Mechanisms may include compromised cerebral vasoreactivity due to endothelial dysfunction, atherosclerosis of larger feeding vessels and build-up of beta-amyloid plaques.

Evidence for the relationship of BP and CBF has been supported by some studies investigating the utility of intensive BP lowering. One study in elderly participants found that GM CBF increased in an intensive intervention group (target $<130/80\text{mmHg}$) compared to participants on a conventional BP lowering regime (target $<140/85\text{mmHg}$) over a 12-week period (122). Using cognitive outcomes, the Systolic Blood Pressure Intervention Trial (SPRINT MIND) tested the efficacy of treating individuals to a low BP target of $<120\text{mmHg}$ in comparison to a control target of $<140\text{mmHg}$. They found beneficial effects in reduction of MCI but not dementia in the intensive BP lowering group (123). However, there has been speculation that the trial was underpowered to detect dementia as fewer cases developed than were projected in the study design (124).

Although these studies suggest good control of hypertension contributes to higher levels of cerebral perfusion, not all studies have found the relationship to be straightforward. One study found that although hypertension was associated with decreased CBF in a sample of 58 elderly adults with vascular disease, use of anti-hypertensive medication did not attenuate this relationship (118). The DANTE trial investigating 203 elderly participants on anti-hypertensive medication and with symptomatic MCI, detected no associations between CBF and systolic BP, diastolic BP, MAP, nor PP over 4 months of continued or discontinued BP lowering treatment (125). This result appears to contradict

previous studies. However, the authors suggested their sample of participants had only moderate hypertension and therefore cerebral autoregulation was maintained within a range to cope with moderate changes in perfusion pressure. The well-defined nature of this cohort (≥ 75 years, moderately high BP, using anti-hypertensive medication, a narrow range of MMSE scores and recruitment from a small geographic area) means that results are difficult to generalise to the wider population.

A study using SPECT to measure CBF found high BP was strongly associated with lower regional CBF in men, accounting for up to 28% of variance depending on brain region, but the association was not evident in women after adjustment for age, brain atrophy, and vascular risk (126). Although the authors acknowledge their study may have been underpowered to detect associations in women (32% of 74 participants), most of the associations of CBF and high BP were positive in women and negative in men. The authors hypothesised that later expression of cardiovascular disease in women was responsible for this result.

The CRESCENDO/3C study did not find cross sectional associations of CBF with systolic BP, although there was a weak association of change in systolic BP, diastolic BP or MAP over 12 years with decreased CBF (127). The authors speculated this was due to cerebral autoregulation adjusting flow to accommodate BP. However, the 3C Dijon study was small ($n=104$) and may have not been powered to detect small effect sizes, the majority of the sample were women (67.3%), and the cohort was homogeneously high income and highly educated, with unspecified ethnicity.

In a systematic review of studies investigating VRFs and brain changes in non-symptomatic participants, a diagnosis of hypertension was consistently associated with decreased global brain volume (128). However, the relationship appeared to be U-shaped as both high and low diastolic BP was associated with reduced cortical volume. The authors also found variability in

response to anti-hypertensive medication. A similar systematic review and meta-analysis of BP and brain atrophy concluded that high BP was associated with, and was predictive of brain volume reduction in 92.9% of studies (129). Discrepancies were attributed to methodological differences used to measure brain volume, differing definitions of hypertension, effect modification by age group, and use of anti-hypertensive medications. Both systematic studies point out that cross-sectional studies may be liable to confounding as increased BP and reduced brain volume are both more prevalent with ageing.

Confounding by age is also problematical when considering associations of WMHs and BP which both increase with age. Several studies on large populations have found only weak or complex associations of hypertension with WMHs, even though WMHs have been purported to have a vascular aetiology. For example, the ARIC study (130) found single BP measurements were not associated with WMHs although cumulative longitudinal measurements of BP were predictive of WMH progression. An early finding from the Rotterdam study indicated associations of WMHs with BP and cholesterol only in participants aged 65-74 after analysis was stratified by age, whereas this association was not apparent in an older group (131). In the Lothian Birth Cohort (132) the effect size of BP in association with WMHs appeared to be small (explaining 2% of total WMH variance) which may explain the apparent lack of effect of anti-hypertensive medication on WMHs volume. In this study the strongest predictor of WMH progression was the volume of WMHs measured at baseline.

1.6.4 Diabetes, cerebral blood flow and the MR markers of brain ageing

There is mixed evidence regarding the effect of T2DM on macrovascular and microvascular blood flow in the brain. Several studies have suggested that macrovascular flow is preserved but tissue perfusion is reduced in participants with T2DM. In a study that measured only total blood flow to the brain using PC-MR, no reduction was found in participants with diabetes (133). In concurrence with this finding Jansen et al (134) found no association of T2DM

with lower flow in the ICAs, but participants with diabetes had decreased cerebral tissue perfusion measured by ASL. However, the association was small; it was only discernible using a method of analysis that calculated the number of voxels deviating from a normal level, and results were not statistically significant using regions of interest (ROIs) nor voxel based statistical parametric mapping (VBM) techniques. Furthermore, after correction for atrophy, the effect only remained significant in subcortical GM, not cortical GM. The authors attributed lower flow in subcortical GM to the absence of collateralisation and lower vessel density in these deep brain areas where there is little compensatory flow for microvascular damage.

The theory that macrovascular and microvascular flow are uncoupled in T2DM is supported by a study in middle-aged adults (135). This study found that, although high IR was associated with both lower arterial blood flow in the ICAs and lower regional cerebral perfusion, there was an interaction between IR and arterial blood flow. High flow in the ICAs only translated to higher regional tissue perfusion in the right superior frontal gyrus in individuals who had lower levels of IR. This finding supports the theory that microvascular damage associated with IR is independent of macrovascular damage.

Other studies (136) reporting hypoperfusion in T2DM using ROI methods in older participants, may indicate effects of T2DM are chronic and the effect of IR on CBF is moderated by age. In support of this theory, cognitive decline as a result of microstructural damage in the presence of diabetes appears to be evident only in ages > 65 years (137, 138).

The effect of medication on CBF is raised by an interesting finding from a study comparing middle-aged groups with a diagnosis of T2DM, an untreated 'prediabetic' group, and control participants (139). Lower CBF was only associated with the prediabetes group. The authors suggested the result may have been confounded by medication. The medicated 'diagnosed diabetes' group may have benefited from, not only blood glucose control medication, but

also lipid lowering and anti-hypertensive medication that contributed to preservation of CBF.

Despite the difficulties encountered in comparing studies due to differences in samples, study design and statistical methodologies, there was a broad consensus between two reviews of T2DM and brain imaging (140) (141) that, in larger population-based studies, decreased brain volume was consistently associated with T2DM, (142) (130) (143, 144) (145) (146) whereas the evidence for the association of T2DM and WMHs was inconsistent. Despite early smaller sample studies suggesting T2DM was associated with SVID represented by the presence of WMHs (147) (143), some large community based studies such as ARIC (130), the Framingham Study (148), CARDIA (145) and ACCORD-MIND (146) have not found convincing evidence of a relationship. In contrast, the SMART study in participants with pre-existing cardiovascular disease, found participants with T2DM had decreased GM volume and larger WMH volume, and these markers progressed at a slightly higher rate than in those without T2DM (149) (144). The authors speculated that this relationship could be due to the effects of T2DM in combination with atherosclerotic disease as their sample were all individuals with high cardiovascular risk.

1.6.5 Lipoproteins, cerebral blood flow and the MR markers of brain ageing

There is mixed evidence to associate cholesterol levels with dementia. A large longitudinal study in elderly adults observed that higher total cholesterol was associated with decreased risk of dementia (109). Another study on a large sample of community based older adults found decreased HDL, and increased LDL and non-HDL cholesterol were associated with vascular dementia but not AD (150). Although, few studies have found strong relationships between CBF and dyslipidaemia one study indicated there was a statistically significant relationship between higher serum cholesterol and lower CBF in patients with transient ischaemic attacks (TIAs) (151). The close association of cholesterol levels with other features of cardiovascular risk make it difficult to extract the

importance or clarify the role of mechanisms linking lipoprotein fractions to cerebral microvascular damage (152).

Protective properties of HDL have been indicated in some studies that found associations of low HDL with reduced regional brain volumes (97) (153). LDL cholesterol has been associated with DWMHs (154) and total cholesterol has been linked with WMHs in older participants 65-74 years (131).

1.6.6 Smoking, cerebral blood flow and the MR markers of brain ageing

There is a general consensus that long term smoking decreases CBF due to impairment of vasodilatation due to increased oxidative stress and inhibited eNOS processes in the endothelium (155) (156, 157). However, the short-term effect of smoking may boost CBF. The CARDIA study in middle aged adults found, compared to never smokers, current smokers had higher regional CBF and former smokers had a trend towards lower regional CBF (158). The authors suggested this pattern of association was due to an acute response to nicotine cravings or recent tobacco exposure in current smokers. Furthermore, they speculated this effect would disappear with increasing age in agreement with other studies on older smokers (159) as they would be unable to sustain compensatory flow mechanisms.

A meta-analysis of studies comparing smokers with non-smokers concluded that regional GM volume was reduced in chronic smokers (160). The Framingham study (148) identified smoking as a risk factor strongly associated with the prevalence and severity of WMHs. The ARIC study agreed with this finding and found this association was stronger in African Americans than Caucasians (161).

1.6.7 Multifactorial vascular risk, cerebral blood flow and the MR markers of brain ageing

The Kaiser Permanente Study (105) found increased risk of dementia in late life was linearly associated with VRFs in midlife. A higher score in an additive composite rating of VRFs increased dementia risk in a 'dose-dependent' relationship. In a longitudinal study in an elderly population, an additive vascular risk score was more strongly associated with AD than single VRFs (104). Certain combinations of risk factors were also found to be particularly strongly associated, with diabetes and smoking the strongest combination. Similarly, the CAIDE study suggested clustered VRFs increased dementia risk (162).

In a sample of middle-aged adults, those with metabolic syndrome (MetS) had lower CBF than controls, with obesity and high triglycerides the most important factors within this combined metric (163). MetS has also been associated with accelerated cognitive decline in 3 related studies in which the authors considered presence of high serum levels of inflammatory markers to be additionally damaging (164). The concept of MetS has been criticised for its lack of sensitivity to ethnic differences such as variation of IR in response to adiposity (165). Also, it is a simple binary categorisation that does not capture linear dose-response effects of vascular risk on outcomes and omits factors such as smoking and socio-economic considerations.

An examination of relationships between vascular risk burden (cumulatively measured as 1 point per risk factor), age, CBF and cognition in older individuals found high vascular risk burden interacted with age to give reduced cortical CBF (103). Elevated vascular risk and lower CBF were also associated with lower cognitive scores leading the authors to conclude 'older adults with an elevated vascular risk burden may be particularly vulnerable to cognitive change as a function of CBF reductions. However, the simple method of scoring 1 point per risk factor does not weight risk factors according to their potential impact on cardiovascular outcomes and may therefore miscalculate the summative risk.

Weighted multifactorial algorithms such as the FRS, QRISK2 and ASSIGN are more robust measures of vascular risk as they are based on outcomes from large cohorts and have been validated in multiple studies.

A small study (n = 33) found FRS was correlated with PV WMHs but not DWMHs, and FRS was negatively correlated with vasoreactivity but not with CBF (166). The authors speculated that WMHs may either be a consequence of adverse VRFs, or that WMHs may impair vasoreactivity through an effect on receptors in the PV zone that are involved in vasoregulation. A larger study of middle-aged adults using composite vascular risk measurements and CBF measured by ASL, found 'a modest but consistent relationship between CBF and cardio-metabolic risk' in midlife (167).

1.6.8 Associations of cerebral blood flow with brain atrophy and white matter hyperintensities

Many studies have indicated that lower CBF is associated with increased brain atrophy and increased volume of WMHs (80, 168, 169). However, not all evidence is in agreement. For example, the PROSPER trial found an apparent strong association between CBF and brain tissue volume that disappeared on adjustment for head size (114), and in the SMART study, lower CBF was related to subcortical atrophy only if participants had moderate to severe WMHs (170). The Rotterdam Study found lower perfusion and increased total WMH volume were correlated in a mainly Caucasian population sample (116), whereas the PROSPER trial in a cardiovascular high-risk population, showed decline in CBF was associated with increased volume of PV but not DWMHs (115). A meta-analysis concluded that WMHs were associated with decreased CBF in most studies, although the strongest associations were in cohorts including individuals with severe cognitive impairment, and studies should be wary of confounding by age (171). Comparison of study results is complex due to differences in CBF acquisition and calculation methods, and samples vary widely by size, ethnic background, age, health and cognitive status.

1.7 Limitations of previous studies

Most of the large cohort studies have used 2D PC-MR methods rather than ASL to estimate cerebral perfusion. The PC-MR technique measures blood flow through the ICAs and basilar artery (mL/min) rather than capillary flow in perfused tissue as in ASL (mL/100g/min). The PC-MR method is restricted to measuring total blood flow to the brain. Results need to be adjusted for head size and this method is unable to provide spatial information so perfusion of GM and WM cannot be distinguished. Although comparison of results using different imaging methods is problematical, PC-MR is an established and validated technique in terms of accuracy and reproducibility (172) and a meta-analysis of these studies considered the strengths of associations between CBF and brain markers within each study to be valid (171).

The large SMART study and PROSPER trial were restricted to participants with pre-existing vascular disease or individuals considered to be at increased vascular risk. Many other studies have drawn participants from memory clinics where all participants have a cognitive complaint ranging from self-reported memory loss to dementia. Extrapolation of these findings to the general population should therefore be treated with caution. Participants in the Rotterdam study are predominantly of white European origin limiting confidence in the generalisability of findings to other ethnic groups.

Most results have been reported from cross-sectional studies which do not allow causal inferences between CBF and brain atrophy or presence of WMHs. Both directions of causality have been hypothesised. Decreased CBF could cause shrinkage in brain tissue. Alternatively, lower metabolic demand from a smaller volume of neurons and fewer synapses requires a lower blood flow rate to maintain brain function. Evidence for the direction of causality has been provided by the Rotterdam Study (117) which conducted analysis of longitudinal data. 3011 individuals, age range 45 to 96 years, underwent 2 MRI examinations with a mean interval between scans of almost 4 years. A smaller brain volume at the first time point was associated with a steeper decrease in

CBF. However, in participants older than 65 years, lower CBF at the first scan was associated with a steeper decline in brain volume. The authors suggested that atrophy precedes CBF decline in middle age, but in older individuals the relationship may be bi-directional. They hypothesised that older individuals have decreased capacity to autoregulate cerebral blood supply when metabolic demand rises and are therefore more susceptible than younger individuals to cerebral hypoperfusion leading to neuronal cell death (117). However, Benedictus et al, hypothesized that decreased CBF associated with both lower total brain volume and higher volume of WMHs in AD participants was determined by decreased neuronal demand and/or small vessel disease (169).

1.8 Conclusion

This chapter has provided a summary of the physiological aspects of cerebral perfusion and the MRI markers of brain ageing along with an overview of the methods used to evaluate MR findings. The scale and importance of the problem of cognitive decline and its likely association with vascular risk in ageing populations has been presented. A review of the literature has discussed a wealth of studies investigating the associations of vascular risk and cognitive and brain imaging outcomes. However, the role of cerebral perfusion in these relationships is still unclear. Most studies have assumed effect homogeneity by pooling results of complete cohorts into a single analysis which omits consideration of ethnic and gender differences.

This thesis aims to investigate the association of brain perfusion with a range of VRFs by employing PCASL to quantify CBF in a large, ethnically diverse sample. It will explore whether these relationships are subject to effect modification by ethnicity and sex. Furthermore, it aims to contribute some understanding of the role of CBF as a mediator between vascular risk and the markers of brain ageing visualized on MRI.

2 . Research questions

2.1 Aims

This thesis aims to:

- a) examine the importance of including measured Hct compared to a population mean value of Hct when ASL is used to calculate CBF in a multi-ethnic elderly population,
- b) investigate whether the FRS, a measure of aggregated vascular risk, is associated with CBF in old age,
- c) investigate which single factors of the combined vascular risk algorithm FRS are most strongly associated with CBF in old age,
- d) investigate whether combined vascular risk is associated with cortical tissue brain volume and the volume and distribution of WMHs in old age,
- e) examine whether CBF mediates associations of combined vascular risk with cortical brain volume and WMH volumes,
- f) investigate the roles of sex and ethnicity as effect modifiers in the relationships of vascular risk, CBF, cortical volume and WMH volumes.

2.2 Hypotheses

This thesis aims to test the following hypotheses:

Chapter 4

1.

- a) The inclusion of individualised measurements of Hct in the calculation of CBF from ASL improves accuracy when investigating group associations of cerebral perfusion.

Chapter 5

1.

- a) Individual components of the FRS are associated with CBF in elderly populations.
- b) Sex and ethnicity are in some instances effect modifiers of this relationship.

2.

- a) Elevated combined vascular risk represented by the FRS is associated with decreased cortical CBF in elderly populations.
- b) Sex and ethnicity are effect modifiers in this relationship.

Chapter 6

1.

- a) Elevated combined vascular risk represented by the FRS is associated with decreased cortical tissue volume and increased WMH volume in an elderly ethnically diverse population.

- b) Sex and ethnicity are in some instances effect modifiers of the association of combined vascular risk and brain outcomes.

2.

- a) Hypoperfusion is associated with decreased cortical tissue volume and increased WMH volume in elderly populations.
- b) Sex and ethnicity are in some instances effect modifiers of the associations of CBF and brain outcomes.

3.

- a) Cortical CBF is a mediator in associations of combined vascular risk with cortical tissue volume and WMH volume in elderly populations.
- b) The strength of CBF as a mediator in the association of combined vascular risk with WMH volume will vary with zonal location.

3 . General methods

3.1 Study sample

Participants were recruited from the Southall and Brent Revisited (SABRE) study. Approval for investigations was obtained from the Fulham Research Ethics Committee (ref:14/LO/0108) and participants gave written informed consent.

SABRE is a longitudinal study principally investigating cardio-metabolic disease in a tri-ethnic population cohort; details have been published elsewhere (173). The study was originally conceived to investigate the increased risk of cardiovascular disease in Indian Asian and African Caribbean migrant populations to the UK in comparison to the host population. Participants were community dwelling elderly men and women, resident in north and north-west London at the commencement of the SABRE study in 1988. Original participants were recruited via GP practices and industrial workplaces with a diverse ethnic mix. Spouses or significant others were invited to join their partners in the third clinical visit commencing in 2014.

In our study the ethnic group 'Europeans' were of white European descent. 'South Asians' were of Indian Asian origin comprising those of Gujarati/Hindu Punjabi/Sikh, Pakistanis and Bangladeshi descent. 'African Caribbeans' were of Black African descent having migrated from the Caribbean or West Africa. An additional booster sample of African Caribbeans from the same area of London as the original cohort were recruited to increase numbers and therefore enhance the power of the study. Ethnicity was defined based on country of origin of all four grand-parents stated on self-administered participant questionnaires.

During the SABRE v3 (visit 3) study there was a gap in recruitment due to a temporary enforced closure of the clinic. Although the total number of participants undergoing MRI was projected to be ~900, it was decided that analyses for this thesis should be based on participants attending between 2014 and 2016. It seems reasonable to assume the clinic closure was a 'random event' in statistical terms, so the subsample used in this thesis should be representative of the entire sample. During the selected period between August 2014 and October 2016, 541 participants attended MRI. 493 (91%) completed the whole MRI scan and these examinations were processed for CBF (**Figure 3-1**). 485 (90%) participants had both MRI and sufficient cardiovascular results to construct a FRS.

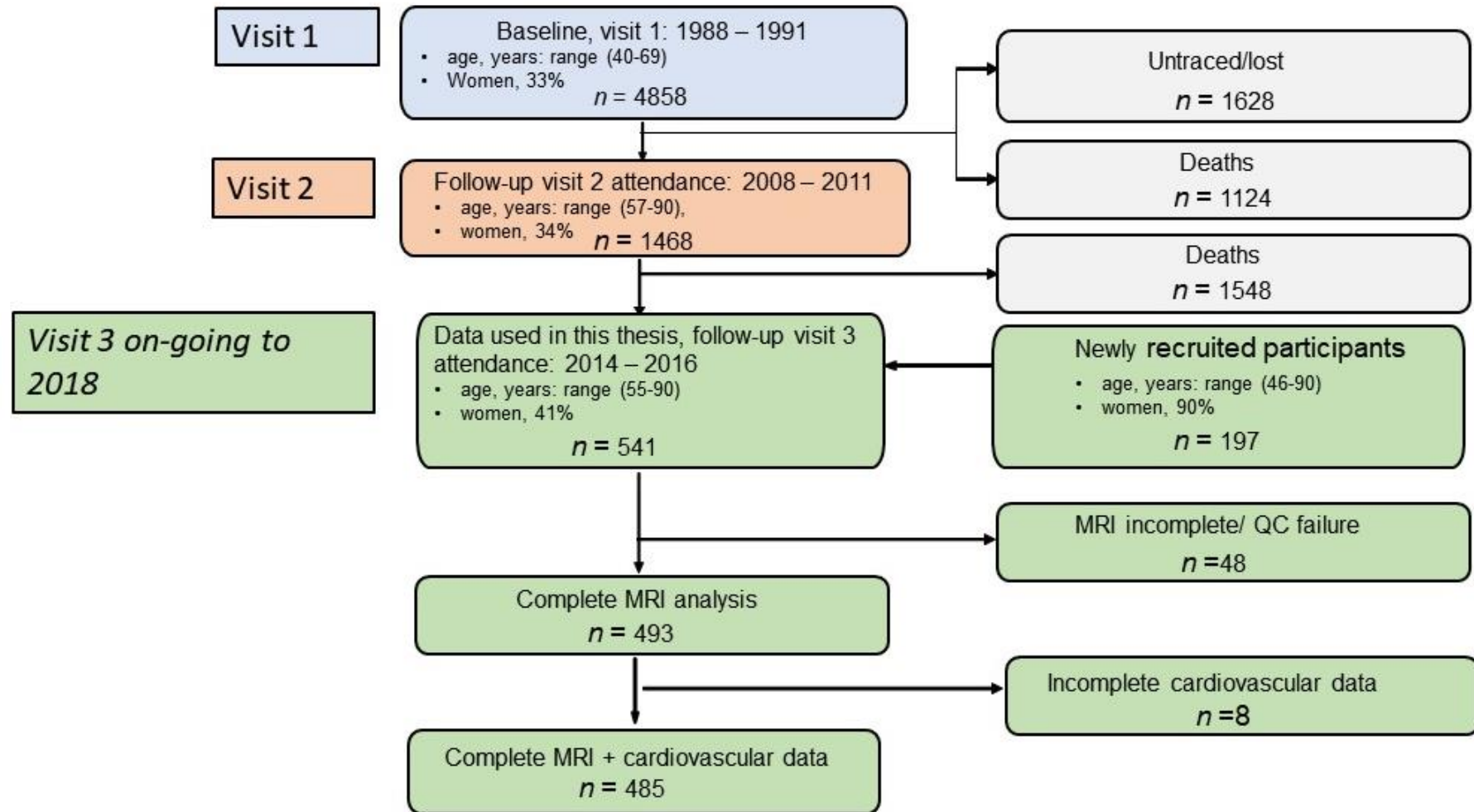


Figure 3-1. Consort diagram, showing sample from the SABRE study. (figure adapted from (174))

3.2 MRI methods

3.2.1 MRI acquisition

All participants were examined at University College Hospital on a 3T MRI (Philips Achieva, Eindhoven, Netherlands) using an 8 channel phased array head coil. The study was entirely performed on one scanner with only minor software upgrades. MRI scanning was planned to optimise morphological measurement precision through its single centre design, protocol adherence, automated planning, staff training and segmentation pipeline. Participants underwent all MRI examinations on the same day as attendance at the SABRE clinic. They were requested to consume no more than a light breakfast with only 1 small cup of a caffeinated drink, and to abstain from smoking and alcohol on the morning of attendance to minimise physiological variation in ASL.

This thesis will primarily utilise T1 3D TFE for structural analysis, FLAIR and T2 3D TSE for WMH detection, and PCASL and B0 sequences for perfusion analysis. Additional sequences were acquired for future assessment of neurovascular disease. Sequence parameters are listed in **Table 3-1**.

The Philips SmartExam automated planning function was utilised for all participants to ensure inter-subject and intra-subject geometric consistency <http://www.philips.co.uk/healthcare/product/HCNMRB514/smartexam-brain-mr-software>. Using SmartExam software, the central slice or mid plane line is positioned on the AC-PC line of the brain in transverse and sagittal planes to minimise shifting and deformation during post processing sequence registration (**Figure 3-2**) Changes in head-foot position were permitted for PCASL sequences to ensure brain coverage of the cerebrum, although angulation remained constant. The RF label was planned in a plane perpendicular to the ICAs using a fast PC-MRI sequence to visualise the vessels. 3D T1, 3D T2 and 3D FLAIR sequences were matched for resolution (isotropic 1mm³) to optimise registration during analysis. PCASL parameters were selected in conformance

with the ISMRM Perfusion Study Group and European Consortium for ASL in Dementia white paper recommendations (42). The only deviation from the white paper recommendation was a 2D readout instead of 3D as at the time of commencement of the study 3D readout for PCASL was not available on the MRI scanner. Planning of the PCASL sequence is illustrated in **Figure 3-3**.

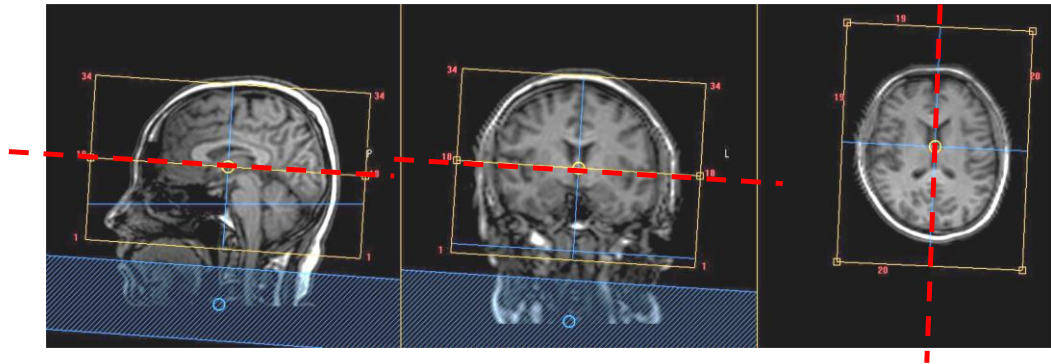


Figure 3-2. MRI survey showing example of SMARTEXAM automated planning. (Dotted red line shows alignment of slices through anterior/posterior commissure line and perpendicular to this line on coronal and transverse planes). (Images are from the SABRE v3 study).

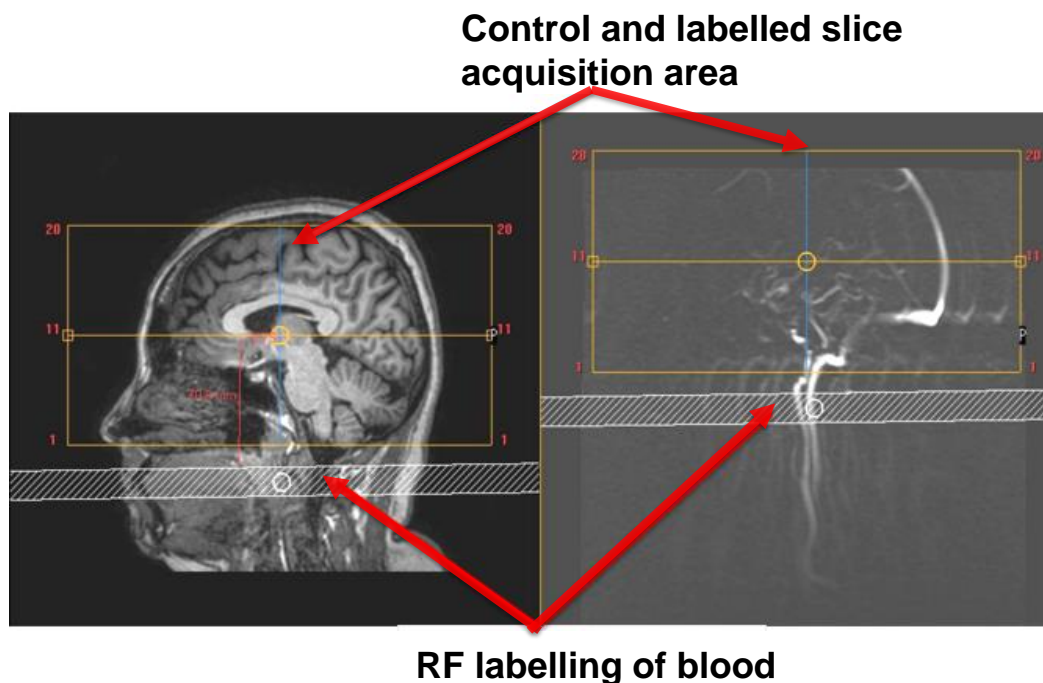


Figure 3-3. MRI planning of PCASL on T1w sagittal (left) and fast PC-MRI (right) showing slice acquisition and RF labelling planes. (Images are from the SABRE v3 study).

All MRI scans and processed images were visually inspected for artefacts. Scans with susceptibility artefacts such as dental work affecting the RF label (n=12), excessive head movement (n=3), claustrophobia/inability to tolerate the scan (n=9), processing errors (n=22), pathology (n=1), and scanner artefact (n=1) were excluded from analyses. Examples of artefacts displayed in scans from this study are illustrated in **Figure 3-4**, **Figure 3-5**, **Figure 3-6**, and **Figure 3-7**.

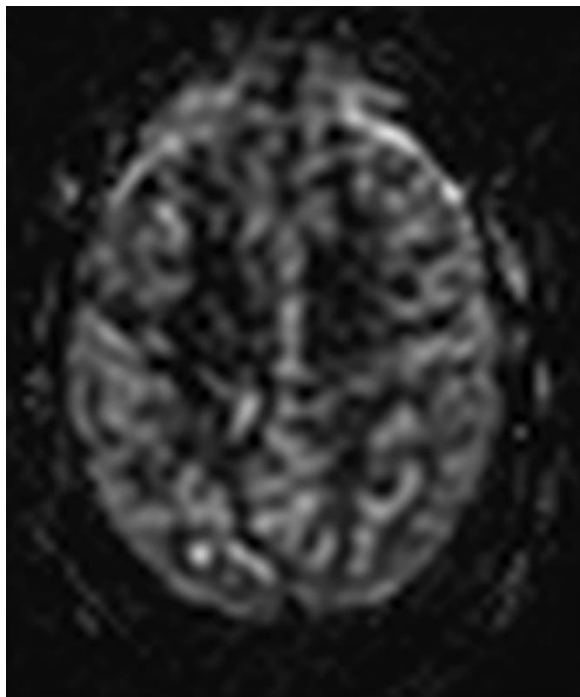


Figure 3-4. Perfusion weighted ASL image in transverse plane illustrating movement artefact (Image is from the SABRE v3 study).

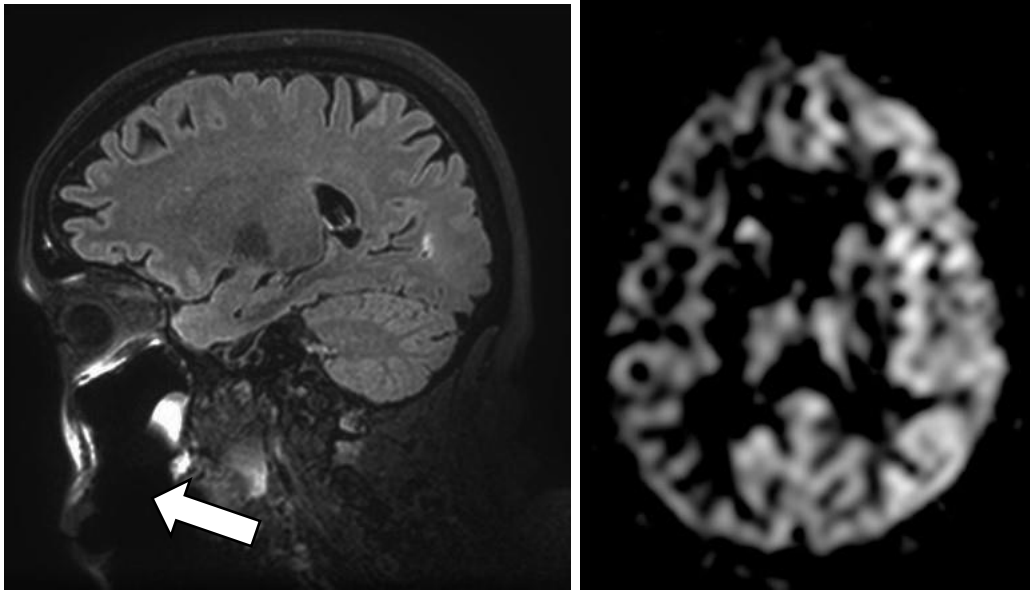


Figure 3-5. T1w sagittal and subtracted ASL images in transverse plane illustrating susceptibility artefact from dental work (white arrow) causing loss of signal in right hemisphere (Images are from the SABRE v3 study).

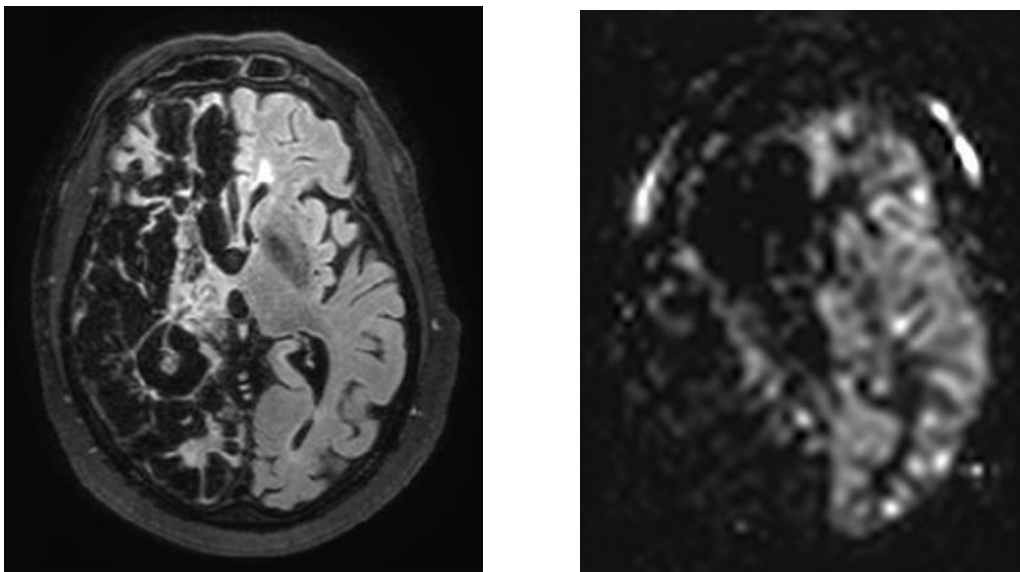


Figure 3-6 T1w transverse and subtracted ASL image in transverse plane illustrating hypointense perfusion deficit resulting from extensive mature damage in right cerebral hemisphere secondary to ischaemic stroke (Images are from the SABRE v3 study).

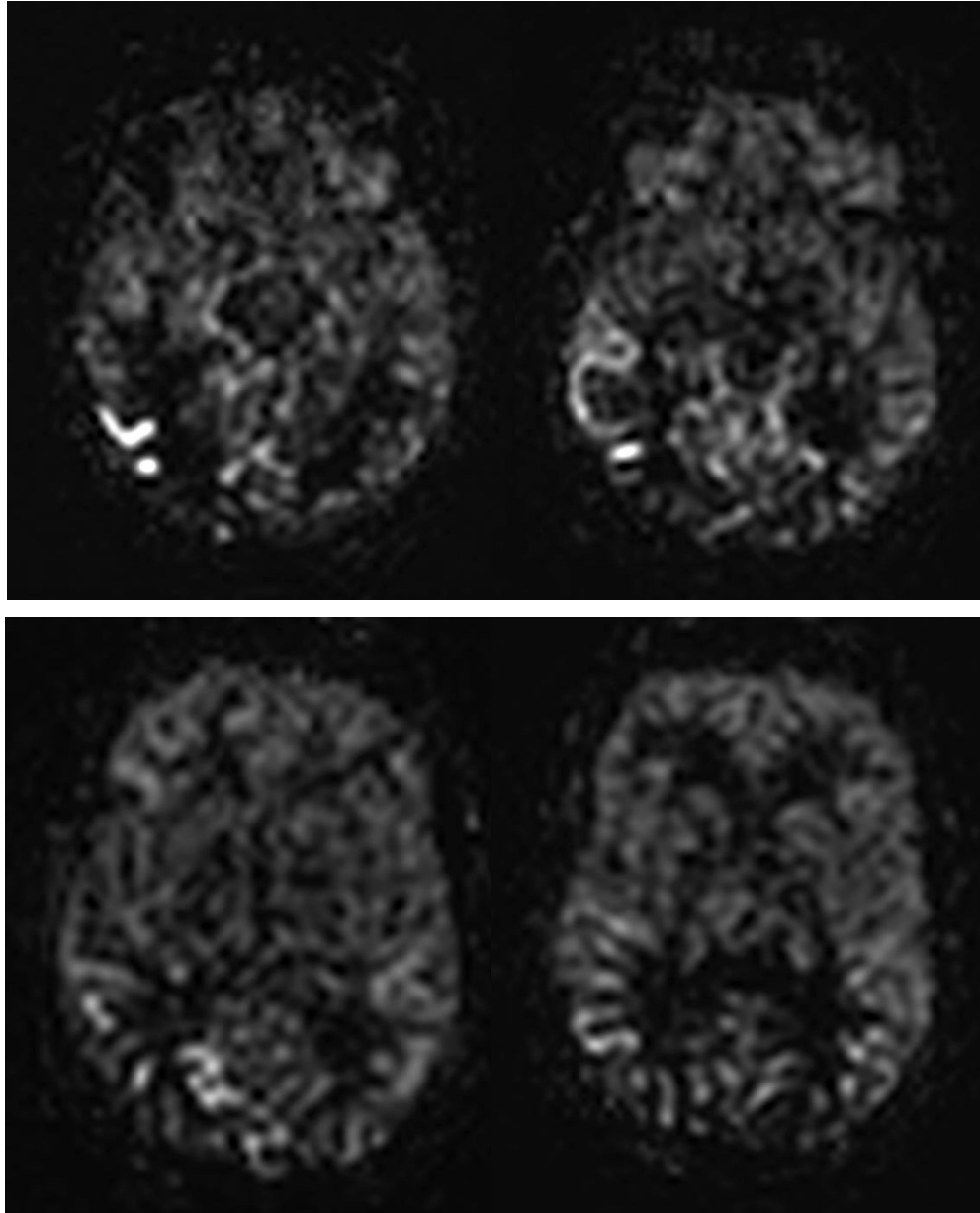


Figure 3-7. Subtracted ASL images in transverse plane illustrating hyperintense signal in vessels due to arterial transit artefacts (ATAs) as a result of delayed perfusion in the posterior circulation which is more marked on the right. (Images are from the SABRE v3 study).

Sequence	Technique	Plane	Voxel size (mm)	TR(ms)	TE(ms)	TI (ms)	flip angle	b-values	SENSE	Duration (min/sec)
T2w	2D FFE	Tra	1,1,3	1223	21	-	18	.	1.3	3.01
T1w	3D FFE	Sag	1,1,1	7	3.2	836	8	.	2.0	3.55
FLAIR	3D IR TSE (SPIR)	Sag	1,1,1	4800	294	1650		.	2.5	6.09
DTI	EPI DTI (SPIR)	Tra	2,2,2	8492	83	.	90	0,1000 (6 dir)	2.3	2.58
MRA	3D FFE (ToF)	Tra	0.4,0.7,0.5	25	3.5	.	20	.	2.0	6.00
PCA	FFE	Tra	1.1,1.1,40	20	6.3	.	15	.	-	0.27
PCASL	EPI	Tra	3.75,3.75,5	4615	15	.	90	.	2.3	5.32
PCASL (calibration)	EPI	Tra	1,1,1	9000	15	.	90	.	2.3	0.36
T2w	3D TSE (SPIR)	Sag	1,1,1	2500	227	.	100	.	2.5	3.50
B0	3D FFE	Tra	3,3,4	10	4.6	.	5	.	2.3	1.02

Table 3-1. MRI protocol for SABRE v3 study

Abbreviations used in Table 3-1

B0	B0 field map
CoW MRA	Circle of Willis magnetic resonance angiography
DTI	diffusion tensor imaging, dir = directions
EPI	echo planar imaging
FLAIR	fluid attenuated inversion recovery
FFE	fast field echo
IR TSE (SPIR)	inversion recovery turbo spin echo spectral inversion recovery
PCA	phase contrast angiography
PCASL	pseudo continuous arterial spin labelling (cal) calibration
TFE	turbo field echo
TE	echo time
TI	time to inversion
ToF	time of flight
TR	repetition time
Tra	transverse
TSE	turbo spin echo
Sag	sagittal
SENSE	sensitivity encoding

3.2.2 MRI processing

The Translational Imaging Group (TiG) at the Centre for Medical Image Computing (CMIC) UCL, performed all brain analyses for the SABRE v3 study.

3.2.2.1 Brain segmentation and parcellation: geodesic information flow

In this thesis the geodesic information flows (GIF) framework was used to produce tissue segmentation and regional parcellation of the brain (175). Previous methods of atlas based structural brain segmentation and parcellation have relied on registration of imaging data to a pre-labelled mean brain template i.e. groupwise space, usually derived from a young healthy population. This method can produce anatomical labelling inaccuracies due to misregistration, the large normal variance of brain morphology particularly in sulcal conformation, as well as difficulties accommodating participants with extensive pathological changes (176). These issues are particularly relevant to ageing populations who are susceptible to regional volume loss and large areas of parenchymal damage such as infarction and WMHs altering the MRI appearance. Further variance is introduced by gender and ethnic differences. Multi atlas templates including brains relevant to the sample and disease characteristics of the dataset have been used to improve accuracy (177). However, such an approach relies on the availability of relevant atlases wherein the creation of such atlases is time intensive in terms of skilled manual input. Building on this approach LEAP (Learning Embeddings for Atlas Propagation) measured the similarity between morphological areas such as the hippocampus between datasets (178). The use of a similarity measure enables propagation between datasets by using intermediate datasets to move between standard populations and sample populations, such as propagating the ‘training’ young healthy dataset onto healthy ageing and AD participants. In this way segmentation and labelling are diffused in steps throughout the dataset. The GIF algorithm improves on this method by measuring regional rather than global similarities between pairs of images. It performs segmentation and regional labelling by voxel-wise voting between several propagated atlases, guided by

local image similarity. This is accomplished through use of a spatially variant graph i.e. pixels are not graphed according to spatial distance but by other characteristics such as image intensity and type of deformation between a pair other types of data can also be included such as age, ethnicity or pathology. Strength of connectivity is derived between each pair of images in a dataset. The strength of connectivity is used to propagate information throughout the dataset utilising estimates of accuracy of the propagation through methods such as the amount of iterations required before a label is assigned in order to assign probability weightings Iterations continue until all images are segmented or labelled (**Figure 3-9**) (179). An example slice is shown in **Figure 3-8** (175). GIF is available online: <http://niftyweb.cs.ucl.ac.uk/>.

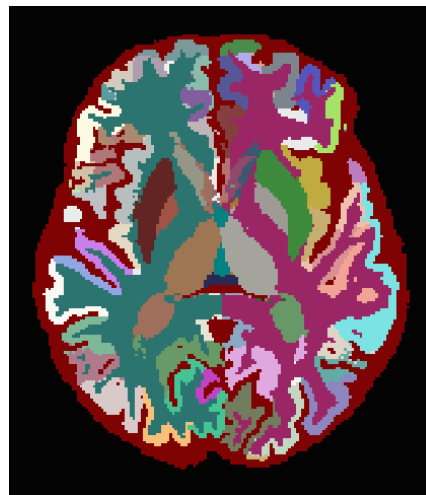


Figure 3-8: Example of regional brain parcellation (image is from the SABRE study).

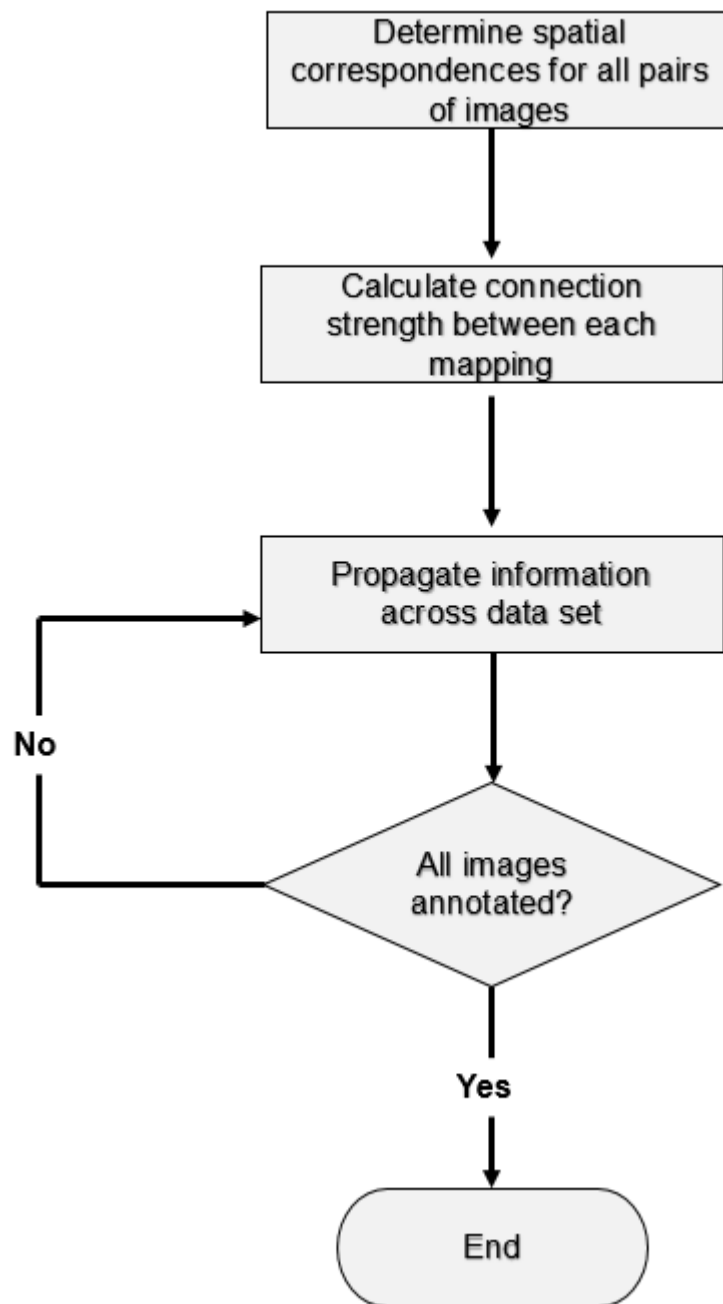


Figure 3-9 Geodesic information flow flowchart showing propagation steps and iterative process. Figure from (179)

3.2.2.2 Quantification of white matter hyperintensities:

Bayesian model selection

Traditionally, WM disease has been classified by manual assessment such as the Fazekas, Scheltens and Manolio scales (180-182) which categorise severity of disease into relatively broad classes. More recently, fully automated algorithms that quantify and spatially locate hyperintensities have allowed detailed analysis of WMHs to be applied in large population studies (183) (184). This provides the opportunity to model the associations of cardiovascular risk with WMHs with greater precision than broad categorical divisions or labour intensive manual segmentation previously allowed.

In this thesis the burden of WMHs was quantified using an automated segmentation method known as Bayesian Model Selection (BaMoS) (183). This model uses T1w, T2w FLAIR and T2w sequences to perform WMH detection. The GIF parcellation method described above is used to define lobes thus allowing regional representation of WMH load. Using the BaMoS model, WMH volumes were calculated by lobe; frontal, parietal, temporal and occipital lobes were defined in right and left hemispheres, basal ganglia and infratentorial were combined. Zonal categories 1 - 4 were defined according to distance from the lateral ventricular surfaces and cortical GM; zone 1 lying closest to the ventricular wall. Examples of segmentation and lobar-zonal distribution are shown in **Figure 3-10**. The BaMoS method has been validated against other automated segmentation methods and gold standard manually segmented datasets (183). For the dataset used in this thesis, visual inspection of each subject's WMH segmentation was performed and those with undetected hyperintensities on FLAIR images were re-segmented using adjusted thresholding parameters ($n = 23$). All examinations that included a full dataset of T1w, FLAIR and T2w sequences were successfully quantified after inspection.

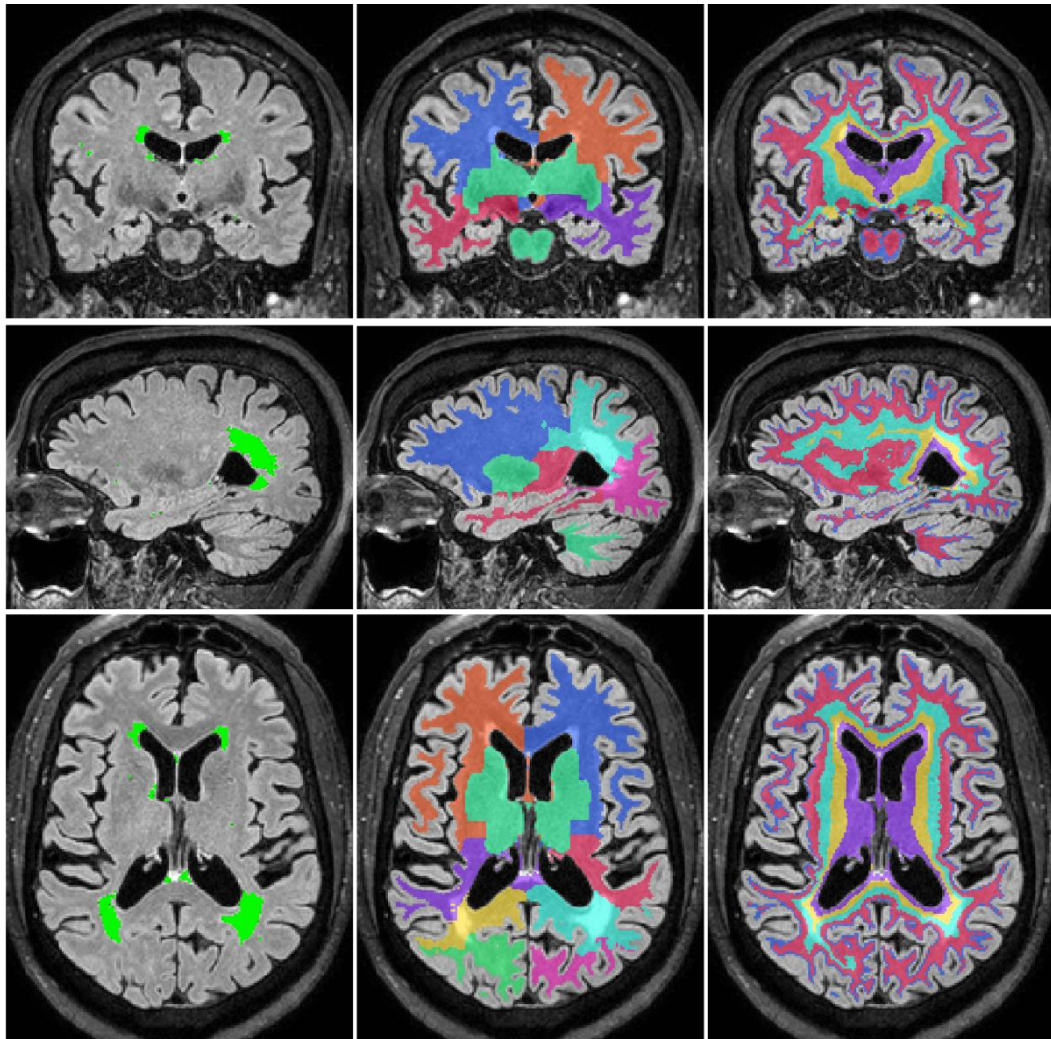


Figure 3-10: FLAIR images illustrating WMH segmentation with lobe and zone allocations. WMHs are highlighted in green (left column), lobular segmentation (middle column), and zonal distribution (1-4), zone 1 is periventricular shown here in purple, zone 4 is sub-cortical shown here in pink (right column) (185)

3.2.3 Cerebral blood flow quantification

CBF was processed using the NiftyFit for ASL open source software package <https://cmiclab.cs.ucl.ac.uk/CMIC/NiftyFit-Release> (186). Determination of CBF maps from ASL data followed the simple derived form for PCASL (Equation 3-1) drawn from the statement of recommendation from the ISMRM Perfusion Study Group and the European Consortium for ASL in Dementia (42) presented in units of mL/100g/min. 35 control, (SC) and label (SL) pairs and 5 proton density (SPD) images were averaged to generate single voxel values for the control

and label in Equation 3-1, where λ is the blood/brain partition coefficient (0.9mL/g), PLD the post-labelling delay between end of bolus and start of imaging (2000ms), $T1_{blood}$ the blood T1 relaxation time, α the labelling efficiency (85%) and τ the labelling duration (1800ms).

$$CBF = 6000 \cdot \lambda \cdot (SI_{control} - SI_{label}) \cdot e^{\frac{PLD}{T1_{blood}}} / SI_{PD} \cdot \left(2 \cdot \alpha \cdot T1_{blood} \cdot (1 - e^{-\tau/T1_{blood}}) \right) \left[\frac{mL}{100g} / min \right]$$

Equation 3-1

Assumptions of this model include; the entire labelled bolus has been delivered to the tissue, there is no significant venous outflow of the labelled bolus upon measurement, and the T1 relaxation of the label is exclusively due to the T1 of blood. In chapters 5 and 6 of this thesis $T1_{blood}$ was calculated based on the formula: $T1 = (0.52 \cdot Hct + 0.38)^{-1}$ (187) where the value for Hct is measured from each participant. (Based on evidence presented in chapter 4.) CBF maps were registered to down-sampled segmentations derived from GIF processed T1w images in order to derive cortical GM CBF values. Regional CBF was not included in analyses as the repeatability and reproducibility of GM CBF is superior to that of regional CBF. Increased variability of lobar CBF is due to inclusion of vascular high signal from arterial transit artefacts (188).

PVC was applied based upon the method used in (48). In this method, weighting coefficients are allocated according to the volume of each tissue type estimated to be present within a voxel in order to improve calculation of the intensity of the voxel by minimizing partial volume effects. The method uses a 'least squares' fit in a kernel which assumes a constant CBF value in the local GM and WM. The algorithm relies on accurate segmentation of GM and WM and precise registration to the structural image. The use of this algorithm is considered to provide valuable adjustment to CBF estimation especially in cases of cerebral atrophy (186). Results for CBF of cortical GM with PVC are therefore presented as the primary measure of CBF throughout this thesis.

3.3 Cardiovascular risk measurements

Participants underwent all clinic examinations on the same day as MRI.

Participants were requested to consume no more than an early light breakfast prior to arrival at the clinic.

3.3.1 Anthropometrics

Weight and height were measured according to a standardized protocol using a Tanita Pro BC-418 Body Composition Analyser and a Seca 216 Stadiometer respectively and BMI (kg/m^2) calculated from this data.

3.3.2 Blood pressure and heart rate

Seated brachial BP was measured using an Omron MIT Elite Plus BP monitor after 5 minutes of rest. Clinic BP was calculated in accordance with the European Society of Hypertension/European Society of Cardiology Guidelines (2013) (189), as the average of the final two of three measurements in the left arm unless the difference between arms was $>10\text{mmHg}$ in which case the arm with the higher BP was used. Heart rate and mean arterial pressure (MAP) were measured using a Pulsecor device (BP+; <https://www.uscom.com.au/>) (190).

3.3.3 Haematocrit

Hct was measured using an impedance based, direct current sheath flow method (Sysmex XE-2100, www.sysmex.co.uk) from a venous blood sample drawn on the same morning as the MRI examination.

3.3.4 Blood analyses

Blood was analysed for glycosylated haemoglobin (HbA1c), serum total cholesterol, high density lipoprotein (HDL) cholesterol and triglycerides. Low density lipoprotein (LDL) cholesterol was calculated using the Friedewald equation (191).

3.3.5 Diabetes mellitus

Diabetes status was determined by the following criteria; diagnosis or prescription of diabetes medication ascertained from primary care records at SABRE study visits 1 and 2, fasting or oral glucose tolerance test or plasma glucose testing ascertained during SABRE study clinic visits 1 and 2 using WHO recommendations (192) ($n = 81$, 61.8%), patient recall of diagnosis or taking antidiabetic medication from health questionnaire completed at SABRE visit 3 ($n = 30$, 22.9%), and those with an HbA1c ≥ 48 mmol/mol when tested in the SABRE study clinic at visit 3 ($n = 20$, 15.3%). HbA1c is a measure of chronic hyperglycaemia; it is recommended by the International Expert Committee (IEC) as the preferred test to diagnose diabetes as it is 'an accurate, precise measure of chronic glycaemic levels and correlates well with the risk of diabetes complications(193). IEC threshold recommendations are: prediabetes HbA1c ≥ 42 mmol/mol, diabetes ≥ 48 mmol/mol. Recent primary care records for participants at visit 3 were not available. Therefore, although it is acknowledged that patient recall is not entirely reliable and HbA1c testing is not the gold standard for diabetes diagnosis, these methods of identifying participants 'with diabetes' were included.

3.3.6 Demographic information

Demographic information was gathered from self-administered questionnaires received by participants prior to their clinic visit. These were checked in clinic and completed as necessary during the visit.

3.3.7 Smoking

Smoking status was determined through self-administered questionnaire. A binary classification of non-smoker/current smoker was used.

3.3.8 Medications

Use of anti-hypertensive and lipid lowering medications were ascertained through GP records and self-administered questionnaire.

3.3.9 Framingham risk score

The Framingham risk score (FRS) was used as an integrated measure of cumulative cardiovascular risk. Using this algorithm has the advantage of minimising the number of parameters in statistical models and integrating information from multiple risk factors to represent combined vascular risk.

The FRS (updated in 2008) was chosen as the most suitable algorithm to use in this thesis due to its extensive validation in various populations giving confidence that it estimates cumulative vascular risk without introducing excessive bias due to ethnicity or gender (194-196). Although FRS does not include adjustment for socio-economic status such as incorporated in the ASSIGN algorithm (197), the relative socio-economic homogeneity of the SABRE cohort minimizes the influence of this factor and in any case assessment of socio-economic status in different ethnic groups is problematic. The advantage of algorithms such as FRS lies in its use of weighted coefficients to reflect the relative contributions of each factor to total risk. The FRS algorithm was designed as a tool to estimate 10-year absolute risk of cardiovascular disease i.e. coronary and cerebrovascular events, peripheral artery disease and heart failure. The model used in this thesis is the updated algorithm from D'Agostino et al (2008) (198). There are sex specific algorithms reflecting differing risk profiles for men and women. Each model comprises multivariable beta coefficients for age, total cholesterol, HDL-cholesterol, untreated systolic BP or treated systolic BP, smoking and diabetes (**Table 3-2**). These variables were found to be statistically significant in Cox proportional-hazard regressions associating measured cardiovascular disease risk factors with incidence of cardiovascular events in the longitudinal Framingham Heart and Framingham Offspring Studies (198).

10-year baseline survival	Estimated beta coefficient	
	Men	Women
Log of age	3.06117	2.32888
Log of total cholesterol	1.12370	1.20904
Log of HDL cholesterol	-0.93263	-0.70833
Log of SBP if untreated	1.93303	2.76157
Log of SBP if treated	1.99881	2.82263
Smoking	0.65451	0.52873
Diabetes	0.57367	0.69154

Table 3-2. Beta coefficients for Framingham risk score algorithm (198)

3.4 Statistical methodology

Details of statistical methodology are described separately in each chapter of this thesis.

Chapters 5 and 6 present stratified analyses in addition to analysis of pooled samples. The rationale for this approach was to avoid confounding by the stratifying factor. All data is shown in order to reveal differences in associations regardless of whether the interaction term showed a statistically significant P -value. As argued by Amrhein et al (199) and many others, reliance on statistical significance can create fallacious binary categorisation of results encouraging a failure to appreciate the nuances of the data behind the test. Therefore, stratification prompted only by the statistical significance of an interaction could potentially miss important distinctions in the associations of variables between sexes, ethnicities and cardiovascular status. Effect modification by sex, ethnicity and diabetes were considered to be reasonable *a priori* assumptions in this study as there is much previous evidence to indicate the effects of cardiovascular disease on end organ damage vary by these factors (200-204). Although stratification reduces the power of the study due to smaller numbers in each sample and therefore P -values more rarely show statistical significance, data presented with confidence intervals and effect sizes should be inspected where possible to avoid loss of potentially important evidence.

4 . Cortical cerebral blood flow in ageing: effects of haematocrit, sex, ethnicity and diabetes

4.1 Abstract

CBF estimates from ASL show unexplained variability in older populations. This chapter studies the impact of variation of Hct on CBF estimates in a tri-ethnic elderly population. PCASL was performed on 493 participants (age 55 - 90) from a tri-ethnic community-based cohort. CBF was estimated using a simplified Buxton equation, with and without correction for Hct measured from blood samples. Differences in perfusion were compared, stratified by sex, ethnicity and diabetes. Results of Student's t-tests were reported with effect size (i.e. Cohen's d, the effect standardized to the standard deviation (SD)). Hct adjustment decreased CBF estimates in all categories except European men. The decrease for women was 2.7 (3.0, 2.4) mL/100g/min (mean (95% confidence interval (CI)), $P < .001$ $d = 0.38$). The effect size differed by ethnicity with estimated mean perfusion in South Asian and African Caribbean women found to be lower by 3.0 (3.6, 2.5) mL/100g/min, $P < .001$ $d = 0.56$ and 3.1 (3.6, 2.5) mL/100g/min, $P < .001$ $d = 0.48$, respectively. Estimates of perfusion in participants with diabetes decreased by 1.8 (2.3, 1.4) mL/100g/min, $P < .001$ $d = 0.23$) following Hct correction. Correction for individual Hct altered sample frequency distributions of CBF values, especially in women of non-European ethnicity. ASL derived CBF values in women, non-European ethnicities and individuals with diabetes are overestimated if calculations are not appropriately adjusted for individual Hct.

4.2 Introduction

ASL is an MRI technique increasingly used in research and clinical settings to calculate CBF non-invasively (205). It has been recognised that ASL can provide an early biomarker for dementia, cognitive decline and small vessel disease (78, 80, 82, 85, 168, 206, 207). Despite statistical differences between groups, e.g. AD, MCI and normal ageing, clinical applications have been hampered by unexplained inter-subject variability (208);(209).

Deriving quantitative perfusion values from the raw MRI signal requires application of a model containing several assumptions that relate to physiological properties of the blood and tissues. The white paper recommendations of the ISMRM and the European Consortium for ASL in Dementia propose PCASL with a single PLD and slice timing correction, and the application of a simplified Buxton equation for quantification of CBF (42, 210). In this model, 1650ms is recommended as the longitudinal relaxation time of blood ($T_{1\text{blood}}$) at 3T. This has been derived from a linear relationship between Hct and blood T1 found in experiments under appropriate physiological conditions (187), assuming an average adult Hct of 43.5% (42).

However, there are well recognised sources of variation in Hct between and within populations that may render CBF estimation inaccurate if these factors are excluded from the model (209) (208). Hct varies by sex with females typically having lower Hct than males (211). Most studies show a lower Hct in blacks than Asians compared to whites (212, 213), although an earlier study found this varied according to age and was not applicable in some younger participants (men aged 15 -24) (214). Higher Hct levels have been associated with obesity (211) and have also been associated with risk of developing diabetes (215). Diabetic patients with long standing disease may have decreased Hct, possibly due to diabetic nephropathy causing erythropoietin deficiency (216), or malabsorption of vitamin B12 as a side-effect of long term treatment with Metformin (217).

The purpose of this study was to identify the variability in cortical CBF using ASL, to investigate the influence of Hct on the estimation of CBF, and to determine how this impacts on the associations of CBF with age, sex, ethnicity and diabetes.

4.3 Materials and methods

See Chapter 3 'General methods' (pp 81 - 91) for study sample, MRI acquisition and processing methods, and collection of cardiovascular data.

4.3.1 Statistical analysis

Analysis was performed using STATA 14.2 (College Station, Texas). All analyses were stratified by sex and ethnicity. Continuous data are presented as mean and standard deviation (SD) or median (interquartile range) for skewed data; categorical data are counts and percentages.

Paired Student's t-tests were used to test for statistical significance between the two methods of CBF calculation. Pearson's correlation coefficient was computed to quantify linear correlations between Hct and CBF estimates, residuals were inspected to look for evidence of linearity or heteroskedasticity. Comparisons by sex and ethnicity were performed using 2-way analysis of variance (ANOVA), followed by individual group-wise comparisons using Fisher's least significant difference (LSD) test if ANOVA was significant ($P < .05$). Multiple linear regression analyses were performed to assess participant characteristic associations with Hct levels with further adjustment for potential confounders, age, mean arterial pressure, diabetes, HbA1C, LDL cholesterol, HDL cholesterol and BMI, chosen *a priori*. Sample frequency distributions of CBF calculated with and without correction for individual Hct were analysed using univariate kernel density estimates.

4.4 Results

4.4.1 Participant characteristics

Table 4-1 shows the basic characteristics of the sample stratified by sex and ethnicity. The sample comprised 493 individuals of whom 40% (n = 196) were women. Women were younger than men (women mean age \pm SD, 69.7 \pm 6.4 years; men 72.9 \pm 5.2 years; $P < .001$). White Europeans represented 46% of the sample, South Asians 35% and African Caribbeans 19%. 27% of participants had type 2 diabetes.

Participant characteristics	n	All	Men	Women	European	South Asian	African Caribbean
Sex, n (female)	493	493 (196)	297	196	226 (78)	175 (67)	92 (51)**
Age, years	493	71.6 ±5.9	72.9 ±5.2	69.7 ±6.4**	72.1 ±5.8	70.8 ±5.6**	72.0 ±6.7
Diabetes (Y), n (%)	493	133 (27)	80 (27)	53 (27)	39 (17)	65(37)	29 (32)**
HbA1c, mmol/mol	486	41.7 ±9.2	41.2 ±8.3	42.5 ±10.3	39.2 ±7.9	43.9 ±8.8**	43.6 ±11.0**
BMI, kg/m²	489	27.5 ±4.2	27.1 ±3.8	28.2 ±4.8**	27.5 ±4.1	26.4 ±3.7**	29.6 ±4.7**
Haematocrit, %	493	41.6 ±3.7	43.0 ±3.5	39.5 ±3.0**	42.7 ±3.6	40.8 ±3.7**	40.7 ±3.4**
Total cholesterol, mmol/L	492	4.7 ±1.1	4.5 ±1.0	5.1 ±1.1**	4.8 ±1.1	4.5 ±1.0**	4.8 ±1.1
LDL, mmol/L	492	2.5 ±0.9	2.4 ±0.9	2.7 ±0.9**	2.6 ±0.9	2.3 ±0.9**	2.5 ±1.0
HDL, mmol/L	492	1.60 ±0.5	1.5 ±0.4	1.8 ±0.5*	1.6 ±0.5	1.5 ±0.4**	1.8 ±0.6**
Systolic BP, mmHg	485	141.2±17.9	141.9±17.4	140.2±18.6	138.0 ±18.2	144.7±18.4**	142.4±14.5*
Diastolic BP, mmHg	480	79.6 ±8.3	79.6 ±8.4	79.4 ±8.0	79.7 ±8.0	78.6 ±7.8	80.9 ±9.5
Heart rate, min⁻¹	481	64.1 ±11.1	62.4 ±10.9	66.7	64.5 ±10.8	63.4 ±11.0	64.7 ±12.1
MAP, mmHg	480	97.0 ±10.0	97.0 ±10.0	96.9 ±10.0	96.7 ±10.1	96.4 ±9.9	98.6 ±10.0
Anti-hypertensive medications(Y) n(%)	493	283 (57)	183 (62)	100 (51)**	101 (45)	119 (68)**	63 (69)**
Lipid lowering medications (Y) n (%)	493	238 (48)	138 (47)	100 (51)	120 (53)	64 (37)**	54 (59)

Table 4-1. Participant characteristics; data are mean ± SD or number of observations (n) (%). *P<0.05, **P<0.01 compared to reference (male/Europeans) by Fisher's LSD test after analysis of variance (ANOVA)

4.4.2 Haematocrit

The mean (SD) Hct of our sample was 41.6% (3.7). This is lower than the population mean Hct of 43.5% suggested in [9], from which a $T1_{\text{blood}}$ of 1650ms at 3T had been calculated. South Asian men had a mean Hct of 42.0% (3.6), lower than either white European (43.8% (3.4)) or African Caribbean men (43.0% (3.5)). Both South Asian (38.8% (3.1)) and African Caribbean women (38.8% (2.4)) had lower mean Hct than European women (40.6% (3.0)), (**Figure 4-1**). Age was not associated with Hct ($r = 0.06$, $P = 0.2$) (**Figure 4-2**).

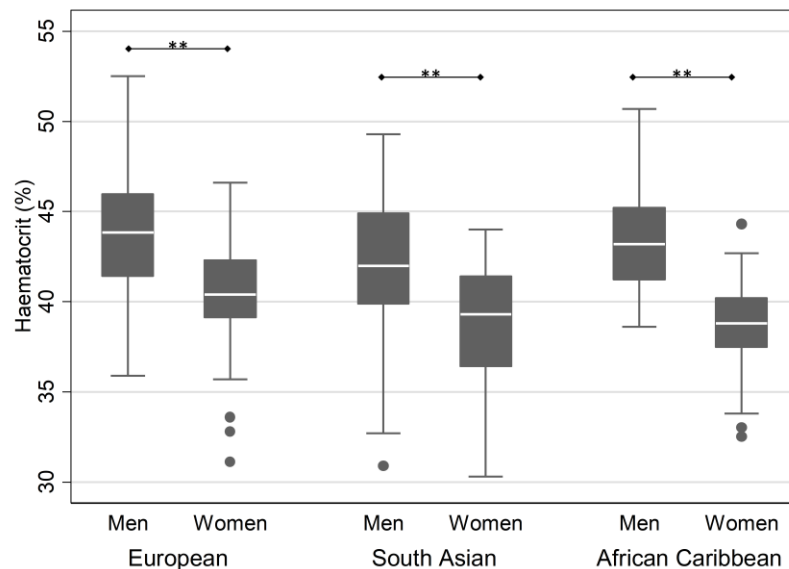


Figure 4-1. Boxplot showing median, interquartile range, upper and lower adjacent values and outside values for Hct by sex and ethnicity. ** = $P < 0.01$ by 2-way analysis of variance followed by Fisher's LSD test.

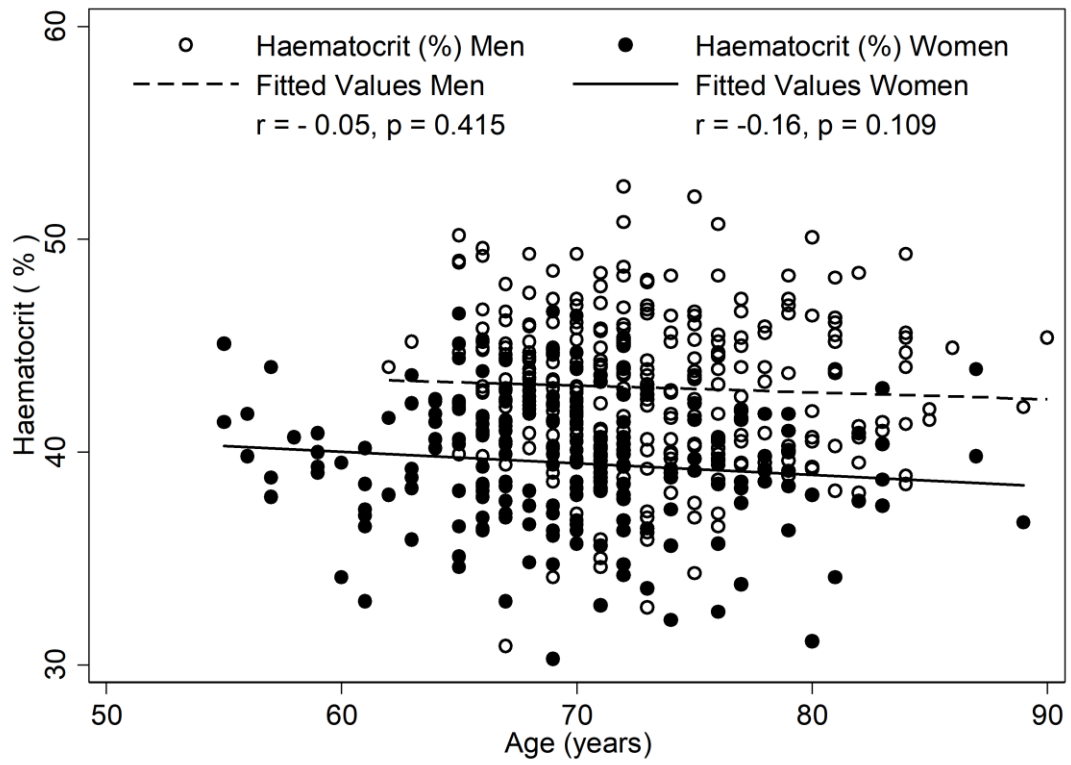


Figure 4-2. Scatterplot with line-fit and Pearson's correlation coefficient (r) showing correlation of age and Hct, by sex

4.4.3 Cerebral blood flow

Table 4-3 shows results for CBF_{fixed} and CBF_{Hct} models stratified by sex, ethnicity and diabetes. As a result of correction for individually measured Hct when calculating $T1_{blood}$, CBF_{Hct} values were lower than CBF_{fixed} values in all categories of sex and ethnicity except for European and African Caribbean men (Figure 4-3). Age was not associated with CBF (men, $r = 0.01$, $P = .861$; women, $r = 0.09$, $P = .237$) (Figure 4-4).

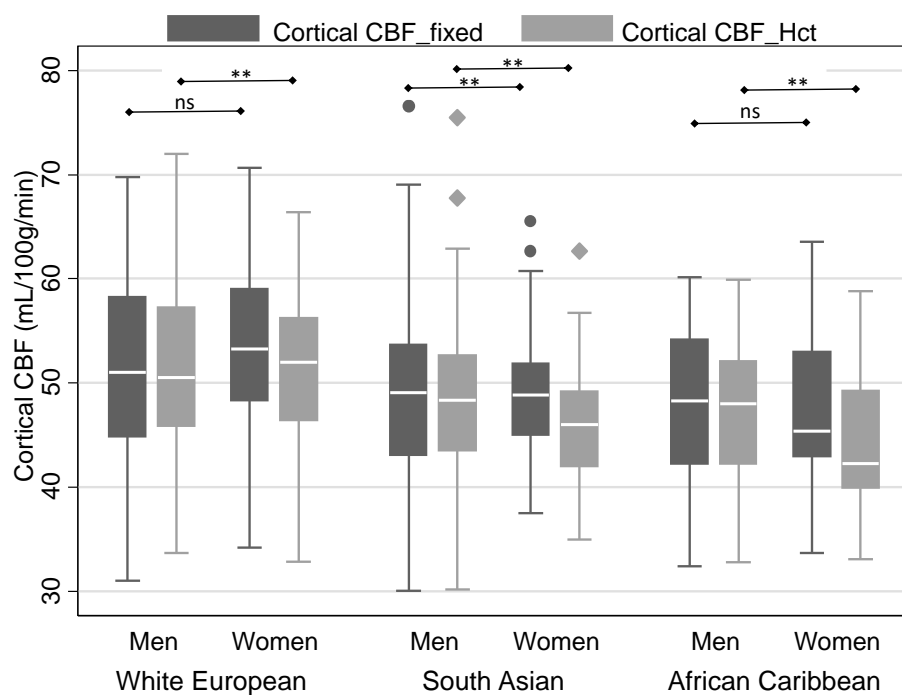


Figure 4-3. Boxplot showing median, interquartile range, upper and lower adjacent values and outside values for CBF without correction for individual haematocrit (CBF_{fixed}) and CBF with correction for individual haematocrit (CBF_{Hct}), by sex and ethnicity. * = $P < 0.05$, ** = $P < 0.01$ by 2 way analysis of variance followed by Fisher's LSD test

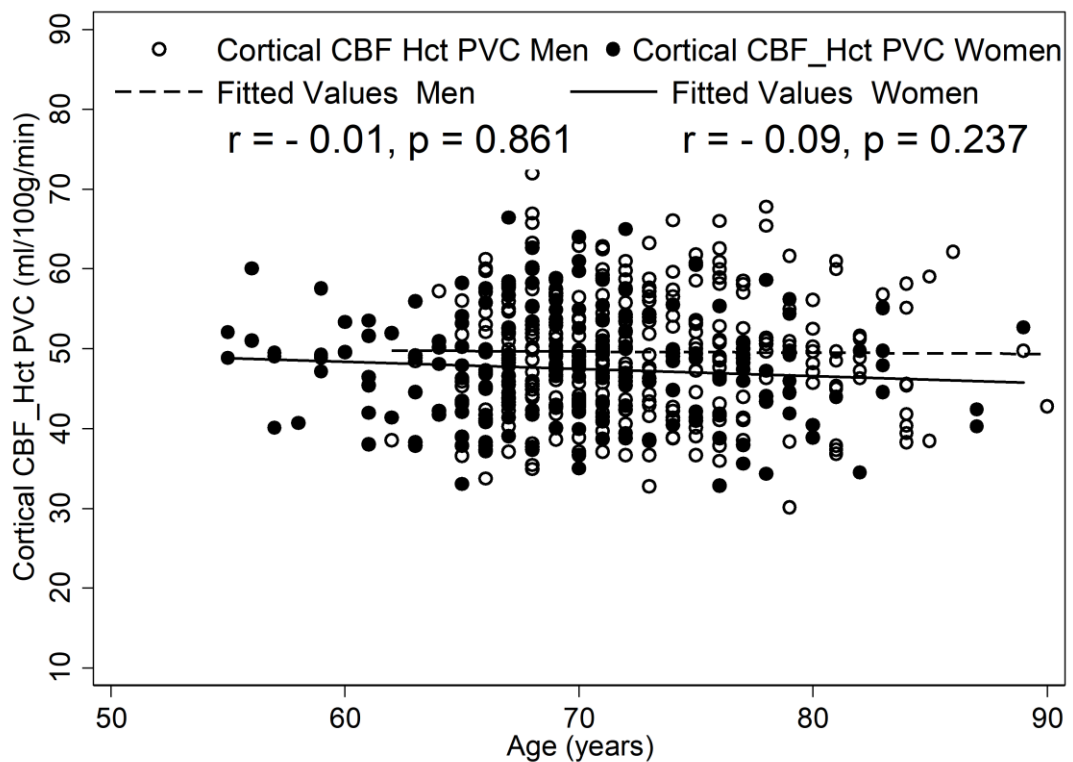


Figure 4-4. Scatterplot with line-fit and Pearson's r showing correlation of age (years) and CBF (mL/100g/min) by sex.

Figure 4-5 demonstrates the inverse linear relationship of Hct with CBF_{fixed} and CBF_{Hct} models. This relationship is attenuated with use of the CBF_{Hct} model although some association of Hct with CBF in men remained ($r = -0.18, P = .002$). Further adjustment for potential confounders of mean arterial blood pressure, BMI, diabetes and dyslipidemia did not affect this relationship when entered in a regression model ($B = -0.3, CI -0.6, -.05 \text{ mL/100g/min}, P = .020$) (**Table 4-2**). (note: Model 2 has fewer participants due to missing cardiovascular data).

Introduction of individualised Hct into CBF estimation altered the distributions of cortical CBF values in this elderly population for all ethnicities (**Figure 4-6**). The mean perfusion difference between models was greater for women in all ethnic

categories than men, with a mean decrease for women of 2.7 mL/100g/min (5.4% of the CBF_{fixed} value), ($t = 17.1$, CI: 3.0, 2.4 mL/100g/min, $P < .001$, $d=0.38$). The perfusion difference for African Caribbean women was -3.1 mL/100g/min (6.5% decrease from the CBF_{fixed} value), ($t = 10.4$, CI: -3.6, -2.5 mL/100g/min, $P < .001$, $d= 0.48$), and for South Asian women it was -3.0 mL/100g/min (6.2% decrease from the CBF_{fixed} value), ($t = 10.9$, CI: -3.6, -2.5 mL/100g/min, $P < .001$, $d= 0.56$). South Asian men were the only male category displaying a significant difference between models with a perfusion difference of -1.0 mL/100g/min (2.0% decrease from the CBF_{fixed} value) ($t = 4.3$, CI: -1.5, -2.0 mL/100g/min, $P < .001$, $d= 0.14$). **Figure 4-7** provides an example of CBF maps illustrating the decrease in CBF estimation of a female subject with an Hct of 37.3%. Application of PVC removed most of the negative association of CBF with age in both models (CBF_{fixed} , $r = -0.02$, $P = 0.7$, and CBF_{Hct} , $r = 0.00$, $P = 0.2$). Adjustment for Hct did not significantly alter this relationship.

	<i>Model 1</i>			<i>Model 2</i>		
Observations (n)	493			466		
Adjusted R²	0.26			0.28		
	<i>B</i>	<i>(95% CI)</i>	<i>P</i>	<i>B</i>	<i>(95% CI)</i>	<i>P</i>
Age (years)	-0.06	(-0.10, -0.01)	.017	-0.04	(-0.09 , 0.00)	.076
Sex (female)	-3.60	(-4.19 , -3.02)	<.001	-3.70	(-4.34 , -3.05)	<.001
South Asian	-1.80	(-2.45 , -1.14)	<.001	-1.67	(-2.36 , -0.98)	<.001
African Caribbean	-1.18	(-1.88 , -0.48)	.001	-1.15	(-1.87 , -0.44)	.002
Diabetes(Y)				-1.15	(-2.14 , -0.16)	.023
LDL cholesterol (mmol/L)				0.44	(0.10 , 0.78)	.012
HDL cholesterol (mmol/L)				-0.07	(-0.77 , 0.63)	.854
MAP (central)(mmHg)				-0.01	(-0.04, 0.02)	.594
HbA1c (mmol/L)				0.03	(-0.01, 0.08)	.160
BMI (m/kg²)				-0.02	(-0.09 , 0.05)	.642

Table 4-2. Multiple linear regression analyses of associations of demographic and cardiovascular risk factors. Hct is dependent variable, model 1 independent variables are age, sex and ethnicity, model 2 is model 1 + independent variables LDL Cholesterol, HDL Cholesterol, mean arterial pressure, HbA1c and BMI.

		<i>n</i>	<i>CBF_fixed</i> (mL/100g/min)		<i>CBF_Hct</i> (mL/100g/min)		<i>Difference</i> (mL/100g/min)	<i>Mean</i> <i>difference (%)</i>	<i>P</i>	<i>Effect</i> <i>size</i>
			<i>mean</i>	<i>SD</i>	<i>mean</i>	<i>SD</i>	<i>mean (95% CI)</i>	<i>mean</i>		<i>d</i>
	All	493	50.1	±7.9	48.8	±7.3	-1.3 (-1.5, -1.1)	-2.6	<.001	0.17
	Men	297	50.0	±8.3	49.6	±7.6	-0.4 (-0.7, -0.1)	-0.8	.005	0.05
	Women	196	50.2	±7.2	47.5	±6.8	-2.7 (-3.0, -2.4)	-5.4	<.001	0.38
European	All	226	51.8	±8.3	51.1	±7.5	-0.7 (-1.0,-0.4)	-1.4	<.001	0.09
	Men	148	51.1	±8.6	51.1	±7.7	0.0 (-0.5, 0.4)	0.0	.815	0.00
	Women	78	53.2	±7.6	51.1	±7.0	-2.1 (-2.6,-1.6)	-4.0	<.001	0.29
South Asian	All	175	49.1	±7.3	47.3	±6.7	-1.8 (-2.2, -1.4)	-3.7	<.001	0.26
	Men	108	49.4	±8.1	48.4	±7.3	-1.0 (-1.5 -0.6)	-2.0	<.001	0.14
	Women	67	48.7	±5.8	45.7	±5.0	-3.0 (-3.6, -2.5)	-6.2	<.001	0.56
African Caribbean	All	92	47.6	±6.7	45.8	±6.3	-1.8 (-2.3, -1.3)	-3.8	<.001	0.29
	Men	41	47.7	±7.0	47.4	±6.4	-0.3 (-0.9, 0.3)	-0.6	.410	0.04
	Women	51	47.6	±6.6	44.5	±6.0	-3.1 (-3.6,-2.5)	-6.5	<.001	0.48
Without diabetes		377	50.5	±7.8	49.4	±7.2	-1.1 (-1.4,-0.8)	-2.2	<.001	0.15
With diabetes		116	49.0	±8.3	47.2	±7.5	-1.8 (-2.3,-1.4)	-3.7	<.001	0.23

Table 4-3. Comparison of CBF without correction for individual haematocrit (CBF_fixed) and CBF with correction for individual Hct (CBF_Hct) by sex, ethnicity and diabetes diagnosis. Data are mean ± SD, except difference (95% CIs), mean difference (%). P values were calculated using a Student's t-test. Effect size is Cohen's d.

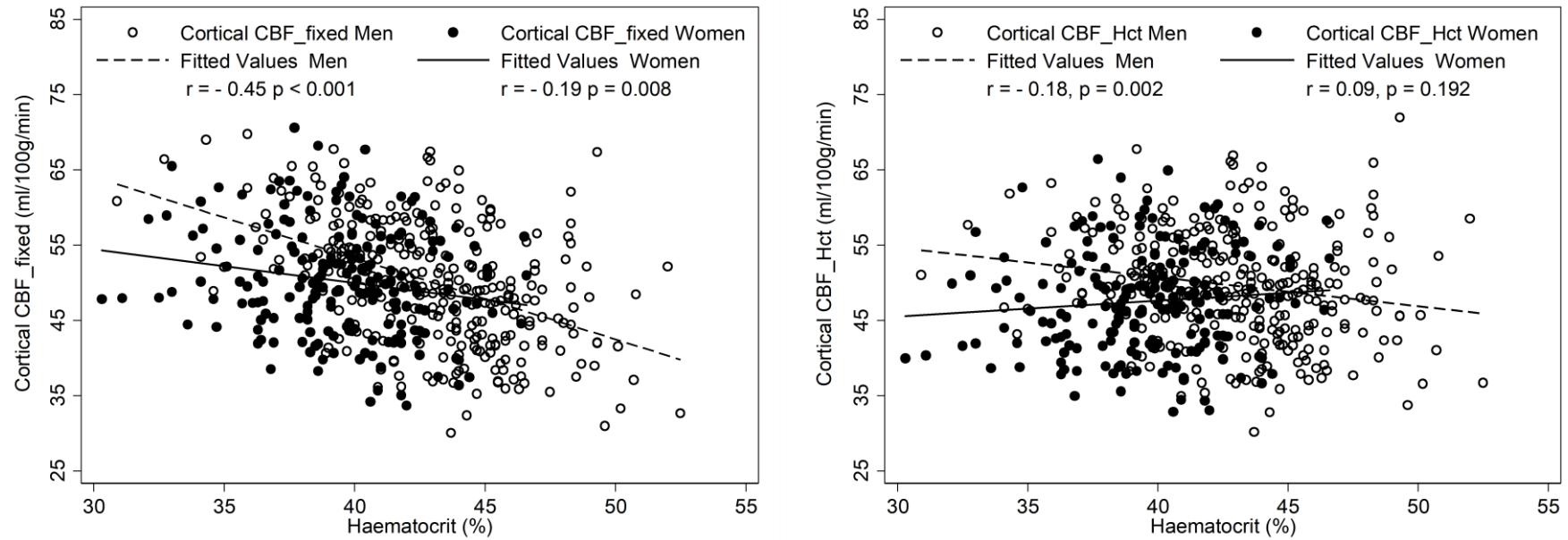


Figure 4-5. Scatterplots showing the effect of correction for individual Hct on the correlation between Hct and cortical CBF in men and women. Left figure shows CBF_{fixed} , right figure shows CBF_{Hct} .

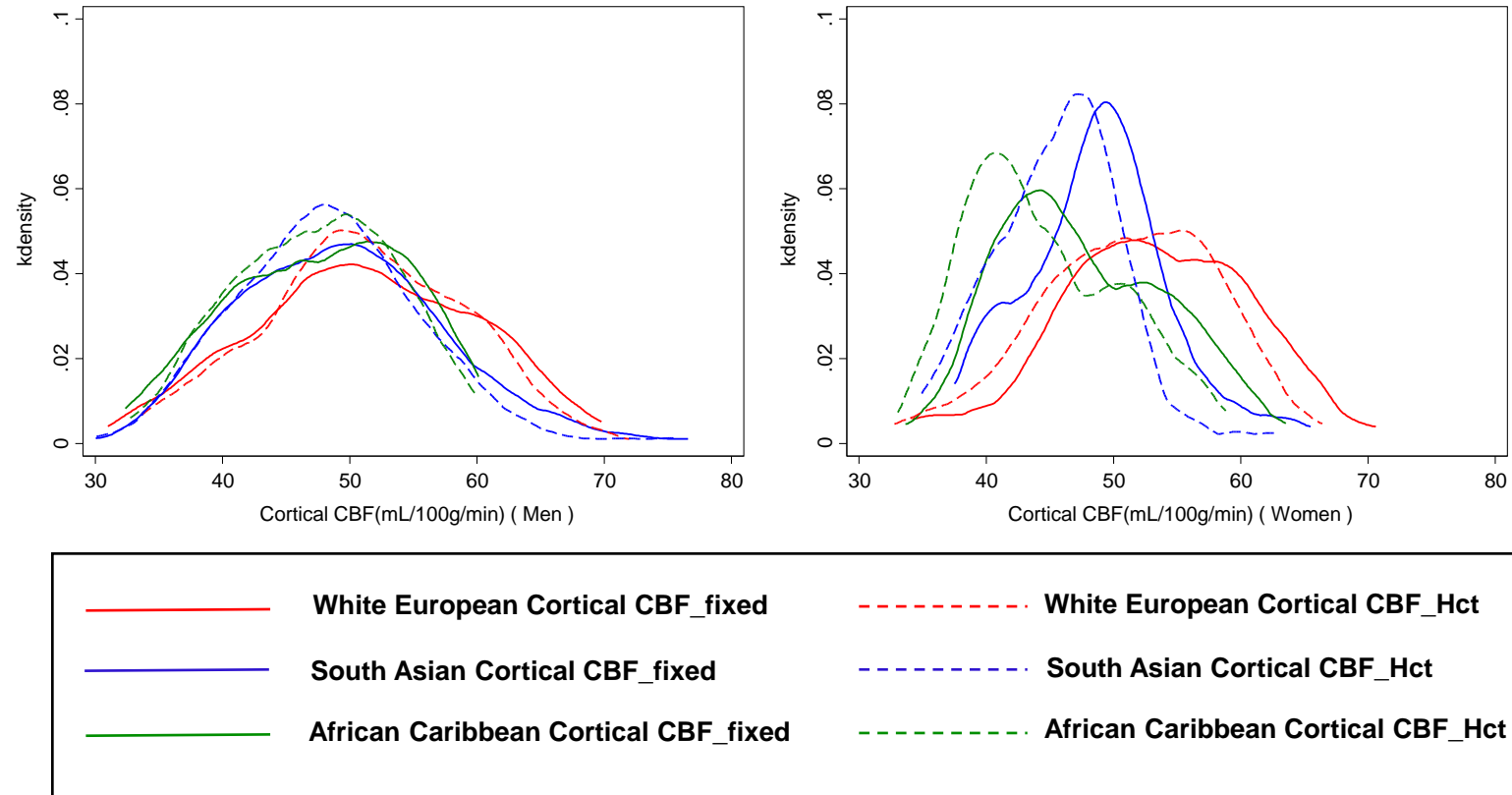


Figure 4-6. Kernel density (kdensity) plots of CBF without correction for individual Hct (CBF_{fixed}) and CBF with correction for individual Hct (CBF_{Hct}) by sex and ethnicity.

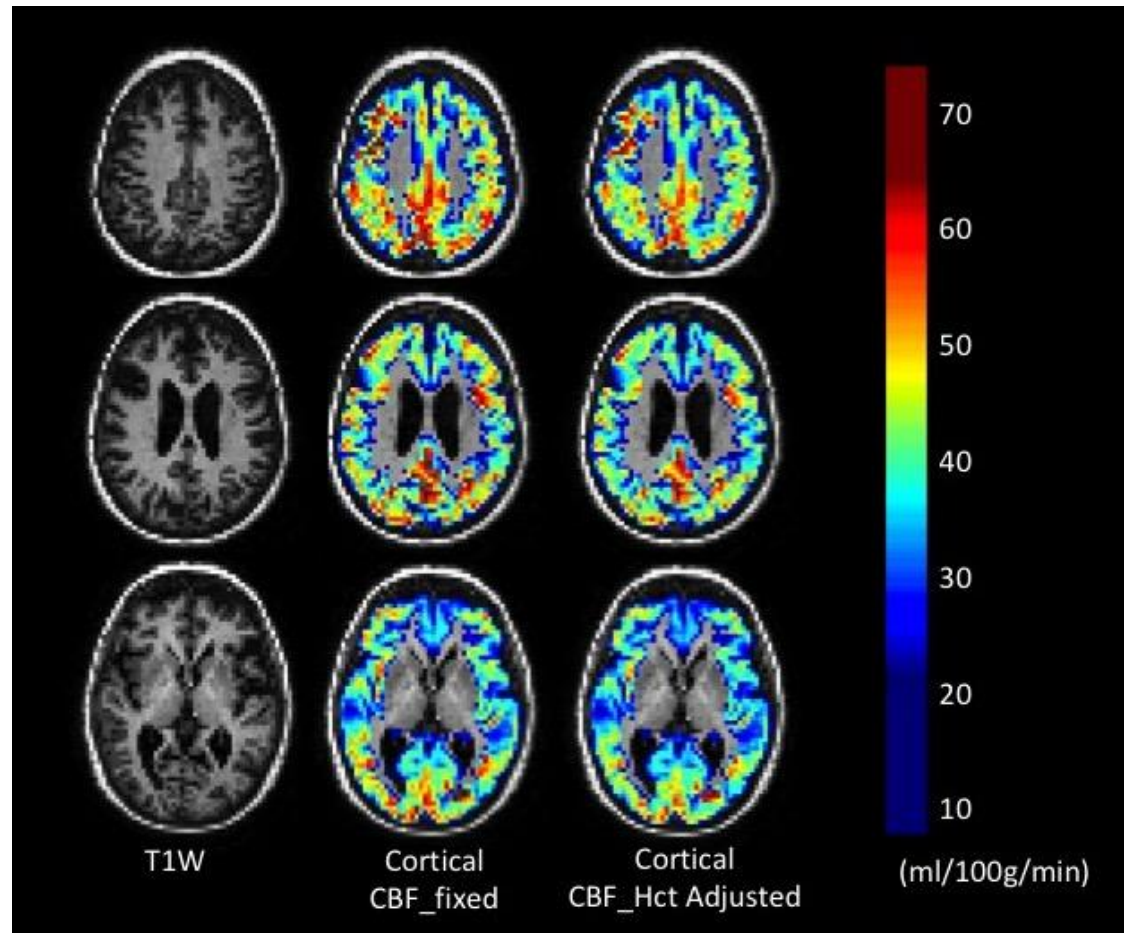


Figure 4-7. CBF maps overlaid on segmented T1w without and with adjustment for measured Hct. The subject was a white European woman with an Hct of 37.3%.

4.4.4 Diabetes

People with diabetes had a mean (SD) Hct of 40.7% (4.1) compared to 42.0% (3.5) for those without diabetes. The perfusion difference between CBF models of people with diabetes was -1.8 mL/100g/min (3.7% of the CBF_{fixed} value) ($t = 7.8$, CI: -2.3, -1.4 mL/100g/min, $P < .001$, $d = 0.23$), whereas those without diabetes only displayed a difference of -1.1 mL/100g/min (2.2% of the CBF_{fixed} value) ($t = 8.4$, CI: -1.4, -0.8 mL/100g/min, $P < .001$, $d = 0.15$) (**Figure 4-8**).

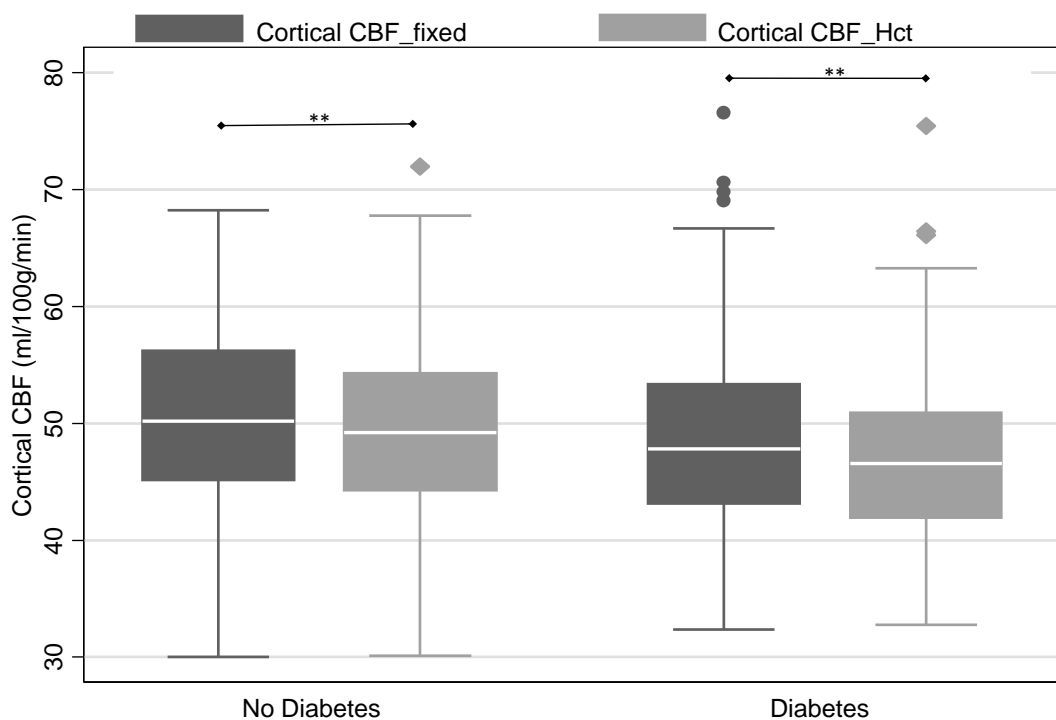


Figure 4-8. Boxplot showing median, interquartile range, upper and lower adjacent values and outside values for CBF without correction for individual Hct (CBF_{fixed}) and CBF with correction for individual Hct (CBF_{Hct}) by diabetes status. . * = $P < 0.05$, ** = $P < 0.01$ by Student's t-test.

4.5 Discussion

This study has shown that Hct levels differ according to sex and ethnicity and that this influences CBF estimated from ASL. Importantly, failure to adjust $T1_{\text{blood}}$ according to sex and ethnic variation in Hct leads to a significant overestimation of CBF in women and non-European populations. Although other studies have investigated the effect of Hct on CBF estimation with ASL in sickle cell (218) and neonatal (219) groups, this is, to the best of my knowledge, the first study to address this in a community based elderly multi-ethnic population.

A study by Parkes et al (220) using continuous ASL found females had higher grey matter CBF than males by 13%. It seems likely that failure to measure individual Hct influenced these observations. This study found a similar difference in CBF between European men and women (+ 9.1% for women) when neither Hct nor PVC were accounted for, but this difference was completely abolished by correction for Hct and PVC. Following correction for PVC and Hct, CBF was slightly lower for women than men in South Asian (-5.6%) and African Caribbean (-6.0%) ethnicities. This finding is broadly aligned with an ^{15}O PET study where differences in CBF between sexes that were evident in younger participants were not apparent in participants older than 65 years (221). It has been suggested that CBF differences by sex in young participants are due to high oestrogen levels in females causing CBF fluctuations during the menstrual cycle (222). Our large elderly sample scanned with age-appropriate parameters such as a long PLD and with CBF calculated using individualised values is likely to provide a more accurate reflection of true physiological differences than studies that have used a 'one size fits all' protocol.

This study also demonstrated that the utilisation of individually measured Hct in the calculation of $T1_{\text{blood}}$ reduced the inverse correlation between CBF and Hct as expected. However, some association remained in men even after adjustment for mean arterial blood pressure, diabetes, and dyslipidemia.

Increased CBF is an expected response to decreases in haemoglobin (and thus Hct) as a mechanism to sustain cerebral metabolic rate of oxygen levels (CMRO₂) as demonstrated by Ibaraki et al. (223). It has also been suggested that higher Hct levels and concomitant increases in blood viscosity may influence capillary flow due to alterations in functional shunting (13). The higher Hct levels found in men may provide an explanation why this study found some association between Hct and CBF only in men as increasing Hct increases blood viscosity in a non-linear relationship, and it has been suggested increased viscosity decreases CBF(224).

Lower values of Hct in those with diabetes indicate that further investigation using larger samples is warranted to investigate the interactions of sex, ethnicity, Hct and the effect of diabetes on CBF. It should be noted that differences in CBF by ethnicity may be confounded by the greater prevalence of diabetes in South Asians (37%) and African Caribbeans (32%) compared to Europeans (17%)(**Table 4-1**) and these relationships warrant further investigation.

Investigation of the association of age and CBF, which had yielded conflicting evidence in previous studies (225) (220) (226) was not the main aim of our study. However, it is noteworthy that this study found an association between age and CBF in the non-partial volume corrected data which disappeared following partial volume correction. A likely explanation for this is decreased brain volume in older participants which makes the ASL perfusion data more prone to partial volume effects with non-perfused CSF, thereby leading to an artificial CBF decrease. However, PVC may introduce overestimation of cortical CBF particularly in examinations hampered by head movement or poor SNR, either in the T1 structural images used for segmentation, or in the ASL acquisition which as a subtraction technique is particularly susceptible to movement artefact. Some movement inevitably remains in a large population study of elderly individuals and this may be a potential source of under or overestimation of partial volume corrected CBF in our cohort.

Despite a more diverse ethnic sample, our cortical CBF values are comparable to previous studies using PCASL on elderly, community-dwelling populations (78, 206). PCASL has some limitations when applied to elderly participants. One factor affecting CBF quantification is blood velocity relative to the labelling plane. Any discrepancies from the expected range of blood velocities due to vascular pathologies such as internal carotid stenosis or vessel tortuosity might result in reduced labelling efficiency and therefore CBF underestimation. Our study used 2D PCASL, rather than a 3D technique, which may be liable to decreased SNR due to longer T1 blood relaxation in slices near the vertex due to sequential slice acquisition (227), despite using slice-timing correction. Inefficiency of background suppression pulses during multiple slice acquisitions may also have affected the ASL signal.

The main strength of this study was its large community-based, elderly, ethnically diverse sample studied in a single centre so that all protocols were consistently applied throughout. Limitations of the study include a potential selection bias towards healthy individuals who were willing and able to attend the research clinic. Another limitation was the absence of direct T1_{blood} measurements, although this was mitigated by the use of a previously published model to account for the effect of Hct (42). Hct is the main determinant of T1_{blood}, but other factors such as serum ferritin and HDL-cholesterol may also contribute to a minor extent (228). Measurement of arterial rather than venous Hct would have been more appropriate to estimate CBF. However, measuring arterial Hct in clinic was impractical and it was considered that venous and arterial Hct were closely related and importantly, that venous Hct could be sampled consistently (229). Although T1_{blood} can be easily directly measured in the left ventricle and has lower test-retest variability compared to measured Hct (230), comparable sequences in the brain are more challenging due to partial volume effects, blood velocity and pulsatility in the measured vessel (219, 231).

Our findings suggest that research studies using ASL to measure CBF should routinely measure Hct to adjust $T1_{\text{blood}}$, especially in inhomogeneous samples. Alternatively, substitution of an appropriate sex and ethnicity specific Hct value derived from population group means or direct measurement of $T1_{\text{blood}}$ during MRI would improve accuracy of CBF measurement. Further research is warranted into whether adjustment to the Hct value in CBF models to accommodate demographic and pathological differences provides stronger associations with cerebrovascular disease, dementia and cognitive decline than previous models using a fixed mean Hct value. Results from previous studies may need to be interpreted with caution where there are ethnic, gender and pathological differences in the sample. Such an approach may improve early risk assessment in ethnic groups and identify potentially vulnerable groups such as those with known vascular or metabolic disease.

4.6 Conclusion

In conclusion, it was demonstrated that CBF values obtained from ASL using a fixed Hct mean may lead to systematic errors, resulting most frequently in an overestimation of CBF in female participants and non-Caucasian ethnicities. It is important to be aware of this when using CBF threshold values to assess disease status or severity. This applies not only to the discrimination between normal ageing and neurodegenerative diseases such as AD but could potentially also influence discrimination between high and low-grade brain tumours (232) or the determination of penumbral threshold values in stroke (233). These conclusions suggest that whenever possible, individualised measures of Hct should be included in CBF calculations by ASL.

5 . Associations of cardiovascular risk with cerebral blood flow in a tri-ethnic elderly population cohort.

5.1 Abstract

The aim of this chapter is to investigate the relationships of CBF and cardiovascular risk in a multi-ethnic elderly population with a high prevalence of diabetes. It was hypothesised that increased cardiometabolic risk (i.e. diabetes and VRFs) would be associated with lower CBF, but these relationships would be moderated by sex, ethnicity and diabetes status. 485 participants from the SABRE study underwent a battery of cardiovascular tests and brain MRI including ASL perfusion scans. CBF was calculated using the formula including individually measured Hct described in Chapter 4 of this thesis. Multiple linear regression analyses were conducted using CBF as the outcome, with demographic variables, cardiovascular measurements and a derived composite cardiovascular risk score (FRS) as predictors.

Based on main effects analyses of the whole sample, women had lower CBF than men. South Asians and African Caribbeans had lower CBF than Europeans and participants with diabetes had lower CBF than those without diabetes. FRS and systolic BP were negatively associated with CBF. HDL cholesterol was positively associated with CBF. Stratified analyses based on sex revealed a more complex pattern of associations. There was evidence that the association between increased systolic BP and lower CBF was stronger in men than women, while the association of FRS with CBF was moderated by both ethnicity and sex. The patterns of association between diabetes and CBF varied by ethnicity suggesting a difference in cardiovascular phenotypes in individuals without diabetes.

Results indicate diabetes and cardiovascular risk are associated with CBF in older age, but ethnicity and sex moderate these relationships. Previous work on more homogenous populations and analysis that has not investigated group effect modification may lack generalisability and miss important differences in sex and ethnic groups in the management of cognitive changes in the elderly.

5.2 Introduction

Studies of elderly subjects have shown increased severity of cognitive impairment to be associated with decreased CBF in memory clinic patients (78-82, 126). Although the shared risks of cardiovascular disease and cerebral ill health in old age have been extensively explored, their associations remain complex and mechanisms are not entirely understood. For example, hypertension has been strongly associated with cerebrovascular disease, but its effect appears to be moderated by a number of conditions such as sex, age, disease duration, age of onset, BP lowering medication, and genetic factors (103, 118, 119, 126). Diabetes has been linked with reduced brain volumes (234), but there is mixed evidence regarding its association with SVID (235) (236) and lower brain perfusion (134, 135, 139). It is not clear whether there is a synergistic effect of multiple VRFs on neurovascular disease. Furthermore, there is sparse evidence for the roles of ethnicity and sex as effect modifiers in these relationships. Differing vulnerabilities of ethnic and gender groups remain under-investigated despite evidence suggesting variable relationships between cerebral outcomes and level of vascular risk. For example, high BP has been associated with reduced CBF in men but not women in a SPECT study measuring cerebral perfusion (126). Ethnic differences in relation to the impact of vascular risk have been found in a number of studies. A study in the US found African Americans to have higher volumes of DWMHs in association with cardiovascular disease compared to Americans of European descent (237). Another study found increased microvascular dysfunction in African Caribbeans with diabetes compared to Europeans even after adjustment for cardiovascular risk (201). Similarly, the SABRE study found excess stroke risk in South Asians and African Caribbeans compared to Europeans that could not be entirely explained by differences in metabolic risk factors (238). Clarification of demographic differences in such associations should be used to underpin evidence-based treatment decisions aimed at reducing the prevalence, progression and severity of cognitive dysfunction resulting from cardiovascular poor health and neurovascular disease.

This chapter examines the relationships of cortical perfusion with vascular risk measured in older age. 485 individuals from a tri-ethnic community-based cohort underwent a battery of cardiovascular tests and brain MRI. Separate measures of vascular risk adjusted for other vascular risk and demographic covariates were used to assess associations with CBF. Secondly, a composite score of multifactorial vascular risk, the FRS, was entered in models in order to evaluate the impact of aggregated vascular risk on CBF. Cerebral perfusion was estimated using CBF calculated from ASL using the method described in chapter 4. It was hypothesised that higher levels of VRFs would be associated with lower CBF, and that sex, ethnicity and diabetes would modify these associations.

5.3 Materials and methods

See Chapter 3: 'General Methods' (pp81-91) for study sample, MRI acquisition protocol, MRI post-processing and cardiovascular data collection methods.

5.3.1 Statistical analysis

All statistical analyses were performed using STATA 14.2 (College Station, Texas).

5.3.1.1 Descriptive statistics

Cardiovascular characteristics were compared by sex and ethnicity. Continuous data are presented as mean \pm SD, categorical data are numbers and percentages. Frequency histograms were inspected to check for normal distribution of continuous variables.

5.3.1.2 Statistical testing

Tests for significance used unpaired 2-tailed Student's *t* tests for continuous variables for independent variable groups with 2 levels and Pearson Chi² for categorical variables. Differences between 3 ethnic groups were assessed by ANOVA for continuous variables followed by individual group-wise comparisons using Fisher's LSD test if ANOVA was significant at $P < .05$. Since ANOVA was used as a permissive test no adjustment was made for multiple testing.

Firstly, bivariate analyses were performed to evaluate unadjusted associations of continuous covariates (correlations) with CBF prior to modelling with multiple linear regression. Boxplots were inspected for relationships of categorical variables with CBF. Bivariate associations between a predictor and an outcome may be due to an omitted confounder associated with both variables. Further analysis was therefore performed using multiple linear regression models to provide estimates of relationships corrected for the influence of possible confounding variables. Inclusion of multiple variables in models (i.e. 'adjustment') estimates the association between predictor and outcome with all other variables in the model 'held constant' at their average value -hence it (potentially) estimates the unconfounded association between predictor and outcome.

Cortical CBF adjusted for PVC and individually measured Hct was the dependent variable in multiple linear regression models. Descriptions of each multiple linear regression model are listed in **Table 5-1** and **Table 5-2**. CBF corrected for both Hct and partial volume was used as the outcome as it was considered to be the most accurate measurement of CBF in our ethnically diverse, elderly sample who were subject to brain atrophy and variation in Hct. As suggested in Chapter 4, variance in Hct affects CBF estimation due to its influence on the calculation of blood T1. PVC aims to adjust for partial volume effects which are particularly common in elderly participants due to age-related brain atrophy. Independent variables were either single VRFs in addition to demographic variables, or FRS, a composite measure of cumulative cardiovascular risk constructed from multiple vascular risk factors. Use of composite algorithms such as the FRS enable the combination of multiple continuous and categorical VRFs to make a single continuous variable. The aim is to capture any additional risk resulting from the presence of multiple VRFs and to enable construction of simple and stable models. Demographic variables of age and sex were not added to FRS models due to their inclusion in the FRS algorithm. VRFs in the single factor models were selected *a priori* on the basis of their inclusion in the FRS (198). Beta coefficients are reported in

unstandardized form with their 95% confidence intervals to reduce reliance on statistical significance. Partial η^2 values are shown to aid comparison between variables of different units and to indicate the strength of an effect by showing the amount of variance in the model accounted for by a specific variable. η^2 was calculated using the STATA 'esize' command which calls $SSEffect/(SSEffect+SSError)$. All single factor VRF models were tested for significant interactions between VRFs and between VRFs and ethnicity. Models with significant interactions are shown. Likelihood ratio (LR) tests compared nested models for goodness of fit. The assumptions of linearity and homoscedasticity which are implicit to linear regression models were checked by inspection of residuals. Model fit was assessed using the Akaike Information Criterion (AIC). Multicollinearity of independent variables were checked by variance inflation factor (VIF) tests with $VIF > 10$ taken to indicate major multicollinearity. Results were considered significant at $P < .05$.

Exploratory analysis indicated that the pooled sample was not homogeneous as sex modified some of the relationships between predictors and outcome variables. Therefore, secondary stratified analyses of men and women as separate samples were performed (see chapter 3 'General Methods' p101). Further analyses of groups with and without diabetes were conducted to detect whether presence of diabetes modified the relationship of vascular risk and CBF.

Dependent Variable: CBF (mL/100g/min)

	Model 1	Model 2	Model 3	Model 4
Independent variables	Sex (If applicable)	Sex (If applicable)	Sex (If applicable),	Sex (If applicable),
	Ethnicity	Ethnicity	Ethnicity	Ethnicity
	Age (Years)	Age (years)	Age, (years)	Age, (years)
		<i>Interaction</i> Age*ethnicity	Diabetes, (Y/N)	Diabetes, (Y/N)
			Systolic BP, (mmHg)	Systolic BP, (mmHg)
			Antihypertensive medication (Y/N)	Antihypertensive medication (Y/N)
			HDL cholesterol, mmol/L	HDL cholesterol, mmol/L
			Total cholesterol, mmol/L	Total cholesterol, mmol/L
			Smoking(current) (Y/N)	Smoking(current) (Y/N)
				<i>Interaction</i> Diabetes*ethnicity*
				<i>Interaction</i> Age*ethnicity**
Sample				
All	1a	2a	3a	4a(l)*, 4a(li)**
Men	1b	2b	3b	4b(l)*, 4b(li)**
Women	1c	2c	3c	4c(l)*, 4c(li)**
Diabetes	1d	-	3d	-
No diabetes	1e	-	3e	-

Table 5-1. Key to multiple linear regression models using vascular risk factors as predictor variables, * and ** denote interaction models.

Dependent Variable: CBF (mL/100g/min)

	Model 5	Model 6
Independent variables	Ethnicity Framingham risk score	Ethnicity Framingham risk score <i>Interaction</i> Ethnicity*Framingham risk score
Sample		
All	5a	6a
Men	5b	6b
Women	5c	6c
Diabetes	5d	6d
No Diabetes	5e	6e
Men, with diabetes	5f	6f
Men, no diabetes	5g	6g
Women, with diabetes	5h	6h
Women, no diabetes	5i	6i

Table 5-2. Key to multiple linear regression models using FRS as predictor variable.

5.4 Results

Basic characteristics and cardiovascular characteristics are presented in **Table 5-3** and **Table 5-4** (all participants), **Table 5-5** and **Table 5-6** (men), **Table 5-7** and **Table 5-8** (women).

5.4.1 Demographic characteristics

40% of the sample were women. The mean (SD) age was 71.6 years (± 5.9) with a range of 55 -90 years. Women were on average ~3 years younger than men, mean (SD) 69.7 (± 6.4) years, compared to 72.9 (± 5.2) years. There were fewer South Asians (35%) and African Caribbeans (19%) than Europeans (46%) (**Figure 5-1**). South Asians were slightly younger than Europeans or African Caribbeans, mean (SD) (70.8 (± 5.6) years; 72.1 (± 5.8) years; 72.0 (± 6.7) years, respectively.

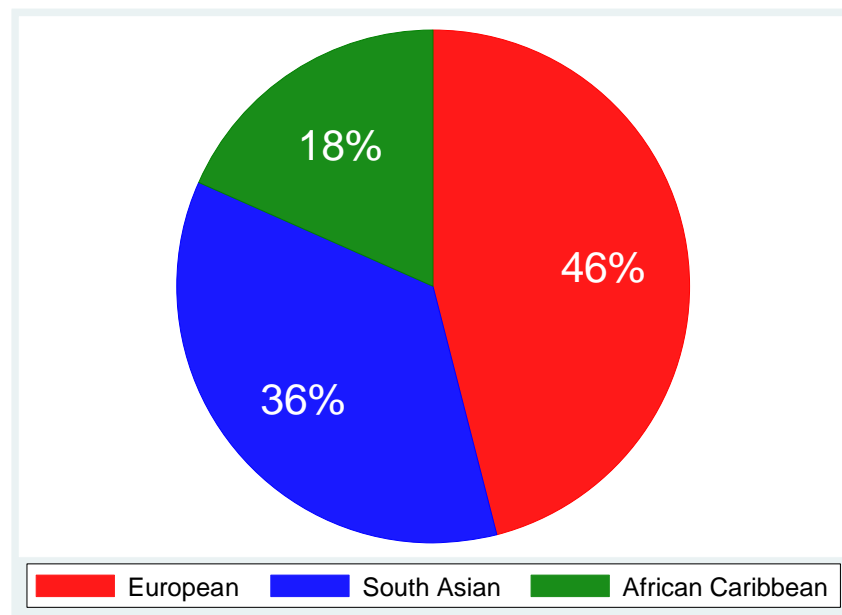


Figure 5-1. Pie chart of distribution of sample by ethnic group (% of sample).

5.4.2 Cardiovascular characteristics

Histograms depicting the distributions of continuous cardiovascular variables are shown in **Figure 5-2** (FRS), **Figure 5-3** (age), **Figure 5-4** (SBP), **Figure 5-5** (HDL cholesterol) and **Figure 5-6** (total cholesterol).

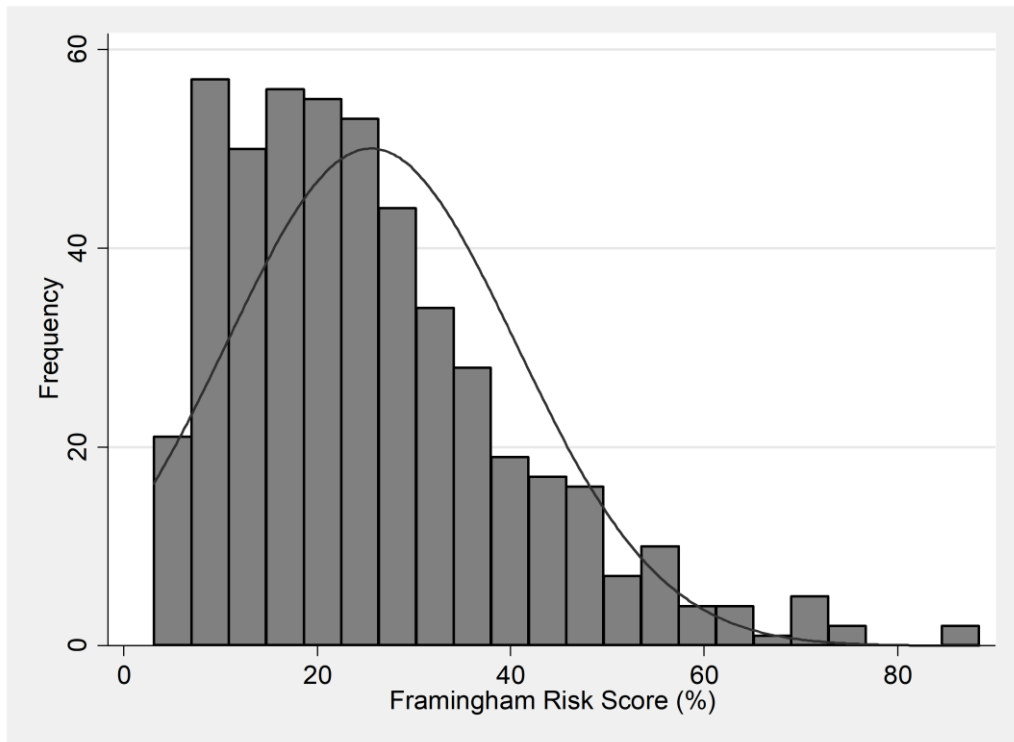


Figure 5-2. Histogram with normal density overlay, showing distribution of FRS, pooled sample.

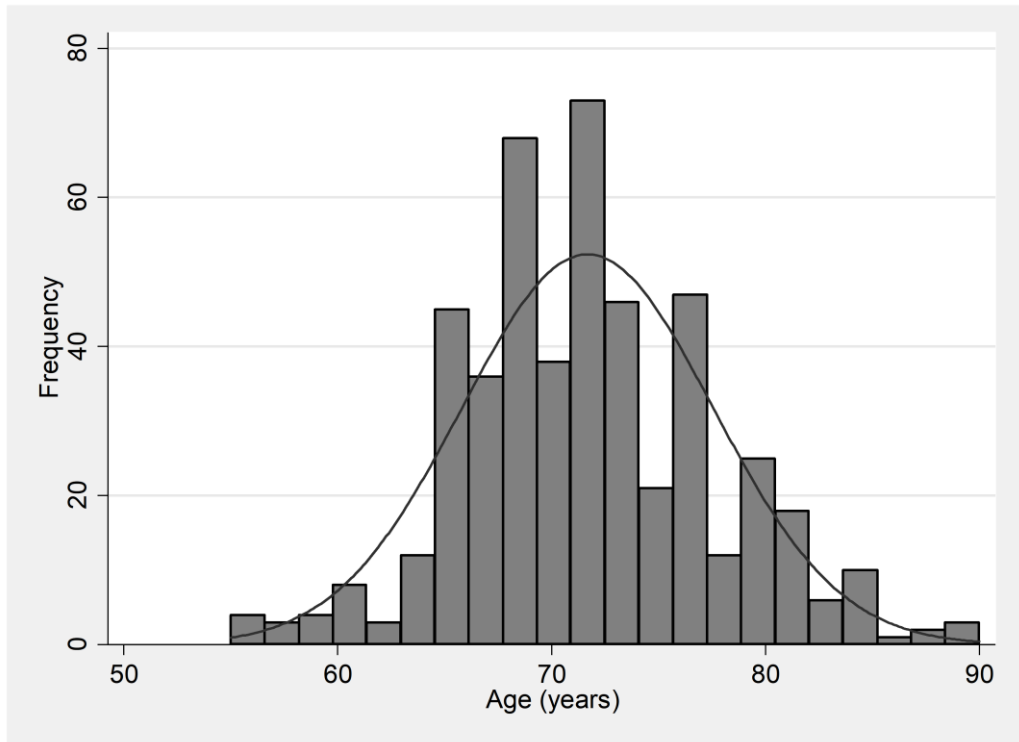


Figure 5-3. Histogram with normal density overlay, showing distribution of age, pooled sample.

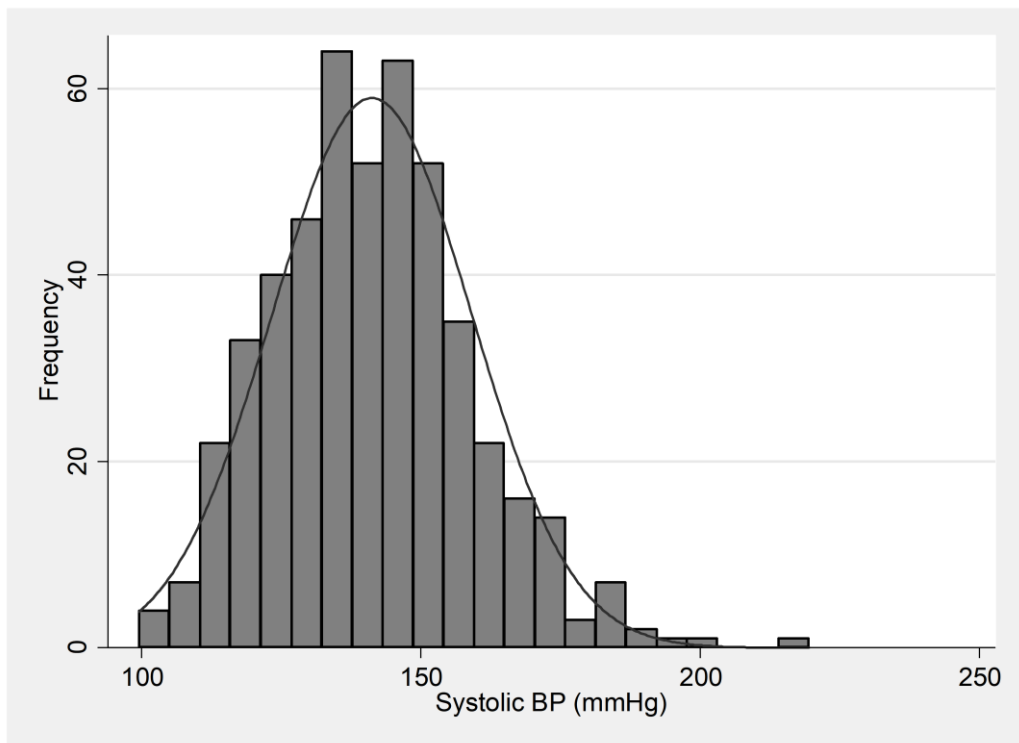


Figure 5-4. Histogram with normal density overlay, showing distribution of systolic BP, pooled sample.

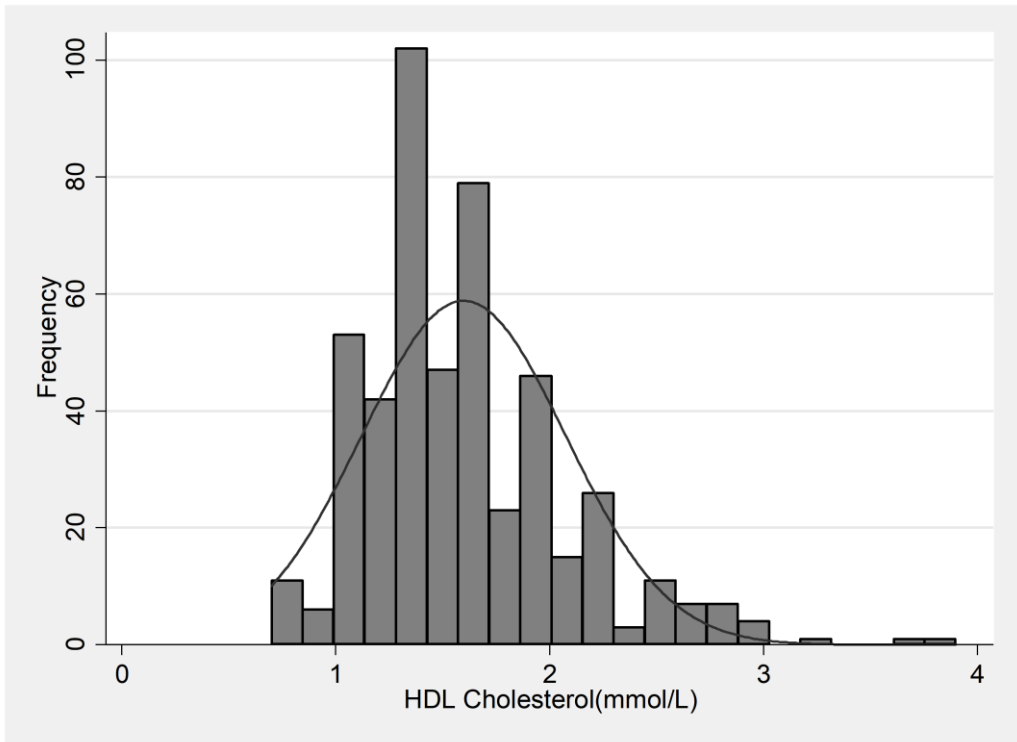


Figure 5-5. Histogram with normal density overlay, showing distribution of HDL cholesterol, pooled sample

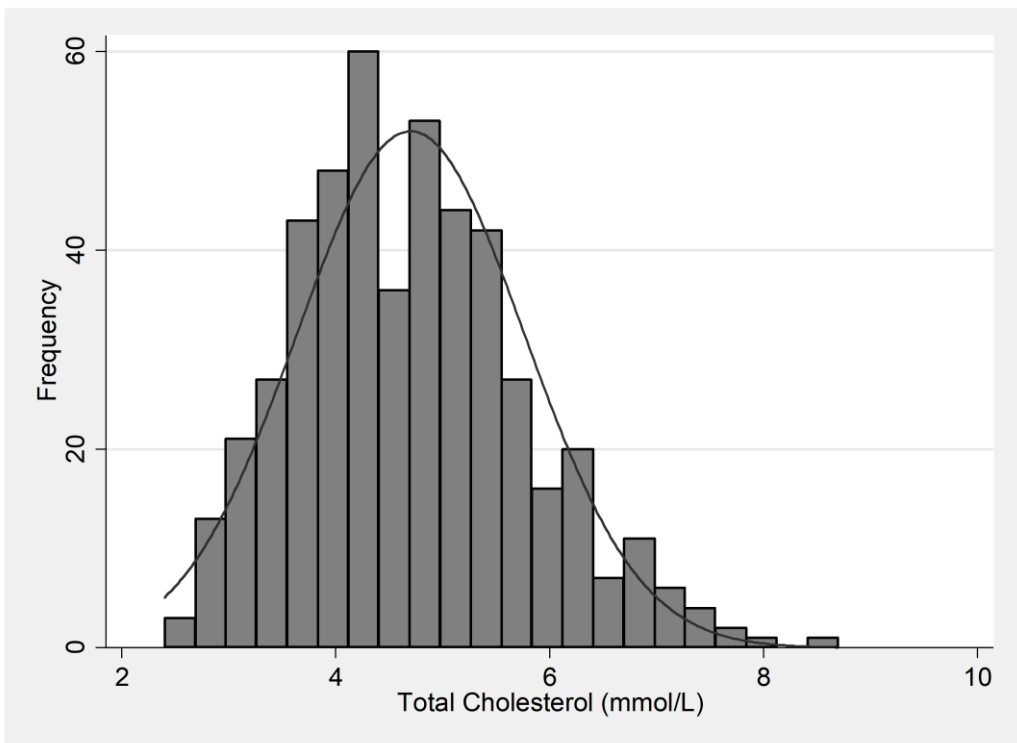


Figure 5-6. Histogram with normal density overlay, showing distribution of total cholesterol pooled sample.

27% of the sample were classified 'with diabetes'. Participants 'with diabetes' were equally distributed between sexes but there was a lower prevalence in Europeans (18%) than South Asians (38%) or African Caribbeans (30%). The majority of South Asians and African Caribbeans took anti-hypertensive medication (69%), compared to 44% of Europeans. 61% of African Caribbeans took lipid lowering medication compared to 53% of Europeans and 36% of South Asians. Very few participants were current smokers. Women had higher BMI than men in all ethnicities. They also had higher LDL, HDL and total cholesterol. The mean (SD) systolic BP of European women (133 mmHg, ± 18.9) was lower than all other groups including European men (140 mmHg, ± 17.5), South Asian women (146.2 mmHg ± 18.5) and African Caribbean women (142.2 mmHg, ± 15.3). Diastolic BP was more uniform across both sexes and all ethnicities.

5.4.3 Framingham risk score

Figure 5-7 shows median and interquartile range (IQR) of FRS by sex and ethnicity. The mean (SD) FRS was 25.6% (± 15.0) risk of a cardiovascular event in 10 years. Overall men had much higher scores than women. South Asians had higher mean (SD) FRS (28.6% ± 16.1) than Europeans (23.9% ± 14.3) or African Caribbeans (23.7% ± 13.5). Amongst men, South Asians had the highest mean (SD) FRS (35.4% ± 15.1), despite being the youngest male group, followed by African Caribbeans (30.1% ± 13.7) and Europeans (29.6% ± 13.8). European women had the lowest mean (SD) FRS (12.9% ± 6.9) compared to South Asian (17.1% ± 11.0) and African Caribbean women (18.4% ± 10.9).

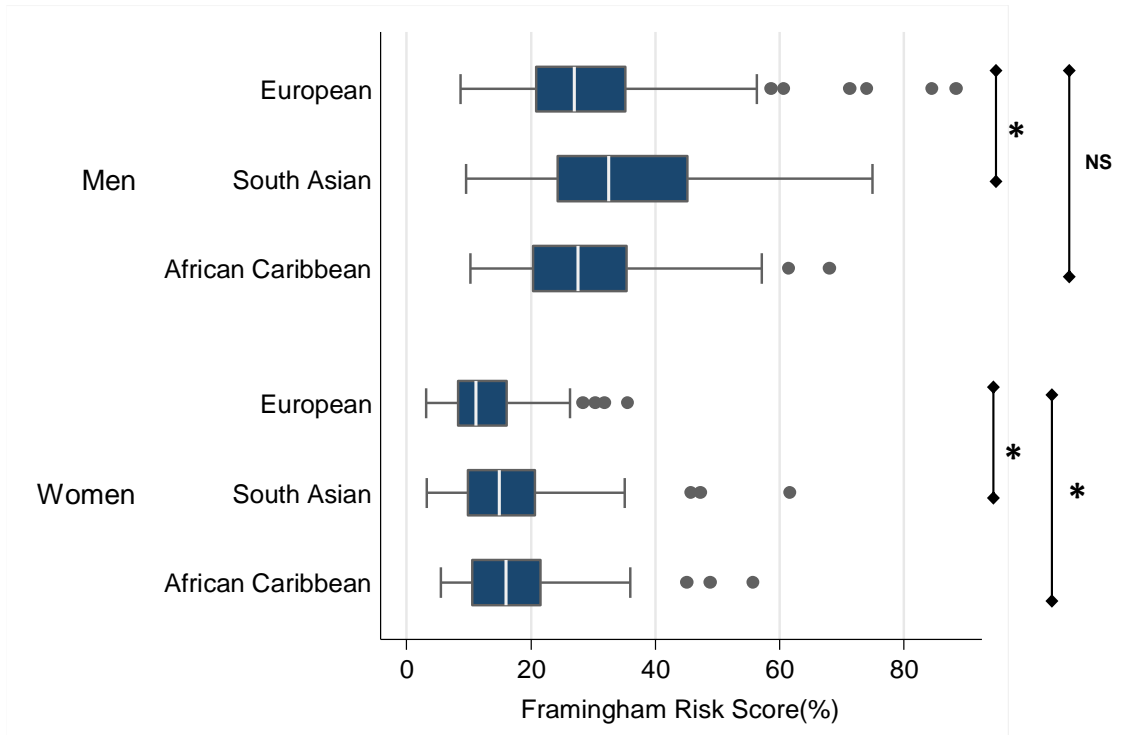


Figure 5-7. Boxplot showing FRS by sex and ethnicity. Data show median (solid white line), IQR (solid blue block), upper and lower adjacent values, (i.e. 1.5 x nearest IQR range), (whiskers), and outliers (dots).

Categorical variables (Pooled sample)	European		South Asian		African Caribbean		P
	n	n (%)	n	n (%)	n	n (%)	
n = 485	223	(46)	173	(36)	89	(18)	<.001**
Sex (female)	223	76 (34)	173	65 (38)	89	49 (55)	.002
Diabetes (Y)	223	39 (18)	173	65 (38)	89	27 (30)	<.001
Anti-hypertensive medication (Y)	223	99 (44)	173	119 (69)	89	61 (69)	<.001
Lipid lowering medication(Y)	223	119 (53)	173	63 (36)	89	54 (61)	<.001
Smoking, (current)	223	9 (4)	173	3 (1.7)	89	3 (3)	.419*
Stroke (Y)	223	7 (3)	173	3 (1.7)	89	4 (5)	.581*
Myocardial infarction (Y)	223	8 (4)	171	9 (5)	89	1 (1)	.297*

Table 5-3: Demographic and cardiovascular characteristics for categorical variables by ethnicity. Data are number of observations and (%). Tests for significance use Chi square or *Fisher's exact, **uses chi square goodness of fit. P <0.05 shown in bold.

Continuous variables (Pooled sample)	European		South Asian		P	African Caribbean		P
	n	mean (\pmSD)	n	mean (\pmSD)		n	mean (\pmSD)	
Age, years	223	72.1 (\pm 5.8)	173	70.8 (\pm 5.6)	.024	89	72.3 (\pm 6.5)	.864
Framingham risk score, %	223	23.9 (\pm 14.3)	173	28.7 (\pm 16.1)	.002	89	23.7 (\pm 13.5)	.896
HbA1c, mmol/mol	220	39.2 (\pm 7.8)	169	43.9 (\pm 8.9)	<.001	89	43.62 (\pm 10.7)	<.001
BMI, kg/m²	223	27.5 (\pm 4.1)	173	26.4 (\pm 3.7)	.006	89	29.6 (\pm 4.4)	<.001
Haematocrit, %	223	42.7 (\pm 3.6)	173	40.8 (\pm 3.8)	<.001	89	40.8 (\pm 3.4)	<.001
Total cholesterol, mmol/L	223	4.8 (\pm 1.1)	173	4.5 (\pm 1.0)	.002	89	4.9 (\pm 1.1)	.746
LDL, mmol/L	222	2.6 (\pm 0.9)	172	2.3 (\pm 0.9)	.011	89	2.5 (\pm 1.0)	.825
HDL, mmol/L	223	1.6 (\pm 0.5)	173	1.5 (\pm 0.4)	.005	89	1.8 (\pm 0.6)	.001
Systolic BP, mmHg	223	138.0 (\pm 18.2)	173	144.7 (\pm 18.4)	<.001	89	142.4 (\pm 14.5)	.048
Diastolic BP, mmHg	223	78.2 (\pm 10.3)	173	78.9 (\pm 10.1)	.511	89	79.6 (\pm 9.2)	.260
Heart rate, bpm	216	64.5 (\pm 10.9)	170	63.5 (\pm 11.0)	.350	87	64.8 (\pm 12.1)	.845
MAP, mmHg	215	96.6 (\pm 10.1)	170	96.6 (\pm 9.8)	.968	87	98.7 (\pm 10.0)	.103

Table 5-4. Demographic and cardiovascular characteristics for continuous variables by ethnicity, pooled sample. Data are mean \pm SD. Tests for significance are compared to reference (white Europeans) by post hoc Fisher's LSD test after ANOVA. *P* <0.05 shown in bold

Categorical variables (men)	European		South Asian		African Caribbean		P
	n	n (%)	n	n (%)	n	n (%)	
n = 295	147	(50)	108	(37)	40	(14)	<.001**
Diabetes (Y)	147	29 (20)	108	43 (40)	40	7 (18)	.001
Anti-hypertensive medication (Y)	147	75 (51)	108	36 (33)	40	25 (63)	<.001
Lipid lowering medication (Y)	147	77 (48)	108	63 (36)	40	25 (63)	.001
Smoking, (current)	147	4 (3)	108	3 (3)	40	1 (3)	.1.00*
Stroke (Y))	147	7 (5)	108	2 (2)	40	1 (3)	.498*
Myocardial infarction (Y)	147	7 (5)	108	9 (8)	40	1 (3)	.366*

Table 5-5. Demographic and cardiovascular characteristics for categorical variables by ethnicity (men), Data are number of observations and (%). Tests for significance use Chi square or *Fisher's exact, **uses chi square goodness of fit. P <0.05 shown in bold.

Continuous variables (men)	European		South Asian		P	African Caribbean		P
	n	mean (\pm SD)	n	mean (\pm SD)		n	mean (\pm SD)	
Age, years	147	73.1 (\pm 5.3)	108	72.4 (\pm 4.8)	.273	40	73.8 (\pm 5.7)	.421
Framingham risk score,%	147	29.6 (\pm 13.8)	108	35.4 (\pm 15.1)	.002	40	30.1 (\pm 13.7)	.847
HbA1c, mmol/mol	147	39.3 (\pm 7.2)	108	44.2 (\pm 9.0)	<.001	40	39.4 (\pm 7.6)	.930
BMI, kg/m ²	147	27.7 (\pm 3.9)	108	25.8 (\pm 3.1)	<.001	40	28.0 (\pm 4.0)	.709
Haematocrit, %	147	43.8 (\pm 3.4)	108	42.0 (\pm 3.6)	<.001	40	43.2 (\pm 2.8)	.364
Total cholesterol, mmol/L	147	4.5 (\pm 0.9)	108	4.3 (\pm 1.0)	.030	40	4.8 (\pm 1.3)	.137
LDL, mmol/L	146	2.4 (\pm 0.8)	108	2.3 (\pm 0.9)	.243	40	2.5 (\pm 1.1)	.351
HDL, mmol/L	147	1.5 (\pm 0.4)	108	1.4 (\pm 0.3)	.006	40	1.8 (\pm 0.6)	.003
Systolic BP, mmHg	147	140.0 (\pm 17.5)	108	144 (\pm 18.4)	.097	40	142.6 (\pm 13.7)	.429
Diastolic BP, mmHg	147	78.9 (\pm 9.9)	108	78.5 (\pm 10.6)	.761	40	78.4 (\pm 9.9)	.522
Heart rate, bpm	143	63.8 (\pm 10.7)	106	61.7 (\pm 10.6)	.128	38	59.5 (\pm 11.9)	.031
MAP, mmHg	143	96.7 (\pm 10.0)	106	96.3 (\pm 10.0)	.735	38	99.1 (\pm 10.0)	.169

Table 5-6. Demographic and cardiovascular characteristics for continuous variables by ethnicity, (men). Data are mean \pm SD. Tests for significance are compared to reference (Europeans) by post hoc Fisher's LSD test after one-way ANOVA. P <0.05 shown in bold.

<i>Categorical variables (women)</i>	<i>European</i>		<i>South Asian</i>		<i>African Caribbean</i>		<i>P</i>
	<i>n</i>	<i>n (%)</i>	<i>n</i>	<i>n (%)</i>	<i>n</i>	<i>n (%)</i>	
<i>n = 295</i>	76	76 (40)	65	65 (34)	49	49 (26)	.052**.
<i>Diabetes (Y)</i>	76	10 (13)	65	22 (34)	49	20 (41)	.001
<i>Anti-hypertensive medication (Y)</i>	76	24 (32)	65	37 (57)	49	36 (74)	<.001
<i>Lipid lowering medication (Y)</i>	76	42 (55)	65	27 (42)	49	29 (59)	.124
<i>Smoking, (current)</i>	76	5 (7)	65	0 (0)	49	2 (4)	.080
<i>Stroke (Y)</i>	76	0 (3)	65	1 (2)	49	3 (6)	.040
<i>Myocardial infarction (Y)</i>	76	1 (1)	65	0 (0)	49	0 (0)	1.000

Table 5-7. Demographic and cardiovascular characteristics for categorical variables by ethnicity, (women). Data are number of observations and (%). Tests for significance use Chi square or *Fisher's exact, **uses chi square goodness of fit. P <0.05 shown in bold.

Continuous Variables (Women)	White European		South Asian		P	African Caribbean		P
	n	mean (\pm SD)	n	mean (\pm SD)		n	mean (\pm SD)	
Age, years	76	70.3 (\pm 6.3)	65	68.2 (\pm 5.8)	.047	49	72.9 (\pm 6.9)	.562**
Framingham Risk Score, (%)	76	12.9 (\pm 6.9)	65	17.1 (\pm 11.0)	.004	49	18.4 (\pm 10.9)	.002
HbA1c, mmol/mol	73	39.1 (\pm 9.1)	61	43.5 (\pm 8.7)	.012	49	46.4 (\pm 11.9)	<.001
BMI, kg/m ²	76	27.1 (\pm 4.6)	65	27.5 (\pm 4.3)	.602	49	30.8 (\pm 4.4)	<.001
Haematocrit, %	76	40.6 (\pm 3.0)	65	38.7 (\pm 3.1)	<.001	49	38.8 (\pm 2.5)	.001
Total Cholesterol, mmol/L	76	5.3 (\pm 1.1)	65	4.8 (\pm 1.0)	.004	49	4.9 (\pm 1.0)	.020
LDL, mmol/L	76	2.9 (\pm 1.0)	64	2.5 (\pm 0.9)	.004	49	2.6 (\pm 0.9)	.032
HDL, mmol/L	76	1.8 (\pm 0.5)	65	1.7 (\pm 0.4)	.117	49	1.9 (\pm 0.5)	.496
Systolic BP, mmHg	76	133.9 (\pm 18.9)	65	146.2 (\pm 18.5)	<.001	49	142.2 (\pm 15.3)	.012
Diastolic BP, mmHg	76	76.9 (\pm 11.1)	65	79.5 (\pm 9.4)	.118	49	79.3 (\pm 10.1)	.188
Heart Rate, bpm	73	66.0 (\pm 11.3)	64	66.4 (\pm 11.0)	.812	49	68.9 (\pm 10.5)	.146
Mean Arterial Pressure, mmHg	72	96.3 (\pm 10.3)	64	97.0 (\pm 9.5)	.705	49	98.2 (\pm 10.2)	.310

Table 5-8. Demographic and cardiovascular characteristics for continuous variables by ethnicity, (women). Data are mean \pm SD. Tests for significance are compared to reference (white Europeans) by post hoc Fisher's LSD test after one-way ANOVA. P <0.05 shown in bold.

5.4.4 Characteristics of cerebral blood flow

Table 5-9 and **Table 5-10** show a summary of CBF by sex, ethnicity and diabetes status. The normal distributions of CBF are shown in histograms by pooled sample (**Figure 5-8**) and by sex (**Figure 5-9**, men, and **Figure 5-10**, women).

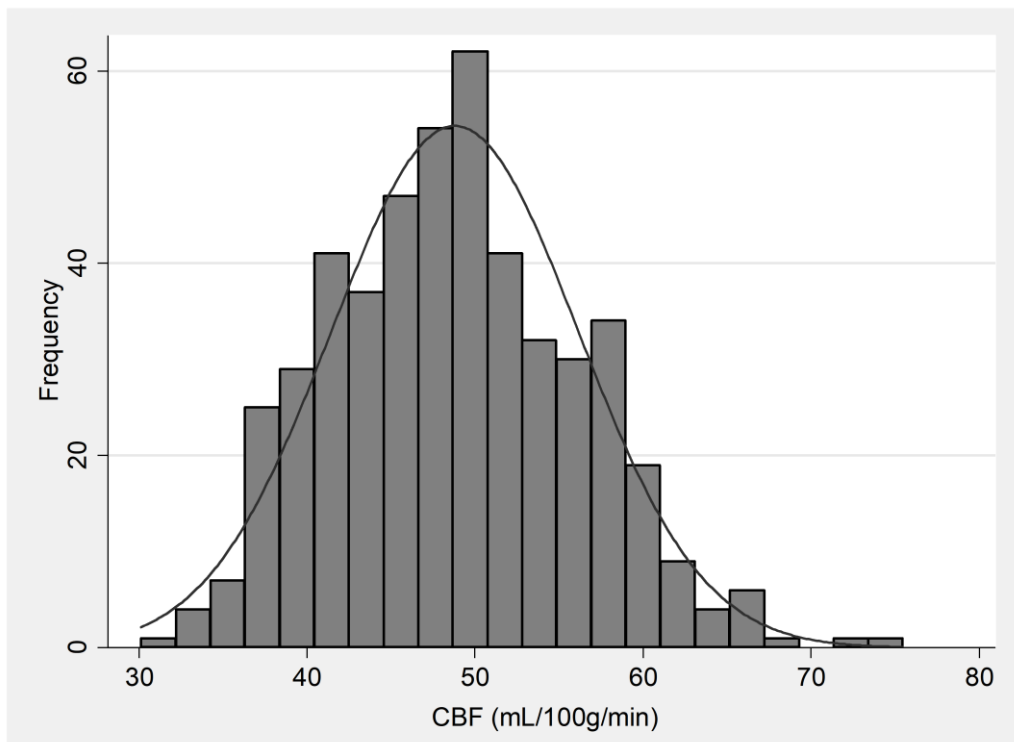


Figure 5-8. Histogram with normal density overlay, showing distribution of CBF, pooled sample.

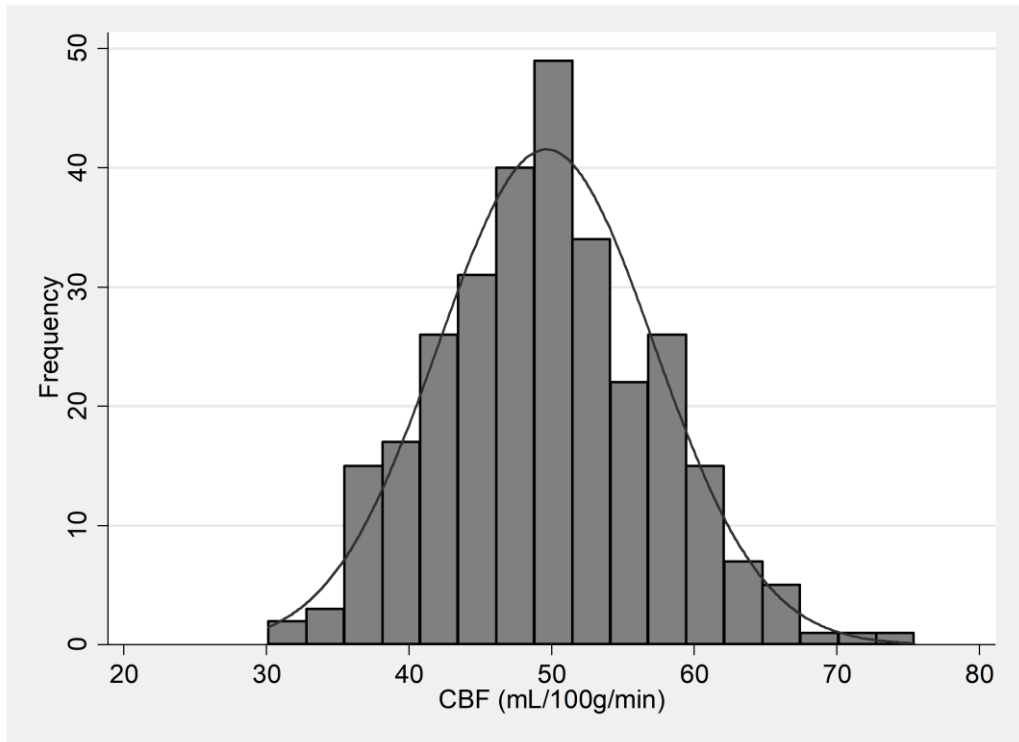


Figure 5-9 Histogram with normal density overlay, showing distribution of CBF,(men).

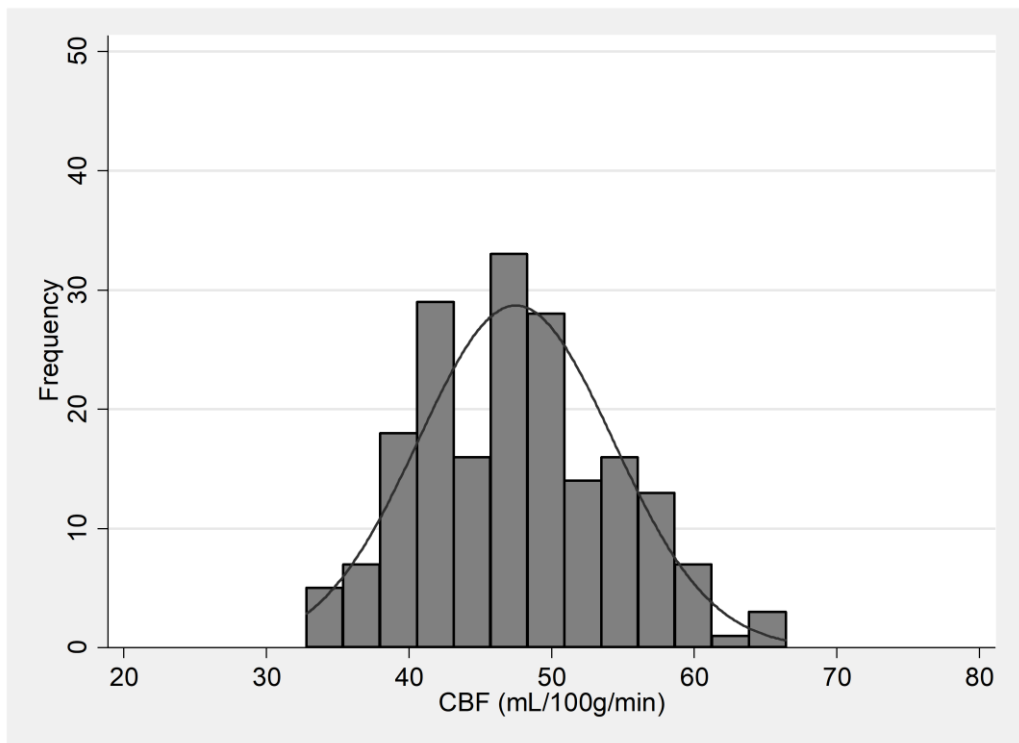


Figure 5-10. Histogram with normal density overlay, showing distribution of CBF, (women).

The mean (SD) CBF corrected for Hct and PVC was 48.8 (± 7.3) mL/100g/min). There were statistically significant differences between men (49.6 (± 7.6) mL/100g/min) and women (47.5 (± 6.8) mL/100g/min) ($P = .002$), and between ethnicities; European (51.1 (± 7.5)) South Asian (47.3 (± 6.7)) African Caribbean (45.8 (± 6.3)) mL/100g/min ($P < .001$) (**Figure 5-11**). South Asian and African Caribbean women had lower CBF than their male counterparts whereas both male and female Europeans had a mean CBF of 51.1 mL/100g/min. The lowest CBF was found in African Caribbean women (44.5 (± 6.0) mL/100g/min (**Figure 5-11**). The mean CBF for the group with diabetes (47.2 (7.5) mL/100g/min) was lower than those without diabetes (49.4 (7.2) mL/100g/min) ($P = .003$) (**Figure 5-12**).

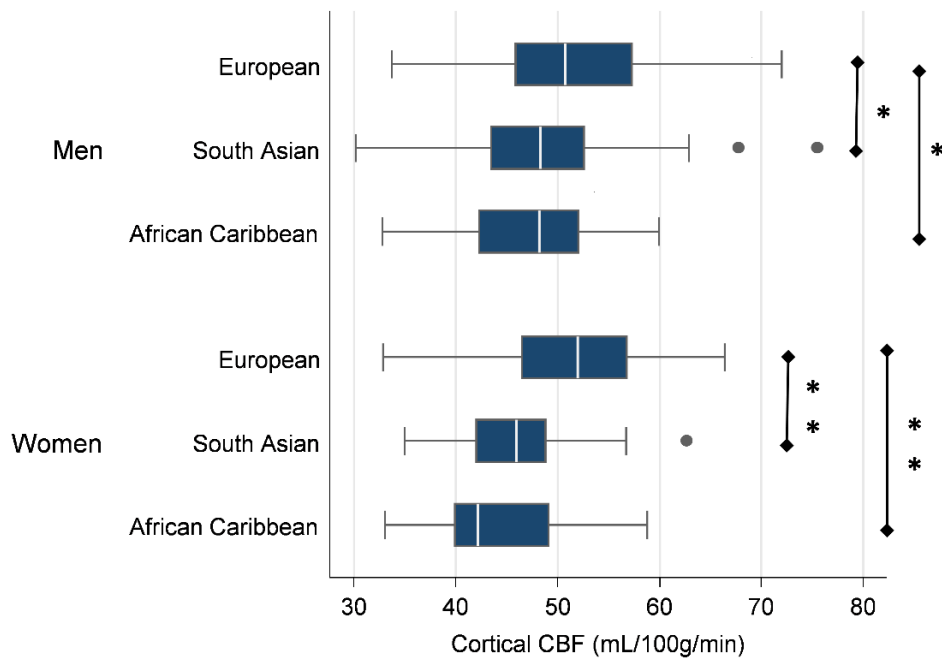


Figure 5-11. Boxplot showing CBF by sex and ethnicity. * $P < .05$, ** $P < .001$.

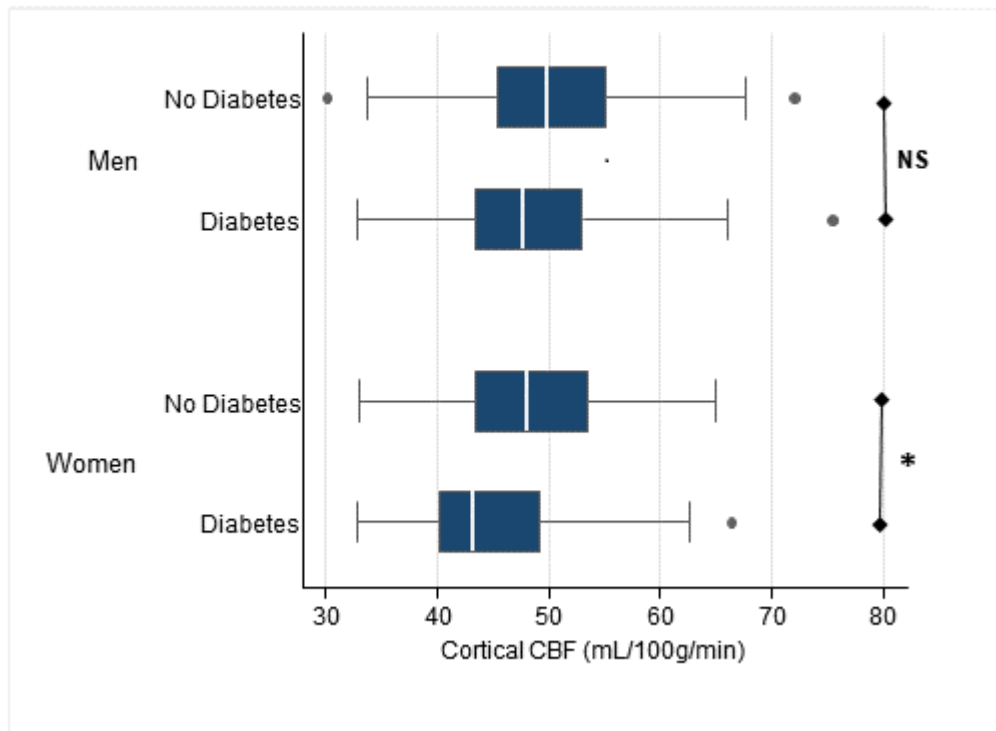


Figure 5-12. Boxplot showing CBF by sex and diabetes status. * $P < .05$, ** $P < .001$.

CBF (mL/100g/min)	European			South Asian			P	African Caribbean			P
	n	mean	±SD	n	mean	±SD		n	mean	±SD	
All, n = 485	223	51.1	±7.5	173	47.3	±6.7	<.001	89	45.8	±6.3	<.001
Men, n = 295	147	51.1	±7.7	108	48.4	±7.3	.004	40	47.4	±6.4	.007
Women, n =190	76	51.1	±7.0	65	45.7	±5.0	<.001	49	44.5	±6.0	<.001

Table 5-9. CBF by sex. Data are mean ±SD. Tests for significance are compared to reference (Europeans) by post hoc Fisher's LSD test after one-way ANOVA, P<0.05 shown in bold.

CBF (mL/100g/min)	No Diabetes			Diabetes			P
	n	mean	±SD	n	mean	±SD	
All, n = 485	354	49.4	±7.2	131	47.2	±7.5	.003
Men, n = 295	216	50.0	±7.5	79	48.6	±7.6	.193
Women, n =190	138	48.5	±6.6	52	45.0	±6.9	.001

Table 5-10. CBF by diabetes status. Data are mean ±SD. Tests for significance use 2 sample unpaired Student's t-test, P<0.05 shown in bold.

5.4.5 Associations of cardiovascular risk factors with cerebral blood flow

5.4.5.1 Bivariate analysis

In a bivariate analysis of continuous variables using Pearson's correlation coefficient r , there was a statistically significant correlation between higher systolic BP and lower CBF. This correlation persisted in sex stratified groups. (Table 5-11). The negative correlation of total cholesterol with CBF and the positive correlation of HDL cholesterol with CBF were stronger in women than men suggesting heterogeneity of effect and therefore investigation of interactions of VRFs and sex should be explored.

	<i>All (n=485)</i>		<i>Men (n=295)</i>		<i>Women (n=190)</i>	
	<i>r</i>	<i>P</i>	<i>r</i>	<i>P</i>	<i>r</i>	<i>P</i>
Age (years)	0.00	.961	-0.01	.883	-0.08	.292
Systolic BP, mmHg	-0.20	<.001	-0.23	<.001	-0.16	.024
HDL cholesterol, mmol/L	0.06	.179	0.08	.188	0.13	.066
Total cholesterol, mmol/L	-0.03	.565	-0.06	.315	0.15	.040
FRS, %	-0.12	.008	-0.22	<.001	-0.26	<.001

Table 5-11: Bivariate analysis, correlations of CBF and continuous cardiovascular risk factors in all participants and stratified by sex, $P < 0.05$ shown in bold.

5.4.5.2 Multiple linear regression models

5.4.5.2.1 Pooled sample

Models including demographic independent variables

i. Associations of CBF with sex and ethnicity

In a model adjusted for age and ethnicity (model 1a, Table 5-12,) women had ~2 mL/100g/min (B -1.78, P =.009, [95%CI -3.12, -0.44] mL/100g/min) lower CBF than men although the effect size was small (1%). After adjustment for

age and sex, South Asian ethnicity was associated with ~ 4 mL/100g/min lower CBF (B -3.87, P < .001, [95%CI -5.26, -2.47] mL/100g/min) and African Caribbean ethnicity with ~ 5 mL/100g/min lower CBF (B -5.12, P < .001; [95%CI -6.86, - 3.38] mL/100g/min) compared to Europeans.

ii. Associations of CBF with age

Age was not associated with CBF in the main effects model adjusted for sex and ethnicity (model 1a, **Table 5-12**). An LR test showed the addition of the interaction term *age*ethnicity* did not improve the fit (model 1a and 2a, **Table 5-12, Figure 5-13**) as the data were equally likely under both models (LR test χ^2 2.02(2) P = .364), (AICs were 3264.155 and 3266.134 respectively).

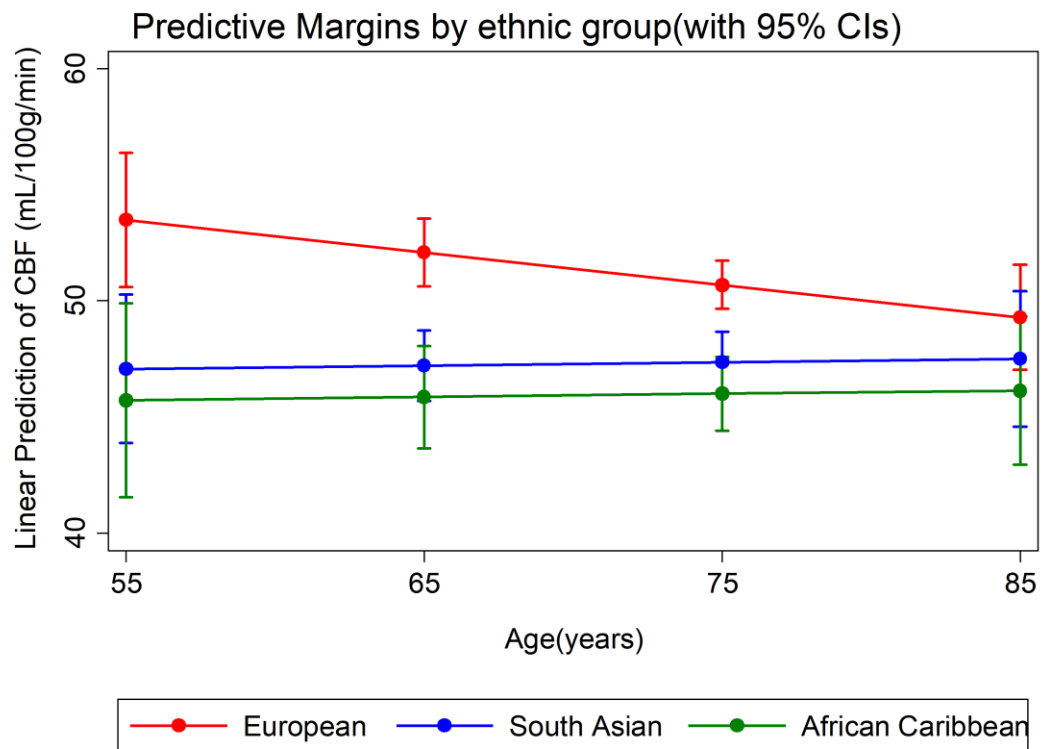


Figure 5-13. Predictive margins plot showing CBF by age, pooled sample

Dependent variable is cortical CBF (mL/100g/min)

<i>Pooled sample</i>	<i>Model 1a</i>				<i>Model 2a</i>			
<i>Observations</i>	<i>n = 485</i>				<i>n = 485</i>			
<i>Adjusted R²</i>	0.10				0.13			
	<i>B</i>	<i>(95% CI)</i>	<i>P</i>	<i>eta²</i>	<i>B</i>	<i>(95% CI)</i>	<i>P</i>	<i>eta²</i>
<i>Sex (female)</i>	- 1.78	-3.12, -0.44	.009	.01	-1.74	-3.09, -0.40	.011	.01
<i>Age (years)</i>	-0.06	-0.17, 0.06	.324	.00	-0.14	-0.30, 0.02	.089	.00
<u><i>Ethnicity</i></u>				.09				.01
<i>South Asian</i>	-3.87	-5.26, -2.47	<.001		-14.90	-32.50, 2.70	.097	
<i>African Caribbean</i>	-5.12	-6.86, -3.38	<.001		-16.26	-36.20, 3.68	.110	
<u><i>Interaction</i></u>								.00
<i>South Asian*age (years)</i>	-	-	-	-	0.15	-0.02, 0.40	.218	
<i>African Caribbean*age (years)</i>	-	-	-	-	0.15	-0.12, 0.43	.271	

Table 5-12 .Multiple linear regression models for dependent variable cortical CBF, demographic independent variables(all participants): shows unstandardized beta coefficients and eta² ,P<0.05 in bold.

Models including vascular risk factors as independent variables

i. Main effects models

When VRFs were added to the model (model 3a, **Table 5-13**), the relationships of age, sex and ethnicity with CBF were maintained although ethnic differences in CBF were modestly attenuated. An increase in systolic BP of 1 mmHg was associated with 0.6 mL/100g/min decrease in CBF (B -0.06, P =.001, [95%CI -0.10, -0.03] mL/100g/min), while 1 mmol/L increase in HDL cholesterol was associated with a 1.88 mL/100g/min increase in CBF (B 1.88, P =.011, [95%CI 0.43, 3.32] mL/100g/min). Diabetes was also associated with a small decrease in CBF (B -1.21, P =.111, [95%CI -2.69, 0.28] mL/100g/min). However, the effect sizes of these covariates were small, each accounting for ~1 to 2% of the sample variance in CBF.

ii. Models with interaction terms

In a model adjusted for VRFs with the interaction term *ethnicity*diabetes*, (model 4a(i)) **Table 5-14** and **Table 5-15**), there was a trend in Europeans and African Caribbeans but not in South Asians, for participants with diabetes to have lower CBF than those without diabetes. Adding both interaction terms *age*ethnicity* and *diabetes*ethnicity* did not improve the fit of the model including VRFs after an LR test (LR χ^2 7.24(4) P =.124 (AIC 3252.743, 3253.507) (**Table 5-15, Figure 5-14**).

Dependent variable is cortical CBF (mL/100g/min)

<i>Pooled sample</i>	<i>Model 3a</i>			
<i>Observations</i>	<i>n = 485</i>			
<i>Adjusted R²</i>	0.13			
	<i>B</i>	<i>(95% CI)</i>	<i>P</i>	<i>eta²</i>
<i>Sex (female)</i>	-2.11	-3.49, -0.72	.003	.02
<i>Age (years)</i>	-0.04	-0.15, 0.08	.538	.00
<u><i>Ethnicity</i></u>				.07
<i>South Asian</i>	-2.98	-4.47, -1.53	<.001	
<i>African Caribbean</i>	-4.89	-6.65, -3.12	<.001	
<i>Diabetes (Y)</i>	-1.21	-2.69, 0.28	.111	.01
<i>Systolic BP, increase 1mmHg</i>	-0.06	-0.10, -0.03	.001	.02
<i>Antihypertensive medication (Y)</i>	-0.36	-1.78, 1.08	.622	.00
<i>HDL cholesterol, increase 1mmol/L</i>	1.88	0.43, 3.32	.011	.01
<i>Total cholesterol, increase 1mmol/L</i>	-0.43	-1.12, 0.26	.221	.00
<i>Smoking (Y)</i>	-0.16	-3.72, 3.39	.928	.00

Table 5-13. Multiple linear regression models using single cardiovascular risk factors (all participants): shows unstandardized beta coefficients and eta², P<0.05 in bold.

Dependent variable is cortical CBF (mL/100g/min)

<i>Pooled Sample</i>	<i>Model 4a(i)</i>			
<i>Observations</i>	<i>n = 485</i>			
<i>Adjusted R²</i>	0.14			
	<i>B</i>	<i>(95% CI)</i>	<i>P</i>	<i>eta²</i>
<i>Sex(female)</i>	-1.93	-3.32, -0.53	.007	.02
<i>Age (years)</i>	-0.03	-0.14, 0.09	.630	.00
<u>Ethnicity</u>				.05
<i>South Asian</i>	-3.82	-5.51, -2.14	<.001	
<i>African Caribbean</i>	-4.37	-6.38, -2.35	<.001	
<i>Diabetes (Y)</i>	-2.13	-4.54, 0.29	.084	.01
<i>Systolic BP, increase 1mmHg</i>	-0.06	-0.10, -0.03	.001	.02
<i>Antihypertensive medication (Y)</i>	-0.36	-1.79, 1.06	.620	.00
<i>HDL cholesterol, increase 1mmol/L</i>	1.79	0.35, 3.24	.015	.01
<i>Total cholesterol, increase 1mmol/L</i>	-0.46	-1.15, 0.23	.194	.00
<i>Smoking (Y)</i>	-0.65	-4.22, 2.92	.720	.00
<u>Interaction</u>				.01
<i>Diabetes (Y)*South Asian</i>	2.68	-0.53, 5.85	.102	
<i>Diabetes(Y)*African Caribbean</i>	-1.40	-5.32, 2.52	.482	

Table 5-14. Multiple linear regression models for dependent variable cortical CBF, single cardiovascular risk factors and diabetes/ethnicity interaction terms (all participants): shows unstandardized beta coefficients and eta², P<0.05 in bold.

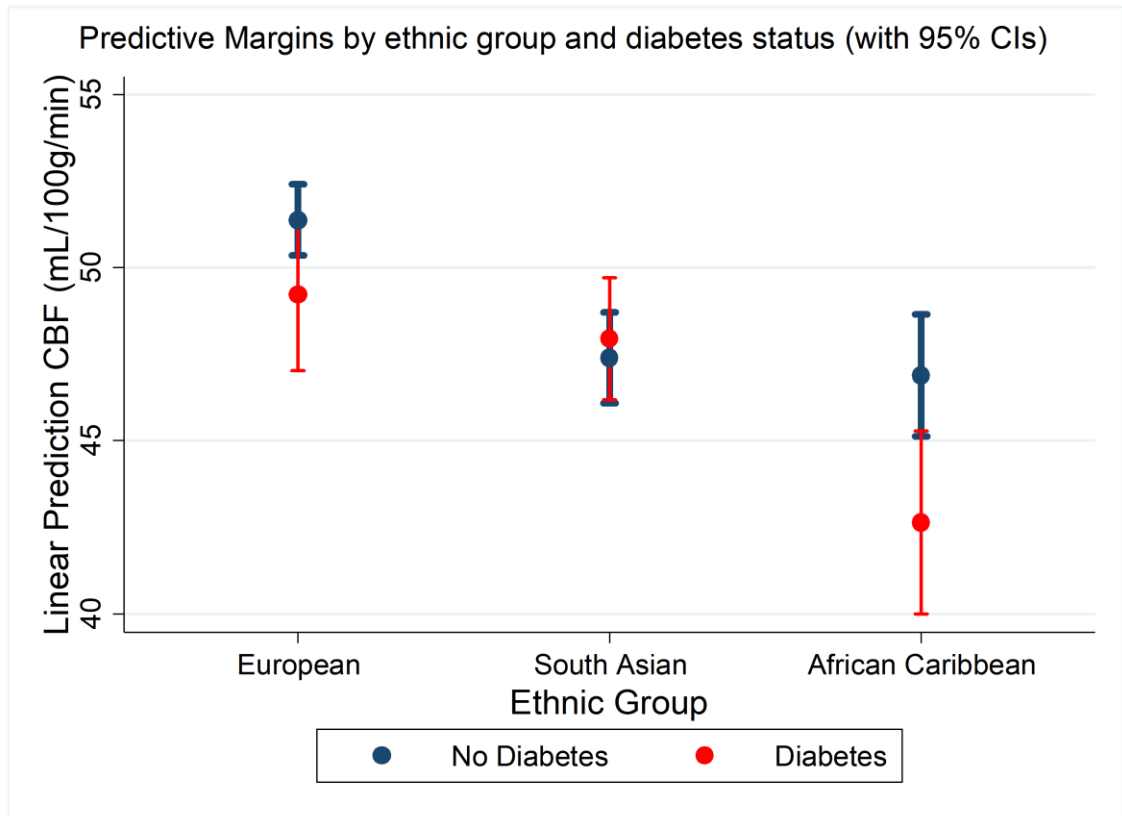


Figure 5-14. Mean linear predictions of CBF by ethnicity and diabetes status (all participants) with 95% CIs adjusted for all covariates (see model 4a(i), (Table 5-14).

Dependent variable is cortical CBF (mL/100g/min)

<i>Pooled sample</i>	<i>Model 4a(ii)</i>			
<i>Observations</i>	<i>n = 485</i>			
<i>Adjusted R²</i>	<i>0.14</i>			
	<i>B</i>	<i>(95% CI)</i>	<i>P</i>	<i>eta²</i>
<i>Sex (female)</i>	-1.86	-3.26, -0.45	0.010	.01
<i>Age (years)</i>	-0.11	-0.27, 0.06	0.196	<.01
<u><i>Ethnicity</i></u>				.01
<i>South Asian</i>	-14.93	-32.38, 2.51	0.093	
<i>African Caribbean</i>	-13.60	-33.24, 6.04	0.174	
<i>Diabetes (Y)</i>	-2.03	-4.45, 0.40	0.101	.01
<i>Systolic BP, increase 1mmHg</i>	-0.06	-0.10, -0.02	0.001	.02
<i>Antihypertensive medication (Y)</i>	-0.39	-1.81, 1.03	0.588	<.01
<i>HDL cholesterol, increase 1mmol/L</i>	1.81	0.36, 3.25	0.014	.01
<i>Total cholesterol, increase 1mmol/L</i>	-0.51	-1.20, 0.19	0.151	<.01
<i>Smoking (Y)</i>	-0.59	-4.16, 2.98	0.747	. <.01
<u><i>Interaction</i></u>				<.01
<i>Age (years)*South Asian</i>	0.15	-0.09, 0.40	0.210	
<i>Age(years)*African Caribbean</i>	0.12	-0.14, 0.40	0.353	
<u><i>Interaction</i></u>				.01
<i>Diabetes (Y)*South Asian</i>	2.60	-0.60, 5.79	0.111	
<i>Diabetes(Y)*African Caribbean</i>	-1.52	-5.45, 2.41	0.449	

Table 5-15. Multiple linear regression model for dependent variable cortical CBF, single cardiovascular risk factors and diabetes/ethnicity and age/ethnicity interaction terms (all participants): shows unstandardized beta coefficients and eta², P<0.05 in bold.

5.4.5.2 Stratified analyses

5.4.5.2.1 Stratification by sex

Models including demographic independent variables

i. Main effects models

In models stratified by sex and adjusted for age and ethnicity (models 1b and 1c, **Table 5-16** and **Table 5-17**), the adjusted R^2 of the women's model was .21, with ethnicity accounting for almost all of the explained sample variance in CBF. African Caribbean women had ~ 7 mL/100g/min (B 7.02, $P < .001$, [95%CI -9.26, -4.82] mL/100g/min) and South Asian women ~ 6 mL/100g/min (B 5.92, $P < .001$, [95%CI -7.97, -3.68] mL/100g/min) lower CBF than European women. The men's model had a smaller adjusted R^2 of .03 which was also largely explained by ethnic differences. African Caribbean men had ~ 3.5 mL/100g/min (B 3.61, $P = .007$, [95%CI -6.22, -0.99] mL/100g/min), and South Asian men ~ 3 mL/100g/min (B 2.76, $P = .004$, [95%CI -4.62, -0.90] mL/100g/min) lower CBF than European men.

An LR test between nested models 1c and 2c (**Table 5-17**) was significant for women (LR 6.39(2). $P = .041$) but not men (LR 0.92(2). $P = .632$) (models 1b and 2b, **Table 5-16**), indicating that ethnicity had a moderating effect on the association of age and CBF only in the women's group (**Figure 5-15** and **Figure 5-16**). Although the CBF of European women was higher than other ethnicities at younger ages, it decreased by ~ 0.3 mL/100g/min per year (B -0.32, $P = .005$, [95%CI -0.53, -0.10] mL/100g/min) until at oldest ages their CBF was at a similar level to other ethnicities. There was a small decrease with age for South Asian women, (B 0.29, $P = .087$, [95%CI -0.04, 0.63] mL/100g/min) and a small increase with age for African Caribbean women (B 0.40, $P = .018$, [95%CI 0.07, 0.73] mL/100g/min) (model 2c, **Table 5-17**).

Dependent variable is cortical CBF (mL/100g/min)

Men	Model 1b				Model 2b			
Observations	n = 295				n = 295			
Adjusted R ²	0.03				0.04			
	<i>B</i>	(95% CI)	<i>P</i>	<i>eta</i> ²	<i>B</i>	(95% CI)	<i>P</i>	<i>eta</i> ²
Age (years)	-0.02	-0.18, 0.15	.839	.00	0.04	-0.19, 0.27	.741	.00
<u>Ethnicity</u>				.04				.00
South Asian	-2.76	-4.62, -0.90	.004		1.60	-25.55, 28.75	.908	
African Caribbean	-3.61	-6.22, -0.99	.007		13.14	-21.77, 48.06	.459	
<u>Interaction</u>								.00
South Asian*age (years)	-	-	-	-	-0.06	-0.43, 0.31	.753	
African Caribbean*age (years)	-	-	-	-	-0.23	-0.70, 0.25	.344	

Table 5-16. Multiple linear regression models for dependent variable cortical CBF and demographic independent variables (men): shows unstandardized beta coefficients and *eta*², *P*<0.05 in bold

Dependent variable is cortical CBF (mL/100g/min)

<i>Women</i>	<i>Model 1c</i>				<i>Model 2c</i>			
<i>Observations</i>	<i>n = 190</i>				<i>n = 190</i>			
<i>Adjusted R²</i>	0.21				0.23			
	<i>B</i>	<i>(95% CI)</i>	<i>P</i>	<i>eta²</i>	<i>B</i>	<i>(95% CI)</i>	<i>P</i>	<i>eta²</i>
<i>Age (years)</i>	-0.11	-0.25, 0.03	.133	.01	-0.32	-0.53, -0.10	.005	.01
<u>Ethnicity</u>				.22				.05
<i>South Asian</i>	-5.92	-7.97, -3.88	<.001		-26.27	-49.50, -3.05	.027	
<i>African Caribbean</i>	-7.02	-9.26, -4.82	<.001		-35.22	-58.67, -11.78	.003	
<u>Interaction</u>								.03
<i>South Asian*age (years)</i>	-	-	-	-	0.29	-0.04, 0.63	.087	
<i>African Caribbean*age (years)</i>	-	-	-	-	0.40	0.07, 0.73	.018	

Table 5-17. Multiple linear regression models for dependent variable cortical CBF and demographic independent variables (women): shows unstandardized beta coefficients and eta², P<0.05 in bold.

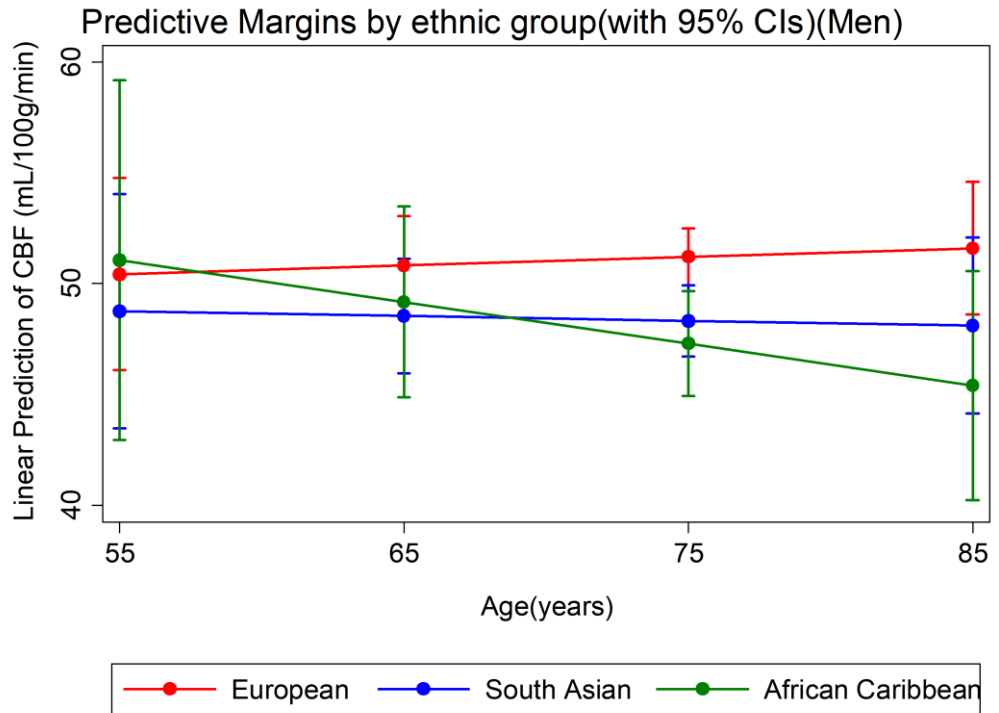


Figure 5-15. Predictive margins plot showing CBF by age, (men)

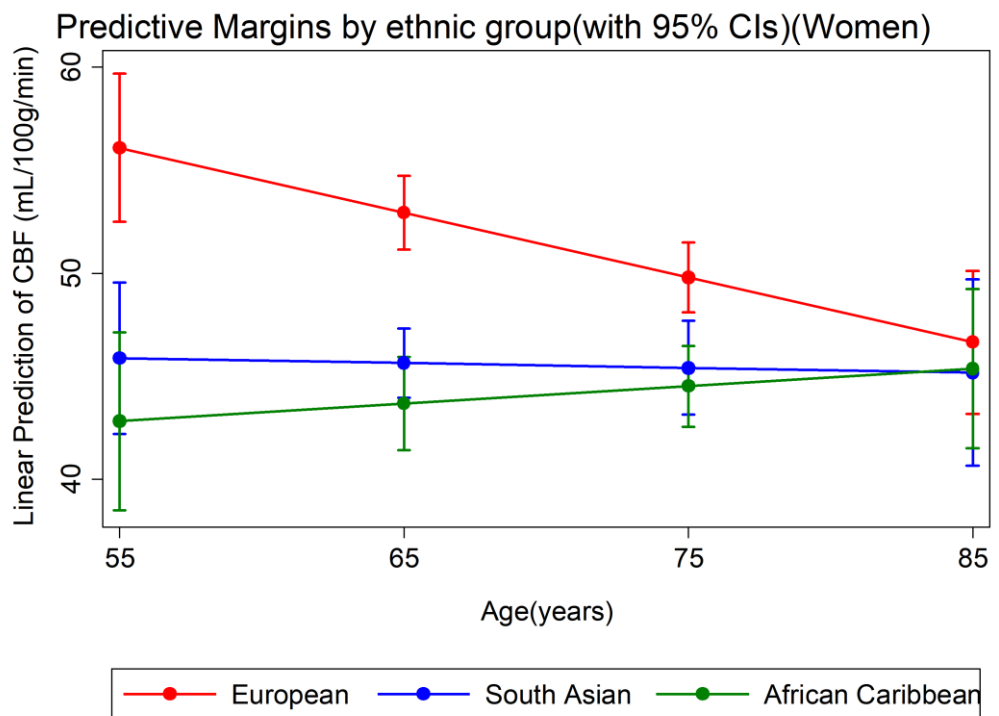


Figure 5-16. Predictive margins plot showing CBF by age, (women)

Models including vascular risk factors as independent variables

i. Main effects

In analyses stratified by sex (models 3b and 3c) (**Table 5-18**) the full model including VRFs and demographic covariates accounted for 22% (adjusted R^2 .22) of the variance of CBF in women compared to 7% (adjusted R^2 .07) in men. The greatest disparity between men and women was the effect size of ethnicity. The partial η^2 of ethnicity in women was .17 compared to .03 in the sample of men.

The association of systolic BP with CBF was stronger in men (B -0.09, P = .001, [95%CI -0.14, -0.04] mL/100g/min) accounting for 4% of CBF variance, a relationship that was not evident in women (B -0.01, P = .733, [95%CI -0.06, 0.04] mL/100g/min). There was a weak association of HDL cholesterol with increased CBF explaining 1 -2% of total variance in both sexes. No other covariates registered effect sizes greater than 1%, nor had confidence margins that were indicative of associations with the dependent variable.

Dependent variable is cortical CBF (mL/100g/min)

	<i>Model 3b (Men)</i>				<i>Model 3c (Women)</i>			
Observations	<i>n</i> = 295				<i>n</i> = 190			
Adjusted <i>R</i>²	0.07				0.22			
	<i>B</i>	(95% <i>CI</i>)	<i>P</i>	<i>eta</i>²	<i>B</i>	(95% <i>CI</i>)	<i>P</i>	<i>eta</i>²
Age (years)	0.03	-0.14, 0.20	.737	.00	-0.12	-0.28, 0.03	.108	.01
<u>Ethnicity</u>				.03				.17
South Asian	-2.02	-3.94, -0.11	.038		-5.20	-7.72, -3.17	<.001	
African Caribbean	-3.59	-6.20, -0.97	.007		-6.46	-9.07, -4.28	<.001	
Diabetes (Y)	-0.81	-2.82, 1.22	.433	.00	-1.52	-3.72, 0.59	.154	.01
Systolic BP, increase 1mmHg	-0.09	-0.14, -0.04	.001	.04	-0.01	-0.06, 0.04	.733	.00
Antihypertensive medication (Y)	-0.62	-2.59, 1.36	.540	.00	-0.35	-2.33, 1.70	.759	.00
HDL cholesterol, increase 1mmol/L	1.74	-0.31, 3.79	.096	.01	2.07	0.11 4.07	.039	.02
Total cholesterol, increase 1mmol/L	-0.69	-1.63, 0.26	.156	.01	-0.38	-1.35, 0.65	.492	.00
Smoking (Y)	0.91	-4.29, 6.10	.731	.00	-1.28	-6.23 3.47	.574	.00

Table 5-18. Multiple linear regression models stratified by sex using single cardiovascular risk factors, (men and women) unstandardised beta coefficients and *eta*², *P*<0.05 in bold.

ii. *Models with interaction terms*

Sex stratified models revealed a difference in the interaction between diabetes and ethnicity in men and women (**Table 5-19 & Table 5-20**). Diabetes in European women was associated with ~5mL/100g/min lower CBF (B 5.07, P =.017, [95%CI -9.24, -0.91] mL/100g/min) compared to European women without diabetes, and ~ 2.5mL/100g/min lower CBF (B 2.53, P =.351, [95%CI -2.81, 7.86] mL/100g/min in African Caribbean women with diabetes compared to African Caribbean women without diabetes. In European and South Asian men, and South Asian women there was no convincing evidence of a difference in CBF in association with their diabetes status. However African Caribbean men with diabetes had ~ 4.6mL/100g/min lower CBF compared to African Caribbean men without diabetes (B 3.98, P =.242, [95%CI -10.66, 2.70] mL/100g/min) although confidence margins were wide (**Figure 5-17 and Figure 5-18, Table 5-19, Table 5-20**).

The model including only men was not improved by the addition of both interaction terms *age*ethnicity* and *diabetes*ethnicity* (model 4b(ii) **Table 5-21**), adjusted R^2 remained .7. The adjusted R^2 of the women's model (model 4c(ii) **Table 5-22**) rose to .25 from .23 reflecting the negative association of age with CBF in women of European ethnicity, and the decrease in CBF of Europeans and African Caribbean women with diabetes which was not evident in South Asian women.

Dependent variable is cortical CBF (mL/100g/min)

	<i>Model 4b(i) (Men)</i>				<i>Model 4c(i) (Women)</i>			
<i>Observations</i>	<i>n = 295</i>				<i>n = 190</i>			
<i>Adjusted R²</i>	0.07				0.23			
	<i>B</i>	<i>(95% CI)</i>	<i>P</i>	<i>eta²</i>	<i>B</i>	<i>(95% CI)</i>	<i>P</i>	<i>eta²</i>
<i>Age (years)</i>	0.02	-0.14, 0.19	.775	.00	-0.09	-0.24,0.07	.263	.01
<u>Ethnicity</u>				.03				.07
<i>South Asian</i>	-2.24	-4.52, 0.04	.054		-6.70	-9.17,-4.23	<.001	
<i>African Caribbean</i>	-2.91	-5.78, -0.04	.047		-6.64	-9.38, -3.90	<.001	
<i>Diabetes (Y)</i>	-0.59	-3.63, 2.45	.703	.01	-5.07	-9.24, -0.91	.017	.02
<i>Systolic BP, increase 1mmHg</i>	-0.09	-0.14, -0.04	.001	.04	-0.02	-0.07,0.04	.533	.00
<i>Antihypertensive medication (Y)</i>	-0.54	-2.52, 1.45	.595	.00	-0.57	-2.57, 1.44	.578	.00
<i>HDL cholesterol, increase 1mmol/L</i>	1.80	-0.25, 1.45	.086	.01	1.95	-0.02, 1.44	.053	.02
<i>Total cholesterol, increase 1mmol/L</i>	-0.68	-1.63, 0.27	.161	.01	-0.42	-1.41, 0.57	.405	.00
<i>Smoking (Y)</i>	0.69	-4.55, 5.93	.796	.00	-2.18	-7.03, 2.66	.375	.00
<u>Interaction</u>				.01				.03
<i>Diabetes (Y)*South Asian</i>	0.40	-3.73, 4.53	.849		6.24	0.10, 11.48	.020	
<i>Diabetes(Y)*African Caribbean</i>	-3.98	-10.66, 2.70	.242		2.53	-2.81, 7.86	.351	

Table 5-19. Multiple linear regression models stratified by sex using single cardiovascular risk factors with interaction term diabetes*ethnicity, unstandardized beta coefficients and eta², P<0.05 in bold.

	<i>European</i>		<i>South Asian</i>		<i>African Caribbean</i>	
	<i>margin (mean)</i>	<i>(95% CI)</i>	<i>margin (mean)</i>	<i>(95% CI)</i>	<i>margin (mean)</i>	<i>95% CI</i>
<u>All</u>						
<i>Diabetic</i>	49.21	47.02, 51.40	47.94	46.19, 49.70	42.64	39.99, 45.28
<i>Non-Diabetic</i>	51.38	50.35, 52.41	47.40	46.08, 48.71	46.88	45.12, 48.64
<u>Men</u>						
<i>Diabetic</i>	50.46	47.77, 53.14	48.61	46.32, 50.91	43.57	38.07, 49.06
<i>Non-Diabetic</i>	51.04	49.68, 52.40	48.80	47.00, 50.60	48.14	45.57, 50.70
<u>Women</u>						
<i>Diabetic</i>	46.83	42.93, 50.72	46.36	43.67, 49.06	42.71	39.93, 45.50
<i>Non-Diabetic</i>	51.90	50.33, 53.46	45.20	43.35, 47.05	45.26	43.00, 47.51

Table 5-20. Marginal means for cortical CBF according to diabetes status by sex and ethnicity data derived from Table 5-14 and Table 5-19.

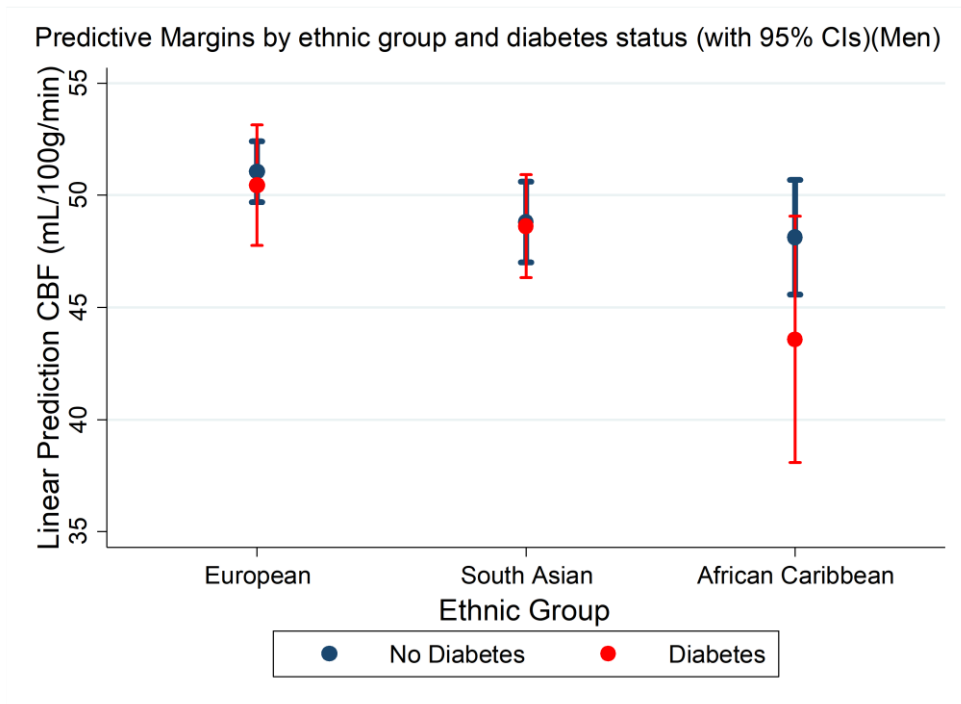


Figure 5-17 Mean linear predictions of CBF by ethnicity and diabetes status (men) with 95% CIs, adjusted for all covariates (see model 4b(i) Table 5-19.)

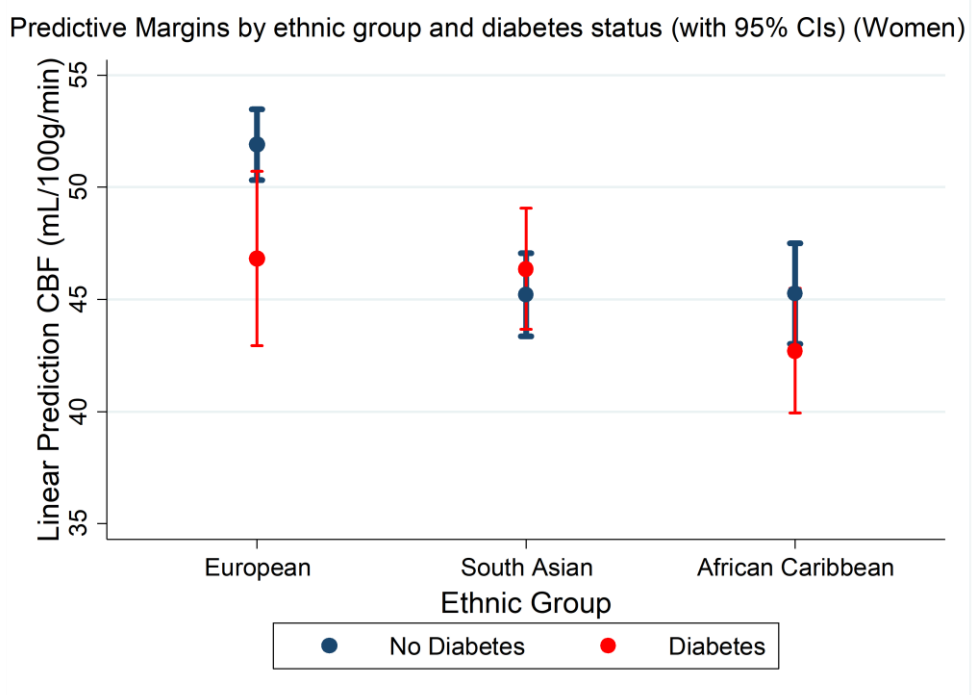


Figure 5-18. Mean linear predictions of CBF by ethnicity and diabetes status (women) with 95% CIs, adjusted for all covariates (see model 4c(i) Table 5-19).

Dependent variable: cortical CBF (mL/100g/min)

Men	Model 4b(ii)			
Observations	n = 295			
Adjusted R²	0.07			
	B	(95% CI)	P	eta²
Age (years)	0.07	-0.16, 0.30	.546	<.01
<u>Ethnicity</u>				. <.01
South Asian	-1.38	-28.08, 25.32	.919	
African Caribbean	16.10	-18.24, 50.44	.357	
Diabetes (Y)	-0.59	-3.64, 2.45	.702	.01
Systolic BP, increase 1mmHg	-0.09	-0.14, -0.04	.001	.04
Antihypertensive medication (Y)	-0.54	-2.52, 1.45	.594	<.01
HDL cholesterol, increase 1mmol/L	1.80	-0.26, 3.87	.086	.01
Total cholesterol, increase 1mmol/L	-0.65	-1.60, 0.31	.182	.01
Smoking (Y)	0.72	-4.53, 5.97	.788	<.01
<u>Interaction</u>				
Age (years)*South Asian	-0.01	-0.38, 0.36	.951	.01
Age(years)*African Caribbean	-0.26	-0.72, 0.21	.276	
<u>Interaction</u>				.01
Diabetes (Y)*South Asian	0.43	-3.71, 4.56	.840	
Diabetes(Y)*African Caribbean	-4.13	-10.82, 2.56	.225	

Table 5-21. Multiple linear regression model for dependent variable cortical CBF, single cardiovascular risk factors and diabetes/ethnicity and age/ethnicity interaction terms (men): shows unstandardized beta coefficients and eta² ,P<0.05 in bold

Dependent variable is cortical CBF (mL/100g/min)

Women	Model 4c(ii)			
Observations	n = 190			
Adjusted R²	0.25			
	B	(95% CI)	P	eta²
Age (years)	-0.28	-0.51, -0.05	.020	.01
<u>Ethnicity</u>				.04
South Asian	-24.19	-48.17, -0.21	.048	
African Caribbean	-32.35	-55.80, -8.91	.007	
Diabetes (Y)	-4.55	-8.71, -0.40	.032	.02
Systolic BP, increase 1mmHg	-0.02	-0.07, 0.04	.559	<.01
Antihypertensive medication (Y)	-0.63	-2.62, 1.36	.534	<.01
HDL cholesterol, increase 1mmol/L	1.83	-0.13, 3.79	.067	.02
Total cholesterol, increase 1mmol/L	-0.48	-1.47, 0.50	.335	.01
Smoking (Y)	-1.40	-6.27, 3.48	.572	<.01
<u>Interaction</u>				.03
Age (years)*South Asian	0.25	-0.09, 0.60	.151	
Age (years)*African Caribbean	0.37	0.04, 0.70	.031	
<u>Interaction</u>				.03
Diabetes (Y)*South Asian	5.82	0.61, 11.04	.029	
Diabetes (Y)*African Caribbean	1.80	-3.53, 7.13	.506	

Table 5-22. Multiple linear regression model for dependent variable cortical CBF, single cardiovascular risk factors and diabetes/ethnicity and age/ethnicity interaction terms (women): shows unstandardized beta coefficients and eta², P<0.05 in bold

5.4.5.2.2 Stratification by diabetes status

Models including demographic independent variables

Sex had a larger effect size in the 'with diabetes' group than in the 'no diabetes' group in models adjusted for demographic variables. In the 'with diabetes' sample women had ~3mL/100g/min (B 2.76, $P = .055$, [95%CI -5.58, 0.64] mL/100g/min) lower CBF than men accounting for ~3% of sample variance (models 1 d and 1e, **Table 5-23**). The effect size of ethnicity was similar in both diabetes groups at 8-9% of sample CBF variance.

Models including vascular risk factors as independent variables

The negative association of systolic BP with CBF had a larger effect size in the 'no diabetes' group (3% of CBF variance) (B -0.07, $P = .001$, [95%CI -0.11, -0.03] mL/100g/min) than in the 'with diabetes' group (1% of CBF variance) (B -0.04, $P = .341$, [95%CI -0.12, 0.04] mL/100g/min) (models 3d and 3e, **Table 5-24**). HDL cholesterol had a slightly larger positive association, explaining 3% of CBF variance in the 'with diabetes' group (B 2.75, $P = .076$, [95%CI 0.43, 3.32] mL/100g/min), compared to the 'no diabetes' group (B 1.48, $P = .079$, [95%CI -0.17, 3.14] mL/100g/min), (explaining 1% of CBF variance).

Dependent variable is cortical CBF (mL/100g/min)

<i>All participants</i>	<i>Model 1d, Diabetes</i>				<i>Model 1e, No diabetes</i>			
<i>Observations</i>	<i>n = 131</i>				<i>n = 354</i>			
<i>Adjusted R²</i>	0.11				0.09			
	<i>B</i>	<i>(95% CI)</i>	<i>P</i>	<i>eta²</i>	<i>B</i>	<i>(95% CI)</i>	<i>P</i>	<i>eta²</i>
<i>Sex (female)</i>	-2.76	-5.58, 0.64	.055	.03	-1.28	-2.81, 0.25	.100	.01
<i>Age (years)</i>	-0.14	-0.38, 0.09	.231	.01	-0.02	-0.14, 0.11	.769	<.01
<u><i>Ethnicity</i></u>				.08				.09
<i>South Asian</i>	-2.00	-4.94, -0.92	.178		-4.39	-6.03, -2.75	<.001	
<i>African Caribbean</i>	-5.65	-9.42, -1.89	.004		-4.41	-6.40, -2.41	<.001	

Table 5-23. Multiple linear regression models for dependent variable cortical CBF, using demographic covariates. shows unstandardised beta coefficients and eta². Groups stratified by diabetes status, P<0.05 in bold.

Dependent variable is cortical CBF (mL/100g/min)

All participants	Model 3d, Diabetes				Model 3e, No diabetes			
Observations	n = 131				n = 354			
Adjusted R ²	0.11				0.12			
	<i>B</i>	(95% CI)	<i>P</i>	<i>eta</i> ²	<i>B</i>	(95% CI)	<i>P</i>	<i>eta</i> ²
Sex (female)	-3.22	-6.22, -0.23	.035	.04	-1.52	-3.13, 0.08	.062	.01
Age (years)	-0.14	-0.39, 0.10	.256	.01	0.01	-0.12, 0.14	.873	<.01
<u>Ethnicity</u>				.06				.08
South Asian	-1.41	-4.55, 1.72	.374		-3.80	-5.49, -2.12	<.001	
African Caribbean	-5.32	-9.32, -1.33	.009		-4.37	-6.40, -2.38	<.001	
Systolic BP, increase 1mmHg	-0.04	-0.12, 0.04	.341	.01	-0.07	-0.11, -0.03	.001	.03
Antihypertensive medication (Y)	-1.19	-1.78, 1.08	.509	<.01	-0.18	-1.74, 1.38	.823	<.01
HDL cholesterol, increase 1mmol/L	2.75	0.43, 3.32	.076	.03	1.48	-0.17, 3.14	.079	.01
Total cholesterol, increase 1mmol/L	-0.99	-1.12, 0.26	.204	.01	-0.30	-1.11, 0.49	.457	<.01
Smoking (Y)	-0.41	-3.72, 3.39	.924	<.01	-0.91	-4.89, 3.07	.652	<.01

Table 5-24. Multiple linear regression models for dependent variable cortical CBF using single cardiovascular risk factors (all participants), showing unstandardised beta coefficients and *eta*². Groups stratified by diabetes status. *P*<0.05 in bold.

5.4.6 Associations of cerebral blood flow with Framingham risk score

5.4.6.1 Bivariate analysis: cerebral blood flow and Framingham risk score

Table 5-25 shows a bivariate analysis using Pearson's correlation coefficient r of FRS with CBF by sex, ethnic and diabetes groups. The correlation of FRS and CBF was similar in each sex. It was much stronger in Europeans than South Asians or African Caribbeans. Scatterplots with linear fit show relationships of FRS with CBF by ethnicity in **Figure 5-19** and **Figure 5-20**.

	<i>n</i>	<i>Pearson's r</i>	<i>P</i>
<i>All</i>	485	-0.12	.008
<i>Men</i>	295	-0.22	<.001
<i>Women</i>	190	-0.26	<.001
<i>European</i>	223	-0.22	<.001
<i>South Asian</i>	173	-0.03	.713
<i>African Caribbean</i>	89	-0.06	.578
<i>Diabetes</i>	131	-0.05	.597
<i>No diabetes</i>	354	-0.09	.111

Table 5-25. Pearson's correlation coefficient of FRS with CBF by sex and ethnic groups, $P < 0.05$ in bold.

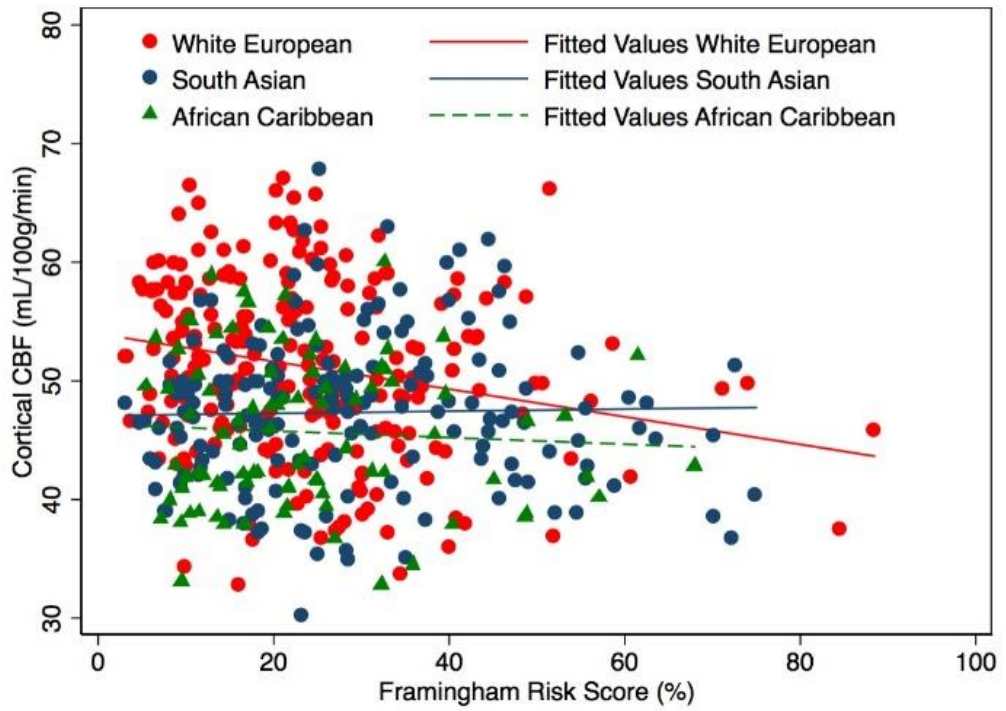


Figure 5-19. Scatterplot with line fit showing associations of CBF and FRS by ethnicity.

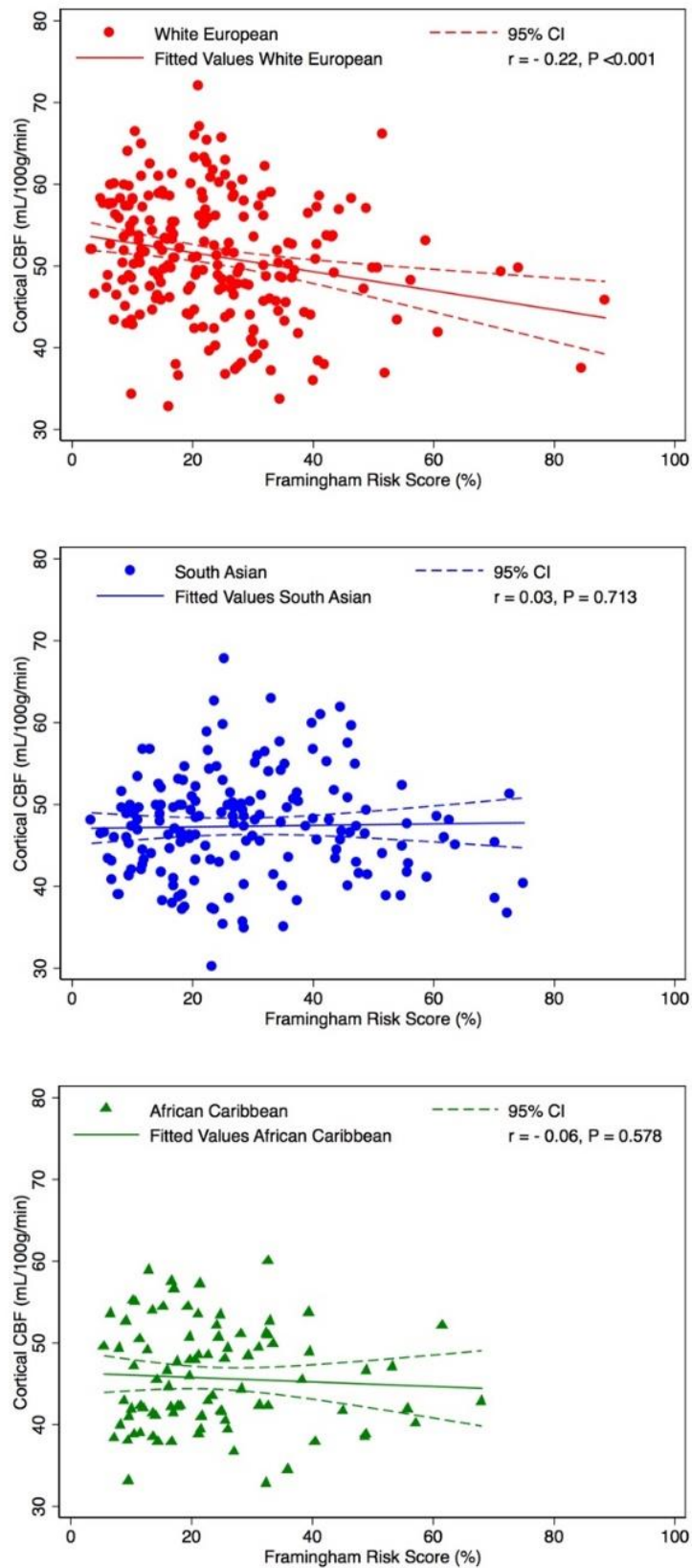


Figure 5-20. Scatter diagrams with line fit and 95% CIs showing associations of CBF and FRS in Europeans (top), South Asians (middle) and African Caribbeans (bottom).

5.4.6.2 Multiple linear regression models

5.4.6.2.1 Pooled sample

Models including Framingham risk score and ethnicity as independent variables

i. Main effects

There was a small decrease of ~ 0.05 mL/100g/min of CBF per 1% increase of FRS (B -0.05, P = .020, CI -0.09, -0.01). On average, South Asians had ~ 3.5 mL/100g/min lower CBF (B -3.62, P <.001, [CI -5.02, -2.21] mL/100g/min) and African Caribbeans ~5.5mL/100g/min lower CBF than Europeans (B -5.51, P <.001, [CI -7.23, -3.80] mL/100g/min) after adjustment for FRS (Model 5a, **Table 5-26**). Ethnicity accounted for 9% of sample variance, whereas the effect size of FRS was 1%.

*ii. Models including FRS and interaction FRS*ethnicity as independent variables*

Ethnicity moderated the association of FRS and CBF (Model 6a, **Table 5-26**). There was a decrease of ~ 0.12 mL/100g/min of CBF for 1% increase of FRS (B -0.12, P < .001, [CI -0.18, -0.05] mL/100g/min) in Europeans. This association was weakly positive in African Caribbeans (B 0.09, P = .165, [CI -0.04, 0.21] mL/100g/min) and in South Asians (B 0.13, P = .006, [CI 0.04, 0.22] mL/100g/min) (**Figure 5-21**).

<i>All participants</i>	<i>Model 5a, Dependent variable: cortical CBF (mL/100g/min)</i>				<i>Model 6a, Dependent variable: cortical CBF (mL/100g/min)</i>			
<i>Observations</i>	485				485			
<i>Adjusted R²</i>	0.10				0.11			
	<i>B</i>	<i>(95% CI)</i>	<i>P-value</i>	<i>eta²</i>	<i>B</i>	<i>(95% CI)</i>	<i>P-value</i>	<i>eta²</i>
<u><i>Ethnicity</i></u>				.09				.06
<i>South Asian</i>	-3.62	-5.02, -2.21	<.001		-6.92	-9.68, -4.15	<.001	
<i>African Caribbean</i>	-5.51	-7.23, -3.80	<.001		-7.62	-11.05, -4.20	<.001	
<i>FRS, %</i>	-0.05	-0.09, -0.01	.020	.01	-0.12	-0.18, -0.05	<.001	.01
<u><i>Interactions</i></u>								.02
<i>FRS(%)*South Asian</i>					0.13	0.04, 0.22	.006	
<i>FRS(%)*African Caribbean</i>					0.09	-0.04, 0.21	.165	

Table 5-26. Multiple linear regression models (all participants) showing associations of CBF with FRS and ethnicity showing unstandardised beta coefficients and η^2 , $P < 0.05$ in bold

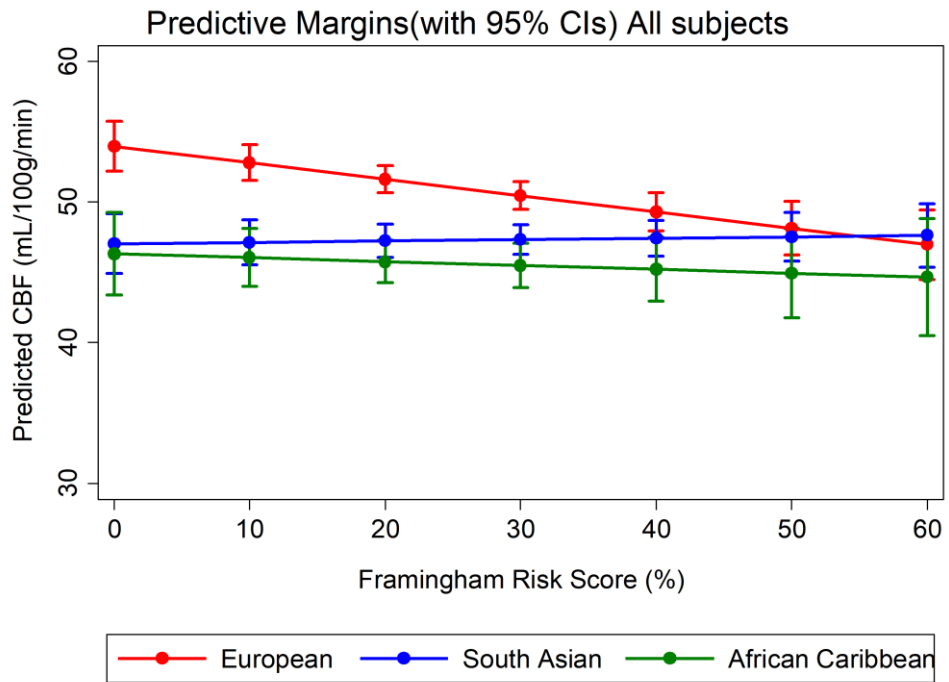


Figure 5-21. Predictive margins plot showing CBF by FRS by ethnicity (all participants), model 6a, (Table 5-26)

5.4.6.2.2 Stratified Models

5.4.6.2.2.1 Stratification by sex

Models including FRS and ethnicity as independent variables

i. Main effects

Men and women showed similar negative associations of FRS with CBF (B -0.11, P < .001, [CI -0.16, -0.04] mL/100g/min; B -0.10, P = .025, [CI -0.20, -0.01] mL/100g/min) respectively (Models 5b and 5c, **Table 5-27** and **Table 5-28**). Men had higher values of CBF than women across the entire range of FRS (**Figure 5-22**).

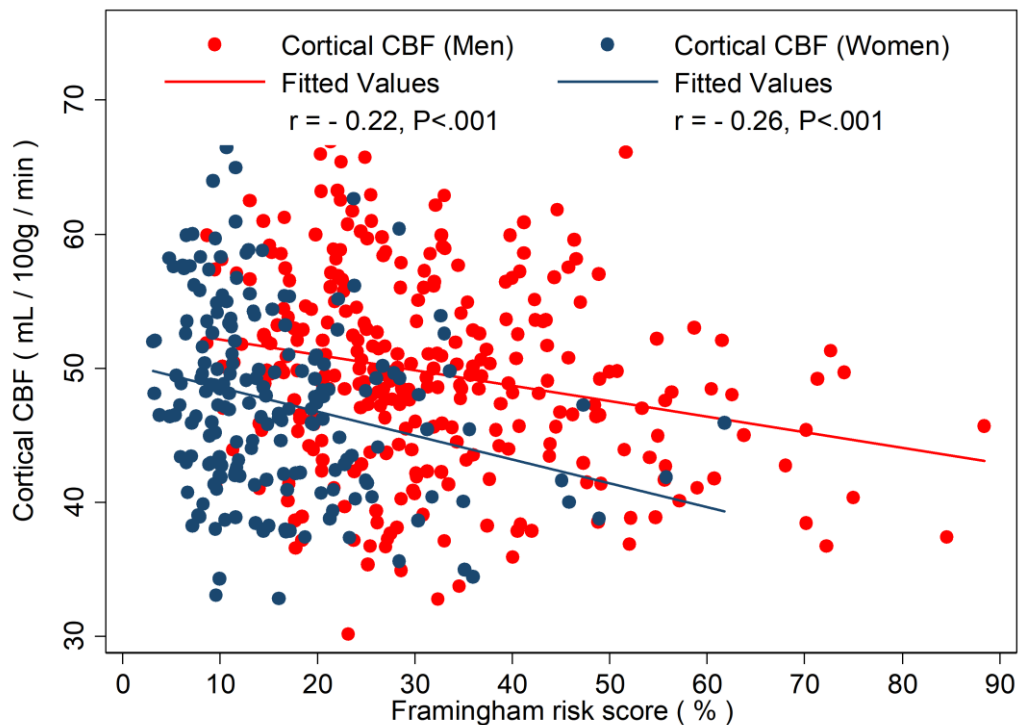


Figure 5-22. Scatterplot showing associations of CBF and FRS by sex

After adjustment for FRS, South Asian and African Caribbean women had ~5mL/100g/min and ~ 6.5mL/100g/min lower CBF than European women (B -5.21, P < .001, [CI. -7.27], -3.16 mL/100g/min; B -6.51, P < .001, [CI -8.75, -4.28] mL/100g/min) respectively. Although the differences in CBF between ethnicities in men was also statistically significant the effect size was smaller; 3% of the sample variance compared to 18% in women. South Asian

men had ~ 2mL/100g/min lower CBF (B 2.14, P =.023, [CI. -3.99, -0.29] mL/100g/min), and African Caribbean men ~ 3.5mL/100g/min lower CBF (B 3.57, P = .006, [CI -6.13, -1.01] mL/100g/min) than European men (**Figure 5-23** and **Figure 5-24**).

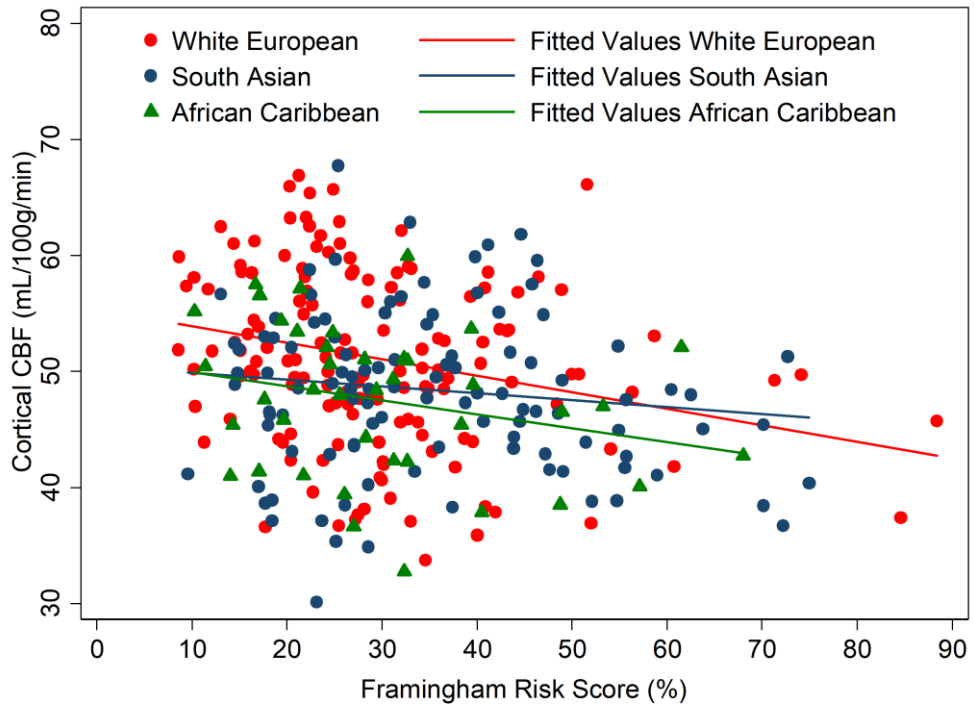


Figure 5-23 Scatterplot showing associations of CBF and FRS by ethnicity, (men).

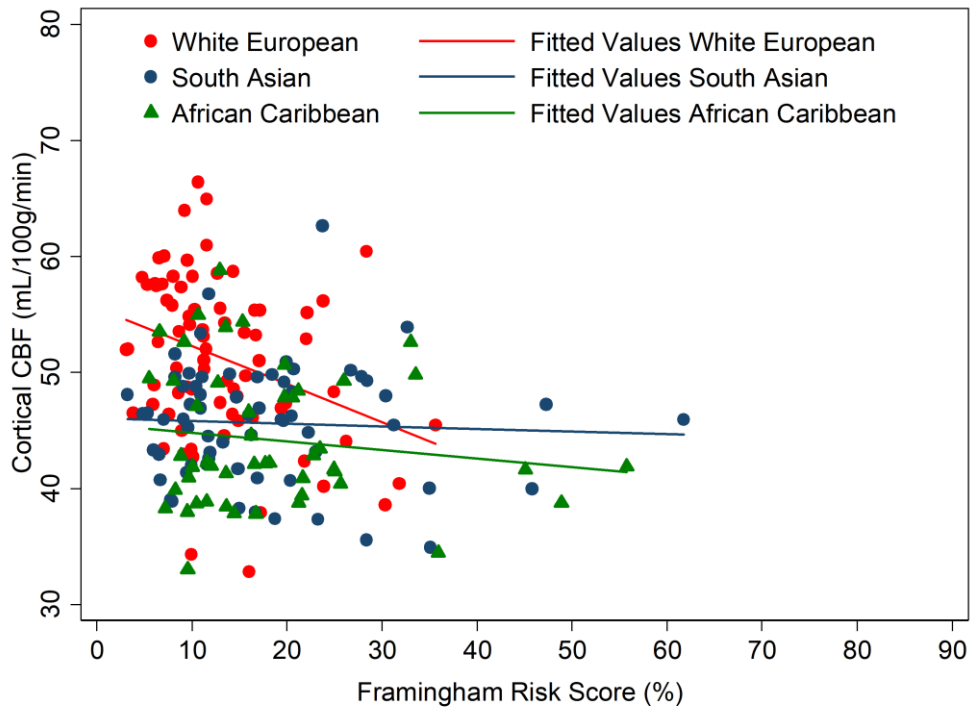


Figure 5-24 Scatterplot showing associations of CBF and FRS by ethnicity, (women).

ii. *Models including FRS and interaction FRS*ethnicity as independent variables*

The interaction of ethnicity and FRS had an effect size of 1% in the men's model and 4% in the women's model (Model 6b, **Table 5-27**, **Figure 5-25**). In the analysis of women (**Table 5-28**, Figure 5-26, model 6c) the strong negative association of FRS with CBF in European women (B 0.33, $P = .001$, [CI -0.53, -0.13] mL/100g/min) was not apparent in South Asian or African Caribbean women. Analysis of interactions suggests this is unlikely to be a chance finding (South Asian*FRS B 0.31, $P = .011$, [CI 0.07, 0.55] mL/100g/min). African Caribbean*FRS B 0.26, $P = .045$, [CI 0.01, 0.51] mL/100g/min) (Model 2c, and **Figure 5-26**). The adjusted R^2 for the women's model containing the ethnicity*FRS interaction term was .24 whereas the adjusted R^2 for the men's model was .07, suggesting a moderate amount of the variance in CBF was accounted for in the women's model.

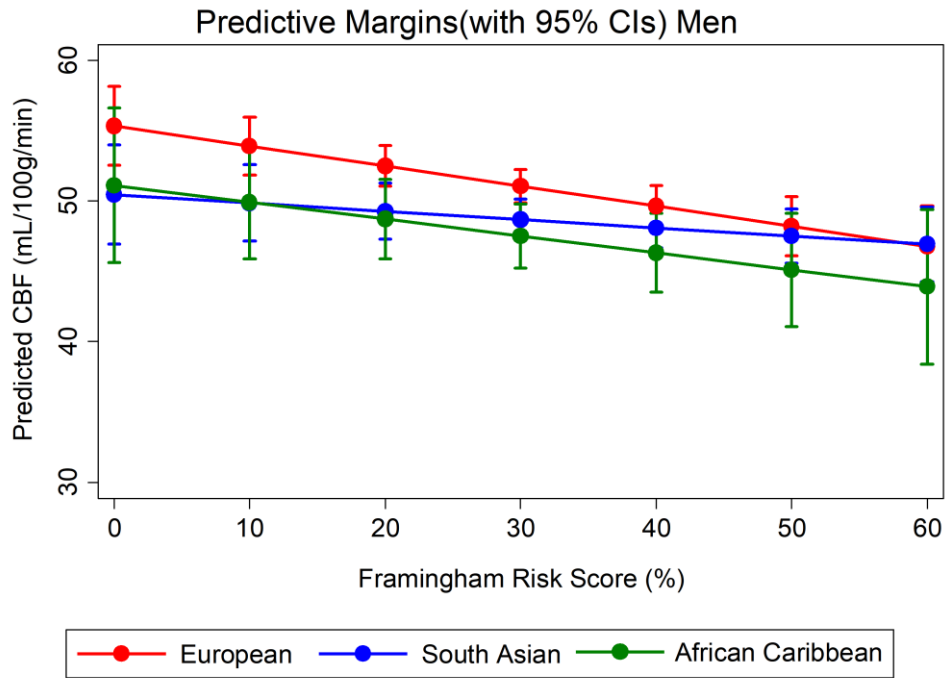


Figure 5-25 Predictive margins plots showing CBF for FRS by ethnicity (men) model 5b.

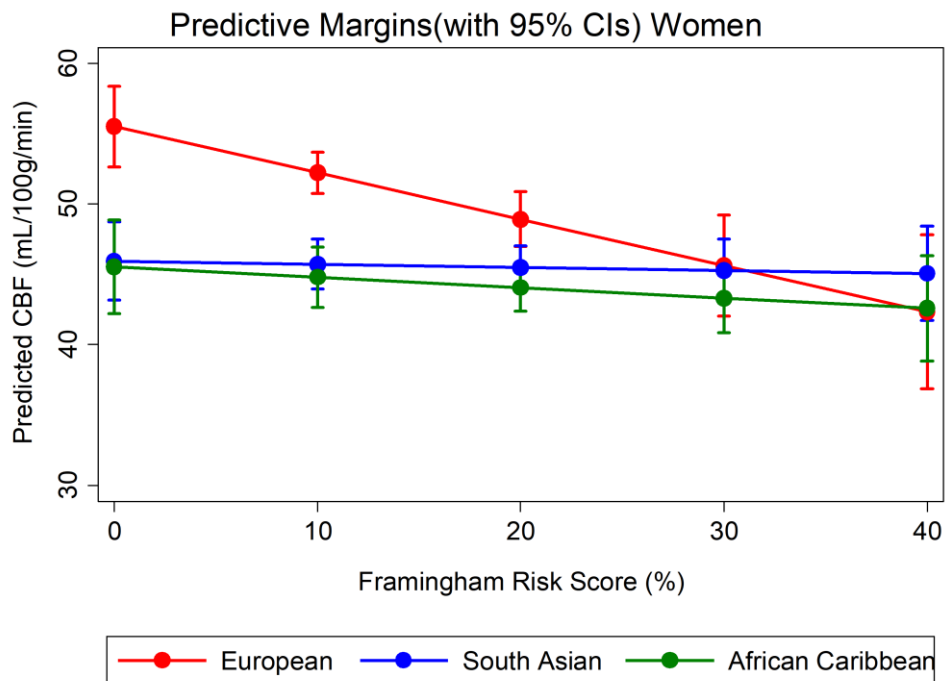


Figure 5-26: Predictive margins showing CBF by FRS by ethnicity (women), model 5c.

<i>Men</i>	<i>Model 5b, Dependent variable: cortical CBF (mL/100g/min)</i>				<i>Model 6b, Dependent variable: cortical CBF (mL/100g/min)</i>			
<i>Observations</i>	295				295			
<i>Adjusted R</i>	0.07				0.07			
	<i>B</i>	<i>(95% CI)</i>	<i>P</i>	<i>eta</i> ²	<i>B</i>	<i>(95% CI)</i>	<i>P</i>	<i>eta</i> ²
<u><i>Ethnicity</i></u>				.03				.09
<i>South Asian</i>	-2.14	-3.99, -0.29	.023		-4.90	-9.41, -0.38	.034	
<i>African Caribbean</i>	-3.57	-6.13, -1.01	.006		-4.23	-10.42, 1.96	.180	
<i>FRS, %</i>	-0.11	-0.16, -0.04	<.001	.04	-0.14	-0.23, -0.06	.001	.03
<u><i>Interaction</i></u>								.01
<i>FRS(%)*South Asian</i>					0.08	-0.04, 0.21	.191	
<i>FRS(%)*African Caribbean</i>					0.02	-0.17, 0.21	.813	

Table 5-27 Multiple linear regression models showing associations of CBF with FRS and ethnicity, (men), showing unstandardised beta coefficients and η^2 , $P < 0.05$ in bold.

<i>Women</i>	<i>Model 5c, Dependent variable: cortical CBF (mL/100g/min)</i>				<i>Model 6c, Dependent variable: cortical CBF (mL/100g/min)</i>			
<i>Observations</i>	190				190			
<i>Adj-R-squared</i>	0.22				0.24			
	<i>B</i>	<i>(95% CI)</i>	<i>P</i>	<i>eta</i> ²	<i>B</i>	<i>(95% CI)</i>	<i>P</i>	<i>eta</i> ²
<u><i>Ethnicity</i></u>				.18				.26
<i>South Asian</i>	-5.21	-7.27, -3.16	<.001		-9.57	-13.56, -5.59	<.001	
<i>African Caribbean</i>	-6.51	-8.75, -4.28	<.001		-10.00	-14.39, -5.60	<.001	
<i>FRS, %</i>	-0.10	-0.20, -0.01	.025	.03	-0.33	-0.53, -0.13	.001	.14
<u><i>Interaction</i></u>								.04
<i>FRS(%)*South Asian</i>					0.31	0.07, 0.55	.011	
<i>FRS(%)*African Caribbean</i>					0.26	0.01, 0.51	.045	

Table 5-28. Multiple linear regression models showing associations of CBF with FRS and ethnicity, (women). showing unstandardised beta coefficients and eta², P<0.05 in bold.

5.4.6.2.2.2 Stratification by diabetes status

i. Main effects

The weak association of FRS with CBF was similar in both 'no diabetes' and 'with diabetes' groups (model 5d and 5e (**Table 5-29**)). South Asians were less differentiated from Europeans in the 'with diabetes' model (B -1.80, P = .228, [CI -4.63, -1.11] mL/100g/min) than in the 'no diabetes' model (B -4.35, P < .001, [CI -6.00, -2.71] mL/100g/min). In the 'no diabetes' group (model 5e) both South Asian and African Caribbean ethnicities had ~4.5mL/100g/min lower CBF than Europeans (B 4.35, P < .001, [CI -6.00, -2.71] mL/100g/min); B 4.56, P < .001, [CI -6.54, -2.58] mL/100g/min) respectively. The CBF of African Caribbeans was lower than either Europeans or South Asians in the 'with diabetes' group (B 7.15, P < .001, [CI -10.75, -3.56] mL/100g/min) (**Table 5-29**).

<i>All participants</i>	<i>Model 5d: Dependent variable: cortical CBF(mL/100g/min), with diabetes</i>				<i>Model 5e: Dependent variable: cortical CBF(mL/100g/min), no diabetes</i>			
<i>Observations</i>	131				354			
<i>Adjusted R²</i>	0.10				0.09			
	<i>B</i>	<i>(95% CI)</i>	<i>P</i>	<i>eta²</i>	<i>B</i>	<i>(95% CI)</i>	<i>P</i>	<i>eta²</i>
<u><i>Ethnicity</i></u>				.11				.10
<i>South Asian</i>	-1.80	-4.63, 1.11	.228		-4.35	-6.00, -2.71	<.001	
<i>African Caribbean</i>	-7.15	-10.75, -3.56	<.001		-4.56	-6.54, -2.58	<.001	
<i>FRS, %</i>	-0.05	-0.12, 0.03	.211	.01	-0.04	-0.10, 0.02	.158	.01

Table 5-29 Multiple linear regression using samples grouped by diabetes status showing unstandardised and eta², P<0.05 in bold.

i. *Models including FRS and interaction FRS*ethnicity as independent variables*

When the interaction term *FRS*ethnicity* was added to the model in the 'no diabetes' group (model 6e, **Figure 5-27**), it provided evidence that the inverse association of FRS and CBF in Europeans (B 0.17, $P < .001$, [CI -0.26, -0.08] mL/100g/min) was not seen in other ethnicities; South Asians (B 0.26, $P < .001$, [CI 0.13, 0.40] mL/100g/min); African Caribbeans (B 0.19, $P = .023$, [CI 0.03, 0.35] mL/100g/min), effect size 4% (**Table 5-30**). The relationship of FRS with CBF in the 'with diabetes' group did not differ much by ethnicity, where the effect size of the interaction term *ethnicity*FRS* was 1% (model 6d, **Table 5-30**, **Figure 5-27**).

All participants	<i>Model 6d: Dependent variable: cortical CBF (mL/100g/min)</i>				<i>Model 6e: Dependent variable: cortical CBF (mL/100g/min)</i>			
	<i>Diabetes</i>				<i>No diabetes</i>			
<i>Observations</i>	131				354			
<i>Adjusted R²</i>	0.09				0.13			
	<i>B</i>	<i>(95% CI)</i>	<i>P</i>	<i>eta²</i>	<i>B</i>	<i>(95% CI)</i>	<i>P</i>	<i>eta²</i>
<u>Ethnicity</u>				.04				.10
<i>South Asian</i>	0.47	-6.25, 7.20	.890		-10.07	-13.42, -6.71	<.001	
<i>African Caribbean</i>	-8.35	-16.49, -0.22	.044		-8.55	-12.50 -4.60	<.001	
<i>FRS, %</i>	-0.03	-0.14, 0.09	.667	.00	-0.17	-0.26, -0.08	<.001	.00
<u>Interaction</u>				.01				.04
<i>FRS(%)*South Asian</i>	-0.06	-0.22, 0.10	.471		0.26	0.13, 0.40	<.001	
<i>FRS(%)*African Caribbean</i>	0.05	-0.18, 0.27	.695		0.19	0.03, 0.35	.023	

Table 5-30 Multiple linear regression including ethnicity/FRS interaction terms, samples grouped by diabetes status, showing unstandardised beta coefficients and eta², P<0.05 in bold.

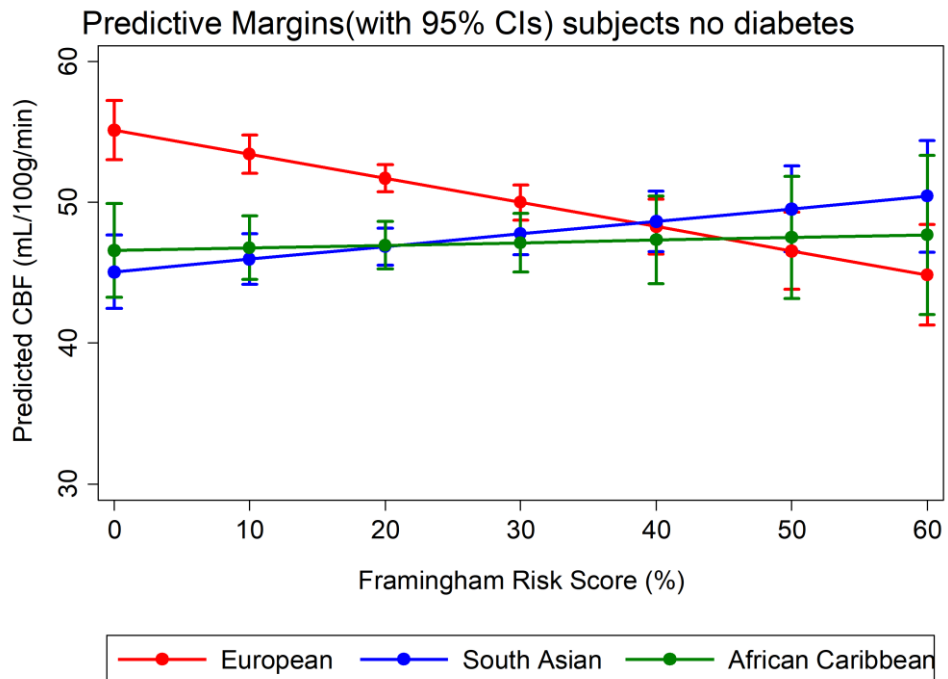
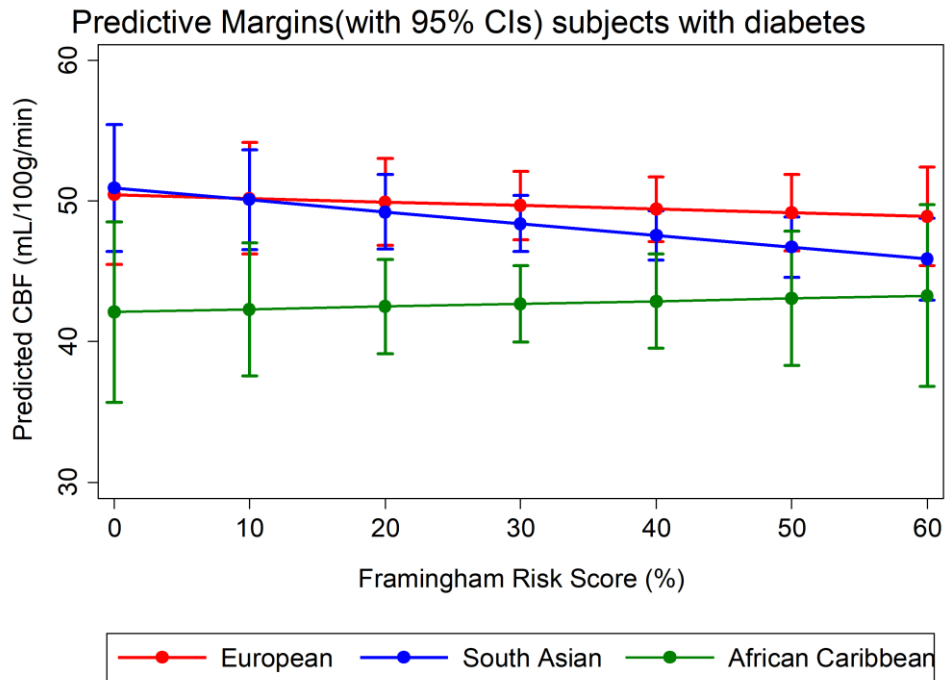


Figure 5-27. Predictive margins plots showing CBF by FRS by ethnicity in groups stratified by diabetes status, all participants, (models 6d and 6e). Top figure shows sample with diabetes, bottom figure shows sample without diabetes..

5.4.6.2.2.3 Stratification by diabetes status and sex

Models including Framingham risk score and ethnicity as independent variables

i. Main effects

The associations of FRS and CBF were similar regardless of diabetes status in main effects models of men and women (models 5f and 5g, **Table 5-31** and models 5h and 5i, **Table 5-33**).

In the 'with diabetes' group (model 5h, **Table 5-33**), there was little difference in CBF between European and South Asian women (B 0.23, $P = .931$, [CI -5.08, 5.54] mL/100g/min), and a moderate difference of ~ 3.5 mL/100g/min CBF (B -3.66, $P = .180$, [CI -9.06, 1.75] mL/100g/min) between European and African Caribbean women. However, in the 'no diabetes' group (model 5i **Table 5-33**) both South Asian (B -6.61 $P < .001$, [CI -8.82, -4.40] mL/100g/min) and African Caribbean women (B -6.39, $P < .001$, [CI -8.90, -3.89] mL/100g/min) 'with diabetes' had ~ 6.5 mL/100g/min lower CBF than European women with diabetes, accounting for 25% of the sample variation.

In the group including only men 'with diabetes', ethnicity accounted for 7% of the sample variance. African Caribbean men had ~ 7 mL/100g/min (B 7.08, $P = .022$, [CI -13.11, -1.05] mL/100g/min) lower CBF than Europeans and there was a moderate difference between South Asian and European men of ~ 2 mL/100g/min CBF (B 1.85, $P = .289$, [CI -5.29, 1.59] mL/100g/min). In the 'no diabetes' group both South Asian and African Caribbean men had ~ 3 mL/100g/min lower CBF than European men (B 2.61, $P = .023$, [CI -4.85, -0.36]) (B 2.79, $P = .055$, [CI -5.63, 0.06] mL/100g/min) respectively with an effect size of .3).

ii. *Models including FRS and interaction FRS*ethnicity as independent variables*

There was little association in the 'no diabetes' group between FRS and CBF in South Asian men (B 0.26, $P = .011$, [CI 0.06, 0.47] mL/100g/min), compared to a ~ 0.2 mL/100g/min decrease in CBF per 1% FRS increase in European men (B 0.23, $P = .001$, [CI -0.36, -0.10] mL/100g/min) and a small ~ 1 mL/100g/min decrease in CBF per 1% decrease in African Caribbean men (B 0.09, $P = .483$, [CI -0.16, 0.33] mL/100g/min) (model 5g). In the 'with diabetes' group the CBF of African Caribbean men increased with increasing FRS (B 0.30, $P = .182$, [CI -0.14, 0.74] mL/100g/min) whereas that of European and South Asian men moderately decreased, (B 0.11, $P = .155$, [CI -0.26, 0.04] mL/100g/min) (B 0.11, $P = .346$, [CI -0.33, 0.12] mL/100g/min) respectively (models 6f and 6g, **Table 5-32**).

The CBF of European women in the 'no diabetes' model declined by ~ 0.3 mL/100g/min with each 1% increase in FRS (B 0.29, $P = .006$, CI -0.50, -0.09), whereas African Caribbean women each 1% increase in FRS was associated with an increase in CBF of ~ 0.2 mL/100g/min (B 0.46, $P = .013$, CI 0.10, 0.83 mL/100g/min) and the CBF of South Asian women was not associated with little or no change in FRS (models 6h and 6i, **Table 5-34**). The moderating effect of ethnicity on the relationship of FRS with CBF was less marked in the 'with diabetes' model, (model 6h,) which had an R^2 of .03 compared to an R^2 of .28 in the 'no diabetes' model but large confidence margins due to small sample numbers make interpretation difficult

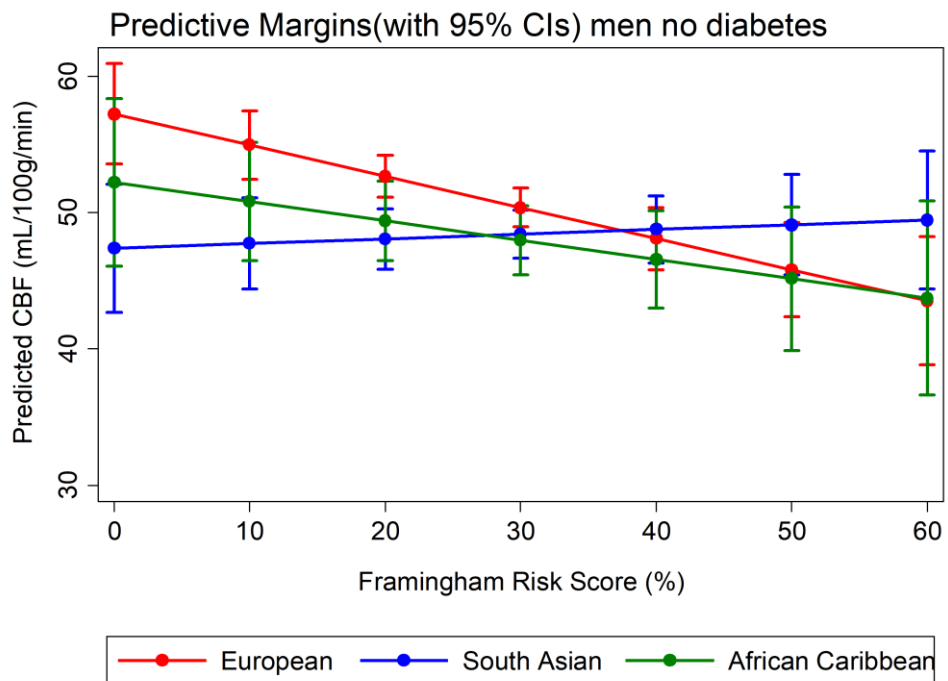
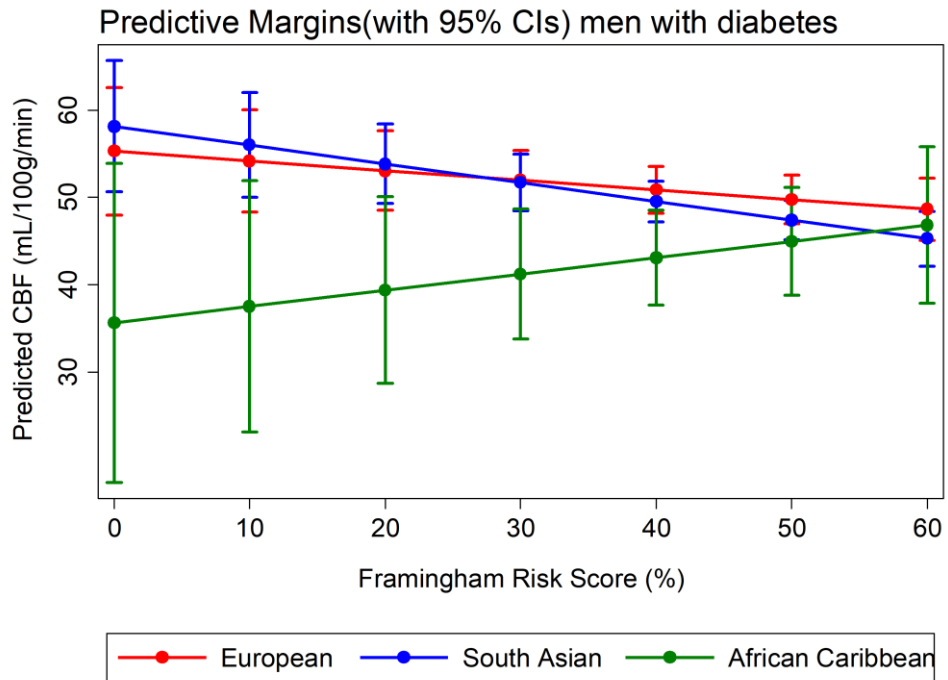


Figure 5-28. Predictive margins plots showing CBF by FRS, by ethnicity (men). Top figure shows sample with diabetes, bottom figure shows sample without diabetes (Table 5-32).

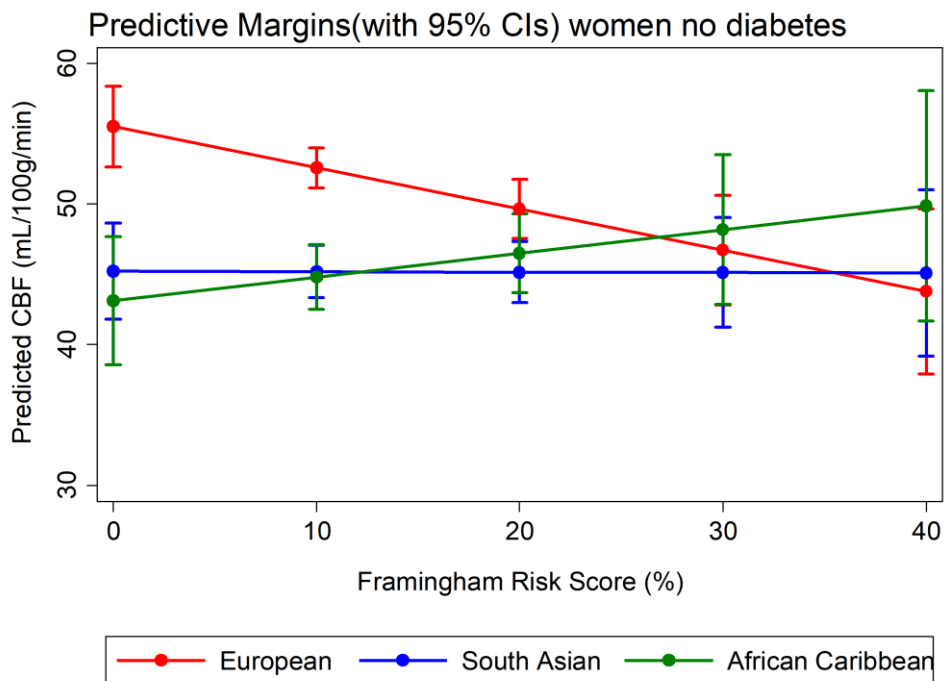
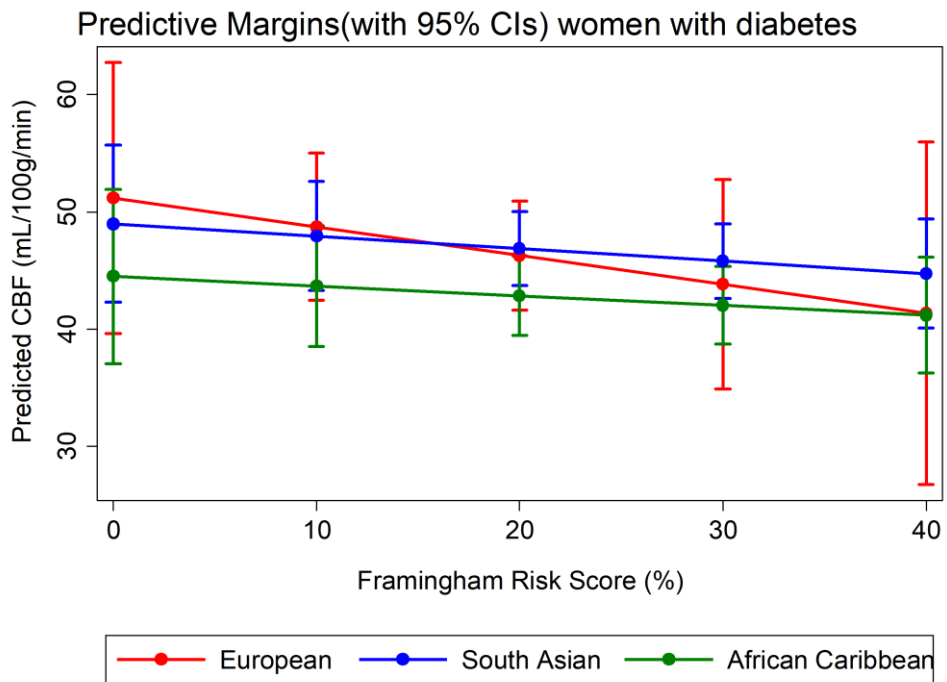


Figure 5-29 Predictive margins plots showing CBF by FRS, by ethnicity (women). Top figure shows sample with diabetes, bottom figure shows sample without diabetes (Table 5-34).

<i>Men</i>	<i>Model 5f, Dependent variable: cortical CBF (mL/100g/min)</i>				<i>Model 5g, Dependent variable: cortical CBF (mL/100g/min)</i>			
	<i>Diabetes</i>				<i>No diabetes</i>			
<i>Observations</i>	79				216			
<i>Adjusted R²</i>	0.10				0.06			
	<i>B</i>	<i>(95% CI)</i>	<i>P</i>	<i>eta²</i>	<i>B</i>	<i>(95% CI)</i>	<i>P</i>	<i>eta²</i>
<u><i>Ethnicity</i></u>				.07				.03
<i>South Asian</i>	-1.85	-5.29, 1.59	.289		-2.61	-4.85, -0.36	.023	
<i>African Caribbean</i>	-7.08	-13.11, -1.05	.022		-2.79	-5.63, 0.06	.055	
<i>FRS, %</i>	-0.14	-0.25, -0.03	.012	.08	-0.12	-0.21, -0.03	.010	.03

Table 5-31. Multiple linear regression using samples grouped by diabetes status (men), showing unstandardised beta coefficients and eta², P<0.05 in bold.

<i>Men</i>	<i>Model 6f, dependent variable: cortical CBF (ml/100g/min)</i>				<i>Model 6g, dependent variable: cortical CBF (ml/100g/min)</i>			
	<i>Diabetes</i>				<i>No diabetes</i>			
<i>Observations</i>	79				216			
<i>Adjusted R²</i>	0.12				0.08			
	<i>B</i>	<i>(95% CI)</i>	<i>P</i>	<i>eta²</i>	<i>B</i>	<i>(95% CI)</i>	<i>P</i>	<i>eta²</i>
<u>Ethnicity</u>				.07				.05
<i>South Asian</i>	2.88	-7.58, 13.34	.584		-9.87	-15.85, -3.89	.001	
<i>African Caribbean</i>	-19.63	-39.31, 0.04	.050		-5.02	-12.19, 2.16	.170	
<i>FRS,%</i>	-0.11	-0.26, 0.04	.155	.01	-0.23	-0.36, -0.10	.001	.03
<u>Interaction</u>				.05				.03
<i>FRS(%)*South Asian</i>	-0.11	-0.33, 0.12	.346		0.26	0.06, 0.47	.011	
<i>FRS(%)*African Caribbean</i>	0.30	-0.14, 0.74	.182		0.09	-0.16, 0.33	.483	

Table 5-32: Multiple linear regression including ethnicity/FRS interaction terms using samples grouped by diabetes status (men), showing unstandardised beta coefficients and η^2 , $P < 0.05$ in bold

<i>Women</i>	<i>Model 5h, Dependent variable: cortical CBF (mL/100g/min)</i>				<i>Model 5i, Dependent variable: cortical CBF (mL/100g/min)</i>			
	<i>Diabetes</i>				<i>No diabetes</i>			
Observations	52				138			
Adjusted R²	0.06				0.25			
	<i>B</i>	<i>(95% CI)</i>	<i>P</i>	<i>eta²</i>	<i>B</i>	<i>(95% CI)</i>	<i>P</i>	<i>eta²</i>
<u>Ethnicity</u>				.07				.25
<i>South Asian</i>	0.23	-5.08, 5.54	.931		-6.61	-8.82, -4.40	<.001	
<i>African Caribbean</i>	-3.66	-9.06, 1.75	.180		-6.39	-8.90, -3.89	<.001	
<i>FRS, %</i>	-0.11	-0.28, 0.06	.206	.03	-0.09	-0.23, 0.05	.187	.01

Table 5-33. Multiple linear regression using samples grouped by diabetes status (women), showing unstandardised beta coefficients and eta², P<0.05 in bold.

<i>Women</i>	<i>Model 6h, Dependent variable: cortical CBF (mL/100g/min)</i>				<i>Model 6i, Dependent variable: cortical CBF (mL/100g/min)</i>			
	<i>Diabetes</i>				<i>No diabetes</i>			
<i>Observations</i>	52				138			
<i>Adjusted R²</i>	0.03				0.28			
	<i>B</i>	<i>(95% CI)</i>	<i>P</i>	<i>eta²</i>	<i>B</i>	<i>(95% CI)</i>	<i>P</i>	<i>eta²</i>
<u><i>Ethnicity</i></u>				.03				.19
<i>South Asian</i>	-2.19	-15.55, 11.18	.744		-10.29	-14.75, -5.84	<.001	
<i>African Caribbean</i>	-6.70	-20.46, 7.07	.332		-12.39	-17.77, -7.01	<.001	
<i>FRS, %</i>	-0.25	-0.86, 0.37	.427	.03	-0.29	-0.50, -0.09	.006	.00
<u><i>Interaction</i></u>				.00				.05
<i>FRS(%)*South Asian</i>	0.14	-0.52, 0.80	.675		0.29	-0.01, 0.59	.057	
<i>FRS(%)*African Caribbean</i>	0.16	-0.51, 0.84	.627		0.46	0.10, 0.83	.013	

Table 5-34. Multiple linear regression including ethnicity/FRS interaction terms using samples grouped by diabetes status (women), showing unstandardised beta coefficients and eta², P<0.05 in bold

5.5 Discussion

Vascular risk in elderly populations has been associated with reduced CBF in previous studies, but there is limited evidence on the effect of multifactorial vascular risk and the moderating effects of sex and ethnicity have not been extensively explored. The current study investigated single VRFs with the aim of establishing each variable's association with CBF, and to evaluate their potential role as mediators of associations between ethnicity, sex and cerebral perfusion. A composite score of vascular risk was also used to investigate the potential role of synergistic effects of multifactorial vascular risk on CBF.

In order to clarify results and facilitate comparison with previous work, pooled sample results are discussed followed by evaluation of stratified analyses.

5.5.1 Study findings

Pooled sample analyses

- *Cortical CBF was lower in women than men in adjusted models.*

Previous studies have frequently found women to have higher CBF than men (127) (220). Adjustment for individual Hct when estimating CBF and the ethnically mixed sample of the present study may account for the disagreement of this finding with previous work.

- *Age was not associated with cortical CBF.*

This finding agrees with the majority of studies using populations of similar restricted age range (127). Studies that have identified lower CBF in old age tend to compare a wide range of young and old age groups or have failed to adequately correct for tissue volume (239). However, stratified analyses showed ethnicity and sex were effect modifiers in the relationship of age and CBF (see below).

- *South Asian and African Caribbean ethnicities had lower cortical CBF than Europeans in adjusted models.*

The use of individual Hct to estimate CBF may have facilitated detection of ethnic differences that have not been noted in previous work. These differences may be due to variation in microvascular damage/dysfunction at the same levels of vascular risk, a hypothesis supported by previous studies (200, 201, 237, 240). However, an alternative explanation may be that South Asian and African Caribbean participants in the SABRE study were first generation migrants, most of whom would have experienced different childhood circumstances to participants who were born in the UK. Early influential factors may include nutrition, exercise, education and environment. Future study of second-generation migrants would reveal whether ethnic differences in CBF in old age persist.

- *Systolic BP was negatively associated with cortical CBF*

The association of high BP with lower CBF is broadly aligned with evidence from previous studies (120) (119) (126) (118). The small effect size is comparable with the DANTE study that found a non-significant 0.21mL/100g/min decrease in CBF per 10mmHg increase of systolic BP in older persons (125). Endothelial damage as a result of prolonged hypertension is a mechanism supported by a substantial body of evidence from previous studies and could account for this association (18, 241).

- *HDL cholesterol was positively associated with cortical CBF*

The association of lipids with CBF was not in agreement with most comparable evidence (127) (242). Differences in sample characteristics may explain these contrasting results. The current study used a larger sample than many previous studies so was better powered to detect the small effect size. It seems a reasonable *a priori* hypothesis that a favourable lipid profile would be associated with less atherosclerosis and increased blood flow. The high prevalence of participants taking lipid-lowering medication may have been a confounder. However, exploratory analyses of models including lipid lowering

treatment as an explanatory variable did not reveal a relationship between lipid lowering treatment and CBF. The weak association of HDL with CBF was similar in stratified models of men and women.

- *There was a weak negative association of diabetes with cortical CBF after adjustment for vascular risk. Ethnicity may moderate this relationship.*

In the present study European and African Caribbean participants 'with diabetes' had lower CBF than those of the same ethnicity 'without diabetes'. This difference was not evident in South Asians. However, this finding should be viewed with regard to effect modification by sex (discussed below in stratified analyses). Although previous studies have not identified strong associations of reduced global brain perfusion with diabetes (133), there is some supporting evidence using regional CBF outcomes that indicates participants with diabetes have lower regional perfusion (135). Furthermore, a study on participants under a hypercapnic challenge observed increased vasoconstriction in participants with diabetes compared to controls, possibly due to endothelial dysfunction (243).

- *Vascular risk measured using the FRS was negatively associated with cortical CBF.*

This finding is consistent with previous investigations that found an inverse relationship of aggregate vascular burden and cerebral perfusion (103, 104, 121, 166). The total variance in CBF accounted for by the model and the effect size of FRS were similar to single factor vascular risk models, suggesting there was not a synergistic effect of VRFs on CBF.

- *The association of FRS and cortical CBF was moderated by ethnicity.*

Europeans with low aggregate vascular risk measured by FRS had higher CBF than South Asians or African Caribbeans with comparable risk scores. Europeans experienced a decrease in CBF as vascular risk increased until, at

the highest levels of risk, CBF was similar in all ethnic groups. South Asians and African Caribbeans appeared to exhibit a perfusion 'floor' effect. Although they had lower CBF at lower levels of vascular risk than Europeans, their CBF did not decrease further with increasing FRS. This phenomenon may be explained by decreases in CBF earlier in the life course as a result of earlier onset and longer duration of VRFs in non-Europeans. This finding is considered further in sex stratified analyses.

Stratified sample analyses

Stratification by sex

- *Ethnicity moderated the association of age with CBF in women*

Ageing in European women was associated with a small decrease in CBF. This relationship was not apparent in the men's model.

- *Ethnic differences in CBF were greater in women than men in models adjusted for vascular risk.*

There was a moderate difference in cortical CBF between European women and South Asian and African Caribbean women. The difference between European men and South Asian and African Caribbean men was smaller. As mentioned previously, non-Europeans in our sample appear to exhibit a perfusion 'floor' at a younger age. This could imply that South Asian and African Caribbean women are more susceptible to microvascular damage in comparison to European women. Further explanations include genetic factors, historical, environmental or lifestyle variables omitted from the current study that could be determinants of lower CBF. Investigation of populations with a wider age range would reveal whether ethnic variation in CBF is evident in younger populations.

- *The negative association of systolic BP with cortical CBF was only observed in men.*

Relatively few comparable studies have conducted secondary analyses by sex. However, this finding is in agreement with Waldstein et al (126) who found higher BP was associated with lower CBF in men but not women. One explanation may be that men and women in the present sample differed by characteristics of hypertension such as longer duration of disease or more variable BP. There may also have been confounding by differing patterns of collinearity of age and BP. However, testing with Pearson's correlation coefficient (r) did not show statistically different relationships of age and systolic BP by sex in our sample (appendix **Figure 8-1**). Other studies have suggested that PP has a greater impact on cerebrovascular damage and, as PP is generally higher in men, they may be more susceptible to cerebral vascular injury. Testing of the relationship of PP and age with Pearson's correlation coefficient (r) showed little difference between sexes in the SABRE sample. (appendix **Figure 8-2**). A possible explanation suggested by previous work (75, 107, 244) is that mid-life BP is more influential than late life BP on the brain changes of old age, information that was not captured in the present study.

- *European women with diabetes had lower cortical CBF than non-diabetic European women. There was less difference between African Caribbean women with and without diabetes and no difference in South Asian women.*

European women 'with diabetes' had similar levels of CBF to South Asian and African Caribbean women who had similar CBF regardless of their diabetes status after adjustment for vascular risk. The same patterns appeared in men, but the trend was weaker.

- *The association of FRS and cortical CBF was moderated by ethnicity in women.*

European women displayed an association of declining CBF with increasing FRS which was not observed in South Asian or African Caribbean women. This

association was similar to the pattern of moderation of age and CBF by ethnicity in the women's stratified sample. This result suggests the 'age' component of the FRS algorithm is mainly responsible for this association. In contrast there was a smaller association of FRS and CBF in men which was not moderated by ethnicity.

Stratification by diabetes status

- *The moderating effect of ethnicity on the relationship of FRS and cortical CBF in the 'no diabetes' group was not evident in the 'with diabetes' group.*

Findings from analyses stratified by diabetes status should be treated with caution due to small sample sizes, wide confidence margins and small effect sizes. Diabetes status in this cohort may also be subject to misclassification as it was not possible to formally exclude the presence of diabetes in participants and the true prevalence of diabetes may therefore be understated. However, the pattern of results indicates the sample 'with diabetes' form a more homogeneous group than the 'no diabetes' sample. Specifically, Europeans 'with diabetes' were not differentiated from other ethnic groups 'with diabetes' in the association of FRS and CBF. In contrast, in the 'no diabetes' stratified sample, Europeans experienced a decline in CBF in association with FRS that was not evident in South Asians or African Caribbeans. One explanation may be that some South Asian and African Caribbean participants 'with diabetes' were misclassified into the 'no diabetes' group. This may be due to clinical under diagnosis, although the inclusion of participants with high HbA1c in clinic goes some way to precluding this. It has been argued in previous work on this cohort that vascular risk does not have a uniform effect across all ethnic groups. For example, the excess risk of CHD in South Asians after adjustment for vascular risk suggested they had lower thresholds of IR and dysglycaemia for adverse cardiovascular outcomes (245, 246). African Caribbeans were found to have lower CHD mortality rates but higher stroke mortality than Europeans for equivalent cardiovascular risk (245). Dichotomisation of individuals 'with' or 'without' diabetes removes sensitivity to the cardiovascular effects of moderate,

yet prolonged dysglycaemia below the cut-off point for T2DM diagnosis (247). Furthermore, South Asians have not only a higher prevalence of diabetes than other ethnicities, but also earlier onset (248). Therefore, it is likely that South Asians in the current study had longer duration of diabetes.

The association of vascular risk and CBF in the female 'with diabetes' group did not appear to be moderated by ethnicity. However, European women in the 'no diabetes' group had higher CBF than South Asian and African Caribbean women, and the CBF of European women also declined with increasing FRS.

Evidence was weak in the analysis of men and there was a paucity of African Caribbean men in the 'with diabetes' group ($n = 7$), so it was not possible to confidently interpret these results from such a small sample .

The apparent greater homogeneity in the 'with diabetes' samples may indicate that South Asians and African Caribbeans classified 'without diabetes' display a vascular risk phenotype closer to those 'with diabetes'. The difference between Europeans with and without diabetes is more distinct. This finding is consistent with previous evidence that in non-diabetic individuals, non-white ethnicities have higher absolute levels of HbA1c than whites although ethnicity did not modify the relationship between HbA1c and the risk of cardiovascular disease (249).

5.5.2 Study strengths

The main strength of our study was its ethnically diverse, community-based, relatively large sample which enables results to be generalised to a wide population. Analyses by strata reduced confounding by sex and diabetes status and thus clarified the role of ethnicity as an effect modifier between vascular risk and cerebral perfusion. All MRI examinations and cardiovascular measurements were conducted in a single centre ensuring robust protocol adherence. As described in Chapter 4 of this thesis, individually measured Hct

was used in CBF estimations to improve the accuracy of T1 blood. This technique was particularly important to estimate CBF in women and non-white European ethnicities where the measured Hct differs substantially from the conventionally assumed mean Hct.

5.5.3 Study limitations

Limitations of our study include a potential selection bias towards physically and mentally healthy individuals who were motivated and physically able to complete a full day of tests in the research clinic. Those with severe cognitive impairment were excluded from the study due to inability to provide informed consent although this was a small number of individuals in the SABRE sample. Our sample was sufficiently powered to detect ethnic differences in the pooled sample, but was somewhat underpowered to detect small effect sizes in VRFs in stratified models. Specifically, women and African Caribbean ethnicity were under-represented at the highest FRS scores (>40%), and African Caribbean men with diabetes were sparse making it difficult to extrapolate results to higher levels of cardiovascular risk.

The FRS has been criticised as it was formulated for mostly white, middle-class North Americans based on outcomes from the Framingham Heart and Offspring studies. It is not validated to assess risk in the very elderly, or individuals with pre-existing cardiovascular events and has been criticised for over-estimating risk in men > 80 years (250). However, it was selected as a reasonable gauge of composite cardiovascular risk in this study as it has been extensively validated and applied in diverse geographic and ethnic population studies (194-196) (251) (252).

The cross-sectional design of the study precludes causal interpretations and does not allow for investigation of associations with complex temporal patterns of VRFs such as periodic hypertension/hypotension.

Omitted variables for which there is some evidence from previous work on cardiovascular risk and CBF include vascular stiffness and pulsatility (253), cardiac index (254), metrics of BP other than systolic BP, exercise and physical activity (255) and genetic factors such as apolipoprotein E4 (APOE4) genotype (256). Further studies incorporating these variables in ethnically diverse and sex stratified models may reveal contributions from these factors on the path to reduced CBF in old age. There may have been residual confounding by age in models using FRS as this adjustment was included as a weighted factor in the FRS. However, although other cerebral outcomes are strongly associated with age it is unlikely to be influential in this context as age was only weakly associated with CBF after PVC.

Although this study showed ethnicity as an effect modifier, the possibility there is a further unidentified confounder responsible for these apparent differences cannot be excluded (257).

5.5.4 Summary

This study has provided evidence of ethnicity as an effect modifier in the relationship between vascular risk and cerebral perfusion. The use of stratified analyses indicated that sex may further impact this relationship. Analysis of pooled samples may be inappropriate in the presence of population heterogeneity in response to cardiovascular risk.

Future studies of longitudinal design would clarify whether ethnic differences in cerebral perfusion are due to earlier onset of CBF decline, longer duration of VRFs or variability in susceptibility to macrovascular or microvascular damage as a consequence of vascular disease. Studies should be powered to provide robust results in studies that can conduct stratified and interaction analyses that do not obscure strata specific relationships.

6 . Associations of Framingham risk score and cerebral blood flow with cortical volume and white matter hyperintensity volumes

6.1 Abstract

This chapter investigates the associations of FRS and CBF with cortical tissue volume, total WMH volume and WMH volumes in PV (zones 1 & 2) and DWM zones (zones 3 & 4) classified using the quantification method described in Chapter 3 'General Methods' (p94).

In this chapter it is hypothesised that increased FRS would be associated with decreased cortical brain volume and increased WMH volume, and that CBF would mediate these relationships. It was further hypothesized the relationship with WMHs in zones 3 & 4 may be more closely related to vascular causes than WMHs in zones 1 & 2 as suggested in previous work (258). Generalized linear models (GLMs) were used to evaluate associations of FRS and CBF with brain outcomes. Structural equation models (SEMs) were used to determine whether CBF was a mediator between FRS and brain outcomes.

FRS was negatively associated with cortical tissue volume and positively associated with WMH volume. The current study suggests these relationships are moderated by ethnicity; in a pooled analysis Europeans experienced less decline in cortical volume and smaller WMH volumes in association with FRS than South Asians and African Caribbeans. However, models using cortical tissue volume as an outcome were also moderated by sex; European men and South Asian women had less decline in cortical volume than other ethnicities in sex stratified analyses. There was no evidence of mediation by CBF on the relationship of FRS and any measured brain outcome variable.

6.2 Introduction

Cerebral atrophy and increases in WMH volume are ‘typical’ features of brain ageing (52, 54, 62, 259, 260). However, there is extensive inter-individual variation ranging from those who age ‘successfully’ with very minor evidence of brain deterioration, to those who experience extensive global or regional volume loss and develop large areas of confluent WMHs. High levels of brain atrophy and large volumes of WMHs have been strongly associated with increased risk of cognitive decline and dementia (56, 261). Previous studies have broadly supported the hypothesis that increased rates of atrophy and WMH volume are associated with increased cardiovascular risk and decreased CBF (262).

Understanding the mechanisms of this relationship would facilitate the development of effective interventional strategies that mitigate cerebral damage and consequent cognitive decline in old age.

In this chapter it was hypothesized that increased FRS would be associated with decreased cortical volume and increased WMH volumes. Furthermore, WMH volume in zones 3 & 4 would be more closely associated with increased FRS and decreased CBF than WMH volume in zones 1 & 2 as it has been suggested by some previous work that the aetiology of WMHs in DWM is more likely to be of vascular origin than WMHs in PV zones. The previous chapter presented evidence of associations of FRS and CBF. This chapter tests the hypothesis that CBF mediates the relationship of FRS and brain outcomes. Ethnicity and sex were considered as potential effect modifiers in these relationships.

6.3 Methods

See Chapter 3 ‘General Methods’ (pp 81-91) for sample description, MRI acquisition and post-processing and VRF data acquisition.

6.3.1 Statistical Analysis

Generalized linear models (GLMs) with gamma family and identity link functions were used to examine associations with cortical volume as the dependent

variable. The distribution of WMH volume was positively skewed but displayed a normal distribution after log transformation (**Figure 6-1, Figure 6-2, Figure 6-3, Figure 6-4, Figure 6-5 and Figure 6-6**), therefore GLMs with gamma family and log link were used for fitting and ease of interpretation for WMH outcomes. Exponentiated regression coefficients ($\exp B$) were calculated and represent percentage change in outcome per unit increase in exposure. Magnitudes of interactions by ethnic group were calculated by multiplying the base $\exp B$ coefficient and the group $\exp B$ coefficient (<https://www.stata.com/statalist/archive/2012-05/msg00919.html>). For example, the calculation of the magnitude of the interaction between South Asian ethnicity and FRS for the outcome variable 'total WMHs' is illustrated below in (Equation 6-1).

$\exp B \text{ base FRS} * \exp B \text{ FRS/South Asian}$ $0.991 * 1.018 = 1.0088$

Equation 6-1 (Example is from Model 4).

This corresponds to a $(1.0088-1)*100 = 0.88\%$ increase in total WMH volume per 1 unit increase in FRS in association with South Asian ethnicity compared with Europeans.

AIC and deviance residuals were inspected to test for goodness of fit and comparison of models when WMHs were outcome variables and log link function was used. TIV was positively associated with brain volume and is therefore included in all models to adjust for head size (263).

SEMs were constructed using SEM builder in STATA (v14) to investigate the role of CBF as a mediator between FRS and cortical volume and WMH volumes in models adjusted for age, TIV and ethnicity. SEM is a tool that facilitates the testing of direct and indirect hypothesized causation in multiple groups of data

through path diagrams and multiple regression style equations. It allows for flexible allocation of variables as dependent or independent variables in the SEM (264). Disadvantages of SEM are similar to other modelling techniques such as OLS in linear regression in that global fit may be good but lower order coefficients may not show large effect sizes and the model may be liable to omitted variables. Ordinal categorical variables are not supported in the STATA implementation of SEM, so ethnicity was used as a dichotomous variable. Multiple group analysis was used to capture effect modification instead of interaction terms (265). The SEM 'group' option was employed to show unconstrained values by ethnicity and effect modification was tested using the Wald test '*estat ginvariant*' option in Stata. The current work employed a complete case analysis, so it was not necessary to use techniques such as full information maximum likelihood to accommodate missing values.

Where WMH volume was the dependent variable a log transform of the outcome was used in SEMs to address the joint multivariate normality assumption. Generalized structural equations (GSEMs) which relax the constraint for multivariate normality allowing for the utilisation of non-linear functional relationships and non-normal sampling distributions. by allowing use of different family and link options were not used for mediation analysis as the STATA post estimation command for analysis of direct and indirect effects is not available after GSEM. All models were re-run with samples stratified by sex to examine sex differences and effect modification looked for as described above for ethnicity. Beta coefficients are reported in unstandardised forms in GLM tables, and standardised forms in SEMs to allow for ease of comparison of effect size of variables in log transformed models.

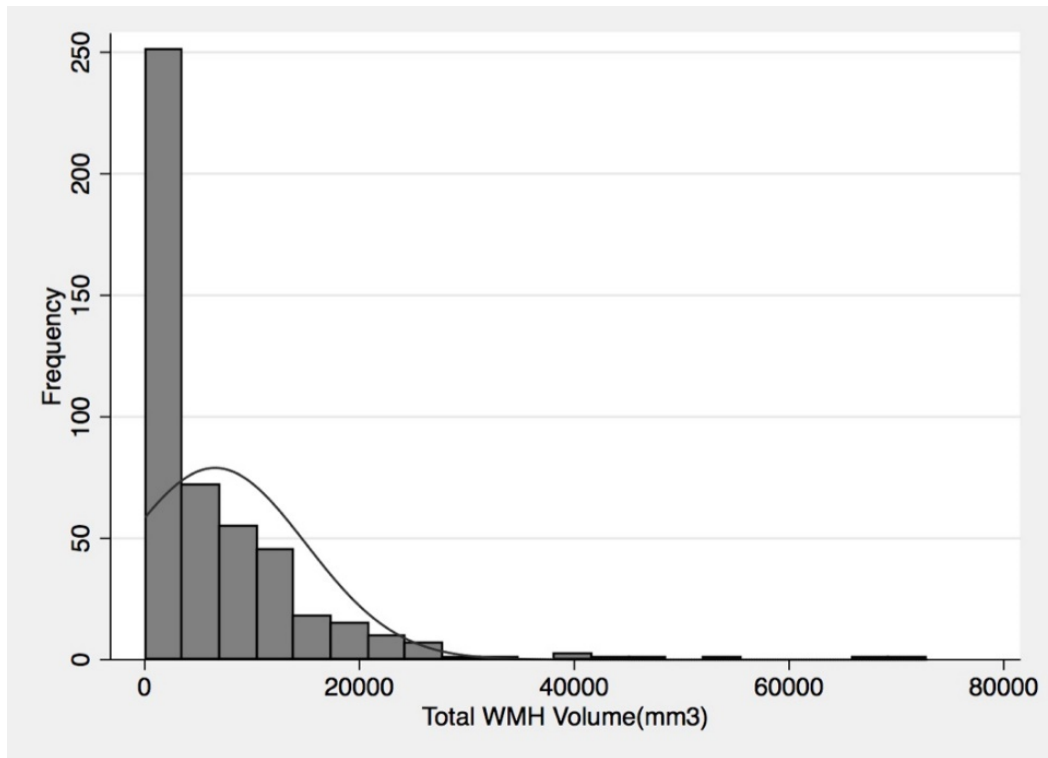


Figure 6-1 Histogram with normal density overlay, distribution of total WMHs.

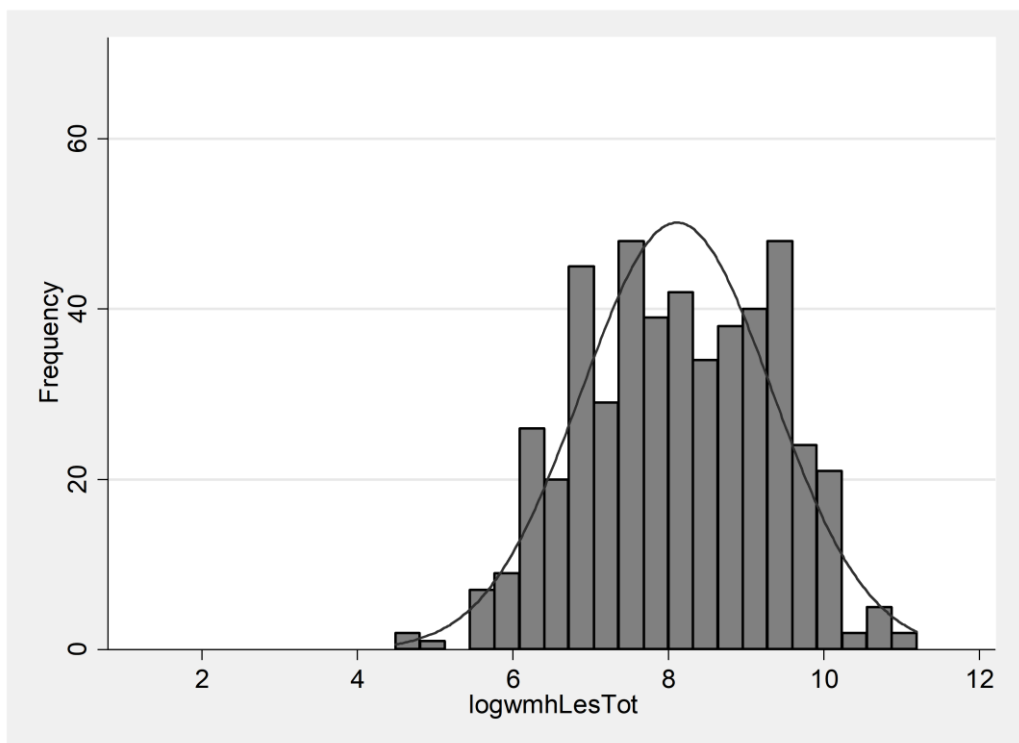


Figure 6-2. Histogram with normal density overlay, distribution of log total WMHs.

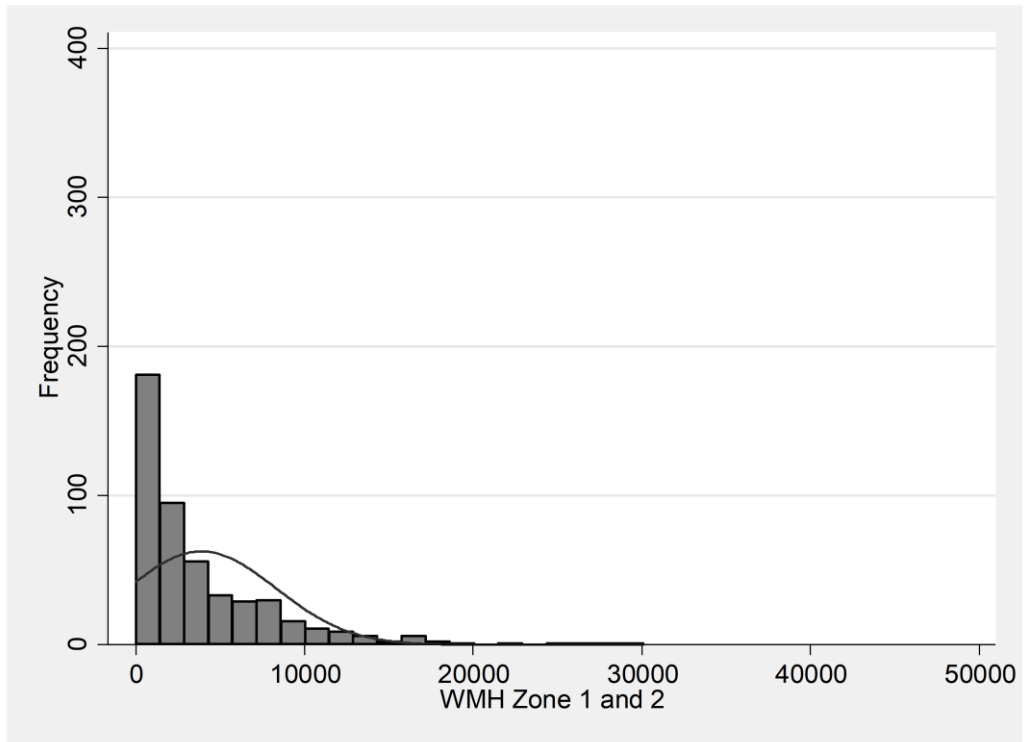


Figure 6-3. Histogram with normal density overlay, distribution of WMHs zones 1 & 2.

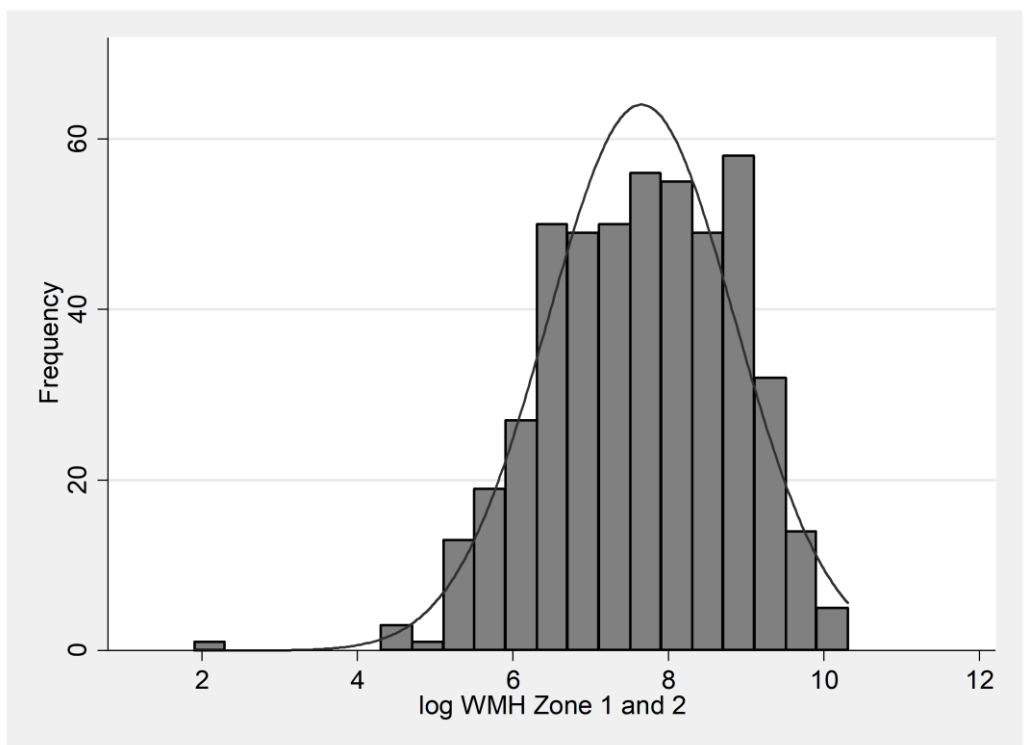


Figure 6-4. Histogram with normal density overlay, distribution of log WMHs zones 1 & 2.

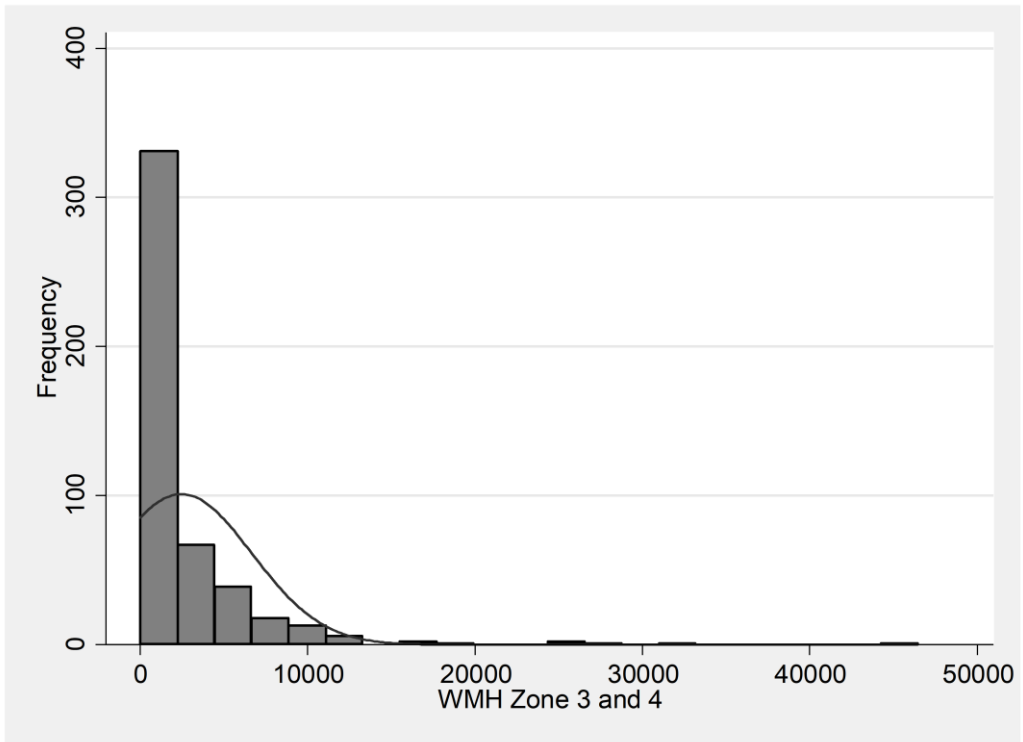


Figure 6-5. Histogram with normal density overlay, distribution of WMHs zones 3 & 4.

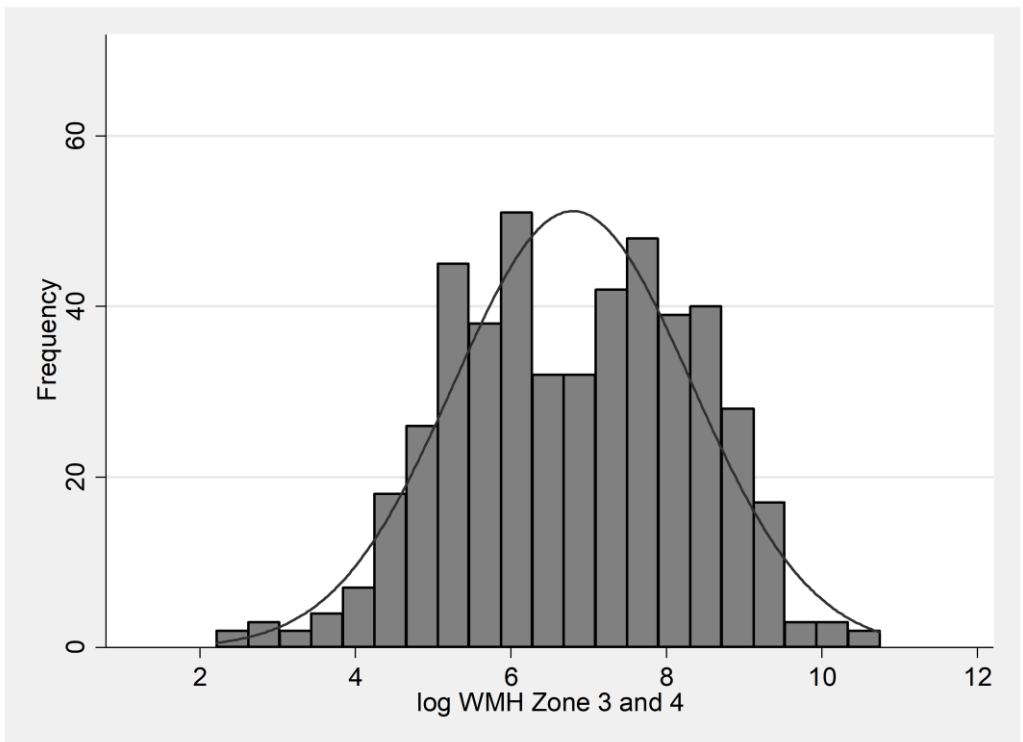


Figure 6-6 Histogram with normal density overlay, distribution of log WMHs zones 3 & 4.

	Model 1	Model 2	Model 3	Model 4	Model 5
Independent variables	TIV Sex (if applicable) Age	TIV Sex(if applicable) Ethnicity Age	TIV FRS	TIV FRS Ethnicity	TIV Ethnicity FRS* ethnicity
Dependent variable: cortical volume (ml)					
All	1a	2a	3a	4a	5a
Men	1b	2b	3b	4b	5b
Women	1c	2c	3c	4c	5c
Dependent variable: total white matter hyperintensity volume (mm³)					
All	1d	2d	3d	4d	5d
Men	1e	2e	3e	4e	5e
Women	1f	2f	3f	4f	5f
Dependent variable: white matter hyperintensity volume zones 1 & 2					
All	1g	2g	3g	4g	5g
Men	1h	2h	3h	4h	5h
Women	1i	2i	3i	4i	5i
Dependent variable: white matter hyperintensity volume zones 3 & 4					
All	1j	2j	3j	4j	5j
Men	1k	2k	3k	4k	5k
Women	1l	2l	3l	4l	5l

Table 6-1. Key to naming of generalized linear regression models using demographic variables and FRS as predictor variables.

	Model 6	Model 7	Model 8
Independent variables	TIV Age Sex CBF	TIV Age Sex (if applicable) Ethnicity CBF	TIV Age Sex (if applicable) Ethnicity CBF*ethnicity
Dependent variable: cortical volume (ml)			
All	6a	7a	8a
Men	6b	7b	8b
Women	6c	7c	8c
Dependent variable: total white matter hyperintensity volume (mm³)			
All	6d	7d	8d
Men	6e	7e	8e
Women	6f	7f	8f
Dependent variable: white matter hyperintensity volume zones 1&2			
All	6g	7g	8g
Men	6h	7h	8h
Women	6i	7i	8i
Dependent variable: white matter hyperintensity volume zones 3&4			
All	6j	7j	8j
Men	6k	7k	8k
Women	6l	7l	8l

Table 6-2. Key to naming of generalized linear regression models using demographic variables and CBF as predictor variables.

6.4 .Results

6.4.1 Brain characteristics

Whole sample and sex stratified mean (SD) absolute brain volumes, and volumes adjusted for TIV are presented in **Table 6-3**. Brain characteristics stratified by ethnicity are shown in **Table 6-4**.

	<i>All</i>			<i>Men</i>			<i>Women</i>			<i>P</i>
	<i>n</i>	<i>mean or %</i>	<i>±SD or IQR</i>	<i>n</i>	<i>mean or %</i>	<i>±SD or IQR</i>	<i>n</i>	<i>mean or %</i>	<i>±SD or IQR</i>	
<i>TIV, mL</i>	485	1340.3	±138.5	295	1400.0	±120.7	190	1247.4	±110.5	<.001
<i>Total brain tissue, mL</i>	485	1025.2	±101.2	295	1064.3	±91.2	190	9646.4	±84.8	<.001
<i>Total brain tissue, % TIV</i>	485	76.6	±2.2	295	76.0	±2.1	190	77.4	±2.2	<.001
<i>Cortical tissue, mL</i>	485	462.0	±46.0	295	479.8	±41.7	190	434.2	±37.9	<.001
<i>Cortical tissue, % TIV</i>	485	34.4	±1.1	295	34.3	±1.1	190	34.9	±1.1	<.001
<i>WM tissue, mL</i>	485	383.3	±44.1	295	398.2	±41.3	190	360.4	±38.1	<.001
<i>WM tissue, %TIV</i>	485	28.6	±1.5	295	28.4	±1.4	190	28.9	±1.5	.002
<i>Total WMH, mm³ *</i>	482	3383.1	(1266.6, 9093.9)	295	3528.0	(1148.6, 9301.1)	187	3073.2	(1368.4, 7960.1)	.549 ^{MW}
<i>WMHz12, mm³ *</i>	482	2253.2	(854.9, 5488.7)	295	2416.3	(814.6, 6094)	187	2106	(958, 4609)	.369 ^{MW}
<i>WMHz34, mm³ *</i>	482	953.9	(271.0, 2963.1)	295	1031.9	(117.2, 2918.6)	187	805.0	(341.4, 3090.0)	.915 ^{MW}
<i>CBF Hct PVC, mL/100g/min</i>	485	48.8	±7.3	295	49.6	±7.6	190	47.5	±6.8	0.002
<i>CBF Hct, mL/100g/min</i>	485	36.6	±6.3	295	36.5	±6.7	190	36.7	±5.8	0.897

Table 6-3. Brain characteristics by sex: data are mean ± SD, percentage of TIV or * median (IQR), tests for significance are calculated by Student's unpaired t-tests, except ^{MW} which denotes P value by rank sum Mann-Whitney test.

	<i>European</i>			<i>South Asian</i>			<i>African Caribbean</i>		
	<i>n</i>	<i>mean or %</i>	<i>±SD or IQR</i>	<i>n</i>	<i>mean or %</i>	<i>±SD or IQR</i>	<i>n</i>	<i>mean or %</i>	<i>±SD or IQR</i>
<i>TIV, mL</i>	223	1415.1	±125.0	173	1281.6	±113.5	89	1266.8	±120.2
<i>Total brain tissue, mL</i>	223	1077.6	±90.5	173	984.3	±85.9	89	973.7	±91.0
<i>Total brain tissue, % of TIV</i>	223	76.2	±2.2	173	76.9	±2.1	89	76.8	±2.3
<i>Cortical tissue, mL</i>	223	486.6	±41.7	173	445.5	±38.0	89	432.2	±37.7
<i>Cortical tissue, % of TIV</i>	223	34.4	±1.1	173	34.7	±0.1	89	34.2	±1.1
<i>WM tissue, mL</i>	223	402.5	±40.5	173	368.0	±39.6	89	365.1	±42.0
<i>WM tissue, % of TIV</i>	223	28.5	±1.4	173	28.7	±1.4	89	28.7	±1.6
<i>Total WMH, mm³ (median, IQR)</i>	223	3438.5	(1272.0, 10117.9)	171	3044.0	(1066.6, 8021.8).	88	3327.4	(545.6, 8564.8).
<i>WMHz12, mm³ (median, IQR)</i>	223	2394.7	(933.0, 6218.0)	171	2105.8	(720.0, 5205.4)	88	2223.3	(1074.1, 4810.4)
<i>WMHz34, (median, IQR)</i>	223	964.7	(278.7, 2972.8)	171	805.0	(265.4, 2391.0)	88	1431.9	(120.4, 3470.5)
<i>CBF Hct PVC, mL/100g/min</i>	223	51.1	±7.5	173	47.3	±6.7	89	45.8	±6.3
<i>CBF Hct, mL/100g/min</i>	223	38.0	±6.7	173	35.3	±5.7	89	35.7	±5.8

Table 6-4. Brain characteristics by ethnicity: data are mean ± SD, percentage of TIV or median (IQR)

6.4.1.1 Cortical volume

The mean (SD) cortical volume was 462.0 (\pm 46.0) mL. Cortical tissue volume decreased by just over 1mL per year of age (B -1.09; P < .001, [95% CI -1.30, -0.89] mL/year) after adjustment for TIV and ethnicity (model 2a, **Table 6-5, Figure 6-7**). Brain tissue volumes adjusted for age and TIV were similar in men and women (**Figure 6-8**, model 2a, **Table 6-6, Table 6-7**). African Caribbeans had ~ 8mL lower cortical volume than Europeans after adjustment for TIV, age and sex (B -7.74 P < .001, [95% CI -11.32, -4.17] mL), (Model 2a, **Table 6-5**) but there was little evidence of a difference in cortical volume between South Asian and Europeans.

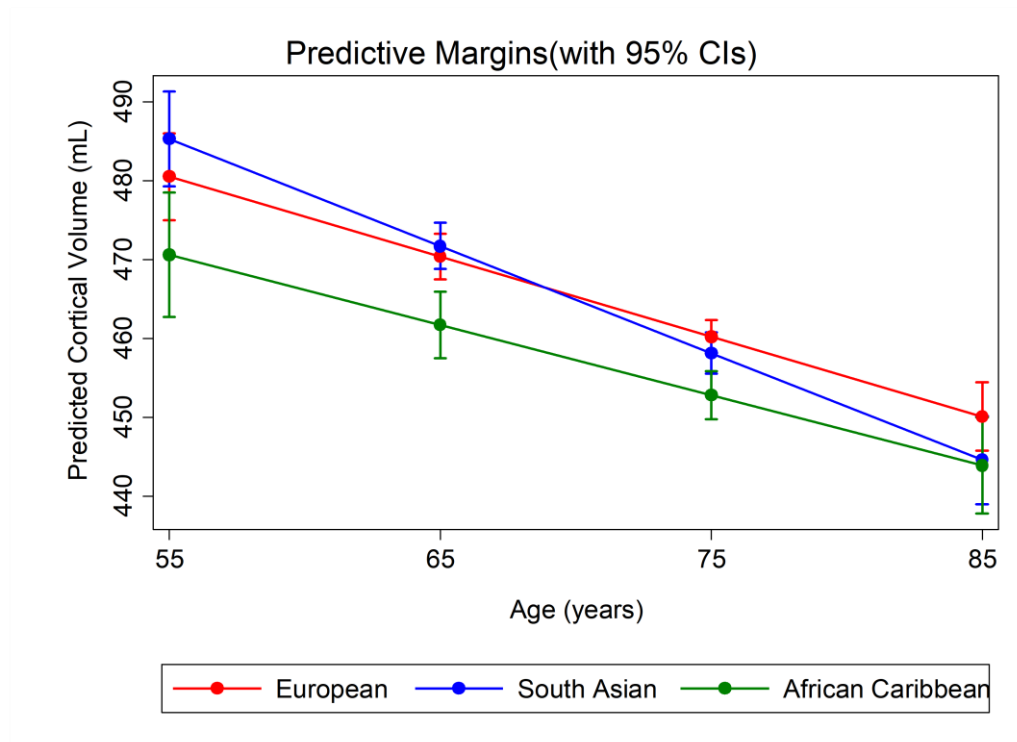


Figure 6-7. Predictive margins plot showing cortical volume by age, (whole sample).

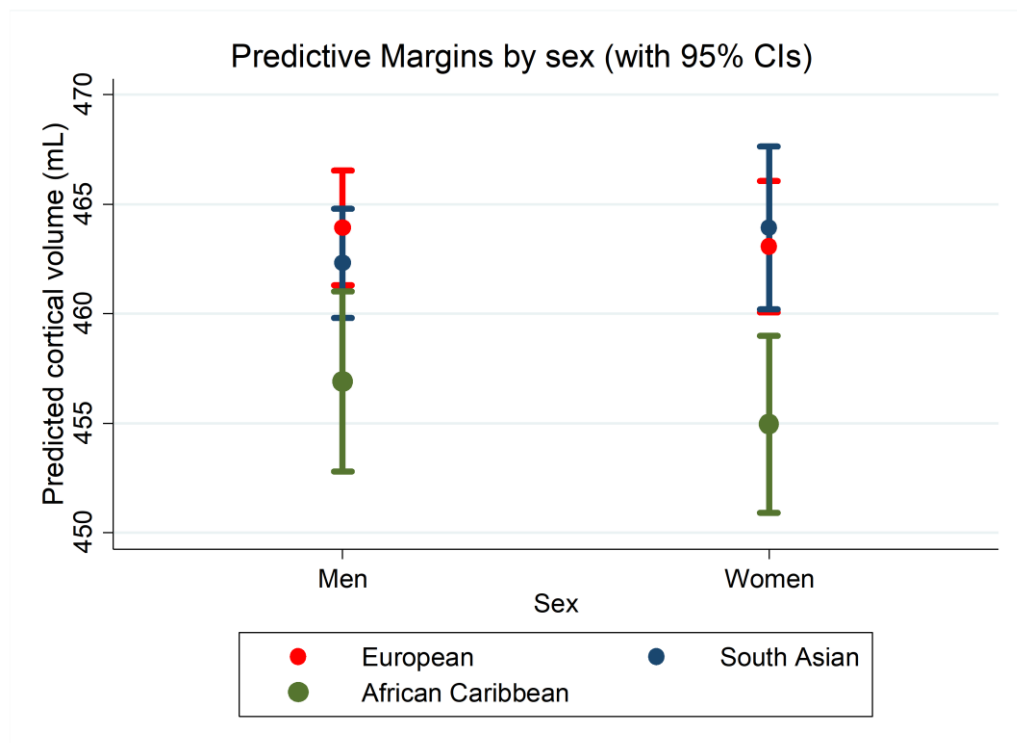


Figure 6-8. Cortical volume by sex and ethnicity, adjusted for age and TIV.

Dependent variable: cortical tissue volume (mL), (all participants)

	<i>Model 1a (n=485)</i>				<i>Model 2a (n=485)</i>			
<i>Adjusted R²</i>	0.92				0.92			
	<i>B</i>	<i>(95%CI)</i>		<i>P</i>	<i>B</i>	<i>(95%CI)</i>		<i>P</i>
<i>Age, years</i>	-1.13	-1.35	-0.92	<.001	-1.09	-1.30	-0.89	<.001
<i>Sex, female</i>	-0.30	-3.28	2.69	.846	-0.20	-3.25	2.85	.900
<i>South Asian</i>	-0.71	-3.76	2.34	.649
<i>African Caribbean</i>	-7.74	-11.32	-4.17	<.001

Table 6-5. Multiple linear regression models 1a, 2a, (all participants), cortical tissue volume is dependent variable. Models are adjusted for TIV, beta coefficients are unstandardised, P <.05 shown in bold.

Dependent variable: cortical tissue volume (mL), (men)

	<i>Model 1b (n=295)</i>				<i>Model 2b (n=295)</i>			
<i>Adjusted R²</i>	0.88				0.88			
	<i>B</i>	<i>(95%CI)</i>		<i>P</i>	<i>B</i>	<i>(95%CI)</i>		<i>P</i>
<i>Age, years</i>	-1.13	-1.45	-0.81	<.001	-1.11	-1.42	-0.79	<.001
<i>South Asian</i>	-1.41	-5.57	2.75	.505
<i>African Caribbean</i>	-6.80	-12.19	-1.41	.014

Table 6-6. Multiple linear regression models 1b, 2b, (men), cortical tissue volume is dependent variable. Models are adjusted for TIV, beta coefficients are unstandardised, P <.05 shown in bold.

Dependent variable: cortical tissue volume (mL), (women)

	<i>Model 1c (n=190)</i>				<i>Model 2c (n=190)</i>			
<i>Adjusted R²</i>	0.90				0.91			
	<i>B</i>	<i>(95%CI)</i>		<i>P</i>	<i>B</i>	<i>(95%CI)</i>		<i>P</i>
<i>Age, years</i>	-1.14	-1.41	-0.88	<.001	-1.07	-1.33	-0.81	<.001
<i>South Asian</i>					0.54	-3.81	4.89	.807
<i>African Caribbean</i>					-8.45	-12.96	-3.94	<.001

Table 6-7. Multiple linear regression models 1c, 2c (women), dependent variable is cortical tissue volume. Models are adjusted for TIV, beta coefficients are unstandardised, P <.05 shown in bold.

6.4.1.2 White matter hyperintensity volumes

The median (IQR) of total WMH volume was 3383 (1266, 9094) mm³ (Table 6-3). WMH volume increased by ~5.0% per year of age (exp *B* 1.05; *P* <.001, [95% CI 1.03, 1.07] mm³/year) (Model 1d,

Table 6-8). Although there was no evidence of a difference in total WMH volume by ethnicity in a pooled analysis (Model 2d,

Table 6-8), in sex-stratified analyses South Asian and African Caribbean men had a greater volume of total WMHs than European men (South Asian (exp *B* 1.42; *P* = .039 [95% CI 1.02, 1.97] mm³); (African Caribbean, exp *B* 1.44; *P* = .107 [95% CI 0.92, 2.23] mm³) after adjustment for TIV and age (Model 2e, **Table 6-9, Figure 6-9**), whereas women of South Asian and African Caribbean ethnicities had lower total WMH volumes than European women (South Asian, exp *B* 0.67; *P* = .093, [95% CI 0.42, 1.07] mm³) (African Caribbean, exp *B* 0.83; *P* = .454 [95% CI 0.50, 1.36] mm³) (Model 2f, **Table 6-10, Figure 6-10**), although the wide confidence limits on these estimates in African Caribbean men and in women of South Asian and African Caribbean descent should be noted. This pattern of results persisted for WMHs measured zonally (WMHz12 & WMHz34), although confidence margins were wide.

6.4.1.3 Cerebral blood flow

See Chapter 5 (p142) for a descriptive summary of CBF.

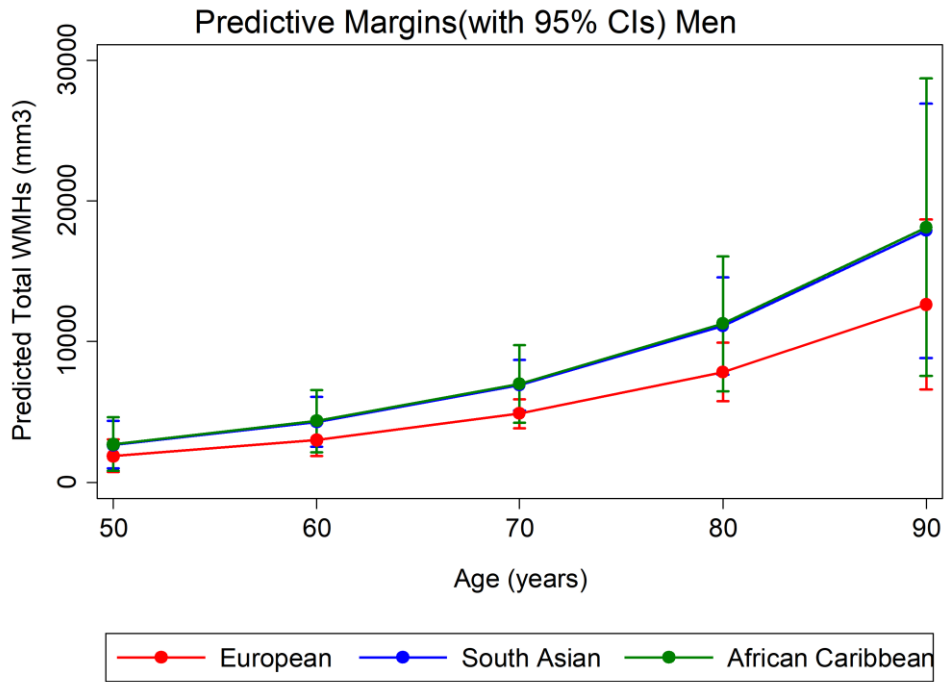


Figure 6-9. Predictive margins plot showing total WMHs by age in men.

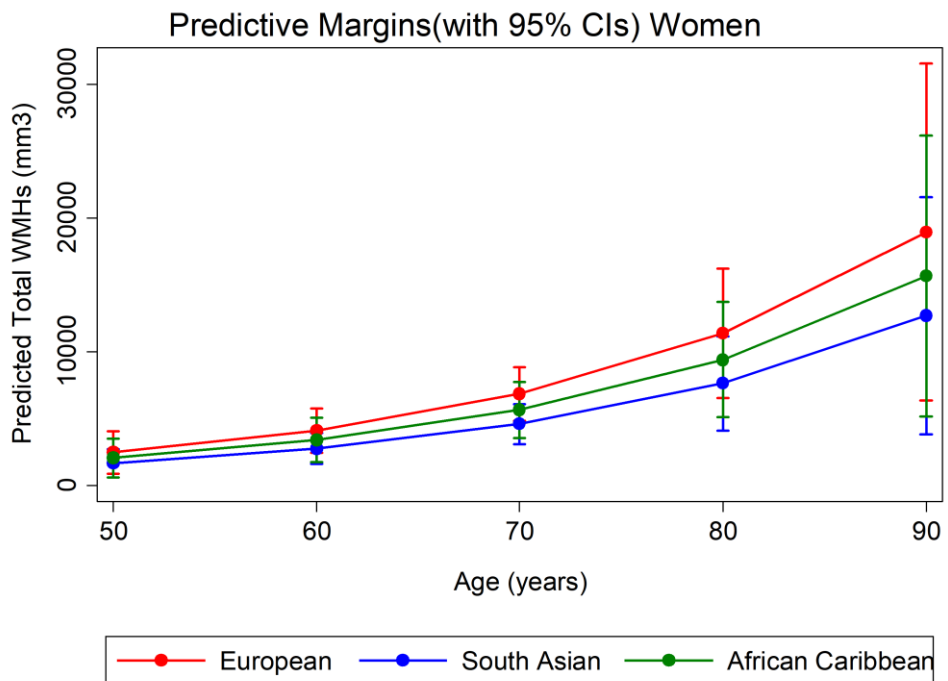


Figure 6-10. Predictive margins plot showing total WMHs by age in women.

Dependent variable: total WMH volume (mm³), (all participants)

	<i>Model 1d (n=482)</i>				<i>Model 2d (n=482)</i>			
<i>AIC</i>	19.49				19.49			
	<i>exp B</i>	<i>(95%CI)</i>		<i>P</i>	<i>exp B</i>	<i>(95%CI)</i>		<i>P</i>
<i>Age, years</i>	1.05	1.03	1.07	<.001	1.05	1.03	1.07	<.001
<i>Sex (female)</i>	1.23	0.93	1.63	.141	1.27	0.95	1.71	.108
<i>South Asian</i>	1.10	0.83	1.45	.524
<i>African Caribbean</i>	1.15	0.82	1.60	.419

Table 6-8. Generalized linear models 1d, 2d (all participants), dependent variable is total WMH volume. Models are adjusted for TIV, exponentiated beta coefficients, P <.05 shown in bold.

Dependent variable: total WMH volume (mm³), (men)

	<i>Model 1e (n=295)</i>				<i>Model 2e (n=295)</i>			
<i>AIC</i>	19.62				19.60			
	<i>exp B</i>	<i>(95%CI)</i>		<i>P</i>	<i>exp B</i>	<i>(95%CI)</i>		<i>P</i>
<i>Age, years</i>	1.05	1.02	1.08	.001	1.05	1.02	1.08	<.001
<i>South Asian</i>	1.42	1.02	1.97	.039
<i>African Caribbean</i>	1.44	0.92	2.23	.107

Table 6-9. Generalized linear models 1e, 2e (men), dependent variable is total WMH volume. Models are adjusted for TIV, exponentiated beta coefficients, P <.05 shown in bold.

Dependent variable: total WMH volume (mm³), (women)

	<i>Model 1f (n=187)</i>				<i>Model 2f (n=187)</i>			
AIC	19.29				19.29			
	<i>exp B</i>	<i>(95%CI)</i>		<i>P</i>	<i>exp B</i>	<i>(95%CI)</i>		<i>P</i>
Age, years	1.05	1.02	1.08	<.001	1.05	1.02	1.08	.001
South Asian	0.67	0.42	1.07	.093
African Caribbean	0.83	0.50	1.36	.454

Table 6-10. Generalized linear models 1f, 2f (women), dependent variable is total WMH volume. Models are adjusted for TIV, exponentiated beta coefficients, P <.05 shown in bold.

Dependent variable: WMH volume zones 1&2 (mm³), (all participants)

	<i>Model 1g (n=482)</i>				<i>Model 2g (n=482)</i>			
<i>AIC</i>	18.43				18.44			
	<i>exp B</i>	<i>(95%CI)</i>		<i>P</i>	<i>exp B</i>	<i>(95%CI)</i>		<i>P</i>
<i>Age, years</i>	1.05	1.04	1.07	<.001	1.05	1.04	1.07	<.001
<i>Sex, female</i>	1.22	0.96	1.55	.108	1.25	0.97	1.61	.089
<i>South Asian</i>	1.07	0.84	1.36	.587
<i>African Caribbean</i>	1.04	0.78	1.39	.787

Table 6-11. Generalized linear models 1g, 2g (all participants), dependent variable is WMH zones 1 & 2 volume. Models are adjusted for TIV, exponentiated beta coefficients, P <.05 shown in bold.

Dependent variable: WMH volume zones 1&2 (mm³), (men)

	<i>Model 1h (n=295)</i>				<i>Model 2h (n=295)</i>			
<i>AIC</i>	18.58				18.58			
	<i>exp B</i>	<i>(95%CI)</i>		<i>P</i>	<i>exp B</i>	<i>(95%CI)</i>		<i>P</i>
<i>Age, years</i>	1.05	1.03	1.08	<.001	1.05	1.03	1.08	<.001
<i>South Asian</i>	1.35	1.01	1.82	.044
<i>African Caribbean</i>	1.32	0.89	1.96	.161

Table 6-12. Generalized linear models 1h, 2h (men), dependent variable is WMH zones 1 & 2 volume. Models are adjusted for TIV, exponentiated beta coefficients, P <.05 shown in bold.

Dependent variable: WMH volume zones 1&2 (mm³), (women)

	<i>Model 1i (n=187)</i>				<i>Model 2i (n=187)</i>			
AIC	18.21				18.21			
	<i>exp B</i>	<i>(95%CI)</i>		<i>P</i>	<i>exp B</i>	<i>(95%CI)</i>		<i>P</i>
Age, years	1.06	1.03	1.08	<.001	1.06	1.03	1.08	<.001
South Asian	0.69	0.47	1.02	.065
African Caribbean	0.73	0.48	1.12	.151

Table 6-13. Generalized linear models 1i, 2i (women), dependent variable is WMH zones 1 & 2 volume. Models are adjusted for TIV, exponentiated beta coefficients, P <.05 shown in bold.

Dependent variable: WMH volume zones 3&4 (mm³), (all participants)

	<i>Model 1j (n=482)</i>				<i>Model 2j (n=482)</i>			
<i>AIC</i>	17.54				17.54			
	<i>exp B</i>	<i>(95%CI)</i>		<i>P</i>	<i>exp B</i>	<i>(95%CI)</i>		<i>P</i>
<i>Age, years</i>	1.05	1.02	1.08	.001	1.05	1.02	1.08	.001
<i>Sex, female</i>	1.26	0.86	1.84	.232	1.30	0.87	1.94	.201
<i>South Asian</i>	1.11	0.76	1.62	.605
<i>African Caribbean</i>	1.32	0.84	2.06	.234

Table 6-14. Generalized linear models 1j, 2j (all participants), dependent variable is WMH zones 3 & 4 volume. Models are adjusted for TIV, exponentiated beta coefficients ,P <.05 shown in bold.

Dependent variable: WMHs zones 3&4 (mm³), (men)

	Model 1k (n=295)				Model 2k (n=295)			
<i>Adjusted R²</i>	17.62				17.62			
	<i>exp B</i>	<i>(95%CI)</i>		<i>P</i>	<i>exp B</i>	<i>(95%CI)</i>		<i>P</i>
Age, years	1.05	1.01	1.08	.010	1.05	1.02	1.08	.004
South Asian	1.49	0.97	2.27	.067
African Caribbean	1.62	0.91	2.86	.099

Table 6-15. Generalized linear models 1k, 2k (men), dependent variable is WMH zones 3 & 4 volume. Models are adjusted for TIV, exponentiated beta coefficients, P <.05 shown in bold.

Dependent variable: WMH volume zones 3&4 (mm³), (women)

	Model 1I (n=187)				Model 2I (n=187)			
Adjusted R ²	17.37				17.34			
	exp B	(95%CI)		P	exp B	(95%CI)		P
Age, years	1.05	1.01	1.09	.028	1.05	1.00	1.09	.040
South Asian	0.61	0.33	1.16	.133
African Caribbean	0.98	0.50	1.94	.959

Table 6-16. Generalized linear models 1I, 2I (women), dependent variable is WMH zones 3 & 4 volume. Models are adjusted for TIV, exponentiated beta coefficients, P <.05 shown in bold.

6.4.2 Independent variable: Framingham risk score

6.4.2.1 .Dependent variable: cortical volume

Pooled sample

Cortical volume decreased by ~2mL per 10% increase in FRS (B -0.22; P <.001, [95% CI -0.30, -0.13] mL) adjusted for TIV (model 3a, **Table 6-17**).

However, this relationship was moderated by ethnicity (model 5a, **Table 6-17**, **Figure 6-11**). Europeans experienced less decline in cortical volume (1.2mL per 10% increase in FRS) with increasing FRS (B -0.12; P = .067, [95% CI -0.26, 0.01] mL) than South Asians who had an excess of ~2.0mL per 10% increase in FRS (B 0.20; P = .035, [95% CI 0.01, 0.38]) or African Caribbeans who had an excess of ~1.6mL decrease per 10% increase in FRS (B 0.16; P = .023, [95% CI -0.42, -0.10] mL). Note: all statistics in brackets cite units as presented in tables i.e. increase in unit outcome variable (mL) per 1% increase in FRS.

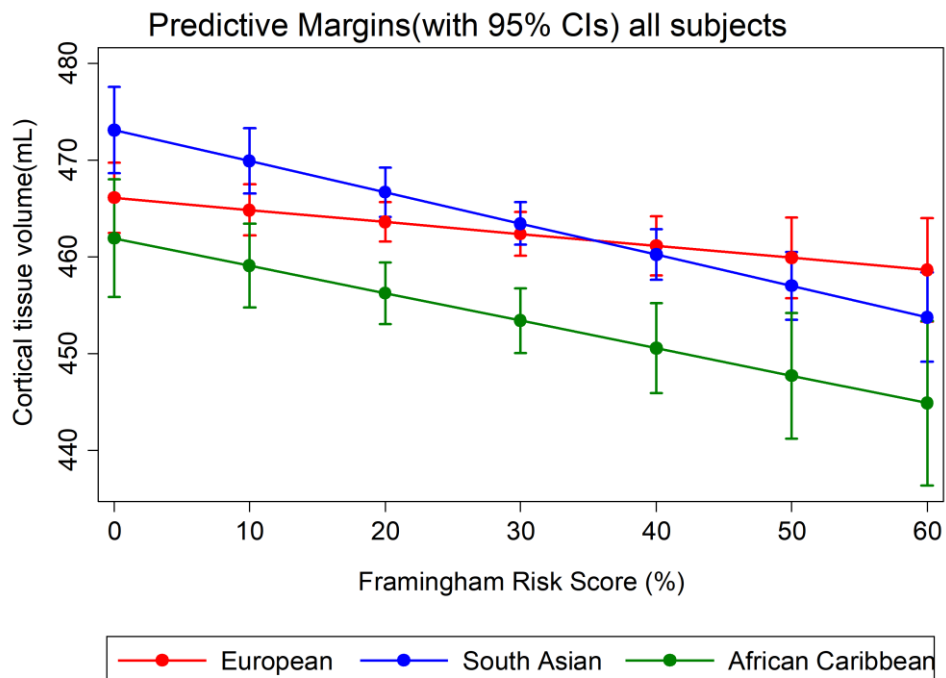


Figure 6-11. Predictive margins plot showing cortical volume and FRS, by ethnicity (all participants), adjusted for TIV.

Dependent variable: cortical tissue volume (mL), (all participants)

	Model 3a (n=485)				Model 4a (n=485)				Model 5a (n=485)			
Adjusted R ²	0.90				0.91				0.91			
	B	(95%CI)		P	B	(95%CI)		P	B	(95%CI)		P
FRS, %	-0.22	-0.30	-0.13	<.001	-0.23	-0.32	-0.15	<.001	-0.12	-0.26	0.01	.067
South Asian					1.97	-1.27	5.20	.234	7.05	1.28	12.81	.017
African Caribbean					-7.88	-11.71	-4.04	<.001	-4.17	-11.26	2.91	.248
South Asian*FRS, %					-0.20	-0.38	-0.01	.035
African Caribbean*FRS, %					-0.16	-0.42	0.10	.218

Table 6-17. Multiple linear regression models 3a, 4a,5a, (all participants), cortical tissue volume is dependent variable. Models are adjusted for TIV, unstandardised beta coefficients, P <.05 shown in bold.

Sex stratified models

South Asian and African Caribbean men had ~ 2-3mL greater decrease of cortical volume per 10% increase in FRS than European men (South Asian , B -0.28; P = .034, [95% CI -0.54, -0.02] mL) (African Caribbean; B -0.20; P = .322, [95% CI -0.58, 0.19] mL) (model 5b, Figure **6-12**, Table **6-18**). However, although the association for the interaction term of FRS with South Asian men was statistically significant, confidence margins for these results are wide, particularly at higher levels of vascular risk where data are sparse, therefore the evidence is weak and should be treated cautiously. Moderation by ethnicity was not evident in women (model 5c, Figure **6-13**, Table **6-19**).

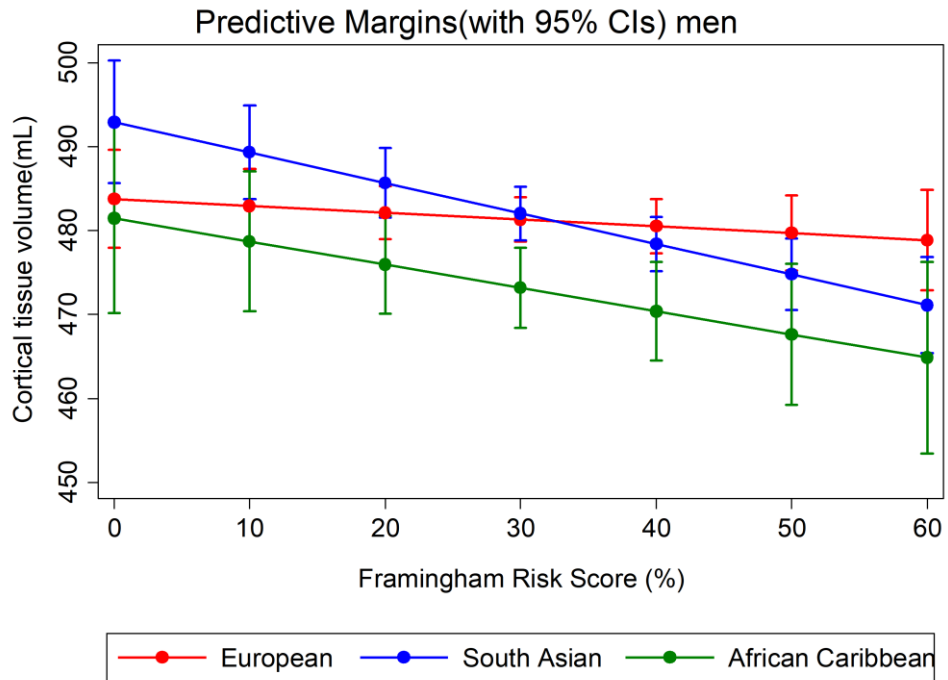


Figure 6-12. Predictive margins plot showing cortical volume and FRS by ethnicity (men), adjusted for TIV.

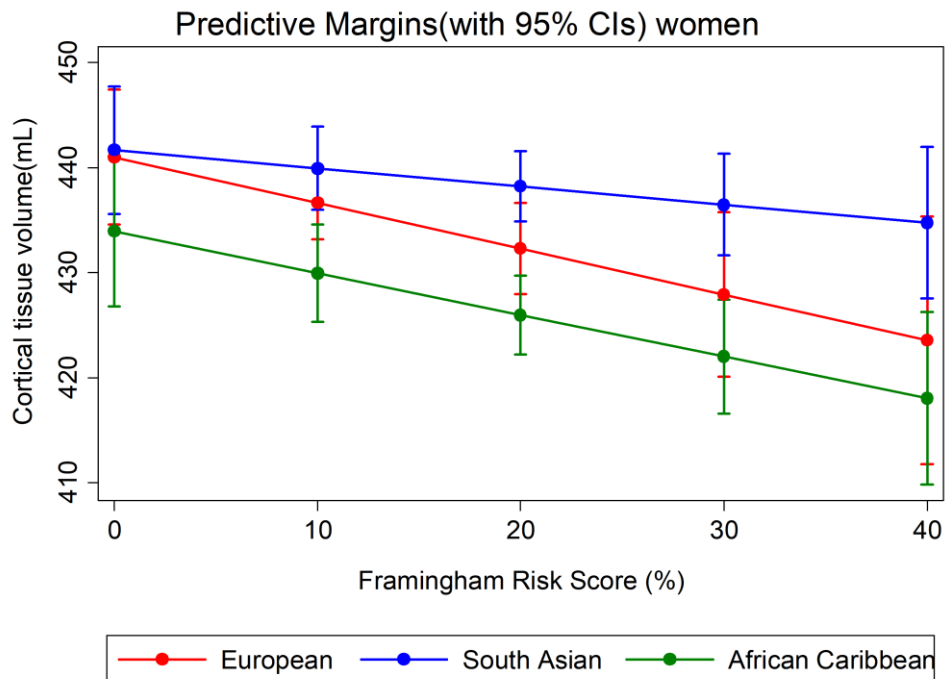


Figure 6-13 Predictive margins plot showing cortical volume and FRS, by ethnicity (women), adjusted for TIV.

Dependent variable: cortical tissue volume (mL), (men)

	Model 3b (n=295)				Model 4b (n=295)				Model 5b (n=295)			
Adjusted R ²	0.87				0.87				0.87			
	B	(95%CI)		P	B	(95%CI)		P	B	(95%CI)		P
FRS, %	-0.20	-0.33	-0.08	.001	-0.22	-0.34	-0.10	<.001	-0.08	-0.26	0.09	.360
South Asian					0.24	-4.17	4.65	.915	9.18	-0.22	18.59	.056
African Caribbean					-7.90	-13.58	-2.21	.007	-2.28	-15.12	10.52	.724
South Asian *FRS, %									-0.28	-0.54	-0.02	.034
African Caribbean *FRS, %									-0.20	-0.58	0.19	.322

Table 6-18. Multiple linear regression models 3b, 4b,5b, (men), cortical tissue volume is dependent variable. Models are adjusted for TIV, unstandardised beta coefficients, P <.05 shown in bold.

Dependent variable: cortical tissue volume (mL), (women)

	Model 3c (n=190)			Model 4c (n=190)			Model 5c (n=190)		
Adjusted R ²	0.87			0.89			0.90		
	B	(95%CI)	P	B	(95%CI)	P	B	(95%CI)	P
FRS, %	-0.32	-0.52 -0.12	.001	-0.30	-0.50 -0.11	.002	-0.44	-0.86 -0.01	.043
South Asian				4.82	-0.13 9.76	.056	0.67	-8.41 9.75	.884
African Caribbean				-6.95	-12.17 -1.72	.009	-7.07	-16.77 2.62	.152
South Asian*FRS, %							0.26	-0.25 0.78	.313
African Caribbean*FRS, %							0.04	-0.50 0.58	.886

Table 6-19 Multiple linear regression models 3c, 4c,5c, (women), cortical tissue volume is dependent variable. Models are adjusted for TIV, unstandardised beta coefficients, P <.05 shown in bold.

6.4.2.2 Dependent variable total WMH volume

Pooled sample

Total WMH load increased by ~1% per 1% increase of FRS adjusted for TIV (exp *B* 1.01; *P* = .083, [95% CI 1.00, 1.01] mm³) (models 3d, **Table 6-20**) in a pooled analysis of all participants. Compared to Europeans, South Asian and African Caribbean participants experienced ~2% greater increase in WMH volume per 1% increase in FRS (Model 5d, **Table 6-20, Figure 6-14**) (exp *B* 1.02; *P* = .048, [95% CI 1.00, 1.03] mm³) (exp *B* 1.02; *P* = .100, [95% CI 1.00, 1.04] mm³) respectively. This result was statistically significant for South Asians (model 5d).

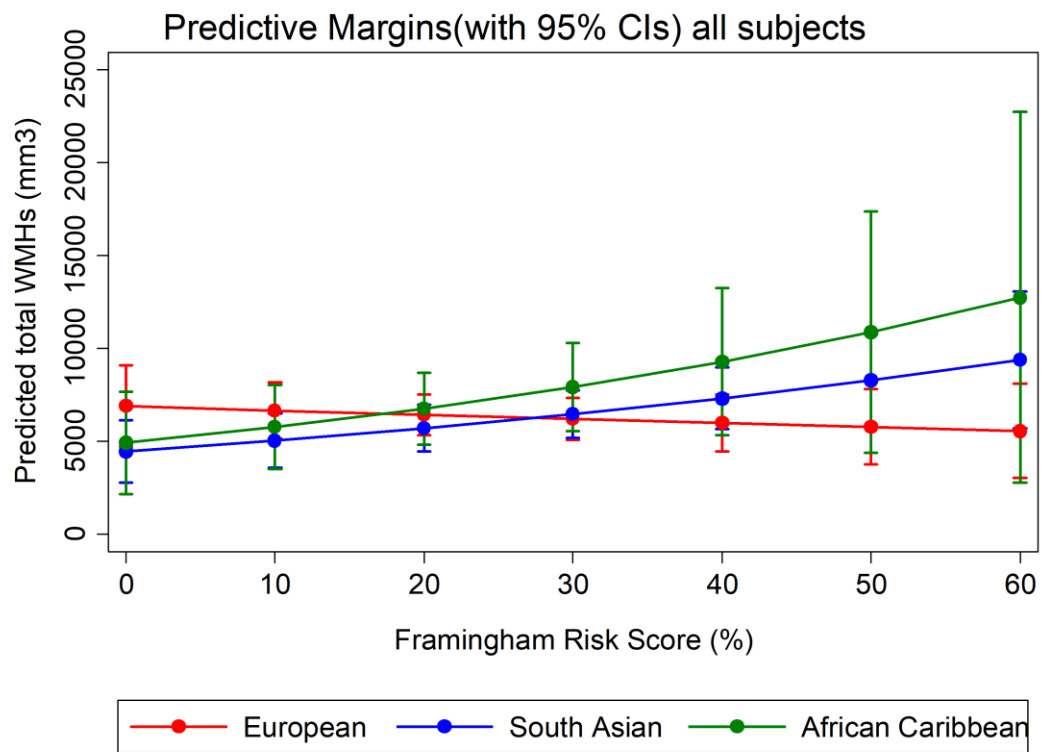


Figure 6-14 Predictive margins plot showing total WMHs and FRS, by ethnicity (all participants), adjusted for TIV.

Dependent variable: total WMH volume (mm³), (all participants)

	Model 3d (n=482)				Model 4d (n=482)			Model 5d (n=482)				
AIC	19.55				19.56			19.55				
	exp B	(95%CI)		P	exp B	(95%CI)		P	exp B	(95%CI)		P
FRS, %	1.01	1.00	1.01	.083	1.01	1.00	1.02	.085	1.00	0.98	1.00	.544
South Asian					0.96	0.72	1.26	.753	0.64	0.40	1.05	.078
African Caribbean					1.11	0.80	1.55	.533	0.71	0.38	1.35	.296
South Asian*FRS, %									1.02	1.00	1.03	.048
African Caribbean*FRS, %									1.02	1.00	1.04	.100

Table 6-20 Generalized linear models 3d, 4d, 5d (all participants), dependent variable is total WMH volume. Models are adjusted for TIV, exponentiated beta coefficients, P <.05 shown in bold.

Sex stratified models

There was some weak evidence that ethnicity was an effect modifier in the relationship of WMH volume and FRS in both sexes (model 5e, model 5f, **Table 6-21**). In stratified models of both men and women, African Caribbeans had a greater increase in total WMH volume in association with increasing FRS than either Europeans or South Asians (**Figure 6-15** and **Figure 6-16**). However, results are somewhat unreliable due to overlapping and wide confidence margins due to paucity of data in stratified models, especially at levels of high vascular risk.

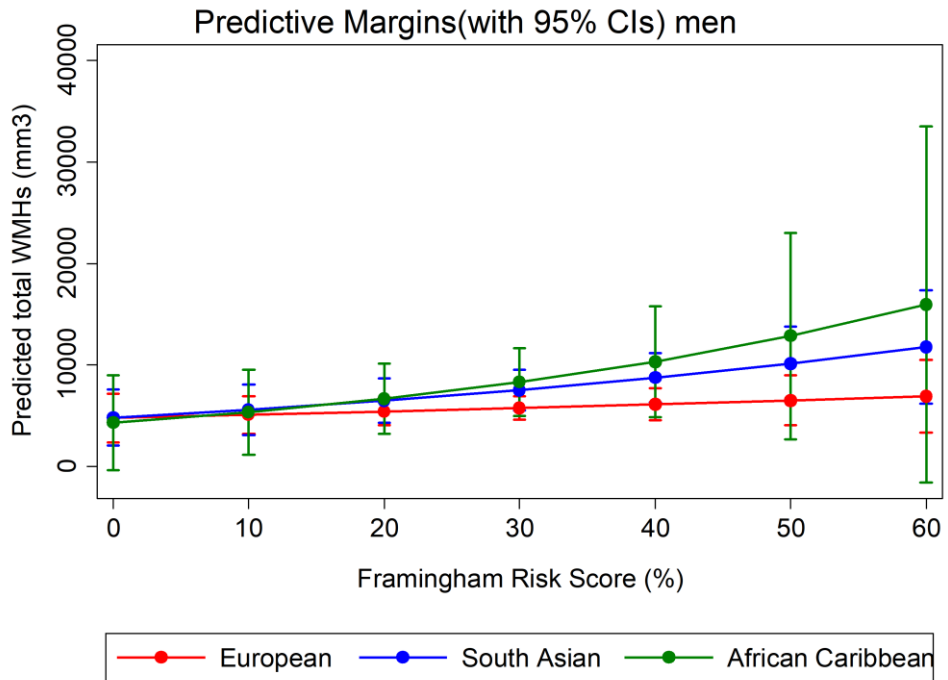


Figure 6-15 Predictive margins plot showing total WMHs and FRS, by ethnicity (men), adjusted for TIV.

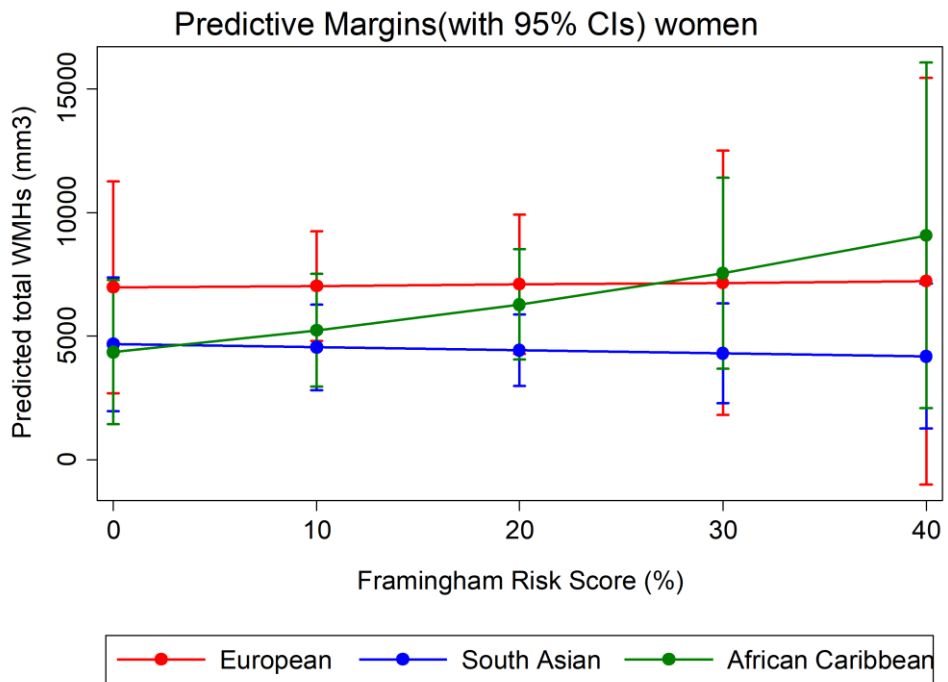


Figure 6-16. Predictive margins plot showing total WMHs and FRS, by ethnicity (women), adjusted for TIV.

Dependent variable: total WMH volume (mm³), (men)

	Model 3e (n=295)				Model 4e (n=295)				Model 5e (n=295)			
AIC	19.65				19.65				19.66			
	exp B	(95%CI)		P	exp B	(95%CI)		P	exp B	(95%CI)		P
FRS, %	1.01	1.00	1.02	.016	1.01	1.00	1.02	.024	1.01	1.00	1.02	.434
South Asian					1.31	0.93	1.84	.124	1.01	0.47	2.15	.989
African Caribbean					1.44	0.91	2.24	.122	0.90	0.27	2.97	.865
South Asian*FRS, %									1.01	0.99	1.03	.432
African Caribbean*FRS, %									1.02	0.98	1.05	.411

Table 6-21. Generalized linear models 3e, 4e, 5e (men), dependent variable is total WMH volume. Models are adjusted for TIV, exponentiated beta coefficients, P <.05 shown in bold.

Dependent variable: total WMH volume (mm³), (women)

	<i>Model 3f (n=187)</i>				<i>Model 4f (n=187)</i>				<i>Model 5f (n=187)</i>			
<i>AIC</i>	19.40				19.39				19.40			
	<i>exp B</i>	<i>(95%CI)</i>		<i>P</i>	<i>exp B</i>	<i>(95%CI)</i>		<i>P</i>	<i>exp B</i>	<i>(95%CI)</i>		<i>P</i>
<i>FRS, %</i>	1.01	1.00	1.00	.024	1.01	0.99	1.03	.532	1.00	0.96	1.04	.965
<i>South Asian</i>					0.62	0.39	0.99	.043	0.67	0.28	1.60	.368
<i>African Caribbean</i>					0.85	0.52	1.39	.510	0.63	0.25	1.58	.322
<i>South Asian *FRS, %</i>									1.00	0.95	1.05	.885
<i>African Caribbean *FRS, %</i>									1.02	0.97	1.07	.510

Table 6-22. Generalized linear models 3f, 4f, 5f (women), dependent variable is total WMH volume. Models are adjusted for TIV, exponentiated beta coefficients, P <.05 shown in bold.

6.4.2.3 Dependent variable WMH volume zones 1 & 2

Pooled sample

The trends of associations between FRS, ethnicity and WMH zones 1 & 2 were similar to those using total volume of WMHs as the dependent variable. FRS was positively associated with WMHs in zones 1 & 2 (exp B 1.01, $P=.019$, [95%CI 1.00, 1.01] mm^3) (model 3g, **Table 6-23, Figure 6-17**). The modifying effect of ethnicity noted for total WMHs volume was similar in WMH zonal areas 1 & 2. African Caribbeans had ~2% greater volume increase per 1% increase in FRS compared to Europeans (exp B 1.02, $P=.073$, [95%CI 1.00, 1.04] mm^3), while South Asians had a 1% greater volume increase per 1% increase in FRS compared to Europeans (model 5g, **Table 6-23, Figure 6-17**), although 95% confidence estimates included unity in both cases.

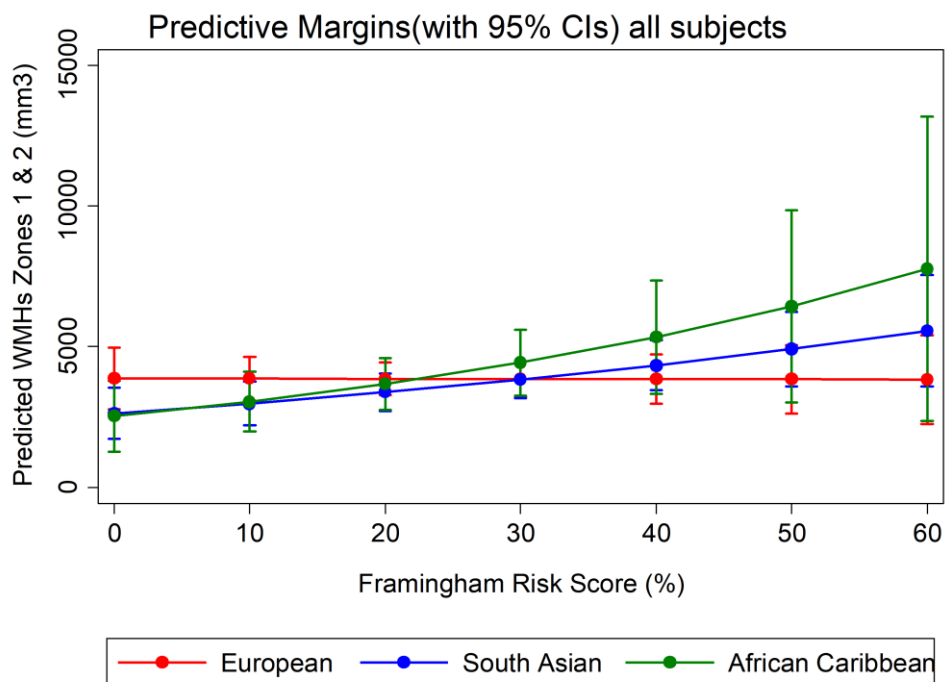


Figure 6-17 Predictive margins plot showing total WMHs zones 1 & 2 and FRS, by ethnicity (all participants), adjusted for TIV.

Dependent variable: WMH volume zones 1&2 (mm³), (all participants)

	<i>Model 3g (n=482)</i>				<i>Model 4g (n=482)</i>				<i>Model 5g (n=482)</i>			
AIC	18.51				18.51				18.51			
	<i>exp B</i>	<i>(95%CI)</i>		<i>P</i>	<i>exp B</i>	<i>(95%CI)</i>		<i>P</i>	<i>exp B</i>	<i>(95%CI)</i>		<i>P</i>
FRS, %	1.01	1.00	1.01	.019	1.01	1.00	1.02	.016	1.00	0.99	1.01	.976
South Asian					0.93	0.73	1.18	.531	0.68	0.44	1.05	.085
African Caribbean					1.01	0.76	1.35	.942	0.65	0.37	1.15	.138
South Asian*FRS, %									1.01	1.00	1.03	.083
African Caribbean*FRS, %									1.02	1.00	1.04	.073

Table 6-23. Generalized linear models 3g, 4g, 5g (all participants), dependent variable is WMH volume zones 1 & 2. Models are adjusted for TIV, exponentiated beta coefficients, P <.05 shown in bold.

Stratified sample

Trends of association were similar in men and women regarding the association of FRS with WMHs zones 1 & 2 and followed similar patterns to models using total WMHs as the dependent variable. In stratified models WMH volume zones 1 & 2 increased with FRS and there were similar indications of interaction with ethnicity although there were wide confidence margins (**Table 6-24, Table 6-25, Figure 6-18**). There was some evidence that South Asian women did not have an increase of WMHs zones 1 & 2 volume with increasing FRS (exp B 0.99, $P=.679$, [95%CI 0.95, 1.04] mm³) whereas European and African Caribbean women had similar increases (**Figure 6-19**).

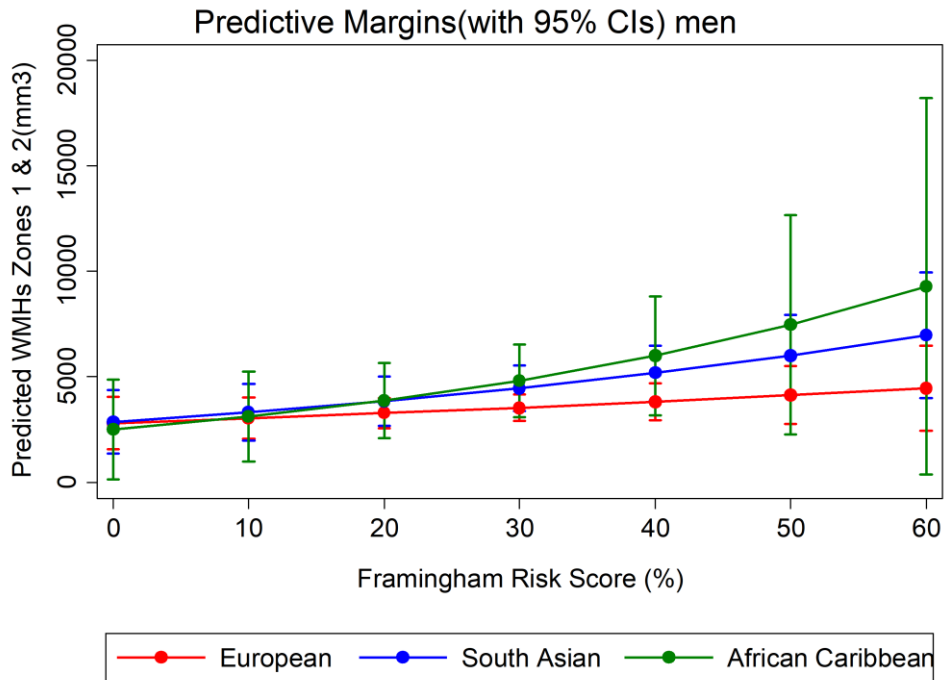


Figure 6-18 Predictive margins plot showing total WMHs in zones 1 & 2 and FRS, by ethnicity (men), adjusted for TIV.

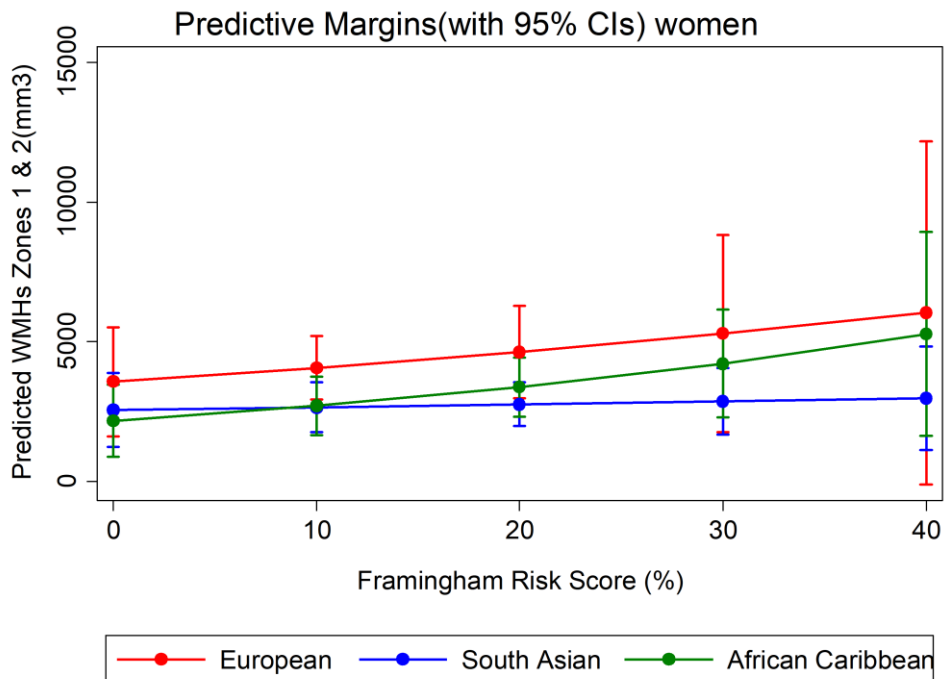


Figure 6-19. Predictive margins plot showing total WMHs in zones 1 & 2 and FRS, by ethnicity (women), adjusted for TIV.

Dependent variable: WMH volume zones 1&2 (mm³), (men)

	<i>Model 3h (n=295)</i>				<i>Model 4h (n=295)</i>				<i>Model 5h (n=295)</i>			
<i>AIC</i>	18.62				18.62				18.62			
	<i>exp B</i>	<i>(95%CI)</i>		<i>P</i>	<i>exp B</i>	<i>(95%CI)</i>		<i>P</i>	<i>exp B</i>	<i>(95%CI)</i>		<i>P</i>
<i>FRS, %</i>	1.01	1.00	1.02	.005	1.01	1.00	1.02	.008	1.01	0.99	1.02	.268
<i>South Asian</i>					1.26	0.93	1.72	.140	1.02	0.51	2.02	.954
<i>African Caribbean</i>					1.35	0.90	2.03	.144	0.89	0.31	2.53	.829
<i>South Asian*FRS, %</i>									1.01	0.99	1.03	.475
<i>African Caribbean*FRS, %</i>									1.01	0.98	1.05	.394

Table 6-24. Generalized linear models 3h, 4h, 5h (men), dependent variable is WMH volume in zones 1 & 2. Models are adjusted for TIV, exponentiated beta coefficients, P <.05 shown in bold.

Dependent variable: WMH volume zones 1&2 (mm³), (women)

	<i>Model 3i (n=187)</i>				<i>Model 4i (n=187)</i>				<i>Model 5i (n=187)</i>			
<i>AIC</i>	18.33				18.32				18.33			
	<i>exp B</i>	<i>(95%CI)</i>		<i>P</i>	<i>exp B</i>	<i>(95%CI)</i>		<i>P</i>	<i>exp B</i>	<i>(95%CI)</i>		<i>P</i>
<i>FRS, %</i>	1.01	1.00	1.03	.260	1.01	1.00	1.03	.140	1.01	0.98	1.05	.482
<i>South Asian</i>					0.61	0.41	0.92	.018	0.72	0.33	1.55	.399
<i>African Caribbean</i>					0.72	0.47	1.11	.137	0.61	0.26	1.38	.234
<i>South Asian*FRS, %</i>									0.99	0.95	1.04	.679
<i>African Caribbean*FRS, %</i>									1.01	0.96	1.06	.699

Table 6-25. Generalized linear models 3i, 4i, 5i (women), dependent variable is WMH volume zones 1 & 2. Models are adjusted for TIV, exponentiated beta coefficients, P <.05 shown in bold.

6.4.2.4 Dependent variable WMH volume zones 3 & 4

Pooled sample

FRS was weakly positively associated with WMHs in zones 3 & 4 (exp *B* 1.01, $P=.308$, [95%CI 1.00, 1.01] mm³) (model 3j, **Table 6-26**) but the data are consistent with a null relationship. There was some evidence of modification of the relationship between FRS and WMH in zones 3 & 4 by ethnicity. South Asians and African Caribbeans appeared to experience an increase of WMH volume in zones 3&4 with increasing FRS (exp *B* 1.02, $P=.030$, [95%CI 1.00, 1.04] mm³) (exp *B* 1.02, $P=.168$, [95%CI 0.99, 1.05] mm³) respectively, in contrast to the weak negative relationship apparent in Europeans (model 5j, **Table 6-26**). However, confidence margins were wide and overlapping, and results should be treated cautiously.

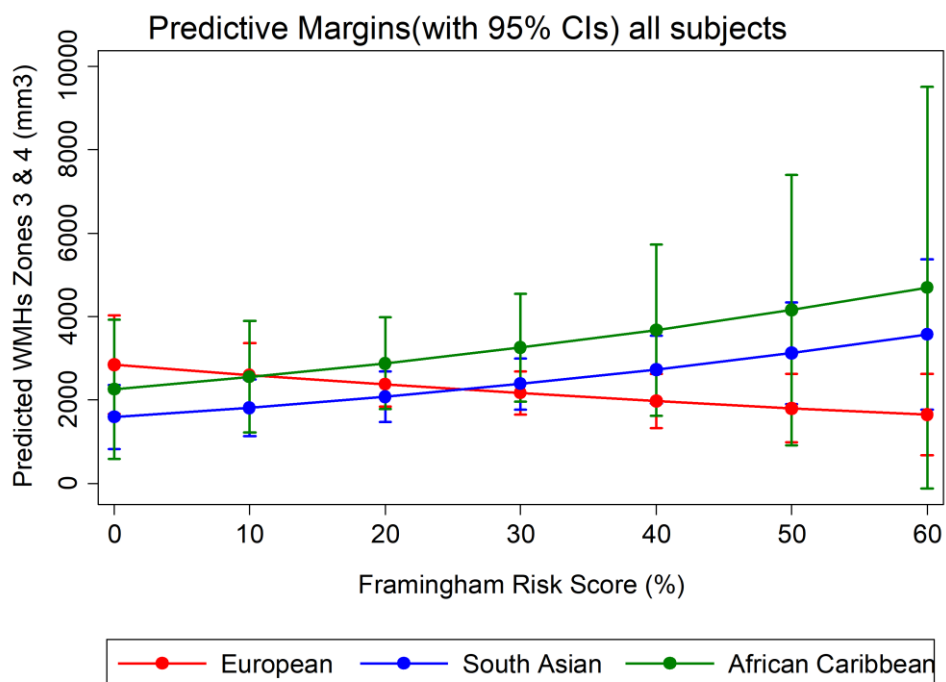


Figure 6-20 Predictive margins plot showing total WMHs zones 3 & 4 and FRS, by ethnicity (all participants), adjusted for TIV

Dependent variable: WMHs zones 3&4 (mm³), (all participants)

	Model 3j (n=482)				Model 4j (n=482)				Model 5j (n=482)			
<i>AIC</i>	17.60				17.60				17.58			
	<i>exp B</i>	<i>(95%CI)</i>		<i>P</i>	<i>exp B</i>	<i>(95%CI)</i>		<i>P</i>	<i>exp B</i>	<i>(95%CI)</i>		<i>P</i>
<i>FRS, %</i>	1.01	1.00	1.01	.308	1.01	1.00	1.02	.322	0.99	0.98	1.01	.234
<i>South Asian</i>					0.98	0.68	1.42	.912	0.56	0.30	1.05	.070
<i>African Caribbean</i>					1.27	0.82	1.99	.285	0.79	0.34	1.83	.589
<i>South Asian*FRS, %</i>									1.02	1.00	1.04	.030
<i>African Caribbean*FRS, %</i>									1.02	0.99	1.05	.168

Table 6-26. Generalized linear models 3j, 4j, 5j (all participants), dependent variable is WMH volume zones 3 & 4. Models are adjusted for TIV, exponentiated beta coefficients, P <.05 shown in bold.

Stratified sample

The men's model showed a weak positive association between FRS and WMHs in zones 3&4 (exp *B* 1.01. *P* = .072, [95%CI 1.00, 1.00] (model 3k, **Table 6-27**). There was no convincing evidence of ethnic variation. (**Figure 6-21**). In the women's sample, there was no overall association of FRS with WMHs in zones 3 & 4 (exp *B* 1.00. *P* = .816, [95%CI 0.98, 1.02] (model 3l, **Table 6-28**). However, FRS was positively associated with WMHs in zones 3 & 4 in African Caribbean women, a relationship that was not evident in European or South Asian women (exp *B* 1.04. *P* = .288, [95%CI 0.97, 1.10] (**Table 6-28, Figure 6-22**).

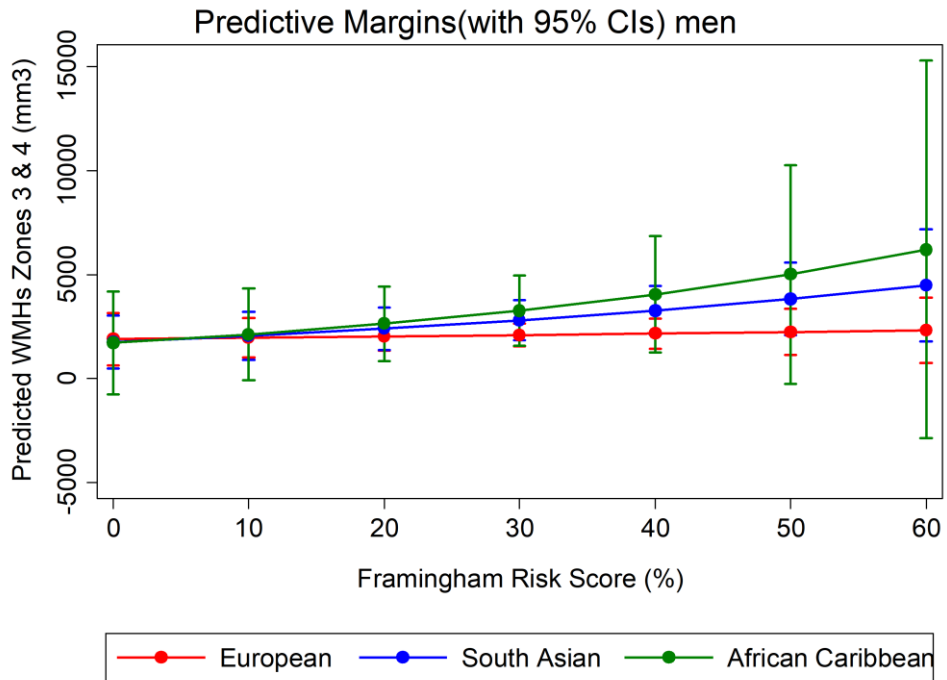


Figure 6-21 Predictive margins plot showing total WMHs in zones 3 & 4 and FRS, by ethnicity (men), adjusted for TIV.

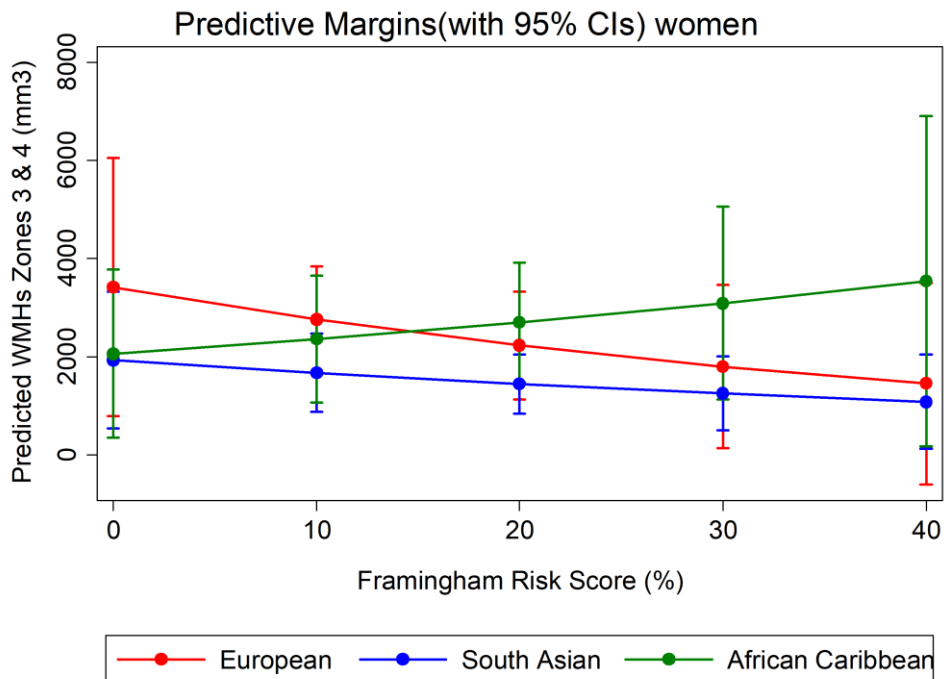


Figure 6-22. Predictive margins plot showing total WMHs in zones 3 & 4 and FRS, by ethnicity (women), adjusted for TIV.

Dependent variable: WMH volume zones 3&4 (mm³), (men)

	<i>Model 3k (n=295)</i>				<i>Model 4k (n=295)</i>				<i>Model 5k (n=295)</i>			
AIC	17.68				17.67				17.68			
	exp B	(95%CI)		P	exp B	(95%CI)		P	exp B	(95%CI)		P
FRS, %	1.01	1.00	1.00	.072	1.01	1.00	1.02	.097	1.00	0.98	1.02	.753
South Asian					1.35	0.87	2.09	.177	0.93	0.35	2.49	.882
African Caribbean					1.54	0.86	2.76	.142	0.91	0.18	4.50	.904
South Asian*FRS, %									1.01	0.98	1.04	.392
African Caribbean*FRS,%									1.02	0.97	1.07	.476

Table 6-27. Generalized linear models 3k, 4k, 5k (men), dependent variable is WMH volume zones 3 & 4. Models are adjusted for TIV, exponentiated beta coefficients, P <.05 shown in bold.

Dependent variable: WMH volume zones 3&4 (mm³), (women)

	Model 3I (n=187)				Model 4I (n=187)				Model 5I (n=187)			
AIC	17.44				17.41				17.41			
	exp B	(95%CI)		P	exp B	(95%CI)		P	exp B	(95%CI)		P
FRS, %	1.00	0.98	1.02	.816	1.00	0.97	1.02	.725	0.98	0.93	1.03	.414
South Asian					0.60	0.33	1.10	.098	0.57	0.19	1.67	.302
African Caribbean					1.08	0.57	2.05	.816	0.60	0.19	1.93	.395
South Asian*FRS, %									1.01	0.95	1.07	.826
African Caribbean*FRS, %									1.04	0.97	1.10	.288

Table 6-28. Generalized linear models 3I, 4I, 5I (women), dependent variable is WMH volume zones 3 & 4. Models are adjusted for TIV, exponentiated beta coefficients, P <.05 shown in bold.

6.4.3 Independent variable: cerebral blood flow

6.4.3.1 Dependent variable: cortical volume

CBF was not associated with cortical volume after adjustment for TIV, age, sex and ethnicity (model 7a, **Table 6-30**). This relationship was not modulated by ethnicity (model 8a, **Table 6-30**) and there were no sex specific differences (model 8b, **Table 6-31**, model 8c, **Table 6-32**).

Dependent variable: cortical tissue volume (mL), (all participants)

	<i>Model 6a (n=485)</i>			
	<i>B</i>	<i>(95%CI)</i>		<i>P</i>
<i>Adjusted R²</i>	0.92			
<i>Age, years</i>	-1.13	-1.34	-0.92	<.001
<i>Sex, female</i>	-0.28	-3.27	2.70	.852
<i>CBF, mL/100g/min</i>	0.08	-0.09	0.25	.354

Table 6-29. . Generalized linear model 6a, dependent variable is cortical tissue volume (all participants), Model is adjusted for TIV, unstandardised beta coefficients, $P < .05$ shown in bold.

Dependent variable: cortical tissue volume (mL), (all participants)

	<i>Model 7a (n=485)</i>				<i>Model 8a (n=485)</i>			
<i>Adjusted R²</i>	0.92				0.92			
	<i>B</i>	<i>(95%CI)</i>		<i>P</i>	<i>B</i>	<i>(95%CI)</i>		<i>P</i>
<i>Age, years</i>	-1.09	-1.30	-0.88	<.001	-1.09	-1.30	-0.88	<.001
<i>Sex, female</i>	-0.18	-3.23	2.88	.909	-0.22	-3.31	2.87	.887
<i>South Asian</i>	-0.65	-3.74	2.45	.681	7.64	-11.68	25.36	.421
<i>African Caribbean</i>	-7.66	-11.31	-4.01	<.001	-9.83	-34.77	11.65	.415
<i>CBF, mL/100g/min</i>	0.02	-0.15	0.19	.821	0.07	-0.18	0.29	.574
<i>South Asian*CBF, mL/100g/min</i>					-0.17	-0.53	0.22	.374
<i>African Caribbean*CBF, mL/100g/min</i>					0.05	-0.40	0.58	.833

Table 6-30.. Generalized linear models 7a, 8a, dependent variable is cortical tissue volume (all participants). Models are adjusted for TIV, unstandardised beta coefficients, P <.05 shown in bold.

Dependent variable: cortical tissue volume (mL), (men)

	<i>Model 7b (n=295)</i>				<i>Model 8b (n=295)</i>			
<i>Adjusted R²</i>	0.88				0.88			
	<i>B</i>	<i>(95%CI)</i>		<i>P</i>	<i>B</i>	<i>(95%CI)</i>		<i>P</i>
<i>Age, years</i>	-1.11	-1.43	-0.79	<.001	-1.10	-1.42	-0.78	<.001
<i>South Asian</i>	-1.45	-5.64	2.73	.495	7.51	-16.49	31.51	.538
<i>African Caribbean</i>	-6.87	-12.30	-1.44	.013	-12.42	-49.75	24.90	.513
<i>CBF, mL/100g/min</i>	-0.03	-0.25	0.20	.827	0.03	-0.28	0.33	.853
<i>South Asian *CBF, mL/100g/min</i>					-0.18	-0.66	0.30	.454
<i>African Caribbean *CBF, mL/100g/min</i>					0.12	-0.65	0.89	.758

Table 6-31. Generalized linear models 7b, 8b, dependent variable is cortical tissue volume (men). Models are adjusted for TIV, unstandardised beta coefficients, P <.05 shown in bold

Dependent variable: cortical tissue volume (mL), (women)

	<i>Model 7c (n=190)</i>				<i>Model 8c (n=190)</i>			
<i>Adjusted R²</i>	0.91				0.92			
	<i>B</i>	<i>(95%CI)</i>		<i>P</i>	<i>B</i>	<i>(95%CI)</i>		<i>P</i>
<i>Age, years</i>	-1.06	-1.32	-0.02	<.001	-1.05	-1.31	-0.79	<.001
<i>South Asian</i>	1.28	-3.31	5.87	.583	-1.10	-30.80	32.99	.946
<i>African Caribbean</i>	-7.56	-12.40	-2.71	.002	-0.43	-31.80	30.94	.979
<i>CBF, mL/100g/min</i>	0.13	-0.13	0.40	.322	0.17	-0.20	0.55	.368
<i>South Asian*CBF, mL/100g/min</i>					0.01	-0.66	0.67	.982
<i>African Caribbean*CBF, mL/100g/min</i>					-0.09	-0.83	0.52	.646

Table 6-32. Generalized linear models 7c, 8c, dependent variable is cortical tissue volume (women). Models are adjusted for TIV, unstandardised beta coefficients, P <.05 shown in bold

6.4.3.2 Dependent variable: white matter hyperintensity volumes

Pooled sample

CBF was not associated with total burden of WMHs, neither in zones 1 & 2 nor in zones 3 & 4 after adjustment for TIV, age, sex and ethnicity (model 7d, **Table 6-34**; model 7g, **Table 6-38**; model 7j, **Table 6-42**).

There was weak evidence that South Asian ethnicity modulated the association of WMHs and CBF. The increase in total WMH volumes for South Asians was ~2% per 1mL/100mg/min CBF, (exp B 1.03; P = 0.075; [95%CI 1.00, 1.07]), compared to small decreases in Europeans (~0.7%), (model 8d, **Table 6-34**). This pattern of effect moderation by ethnicity was also present in both WMH zonal models, (model 8g **Table 6-38**, model 8j, **Table 6-42**).

Stratified sample

The trend for South Asian ethnicity to have greater WMH volumes in association with increasing CBF was discernible in both sexes (model 8e, **Table 6-35**; model 87, **Table 6-36**; model 8h, **Table 6-39**; model 8i, **Table 6-40**; model 8k, **Table 6-43**; model 8l, **Table 6-44**). This association was strongest in the men's model with WMHs zones 3 & 4 as the dependent variable (exp B 1.05; P = 0.053; [95%CI 1.00, 1.11]), (model 8k, **Table 6-43**).

Dependent variable: total WMH volume (mm³), (all participants)

	<i>Model 6d (n=482)</i>			
AIC	19.49			
	<i>exp B</i>	<i>(95%CI)</i>		<i>P</i>
Age, years	1.05	1.03	1.07	<.001
Sex, female	1.23	0.93	1.63	.142
CBF, mL/100g/min	1.00	0.99	1.02	.702

Table 6-33. Generalized linear model 6d (all participants), dependent variable is total WMH volume. Models are adjusted for TIV, exponentiated beta coefficients, $P < .05$ shown in bold.

Dependent variable; total WMH volume (mm³), (all participants)

	<i>Model 7d (n=482)</i>				<i>Model 8d (n=482)</i>			
<i>AIC</i>	19.50				19.49			
	<i>exp B</i>	<i>(95%CI)</i>		<i>P</i>	<i>exp B</i>	<i>(95%CI)</i>		<i>P</i>
<i>Age, years</i>	1.05	1.03	1.07	<.001	1.05	1.03	1.07	<.001
<i>Sex, female</i>	1.27	0.95	1.71	.108	1.29	0.96	1.74	.094
<i>South Asian</i>	1.10	0.83	1.46	.504	0.22	0.04	1.32	.097
<i>African Caribbean</i>	1.17	0.83	1.64	.368	1.26	0.12	12.74	.847
<i>CBF, mL/100g/min</i>	1.01	0.99	1.02	.591	0.99	0.97	1.02	.585
<i>South Asian*CBF, mL/100g/min</i>					1.03	1.00	1.07	.075
<i>African Caribbean*CBF, mL/100g/min</i>					1.00	0.95	1.05	.902

Table 6-34. Generalized linear models 7d, 8d (all participants), dependent variable is total WMH volume. Models are adjusted for TIV, exponentiated beta coefficients, P <.05 shown in bold

Dependent variable; total WMH volume (mm³), (men)

	<i>Model 7e (n=295)</i>				<i>Model 8e (n=295)</i>			
<i>AIC</i>	19.61				19.61			
	<i>exp B</i>	<i>(95%CI)</i>		<i>P</i>	<i>exp B</i>	<i>(95%CI)</i>		<i>P</i>
<i>Age, years</i>	1.05	1.02	1.08	<.001	1.05	1.03	1.08	<.001
<i>South Asian</i>	1.41	1.01	1.97	.041	0.24	0.03	1.80	.166
<i>African Caribbean</i>	1.44	0.92	2.24	.107	1.65	0.07	36.58	.751
<i>CBF, mL/100g/min</i>	1.00	0.98	1.02	.914	0.99	0.96	1.01	.360
<i>South Asian*CBF, mL/100g/min</i>					1.04	1.00	1.08	.082
<i>African Caribbean*CBF, mL/100g/min</i>					1.00	0.93	1.06	.904

Table 6-35. Generalized linear models 7e, 8e (men), dependent variable is total WMH volume. Models are adjusted for TIV, exponentiated beta coefficients, P <.05 shown in bold.

Dependent variable; total WMH volume (mm³), (women)

	<i>Model 7f (n=187)</i>				<i>Model 8f (n=187)</i>			
<i>AIC</i>	19.30				19.32			
	<i>exp B</i>	<i>(95%CI)</i>		<i>P</i>	<i>exp B</i>	<i>(95%CI)</i>		<i>P</i>
<i>Age, years</i>	1.05	1.02	1.08	.001	1.05	1.02	1.09	.001
<i>South Asian</i>	0.67	0.40	1.11	.119	0.49	0.01	29.14	.731
<i>African Caribbean</i>	0.82	0.47	1.44	.496	1.89	0.05	72.42	.732
<i>CBF, mL/100g/min</i>	1.00	0.97	1.03	.988	1.00	0.96	1.05	.893
<i>South Asian*CBF, mL/100g/min</i>					1.01	0.92	1.10	.872
<i>African Caribbean*CBF, mL/100g/min</i>					0.98	0.91	1.06	.643

Table 6-36. Generalized linear models 7f, 8f (women), dependent variable is total WMH volume. Models are adjusted for TIV, exponentiated beta coefficients, $P < .05$ shown in bold.

Dependent variable: WMH volume zones 1&2 (mm³), (all participants)

	Model 6g (n = 482)			
AIC	19.49			
	exp B	(95%CI)		P
Age, years	1.05	1.04	1.07	<.001
Sex, female	1.22	0.96	1.55	.109
CBF, mL/100g/min	1.00	0.99	1.02	.841

Table 6-37. Generalized linear model 6g (all participants), dependent variable is WMH volume zones 1 & 2. Models are adjusted for TIV, exponentiated beta coefficients, P <.05 shown in bold.

Dependent variable: WMH volume zones 1&2 (mm³), (all participants)

	<i>Model 7g (n=482)</i>				<i>Model 8g (n=482)</i>			
<i>AIC</i>	18.44				18.44			
	<i>exp B</i>	<i>(95%CI)</i>		<i>P</i>	<i>exp B</i>	<i>(95%CI)</i>		<i>P</i>
<i>Age, years</i>	1.05	1.04	1.07	<.001	1.05	1.04	1.07	<.001
<i>Sex, female</i>	1.25	0.97	1.61	.089	1.25	0.97	1.61	.085
<i>South Asian</i>	1.07	0.84	1.36	.577	0.24	0.05	1.11	.068
<i>African Caribbean</i>	1.05	0.78	1.41	.754	1.42	0.19	10.40	.731
<i>CBF, mL/100g/min</i>	1.00	0.99	1.02	.806	0.99	0.97	1.01	.447
<i>South Asian*CBF, mL/100g/min</i>					1.03	1.00	1.06	.053
<i>African Caribbean*CBF, mL/100g/min</i>					0.99	0.95	1.03	.710

Table 6-38. Generalized linear models 7g, 8g (all participants), dependent variable is WMH volume in zones 1 & 2. Models are adjusted for TIV, exponentiated beta coefficients, P <.05 shown in bold

Dependent variable: WMH volume zones 1&2 (mm³), (men)

	<i>Model 7h (n=295)</i>				<i>Model 8h (n=295)</i>			
<i>AIC</i>	18.58				18.58			
	<i>exp B</i>	<i>(95%CI)</i>		<i>P</i>	<i>exp B</i>	<i>(95%CI)</i>		<i>P</i>
<i>Age, years</i>	1.05	1.03	1.08	<.001	1.05	1.03	1.08	.001
<i>South Asian</i>	1.35	1.01	1.82	.045	0.34	0.06	2.00	.233
<i>African Caribbean</i>	1.32	0.89	1.96	.166	2.77	0.17	44.10	.471
<i>CBF (mL/100g/min)</i>	1.00	0.98	1.02	.938	0.99	0.97	1.01	.416
<i>South Asian*CBF, mL/100g/min</i>					1.03	0.99	1.07	.123
<i>African Caribbean*CBF, mL/100g/min</i>					0.98	0.93	1.04	.571

Table 6-39. Generalized linear models 7h, 8h (men), dependent variable is WMH volume in zones 1 & 2. Models are adjusted for TIV, exponentiated beta coefficients, *P* <.05 shown in bold.

Dependent variable: WMH volume zones 1&2 (mm³), (women)

	<i>Model 7i (n=187)</i>				<i>Model 8i (n=187)</i>			
<i>AIC</i>	18.58				18.58			
	<i>exp B</i>	<i>(95%CI)</i>		<i>P</i>	<i>exp B</i>	<i>(95%CI)</i>		<i>P</i>
<i>Age, years</i>	1.05	1.03	1.08	<.001	1.05	1.03	1.08	<.001
<i>South Asian</i>	1.35	1.01	1.82	.045	0.34	0.06	2.00	.233
<i>African Caribbean</i>	1.32	0.89	1.96	.166	2.77	0.17	44.10	.471
<i>CBF, mL/100g/min</i>	1.00	0.98	1.02	.938	0.99	0.97	1.01	.416
<i>South Asian*CBF, mL/100g/min</i>					1.03	0.99	1.07	.123
<i>African Caribbean*CBF, mL/100g/min</i>					0.98	0.93	1.04	.571

Table 6-40 Generalized linear models 7i, 8i (women), dependent variable is WMH volume in zones 1 & 2. Models are adjusted for TIV, exponentiated beta coefficients, P <.05 shown in bold.

Dependent variable; WMH volume zones 3&4 (mm³), (all participants)

	<i>Model 6j (n=482)</i>			
<i>AIC</i>	17.54			
	<i>exp B</i>	<i>(95%CI)</i>		<i>P</i>
<i>Age, years</i>	1.05	1.02	1.08	.001
<i>Sex, female</i>	1.25	0.86	1.82	.239
<i>CBF, mL/100g/min</i>	1.01	0.99	1.03	.493

Table 6-41. Generalized linear model 6j (all participants), dependent variable is WMH volume in zones 3 & 4. Models are adjusted for TIV, exponentiated beta coefficients, $P < .05$ shown in bold.

Dependent variable: WMH volume zones 3&4 (mm³), (all participants)

	<i>Model 7j (n=482)</i>				<i>Model 8j (n=482)</i>			
<i>AIC</i>	17.54				17.53			
	<i>exp B</i>	<i>(95%CI)</i>		<i>P</i>	<i>exp B</i>	<i>(95%CI)</i>		<i>P</i>
<i>Age, years</i>	1.05	1.02	1.08	.001	1.05	1.02	1.08	.001
<i>Sex, female</i>	1.29	0.87	1.90	.209	1.33	0.88	2.01	.170
<i>South Asian</i>	1.11	0.77	1.61	.579	0.18	0.01	2.07	.167
<i>African Caribbean</i>	1.37	0.87	2.14	.173	1.19	0.05	27.22	.914
<i>CBF, mL/100g/min</i>	1.01	0.99	1.03	.351	1.00	0.97	1.03	.867
<i>South Asian*CBF, mL/100g/min</i>	1.04	0.99	1.09	.139
<i>African Caribbean*CBF, mL/100g/min</i>	1.00	0.94	1.07	.968

Table 6-42. Generalized linear models 7j, 8j (all participants), dependent variable is WMH volume in zones 3 & 4. Models are adjusted for TIV, exponentiated beta coefficients, P <.05 shown in bold.

Dependent variable: WMH volume zones 3&4 (mm³), (men)

	Model 7k (n=295)				Model 8k (n=295)			
AIC	17.63				17.61			
	exp B	(95%CI)		P	exp B	(95%CI)		P
Age, years	1.05	1.02	1.08	.004	1.06	1.02	1.09	.001
South Asian	1.47	0.96	2.26	.078	0.11	0.01	1.55	.102
African Caribbean	1.62	0.92	2.87	.097	0.67	0.01	34.02	.844
CBF, mL/100g/min	1.00	0.98	1.03	.730	0.98	0.95	1.02	.322
South Asian*CBF, mL/100g/min					1.05	1.00	1.11	.053
African Caribbean*CBF, mL/100g/min					1.02	0.94	1.10	.676

Table 6-43. Generalized linear models 7k, 8kj (men), dependent variable is WMH volume in zones 3 & 4. Models are adjusted for TIV, exponentiated beta coefficients, P <.05 shown in bold.

Dependent variable: WMH volume zones 3&4 (mm³), (women)

	Model 7I (n=187)				Model 8I (n=187)			
AIC	17.35				17.39			
	exp B	(95%CI)		P	exp B	(95%CI)		P
Age, years	1.05	1.00	1.09	.038	1.05	1.01	1.09	.027
South Asian	0.64	0.32	1.28	.209	2.13	0.01	428.31	.781
African Caribbean	1.04	0.49	2.20	.923	4.35	0.04	473.79	.539
CBF, mL/100g/min	1.01	0.96	1.05	.748	1.02	0.96	1.08	.492
South Asian*CBF, mL/100g/min					0.98	0.87	1.09	.663
African Caribbean*CBF, mL/100g/min					0.97	0.88	1.07	.550

Table 6-44. Generalized linear models 7I, 8I (women), dependent variable is WMH volume in zones 3 & 4. Models are adjusted for TIV, exponentiated beta coefficients, P <.05 shown in bold.

6.4.4 SEM mediation analysis

Direct, indirect and total effects of FRS showing potential mediation by CBF on cortical volume and WMH volume estimated from SEMs are summarized in **Table 6-45**. Wald tests for parameter invariance between groups did not suggest effect modification by ethnicity for cortical volume or WMH volume outcomes (**Table 6-46, Table 6-48, Table 6-50 and Table 6-52**). Although GLMs did not show any relationships between CBF and brain outcomes, SEMs were executed to explore potential differences by ethnicity in these relationships.

6.4.4.1 Dependent variable: cortical volume

As shown in section 6.4.3.1 there was no association between CBF and cortical volume. This result is reflected in the SEMs where there was no evidence to suggest a role for CBF as a mediator between FRS and cortical volume (**Figure 6-26, Figure 6-27, Figure 6-28, Figure 6-23, Figure 6-24 and Figure 6-25**).

6.4.4.2 Dependent variables: total WMHs, WMHs zones 1 & 2, WMHs zones 3 & 4

There was also no evidence to suggest CBF was a mediator between FRS and total WMHs (**Figure 6-32, Figure 6-33, Figure 6-34, Figure 6-29, Figure 6-30 and Figure 6-31**), WMH zones 1 & 2 (**Figure 6-38, Figure 6-39, Figure 6-40, Figure 6-35, Figure 6-36 and Figure 6-37**) nor WMH zones 3 & 4 (**Figure 6-44, Figure 6-45, Figure 6-46, Figure 6-41, Figure 6-42 and Figure 6-43**).

SEM path	Sample	Direct Effect		Indirect Effect		Total Effect	
		β	<i>P</i>	β	<i>P</i>	β	<i>P</i>
FRS(%)>CBF(mL/100g/min)>> Cortical Volume (mL)	White European	-0.04	.160	0.00	.536	-0.04	.111
	South Asian	-0.14	<.001	0.00	.767	-0.14	<.001
	African Caribbean	-0.10	.005	0.00	.780	-0.10	.005

Table 6-45. Direct, indirect and total effects of FRS mediated by CBF on cortical volume estimated from SEMs, standardised beta coefficients, $P < .05$ in bold.

Wald test	Chi ²	df	<i>P</i>
>>Cortical volume			
CBF	1.69	2	.429
FRS	5.03	2	.081
TIV	2.83	2	.243
>>CBF			
FRS	7.51	2	.023
>>Joint test	16.05	8	.042

Table 6-46. Wald tests for invariance of parameters across ethnic groups for SEMs including cortical volume using multi group option, $P < .05$ in bold.

SEM path	Sample	Direct Effect		Indirect Effect		Total Effect	
		β	<i>P</i>	β	<i>P</i>	β	<i>P</i>
FRS(%)>CBF(mL/100g/min)>> log Total WMHs (mm ³)	White European	0.00	.981	0.02	.213	0.02	.785
	South Asian	0.22	.004	0.00	.811	0.22	.004
	African Caribbean	0.15	.143	0.01	.555	0.16	.121

Table 6-47. Direct, indirect and total effects of FRS mediated by CBF on log total WMHs volume estimated from SEMs, standardised beta coefficients *P*<.05 in bold.

Wald test	Chi ²	df	<i>P</i>
>>Log total WMH volume			
CBF	4.84	2	.089
FRS	4.30	2	.117
TIV	2.43	2	.296
>>CBF			
FRS	7.28	2	.026
>>Joint test	21.75	8	.005

Table 6-48. Wald tests for invariance of parameters across ethnic groups for SEMs including log total WMH volume using multi group option, *P*<.05 in bold.

SEM path	Sample	Direct Effect		Indirect Effect		Total Effect	
		β	<i>P</i>	β	<i>P</i>	β	<i>P</i>
FRS(%)>CBF(mL/100g/min)>> log WMH Z12 (mm ³)	White European	0.03	.668	0.02	.244	.05	.473
	South Asian	0.23	.002	0.00	.811	.23	.002
	African Caribbean	0.19	.063	0.01	.580	.20	.054

Table 6-49. Direct, indirect and total effects of FRS mediated by CBF on log WMHs zones 1 & 2 volume estimated from SEMs, standardised beta coefficients, *P*<.05 in bold.

Wald test	Chi ²	df	<i>P</i>
>>Log WMH zones 1 & 2			
CBF	4.09	2	.129
FRS	4.07	2	.131
TIV	1.72	2	.422
>>CBF			
FRS	7.28	2	.026
>>Joint test	19.61	8	.012

Table 6-50. Wald tests for invariance of parameters across ethnic groups for SEMs including log WMH zones 1 & 2 volume using multi group option, *P*<.05 in bold.

SEM path	Sample	Direct Effect		Indirect Effect		Total Effect	
		β	<i>P</i>	β	<i>P</i>	β	<i>P</i>
FRS(%)>CBF(mL/100g/min)>> log WMH Z34 (mm ³)	White European	-0.05	.497	0.02	.214	-0.03	.685
	South Asian	0.18	.021	0.00	.814	0.18	.020
	African Caribbean	0.08	.460	0.01	.547	0.09	.401

Table 6-51. Direct, indirect and total effects of FRS mediated by CBF on log WMHs zones 3 & 4 volume estimated from SEMs, standardised beta coefficients, *P*<.05 in bold.

Wald test	Chi ²	df	<i>P</i>
>>Log WMH zones 3&4			
CBF	4.06	2	.131
FRS	4.28	2	.118
TIV	4.11	2	.128
>>CBF			
FRS	7.28	2	.026
>>Joint test	23.07	8	.003

Table 6-52. Wald tests for invariance of parameters across ethnic groups for SEMs including log WMH zones 3 & 4 volume using multi group option, *P*<.05 in bold.

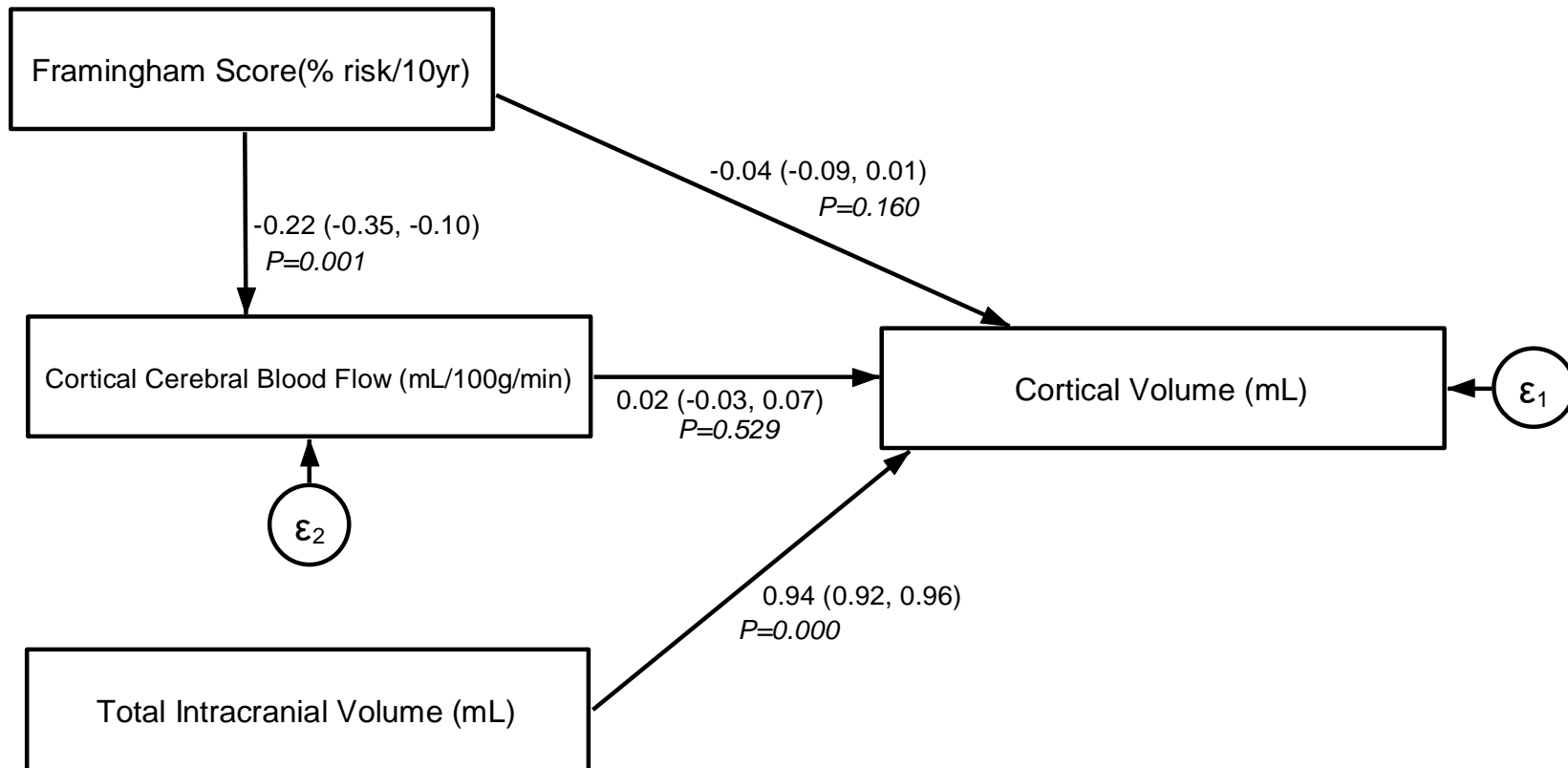


Figure 6-23. SEM diagram examining the role of CBF as a mediator between FRS and cortical volume; Europeans. Connectors show standardised beta coefficients, (95% CIs) and P-values.

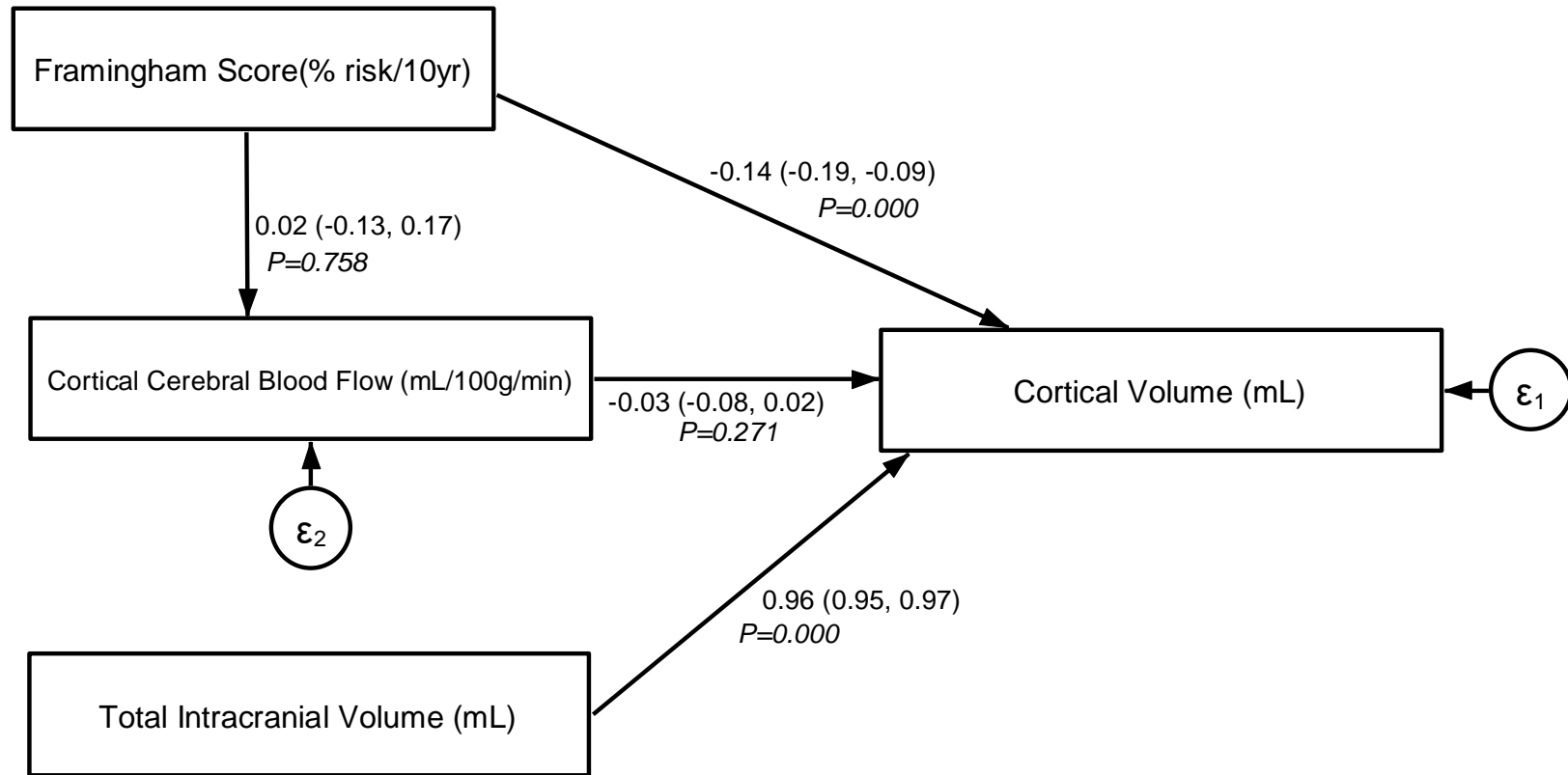


Figure 6-24. SEM diagram examining the role of CBF as a mediator between FRS and cortical volume; South Asians. Connectors show standardised beta coefficients, (95% CIs) and P-values.

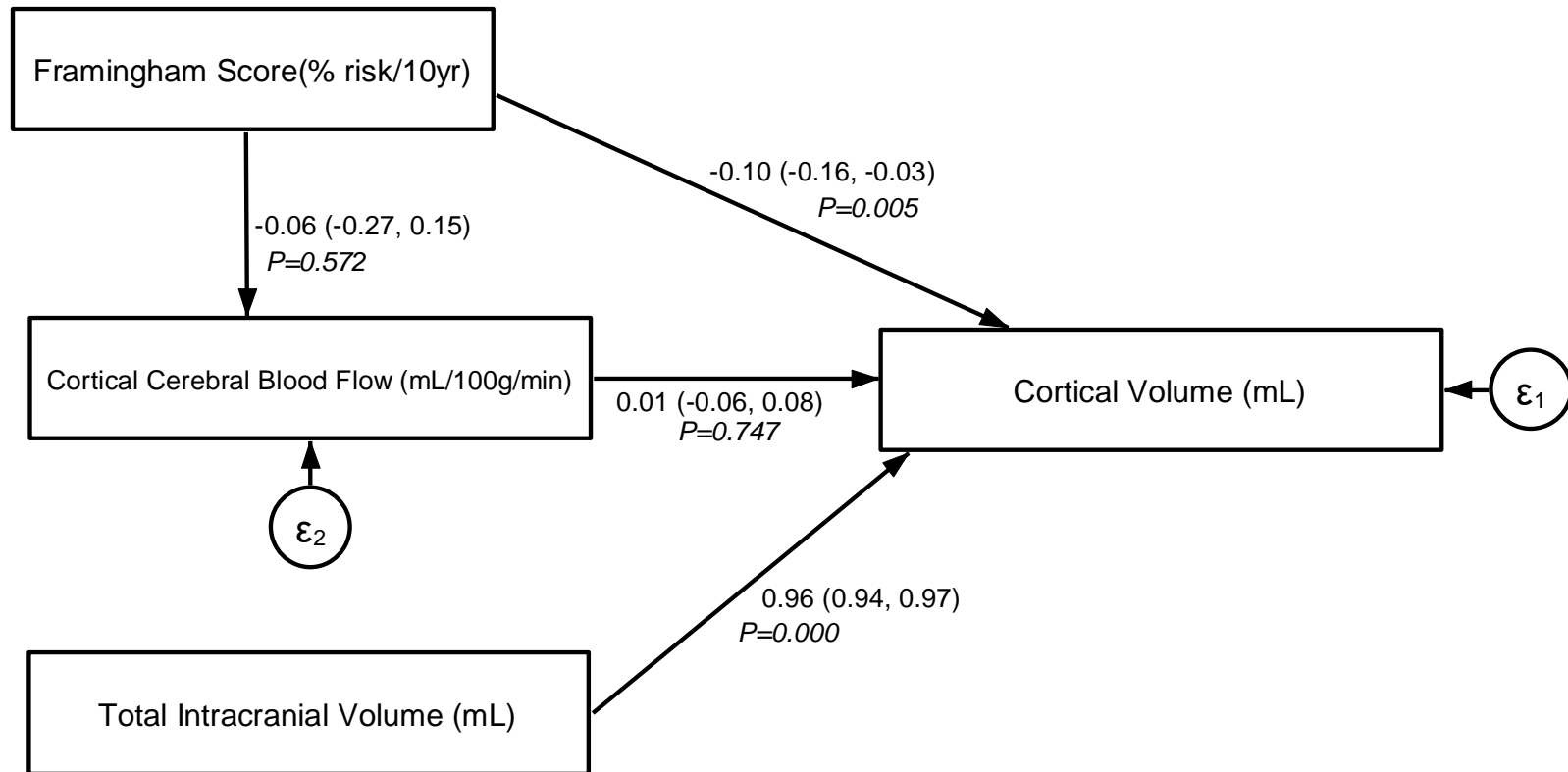


Figure 6-25. SEM diagram examining the role of CBF as a mediator between FRS and cortical volume; African Caribbeans. Connectors show standardised beta coefficients, (95% CIs) and P-values

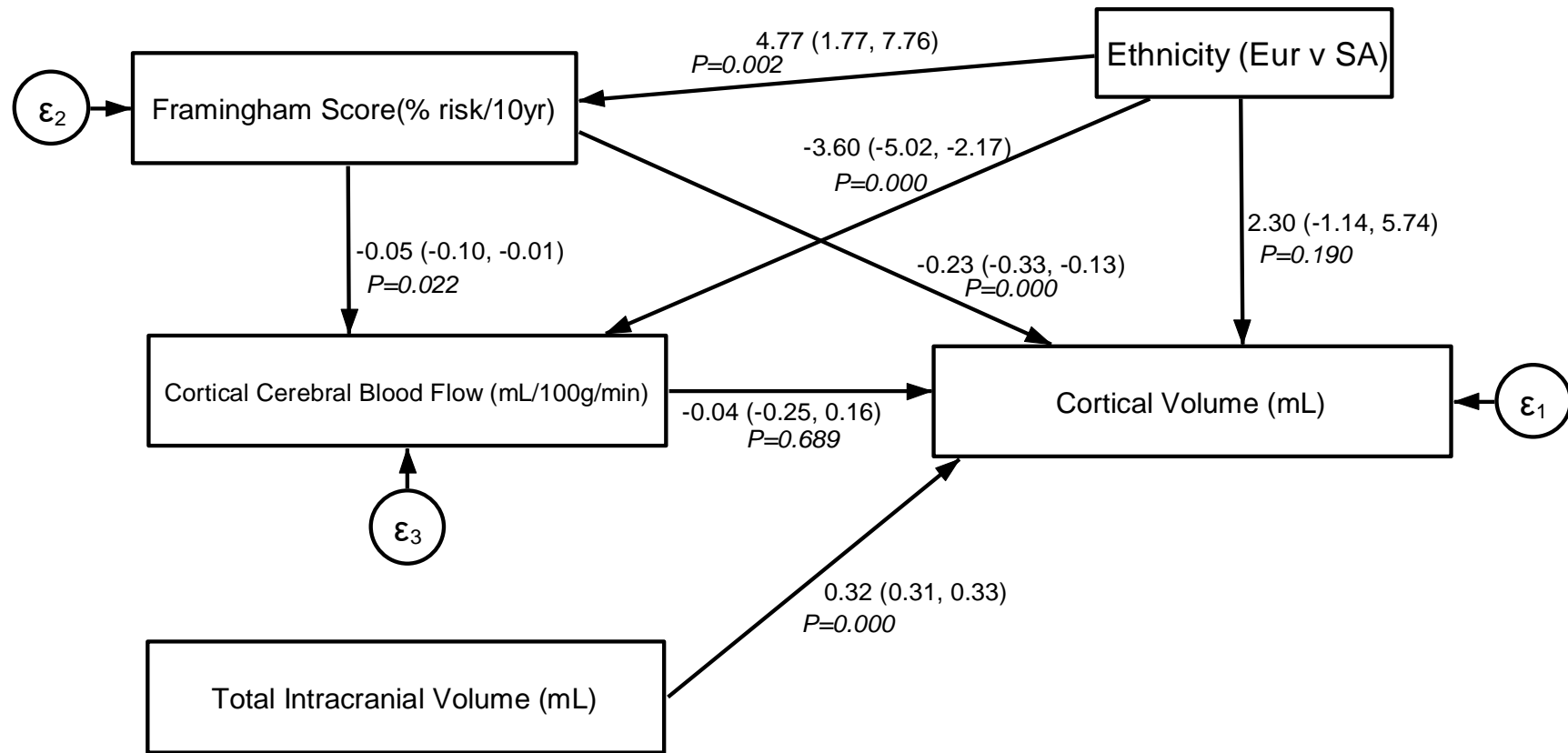


Figure 6-26. SEM diagram examining the role of CBF as a mediator between FRS and cortical volume; Europeans vs South Asians. Connectors show unstandardised beta coefficients, (95% CIs) and P-values.

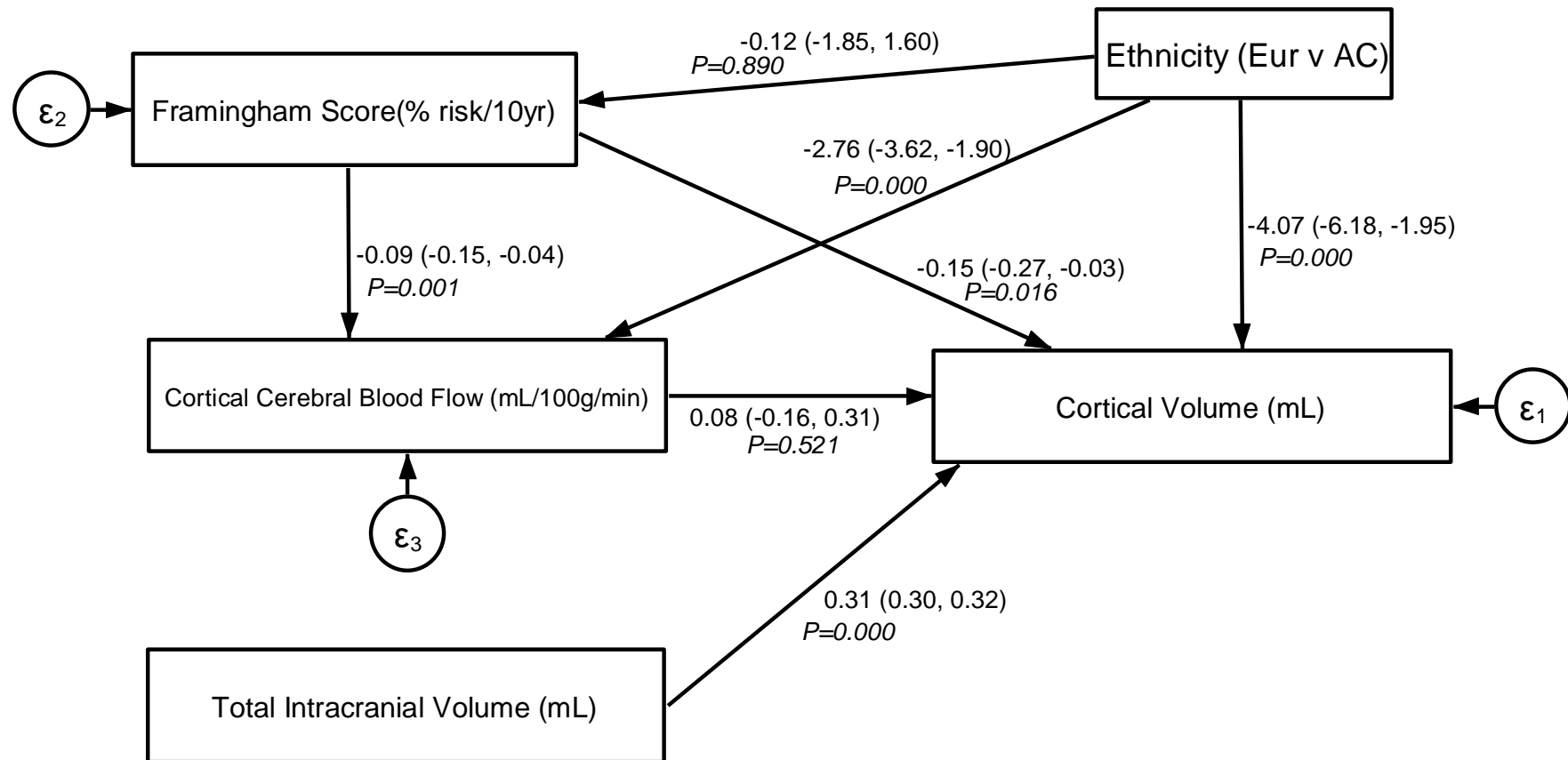


Figure 6-27. SEM diagram examining the role of CBF as a mediator between FRS and cortical volume; Europeans vs African Caribbeans. Connectors show unstandardised beta coefficients, (95% CIs) and P-values.

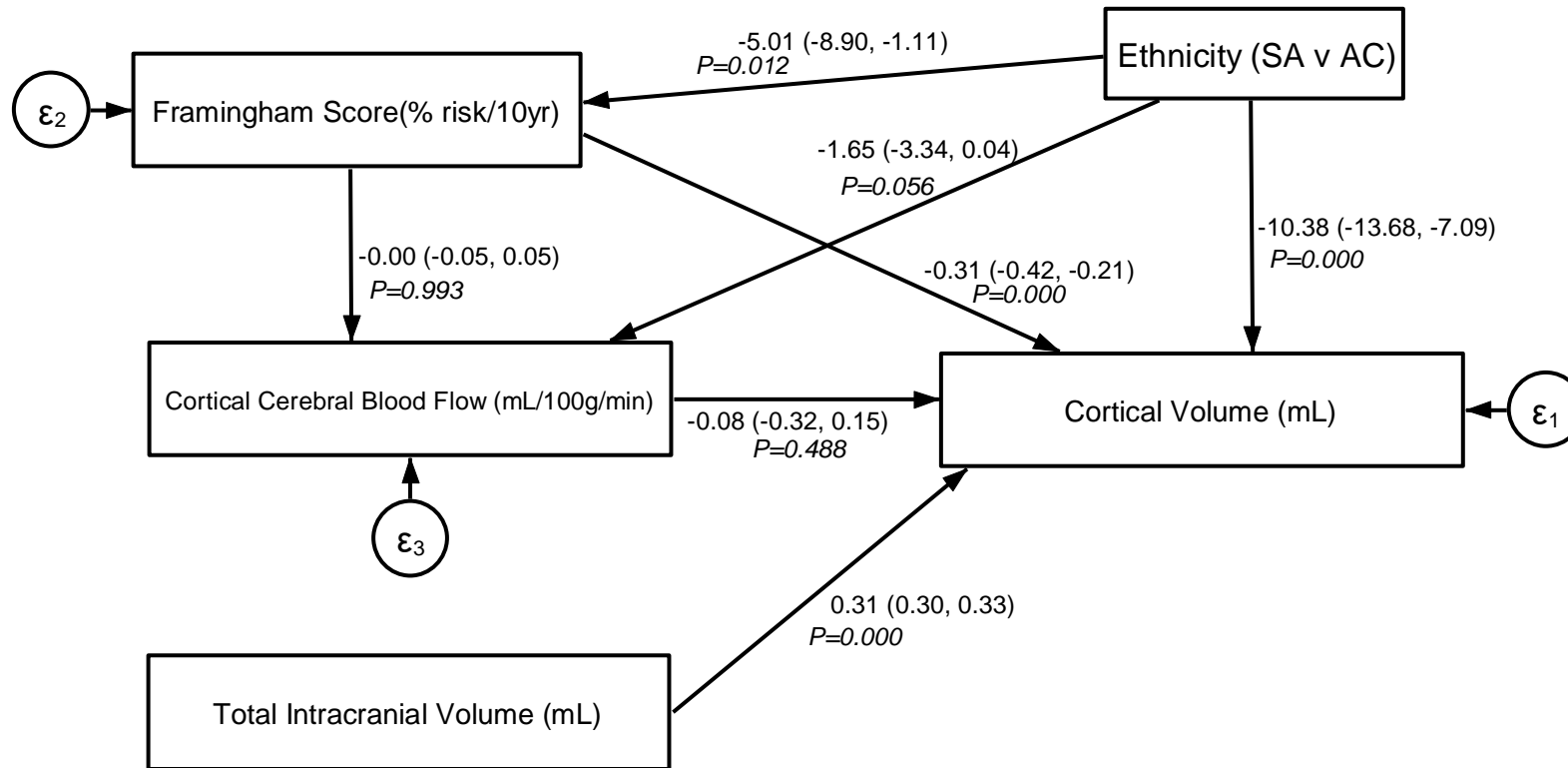


Figure 6-28. SEM diagram examining the role of CBF as a mediator between FRS and cortical volume; South Asians vs African Caribbeans. Connectors show unstandardised beta coefficients, (95% CIs) and P-values.

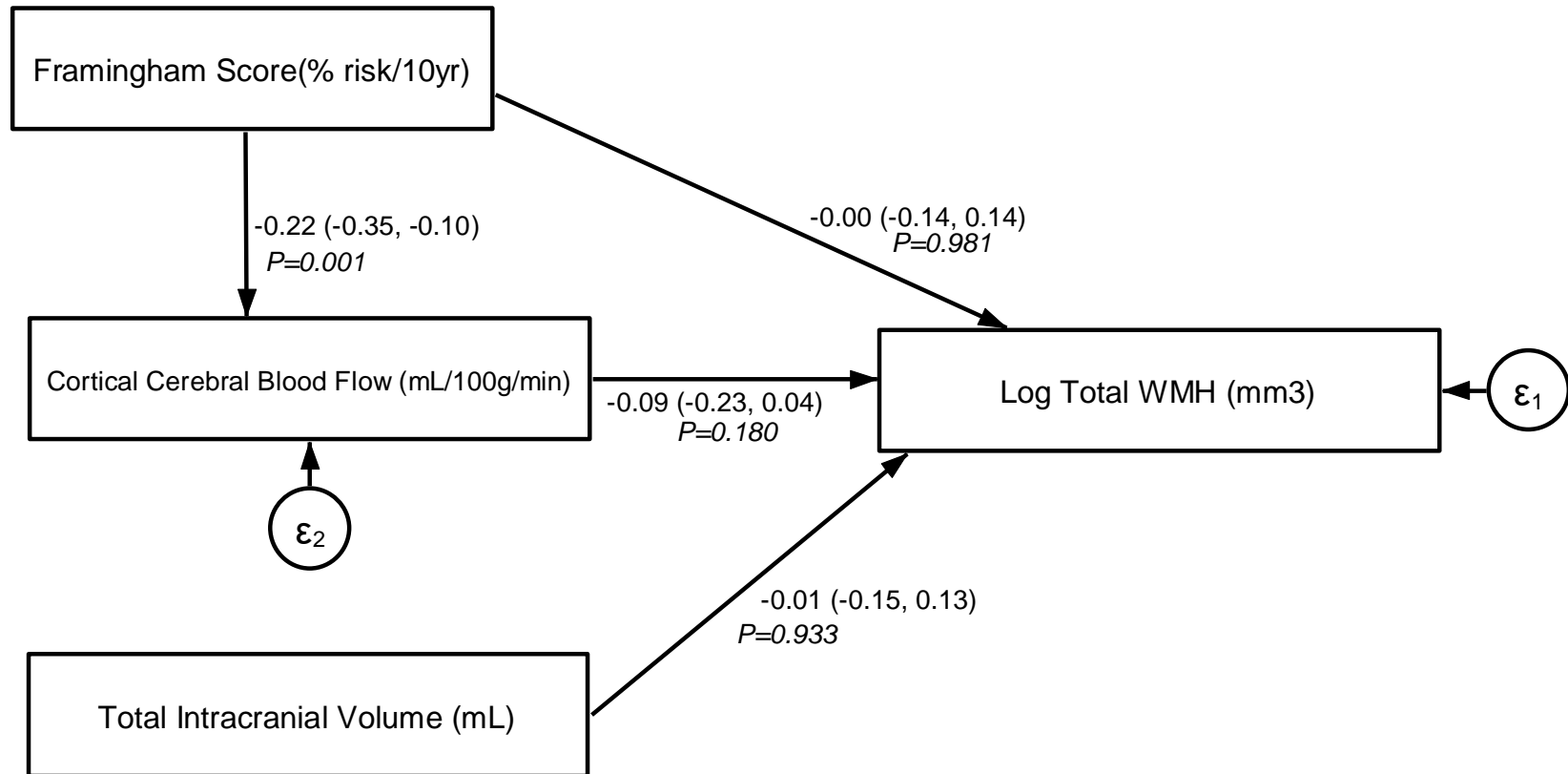


Figure 6-29. SEM diagram examining the role of CBF as a mediator between FRS and log total WMHs; Europeans. Connectors show standardised beta coefficients, (95% CIs) and P-values

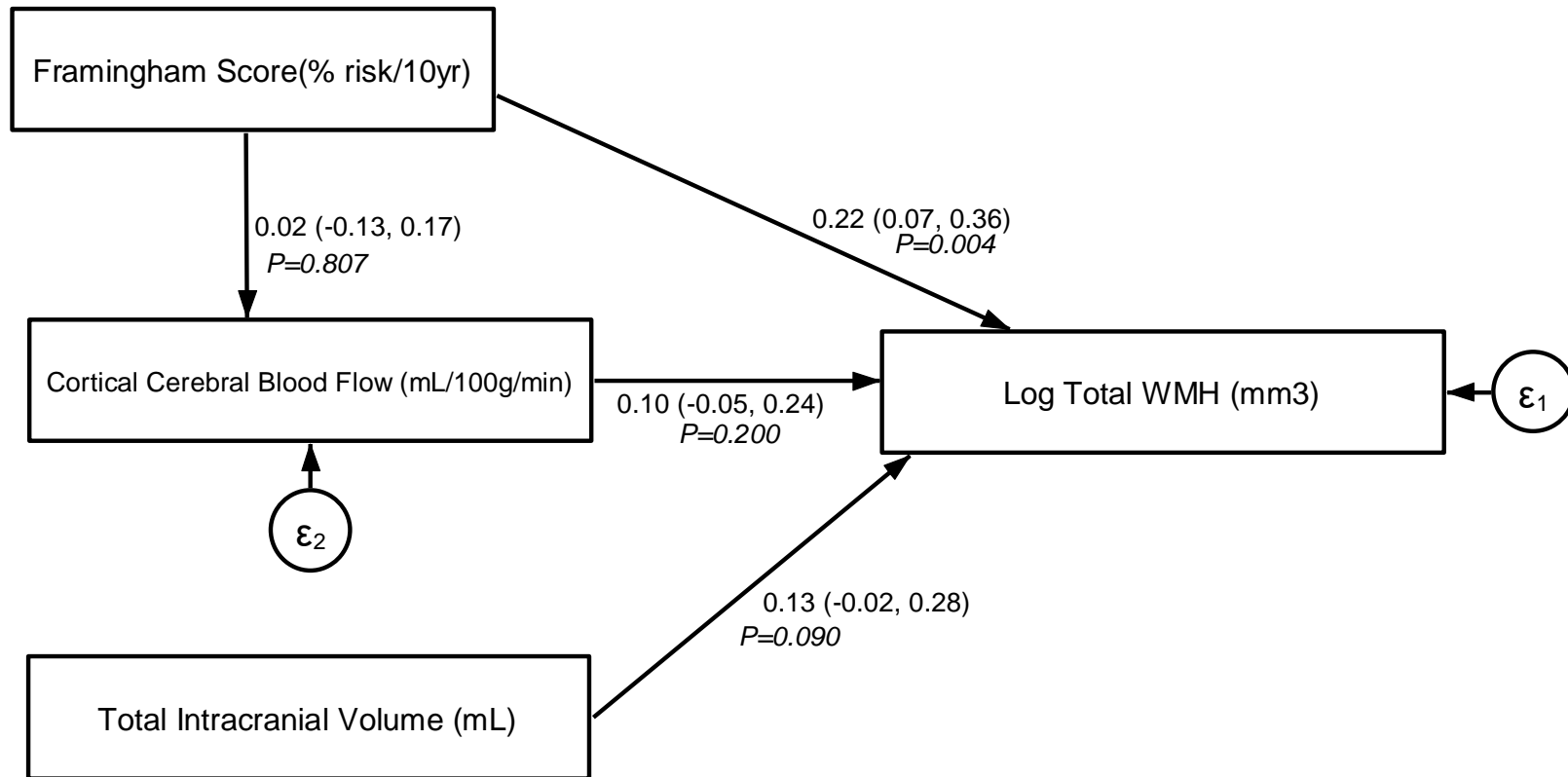


Figure 6-30. SEM diagram examining the role of CBF as a mediator between FRS and log total WMHs; South Asians. Connectors show standardised beta coefficients, (95% CIs) and P-values.

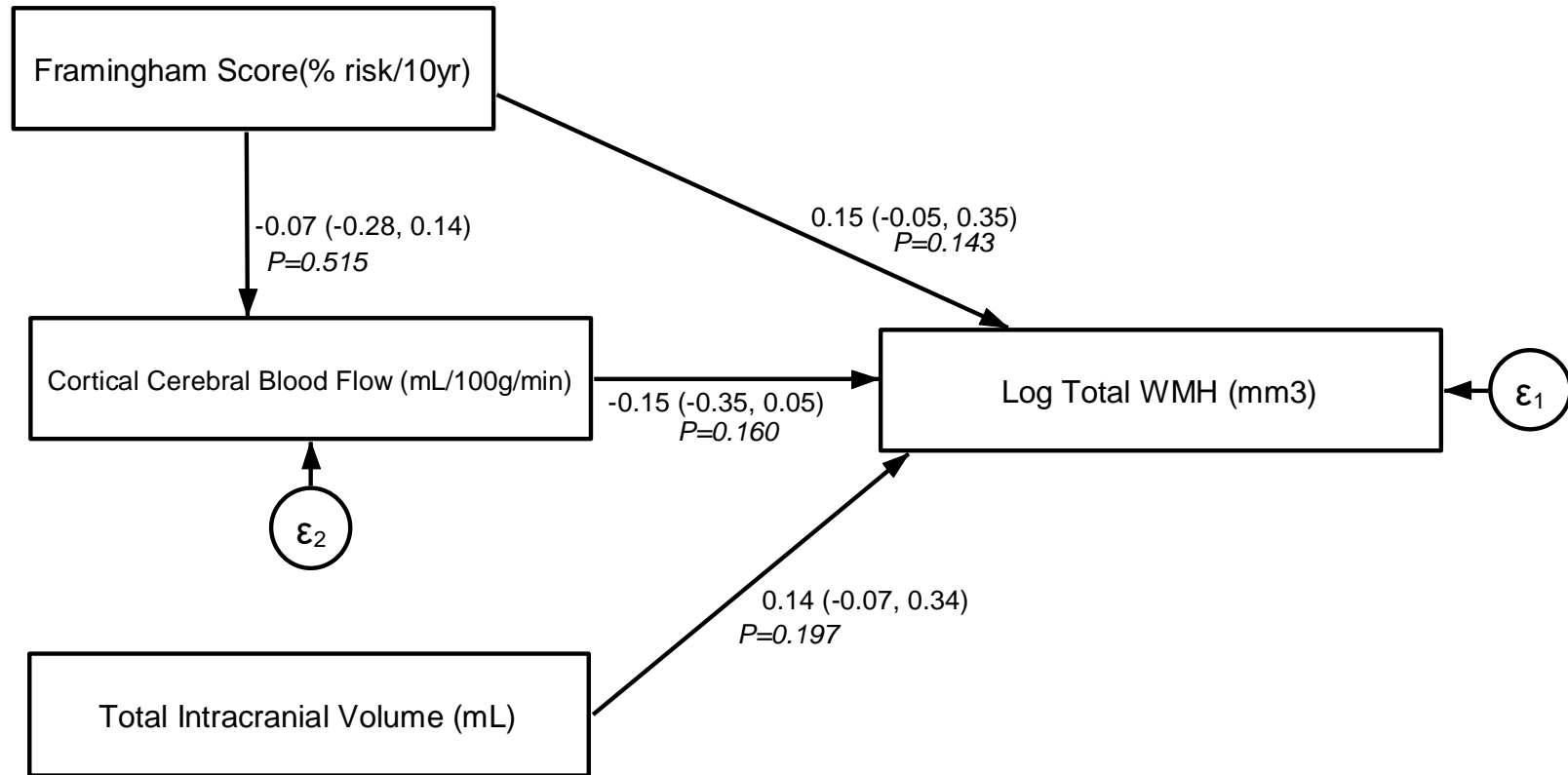


Figure 6-31. SEM diagram examining the role of CBF as a mediator between FRS and log total WMHs; African Caribbeans. Connectors show standardised beta coefficients, (95% CIs) and P-values.

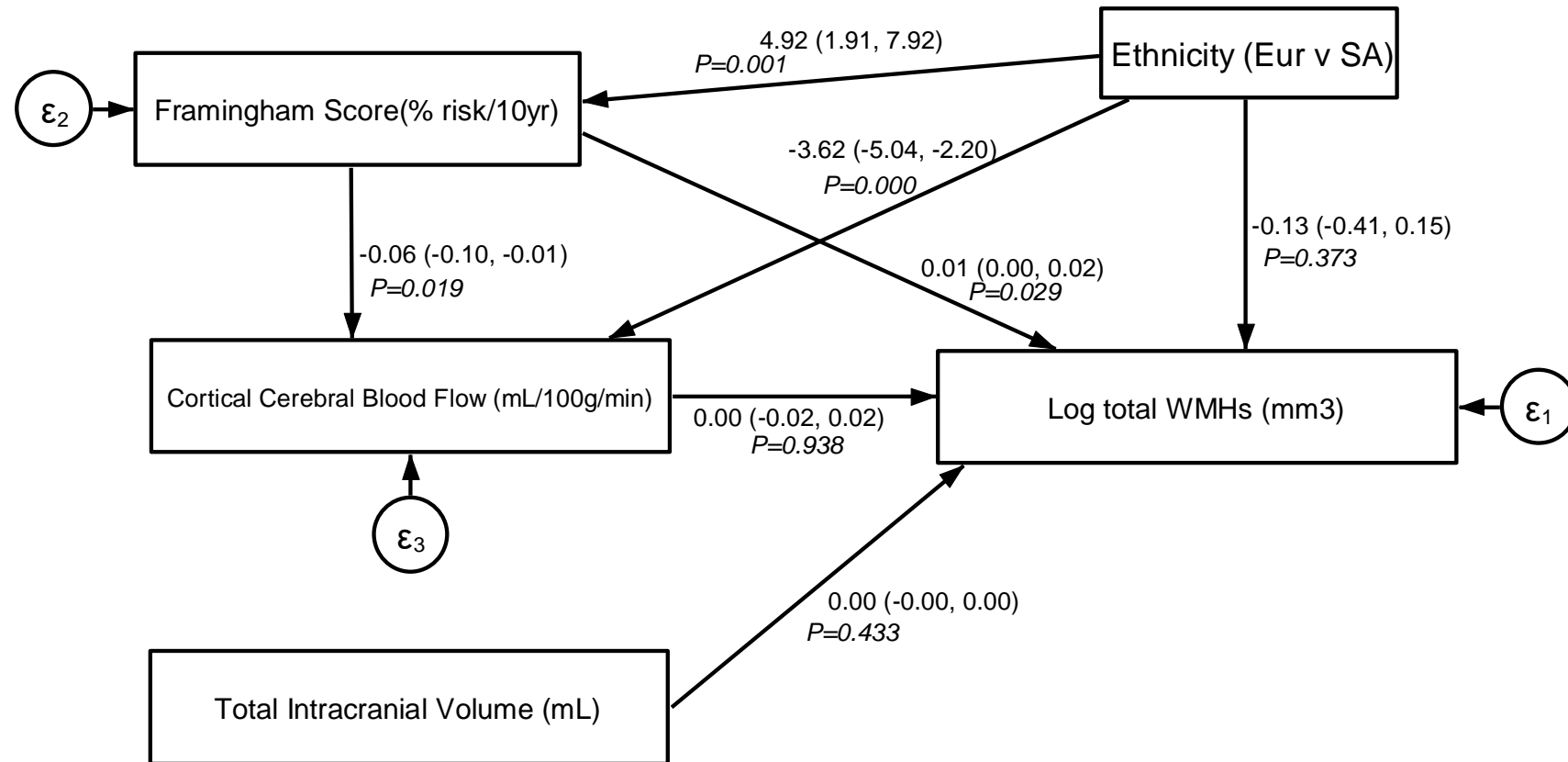


Figure 6-32. SEM diagram examining the role of CBF as a mediator between FRS and log total WMHs; Europeans vs South Asians. Connectors show unstandardised beta coefficients, (95% CIs) and P-values.

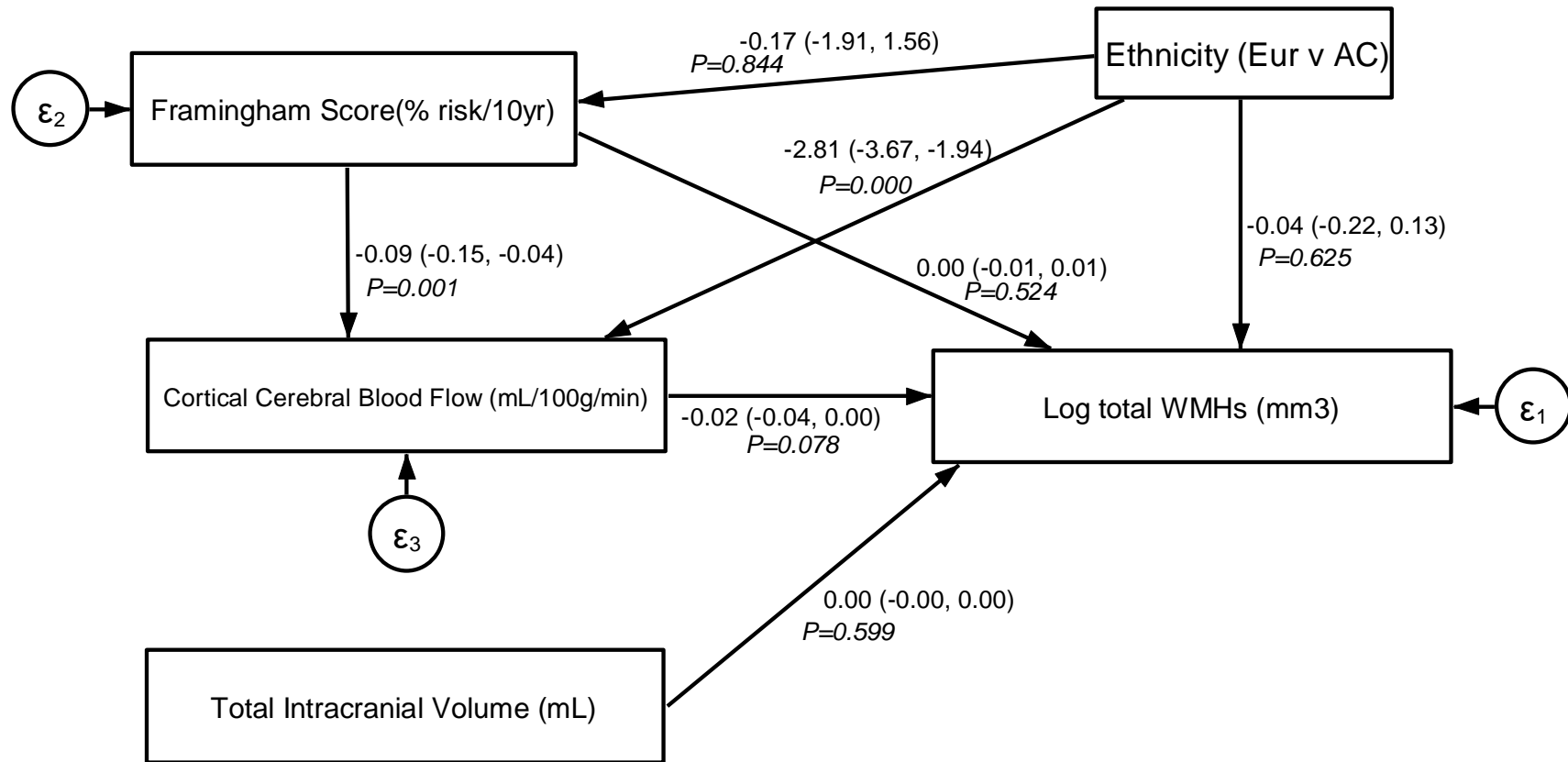


Figure 6-33. SEM diagram examining the role of CBF as a mediator between FRS and log total WMHs; Europeans vs African Caribbeans. Connectors show unstandardised beta coefficients, (95% CIs) and P-values.

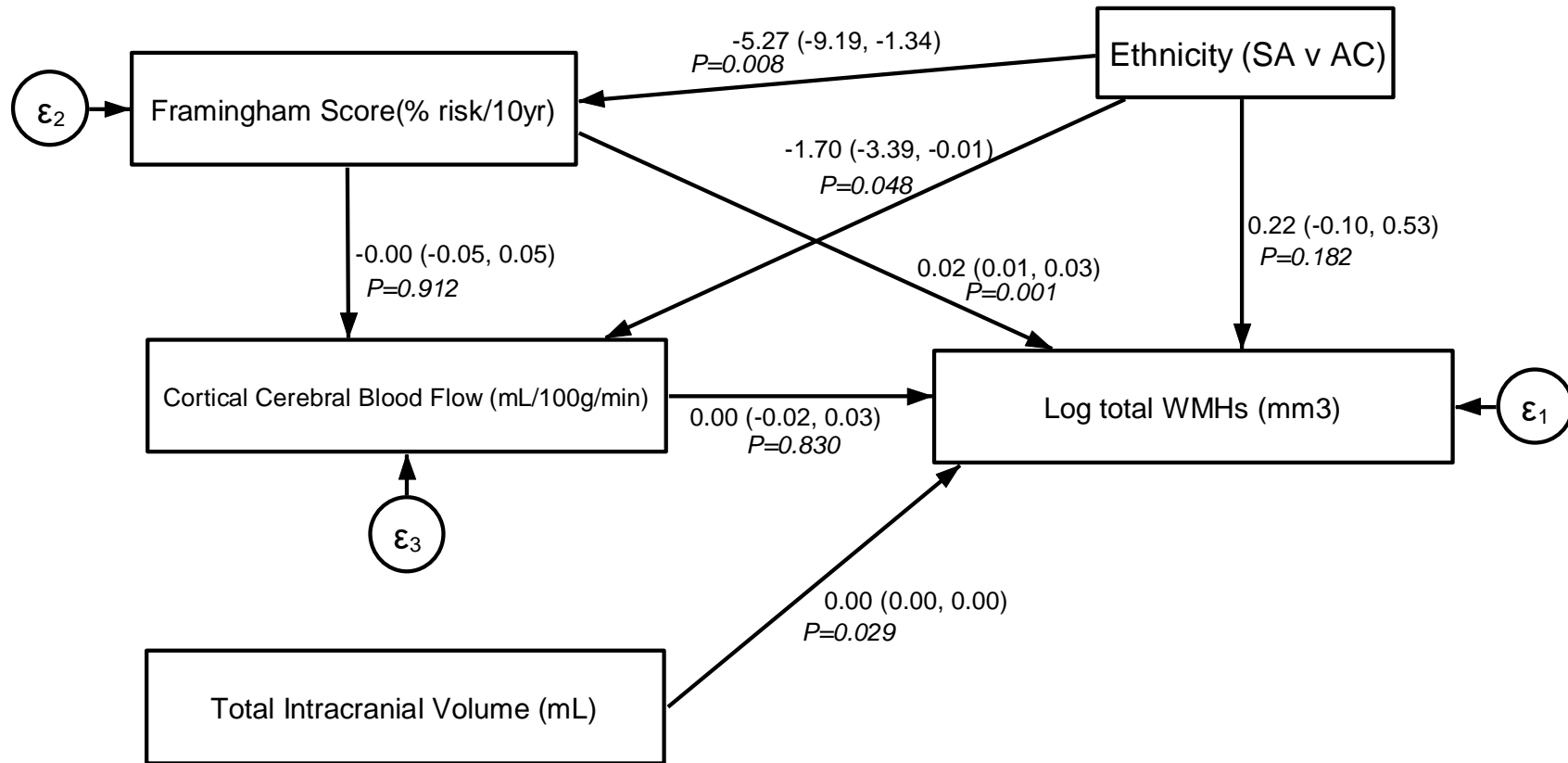


Figure 6-34. SEM diagram examining the role of CBF as a mediator between FRS and log total WMHs; South Asians vs African Caribbeans. Connectors show unstandardised beta coefficients, (95% CIs) and P-values

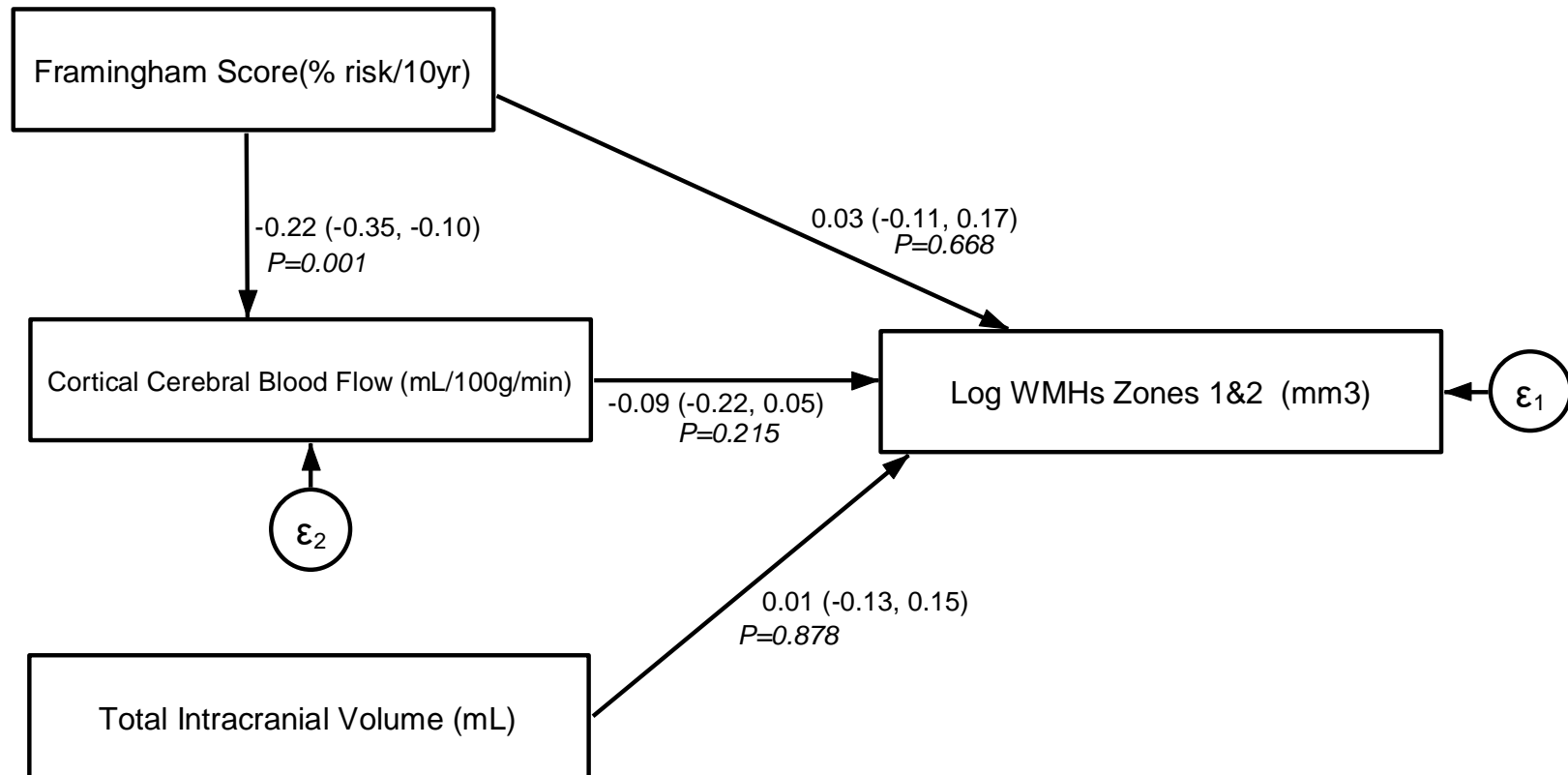


Figure 6-35. SEM diagram examining the role of CBF as a mediator between FRS and log WMHs in zones 1 & 2; Europeans. Connectors show standardised beta coefficients, (95% CIs) and P-values.

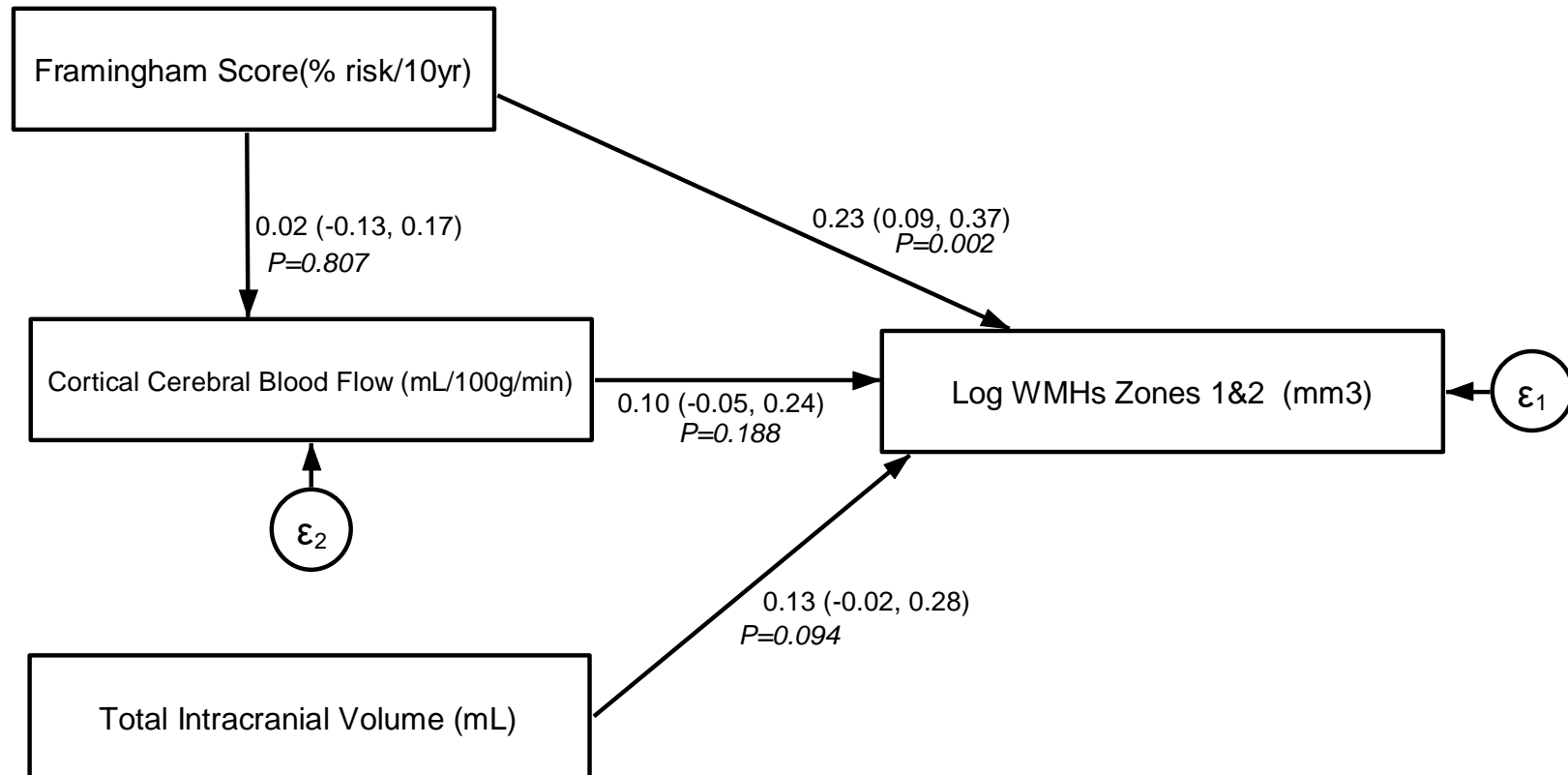


Figure 6-36. SEM diagram examining the role of CBF as a mediator between FRS and log WMHs in zones 1 & 2; South Asians. Connectors show standardised beta coefficients, (95% CIs) and P-values.

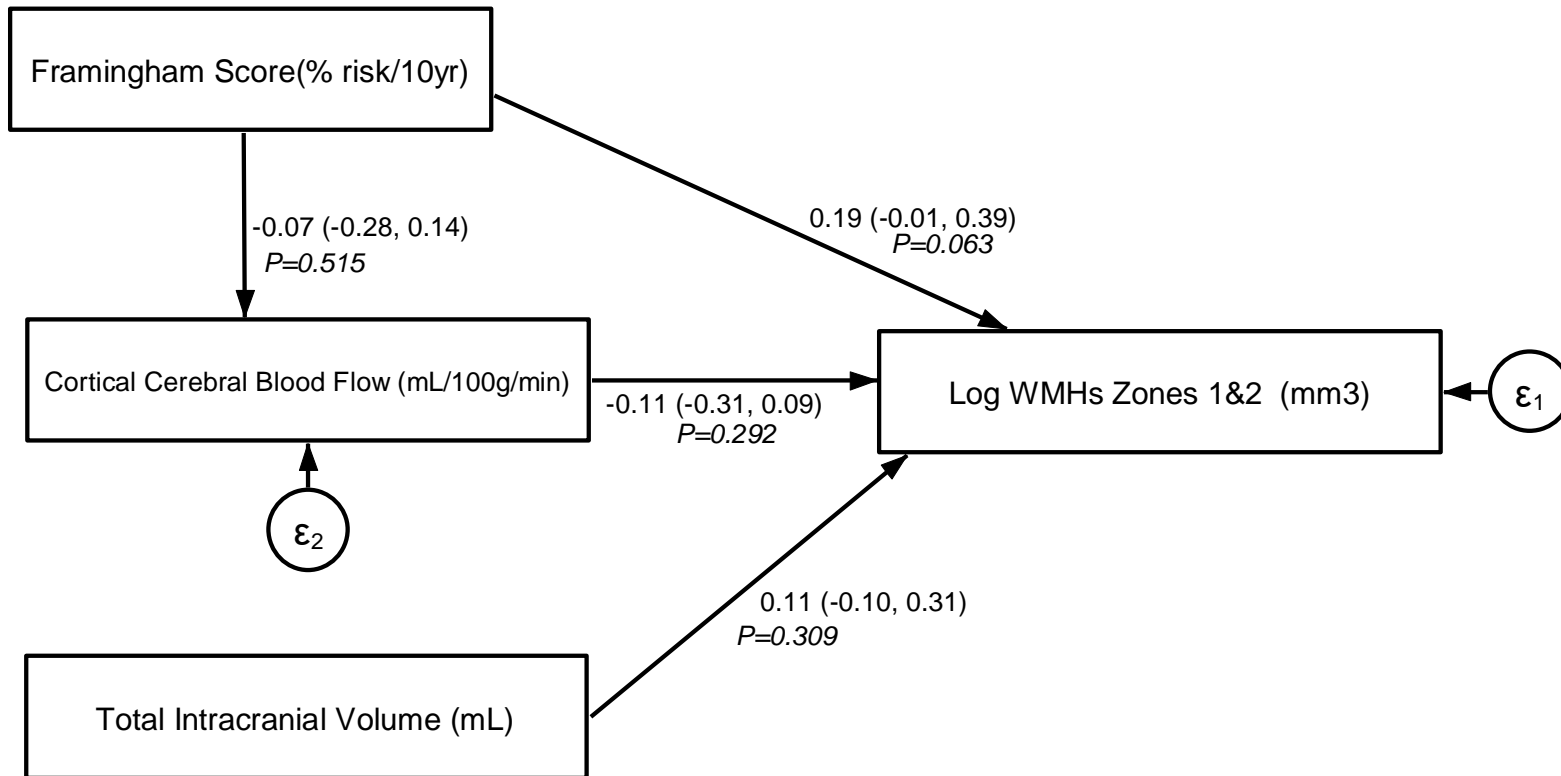


Figure 6-37. SEM diagram examining the role of CBF as a mediator between FRS and log WMHs in zones 1 & 2; African Caribbeans. Connectors show standardised beta coefficients, (95% CIs) and P-values.

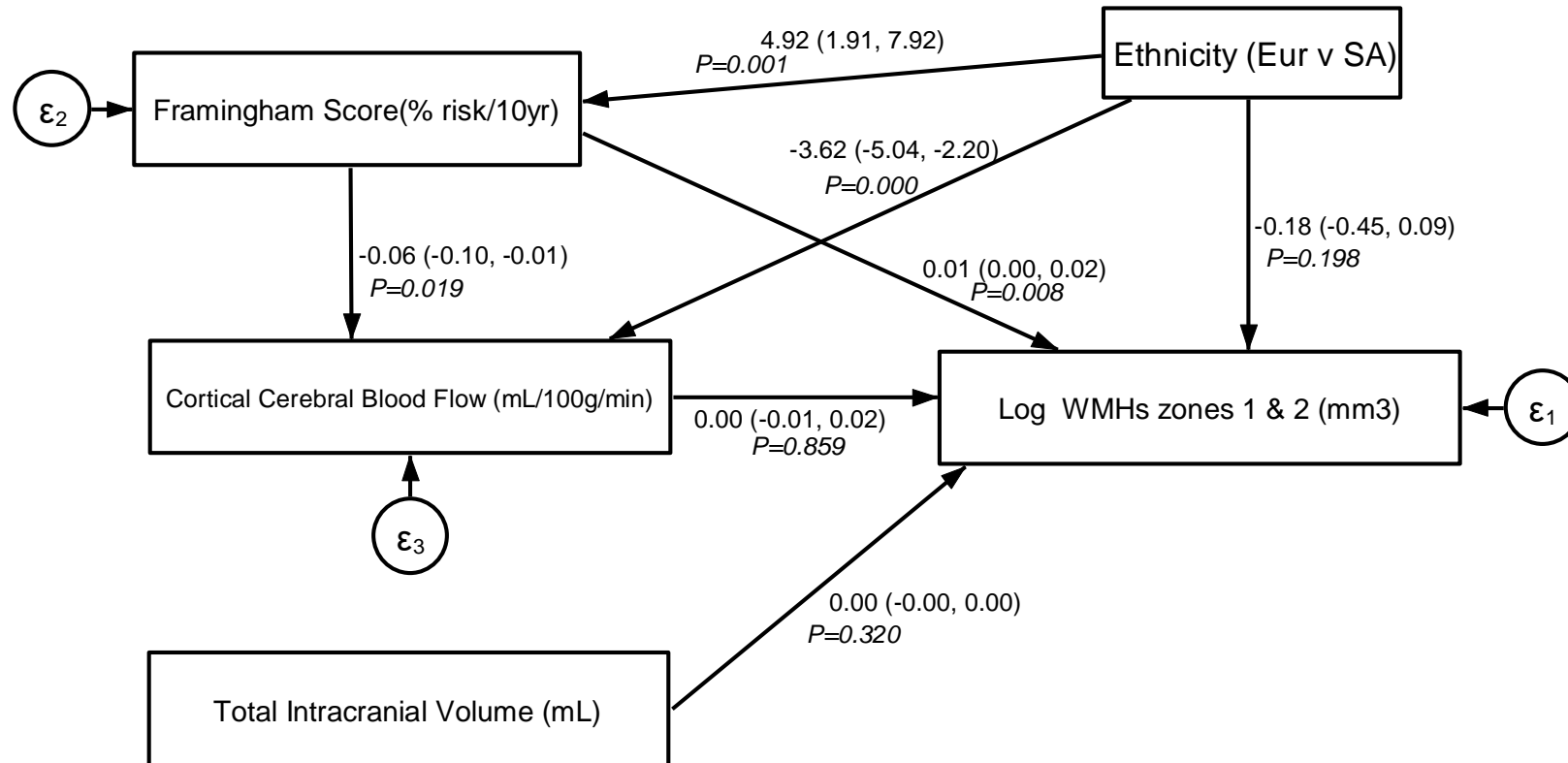


Figure 6-38. SEM diagram examining the role of CBF as a mediator between FRS and log WMHs in zones 1 & 2; Europeans vs South Asians. Connectors show unstandardised beta coefficients, (95% CIs) and P-values.

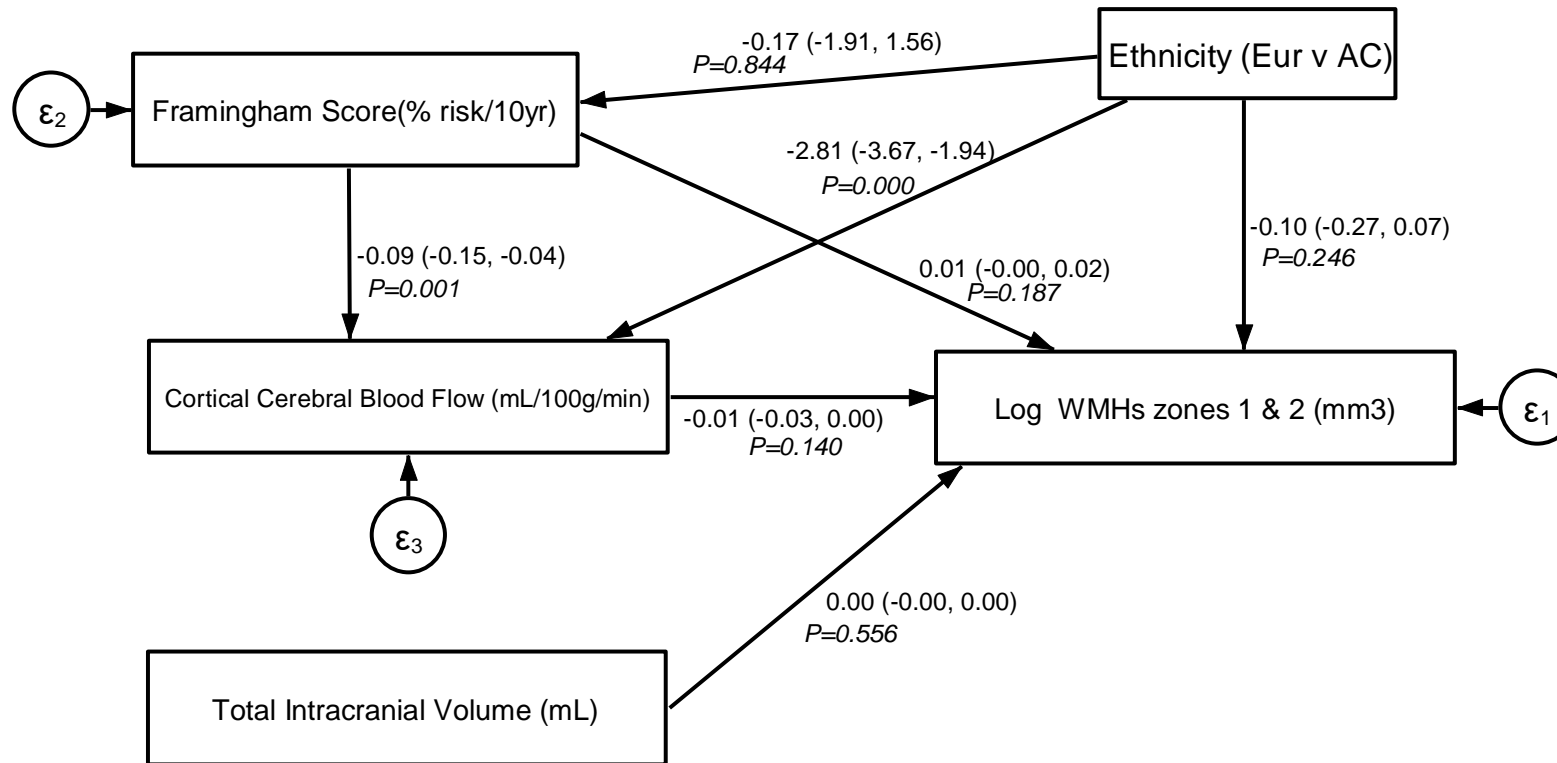


Figure 6-39. SEM diagram examining the role of CBF as a mediator between FRS and log WMHs in zones 1 & 2; Europeans vs African Caribbeans. Connectors show unstandardised beta coefficients, (95% CIs) and P-values.

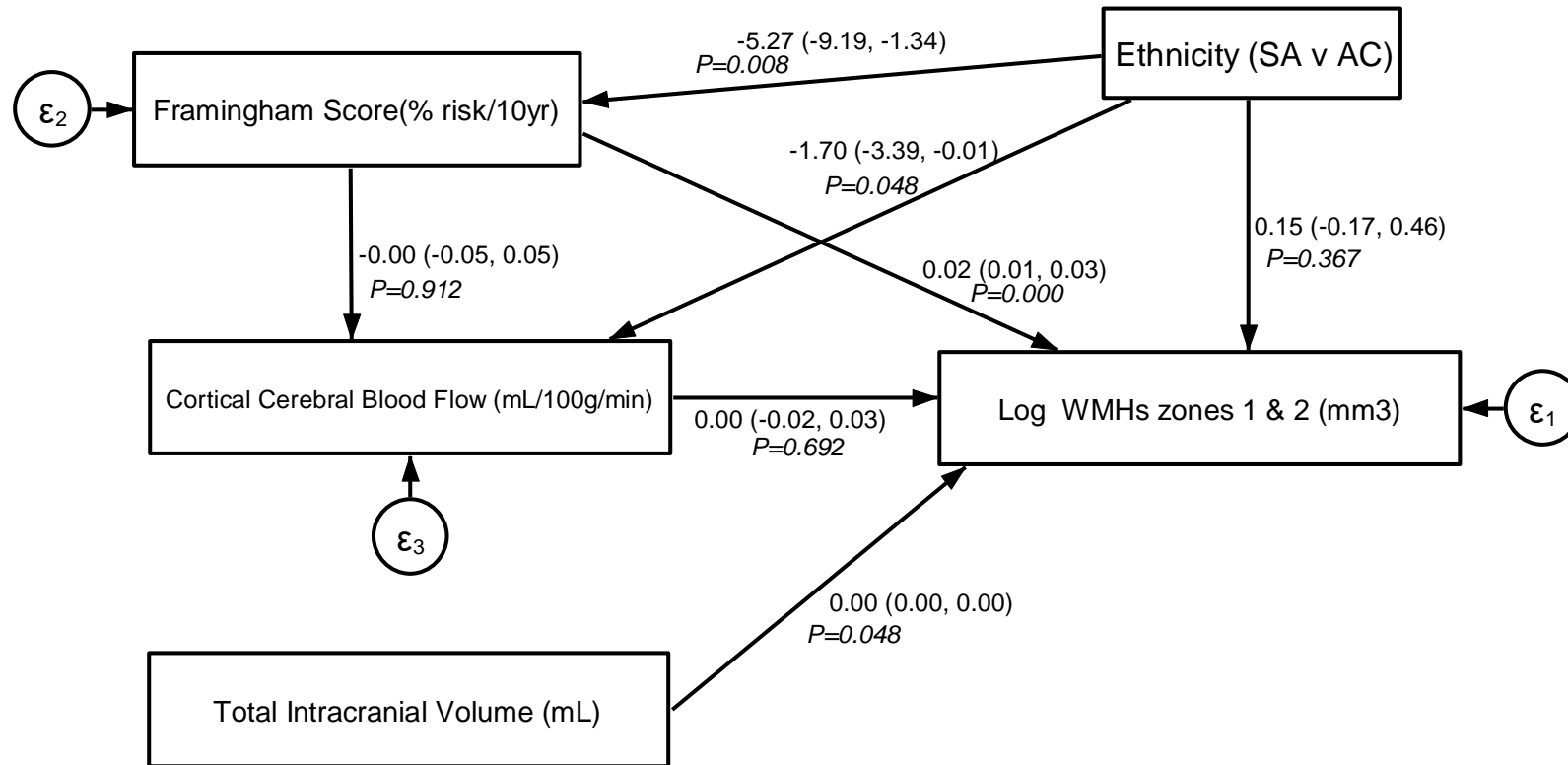


Figure 6-40. SEM diagram examining the role of CBF as a mediator between FRS and log WMHs in zones 1 & 2; South Asians vs African Caribbeans. Connectors show unstandardised beta coefficients, (95% CIs) and P-values.

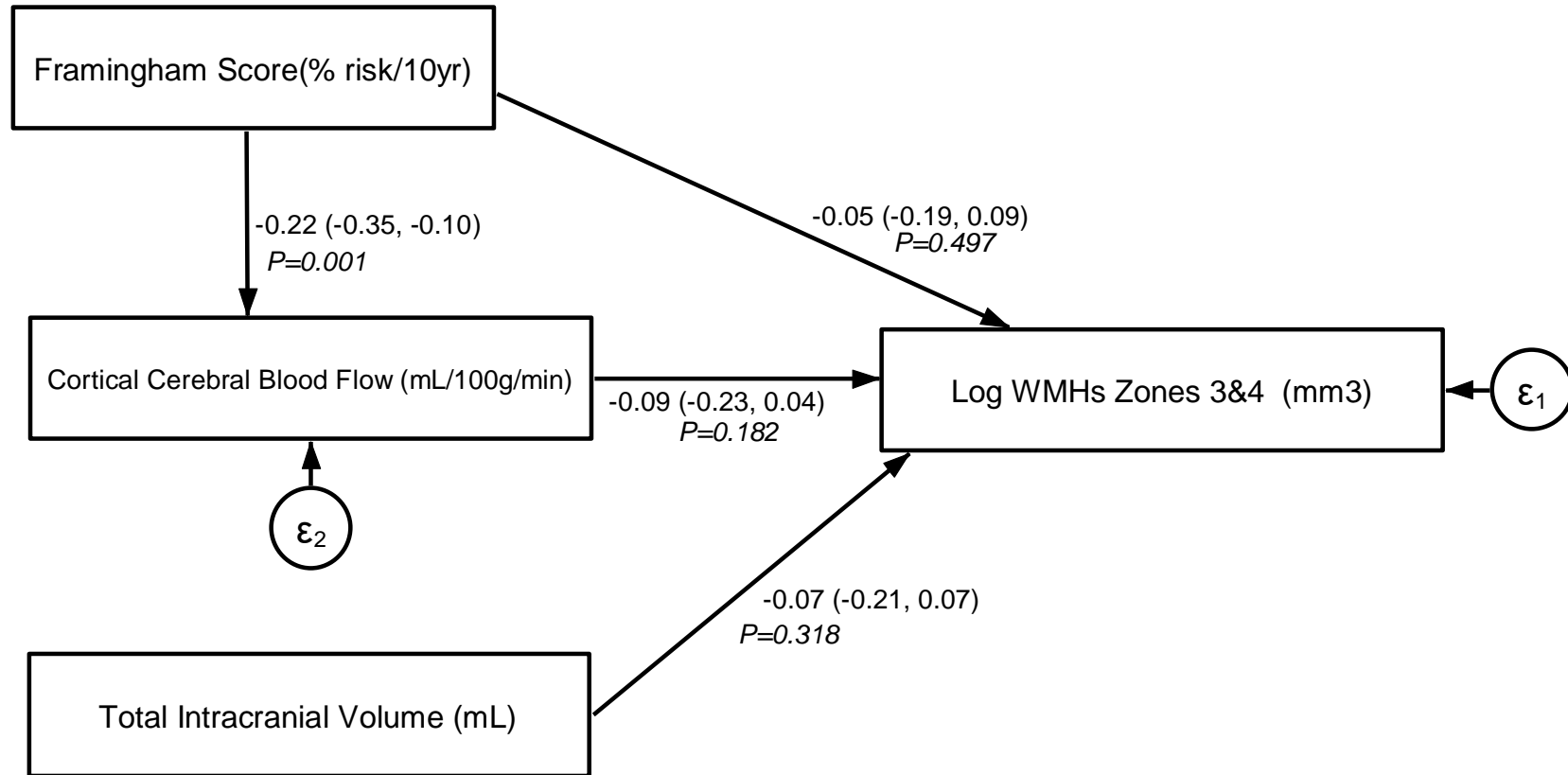


Figure 6-41. SEM diagram examining the role of CBF as a mediator between FRS and log WMHs in zones 3 & 4; Europeans. Connectors show standardised beta coefficients, (95% CIs) and P-values.

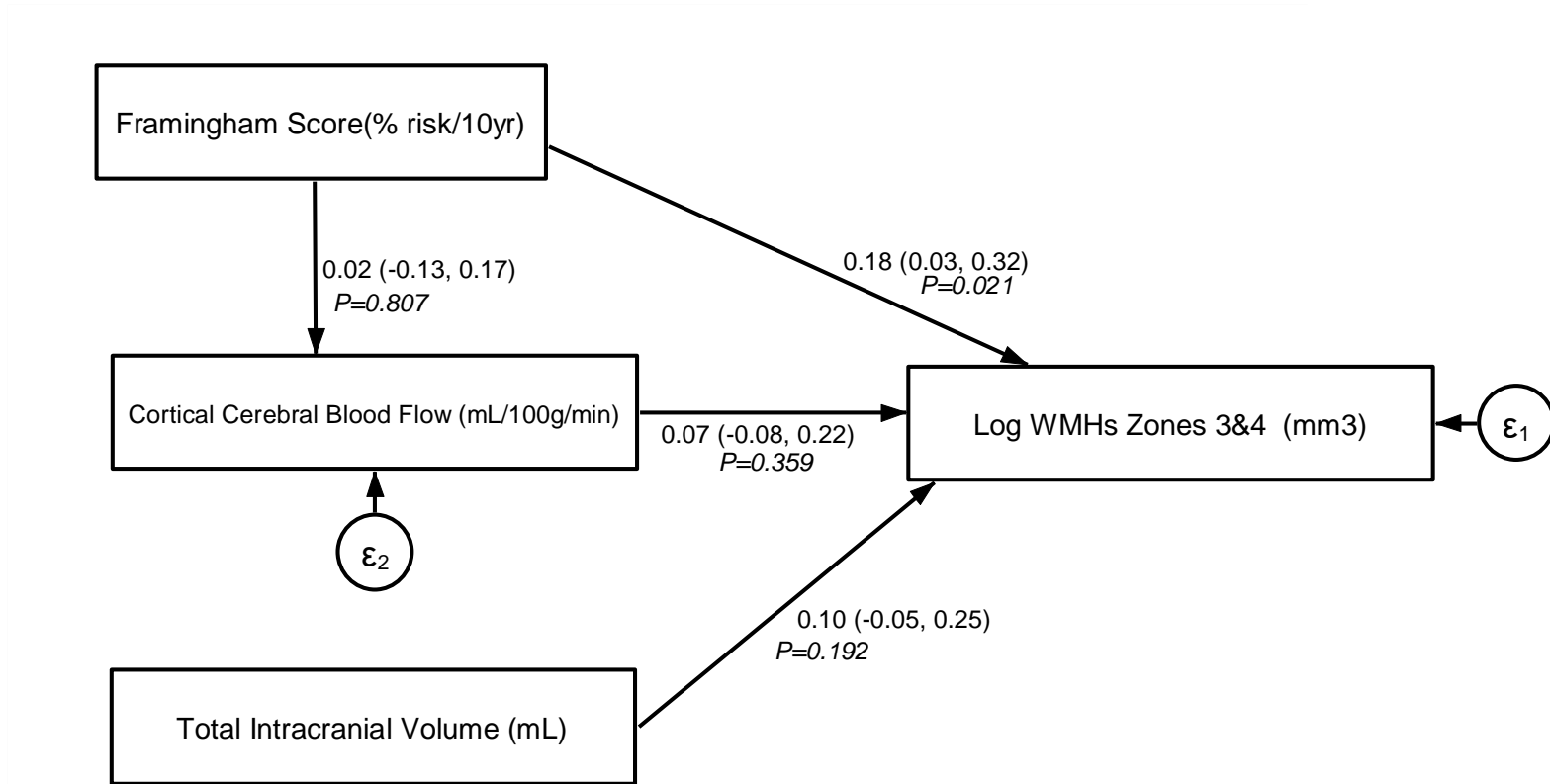


Figure 6-42. SEM diagram examining the role of CBF as a mediator between FRS and log WMHs in zones 3 & 4; South Asians. Connectors show standardised beta coefficients, (95% CIs) and P-values.

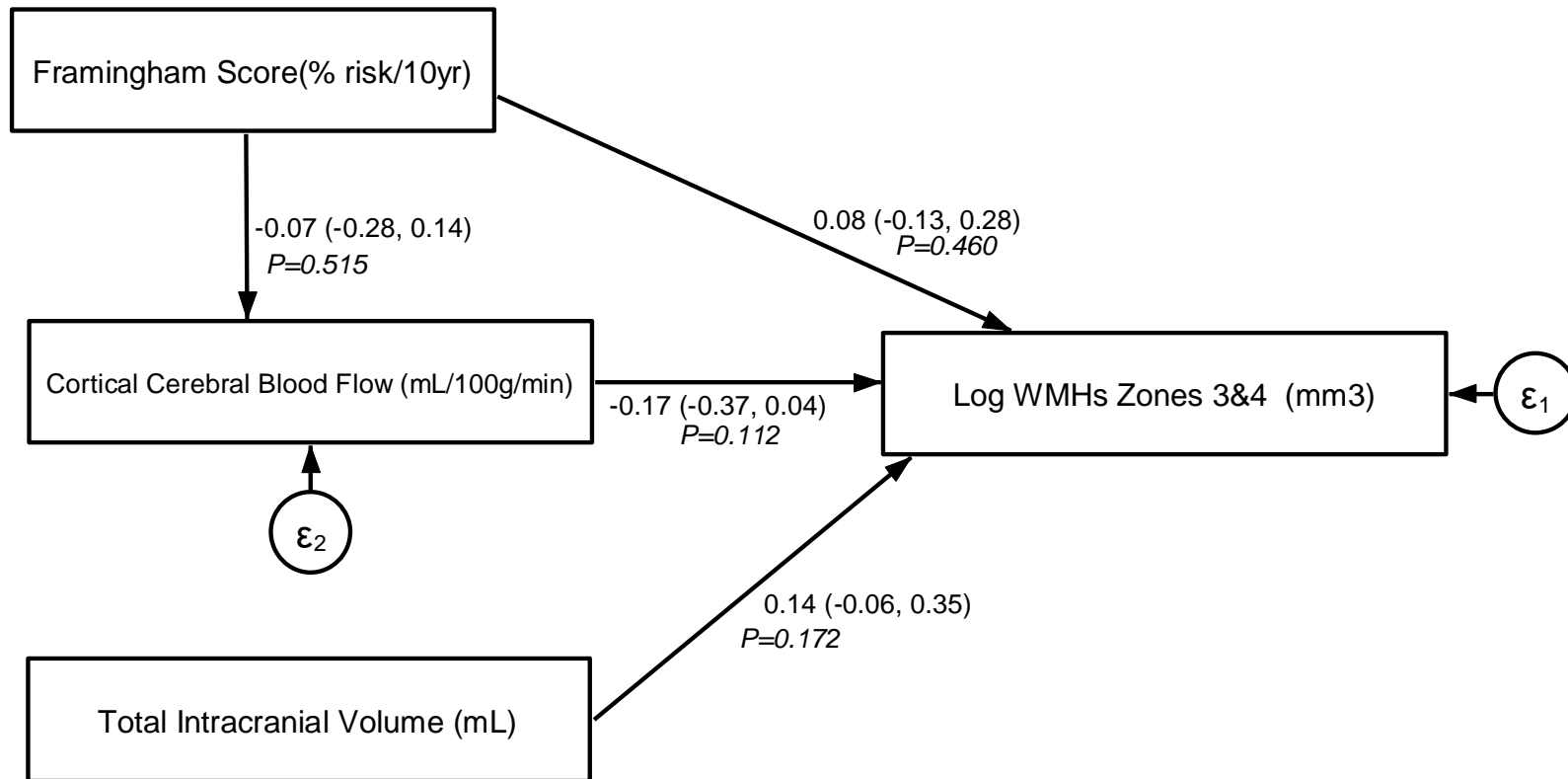


Figure 6-43. SEM diagram examining the role of CBF as a mediator between FRS and log WMHs in zones 3 & 4; African Caribbeans. Connectors show standardised beta coefficients, (95% CIs) and P-values..

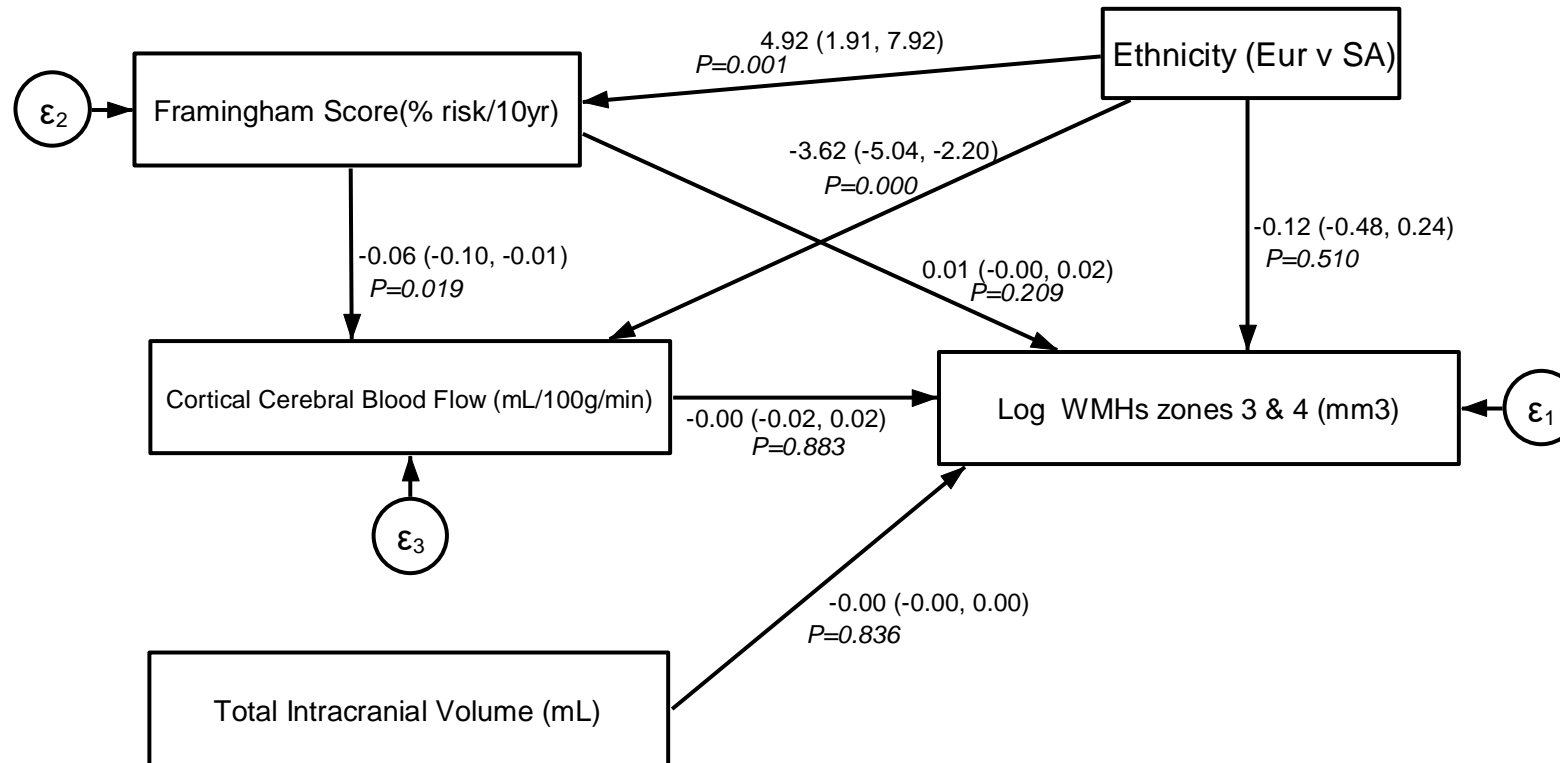


Figure 6-44. SEM diagram examining the role of CBF as a mediator between FRS and log WMHs in zones 3 & 4; Europeans vs South Asians. Connectors show unstandardised beta coefficients, (95% CIs) and P-values.

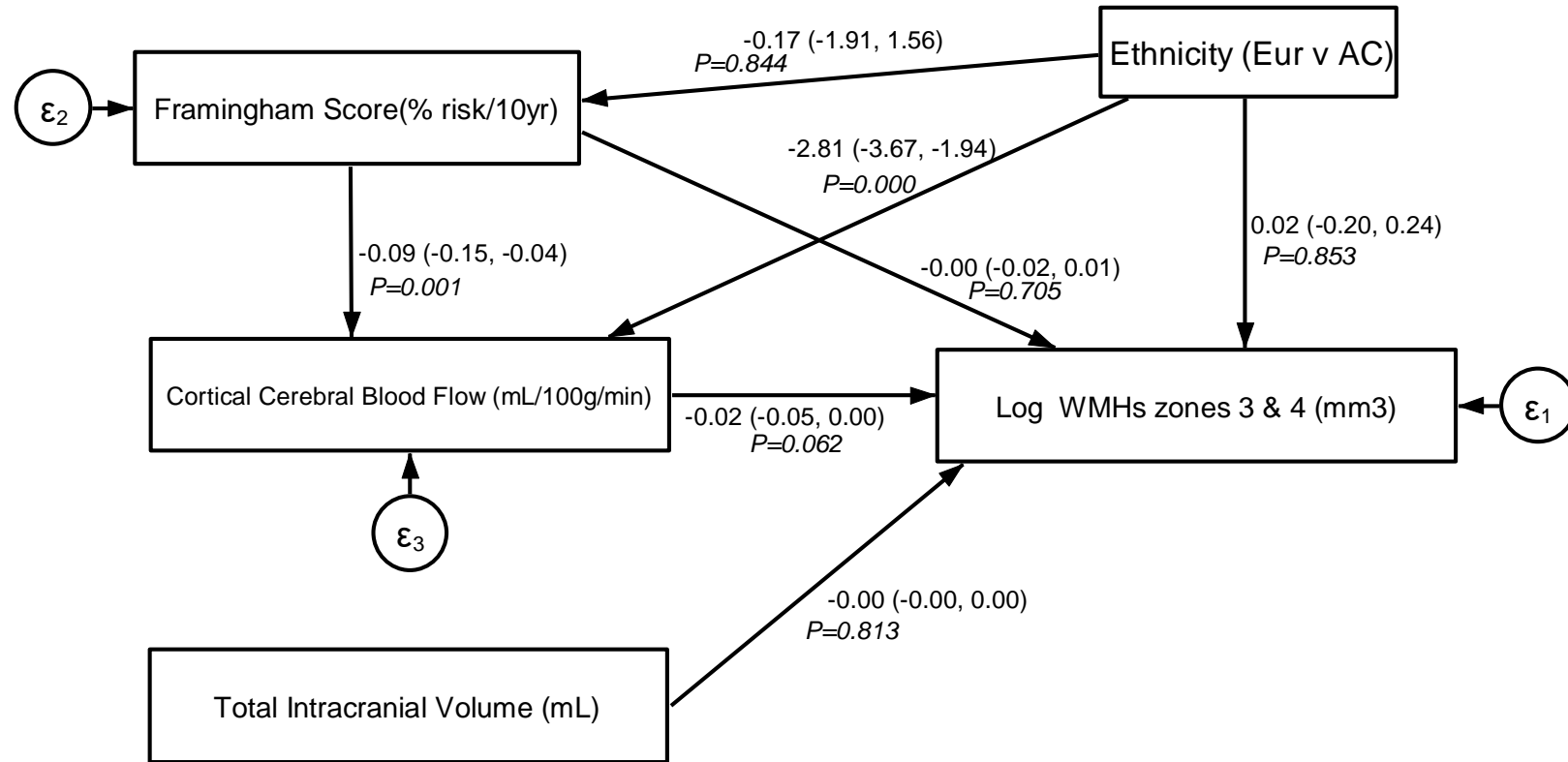


Figure 6-45. SEM diagram examining the role of CBF as a mediator between FRS and log WMHs in zones 3 & 4 Europeans vs African Caribbeans. Connectors show unstandardised beta coefficients, (95% CIs) and P-values.

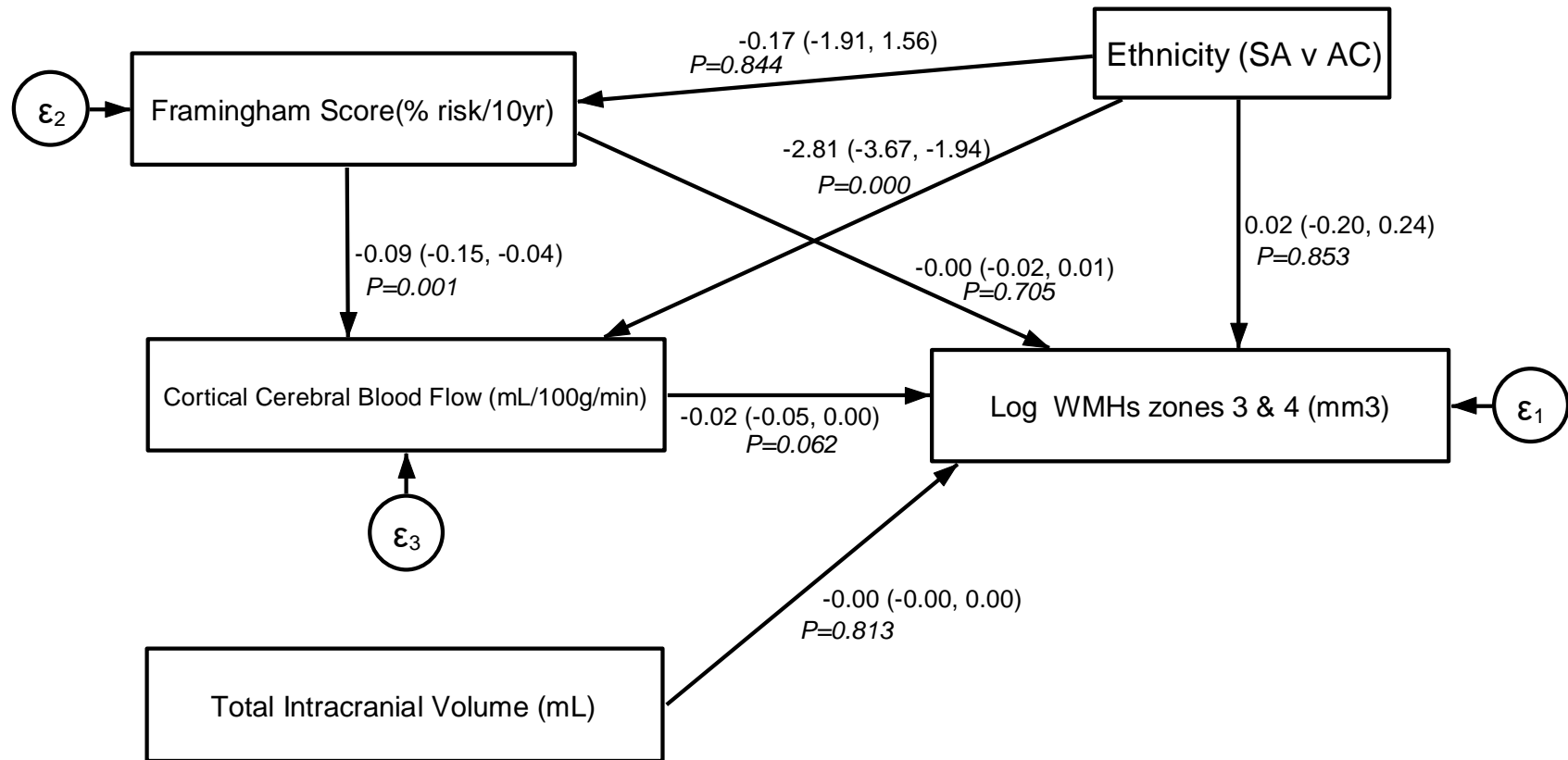


Figure 6-46 SEM diagram examining the role of CBF as a mediator between FRS and log WMHs in zones 3 & 4; South Asians vs African Caribbeans. Connectors show unstandardised beta coefficients, (95% CIs) and P-values.

6.5 Discussion

Cerebral atrophy and increases in WMHs are well documented as typical brain characteristics in old age. Much evidence supports the theory that these alterations are exacerbated by vascular risk. However, the mechanisms responsible for these changes, the wide range of inter-individual variation and variation by ethnicity and gender are not entirely understood. Chapter 5 described associations of vascular risk with CBF and indicated this relationship was modified by ethnicity and sex. In the current chapter it was hypothesised that FRS and CBF (calculated using the method of individualised Hct), would each be associated with cortical volume and burden of WMHs. It was further hypothesised that the strength of these relationships would differ between WMHs zones 1 & 2 and WMHs zones 3 & 4 to reflect differing aetiologies of WMHs in these areas. Ethnicity and sex were also tested as effect modifiers on these relationships. Furthermore, it was hypothesised that CBF is a mediator between vascular risk and MRI brain outcomes.

6.5.1 Main Findings

6.5.1.1 Associations of age, FRS and cortical tissue volume

1. *Increasing age was associated with decreased cortical tissue volume.*

The decrease in cortical volume with increasing age agrees with most previous evidence supporting a largely linear decline of GM volume in this age group. (266) (267) (54) (268).

2. *FRS was negatively associated with cortical volume.*

The majority of previous work supports the theory that more adverse vascular risk factors are associated with cerebral atrophy. Findings from the current study using FRS as a composite measure of vascular risk agree with a range of investigations that employed various vascular risk factors such as hypertension (130), diabetes (235) (243) multiple VRFs and clustering of vascular risk factors

such as metabolic syndrome (269) (270). These factors have all been mechanistically implicated in neurodegenerative changes in old age.

3. Europeans had less decline in cortical tissue volume in association with increasing FRS than South Asians or African Caribbeans.

The steeper gradient of decline in cortical volume in association with increasing vascular risk in South Asians and African Caribbeans compared to Europeans is an interesting finding. One explanation of this finding may be the greater prevalence of diabetes in non-European ethnic groups, (Europeans 18%, South Asians 38%, African Caribbeans 30% in the present study). T2DM has been associated with cortical tissue loss in many previous studies (271). Diabetes is included in the FRS algorithm, but may be insufficiently weighted (and may differ by ethnicity) to account for the effect of diabetes on the outcomes for this study, resulting in residual confounding by differences in prevalence and toxicity of diabetes across ethnic groups. There is some evidence that diabetes exerts more adverse effects on stroke risk in South Asians which is consistent with this suggestion (238). Diabetes is a binary factor in the FRS and therefore does not capture the deleterious effects of duration of diabetes, level of glycaemic control or hyperglycaemia below the threshold for diagnosis of diabetes. Age also has potential for residual confounding in this study. There is considerable evidence that brain atrophy accelerates in old age and the coefficient for age in FRS may not wholly account for the effect of age on cortical volume. However, the mean and distribution of age were similar across ethnic groups in the pooled sample and is therefore unlikely to have had a major influence on findings relating to ethnicity.

4. European men had less decline in cortical volume in association with increasing FRS than South Asian or African Caribbean men.

5. South Asian women had less decline in cortical volume in association with increasing FRS than European or African Caribbean women.

Stratified analyses revealed sex-specific effect modification by ethnicity. The difference in trends of effect modification by sex cannot be explained by

differences in diabetes prevalence as this is similar in men and women in each ethnic group. South Asian women were slightly younger than women in other ethnic groups so there may be some residual confounding by age if FRS does not fully account for age effects. This study cannot exclude the possibility of omitted lifestyle variables or omitted information such as the duration of vascular risk factors or other unmeasured factors confounding results. These findings also may be due to chance as 95% CI margins mostly overlapped, and sex-interactions were generally not statistically significant. However, when the data were stratified by sex and ethnicity, sample sizes were small limiting the power of the study to detect meaningful differences.

6.5.1.2 Associations of age, Framingham risk score and white matter hyperintensity volumes

6. Increasing age was associated with increased WMH volume.

The well documented relationship of increasing severity of WMHs with old age was replicated in this study (131, 161, 272) (62). The trajectories of WMH increase with age were similar in both PV (WMH zones 1 & 2) and DWM areas (WMH zones 3&4) giving no suggestion of differing aetiologies of WMHs by zone.

7. European women had a greater volume of WMHs than European men in age adjusted models. There was little difference between WMH volumes between sexes in South Asian and African Caribbean ethnic groups.

The finding that European women had a greater volume of WMHs than European men in models adjusted for age aligns with the Rotterdam study (62) which was a largely Caucasian sample. However, in the present study there was little difference in WMH volume between sexes in South Asian and African Caribbean groups.

8. *FRS was positively associated with volume of WMHs.*

The increase in WMH severity with old age is a well-documented characteristic of brain ageing (262) (62). Evidence regarding the relationship of WMHs with vascular risk is more controversial. The present study found a positive association of WMHs with FRS, but taking into consideration evidence from previous studies, it is possible that age is the component of the algorithm most influential on this result. Although the association of vascular risk with WM damage is supported by evidence such as the Framingham study that found increased WMHs with higher composite vascular risk scores and hypertension (148), and another study using FA found vascular risk interacted with age to undermine WM integrity (273), the Lothian study found that only a small amount of variance in WMHs was explained by vascular risk (132). This study also argued that lack of convincing evidence regarding the effect of BP lowering medication on progression of WMHs supported this observation. While the use of a composite risk score including age in the current study has a number of advantages as previously discussed, it does not make it possible to disentangle the impact of each component on the outcome.

9. *The strength of association of FRS with WMH volume in zones 1 & 2 and zones 3 & 4 could not be differentiated.*

There was no evidence of differences in the strengths of association of FRS with WMHs in zones 1 & 2 or 3 & 4. No difference in aetiology between WMHs in inner and outer zones can be inferred from this result. This finding disagrees with previous literature that suggested different causal pathways for WM damage in PV and DWM regions due to their differing vascular architectures (63, 115). However, more recent evidence indicates a much more complex picture: phenotypes displaying PV hyperintensities and DWM hyperintensities have both shared and differing genetic loci which are also variously associated with vascular pathologies (274). Heritability may be an important factor in the development of WMHs which cannot be captured in the present study due to the absence of genetic data.

10. South Asians and African Caribbeans had a greater increase in WMH volume in association with increasing FRS than Europeans. This was the case in both sexes in stratified models.

Ethnicity as an effect modifier in the relationship of WMHs and vascular risk is in accordance with previous studies (161). The ARIC study, that found greater progression in WMHs in African Americans compared to Caucasians, considered this could be due to longer duration of hypertension in African Americans (244). The greater prevalence of anti-hypertensive medication in African Caribbeans of both sexes and South Asian women compared to Europeans in the current sample reflects a greater prevalence of hypertension diagnosis and may be indicative of longer duration of pathological levels of BP. Systolic BP measured in clinic was also lower in Europeans. However, the ethnic variation in WMH volume may also be due to residual confounding by age or diabetes. Longitudinal studies indicate that one of the strongest predictors of WMH volume is higher baseline readings. i.e. participants with the largest volume of WMHs at the beginning of a study experience the greatest progression of WMH volume over the period until follow-up (132). Furthermore, non-vascular predictors of WMHs that vary by ethnicity are not included in this study and may act as confounders, such as genetic variants implicated in causal inflammatory pathways leading to WMHs (275).

6.5.1.3 Associations of CBF with cortical tissue volume and WMH volume

11. CBF was not associated with cortical volume nor WMH volumes and did not mediate the relationship of FRS with brain outcomes.

CBF was not associated with brain outcomes in GLM analyses and this lack of association was unsurprisingly reflected in the null results for CBF as a mediator in SEMs. Comparisons with previous studies are difficult due to variation in cohort characteristics and methodological differences for acquiring flow data and estimating flow. Studies that have found associations of CBF and

brain atrophy have generally included clinic cohorts with memory problems or AD or have included participants with other severe neurodegenerative changes (168). A previous study found associations between CBF and atrophy in AD but not controls (169). Other studies did not find convincing associations of CBF and atrophy after adjustment for age (114), or if they did only reported regional brain flow (80, 261). Measurement of regional CBF may be more sensitive to early changes in vulnerable regions of the brain associated with neurovascular degeneration and cognitive decline. There may be reverse causation due to matching of perfusion to the demands of reduced brain volume or lower metabolic demands of rarefied tissue. The direction of causality between perfusion and brain volume remains obscure, although there is some evidence of bi-directionality in old age (117). The independent effect of atrophy on both CBF and brain volume may also act as a confounder. Consideration of total blood flow to the brain by PC-MRI could be used as an additional indicator of brain health, although adjustment for head size is still necessary (114), and this method does not measure tissue perfusion directly.

The lack of a cross-sectional association between WMHs and CBF in the current study is in conflict with the majority of previous evidence summarised in a recent systematic review (171). However, the diversity of methodological approaches used to quantify WMHs and to measure CBF make direct comparisons difficult. For example, in a small study ($n = 26$) Crane et al (276) observed a negative association of WMH volume with GM CBF using PCASL in regional areas but did not report global results, and Bastos-Leite et al (168), using the Fazekas scale to categorise WMH volume, found an association of diffuse confluent WMHs with lower global and whole brain CBF using PASL. In contrast, Wagner et al (277) found no associations between GM CBF, measured using PASL, and WM changes measured using T2* mapping. Furthermore, this systematic review suggested that many investigations were confounded by inadequate adjustment for age which is often associated with both CBF and WMH burden, and some results may have been biased by over-representation of participants with dementia. Age was not associated with CBF in the current work (see Chapter 4). As discussed above this may reflect the

limited age range in the sample and may partially explain why these findings disagree with some but not all others (116). The sample in the present study was healthier and younger than many previous studies. In these circumstances cerebral autoregulation is more likely to be preserved, at least under resting conditions. ASL as implemented in the present study cannot detect abnormal blood flow rates that only occur in response to a stimulant such as a hypercapnic challenge or a drop or elevation of BP. Alternatively, low CBF may be the consequence not the cause of WMHs so that the relatively healthy individuals observed in the current study may be too early in the process of WMH development for lesions to detectably affect CBF. It would be interesting to investigate whether CBF decreased in individuals with high WMH burden in follow up scans as observed in a previous longitudinal study (112).

There were no differences in the strength of associations of CBF with WMHs in zonal analysis. This finding may reflect the limitations in detecting small changes in resting CBF in relatively healthy populations in the early stages of WMH development as mentioned above. Ten Dam et al. did not find an association of WMHs and CBF in cross-sectional analysis, although longitudinal data in this elderly sample revealed an association of decline in CBF with an increase in PV WMHs, indicative of diffuse hypoperfusion, but not DWM hyperintensities which would be indicative of localised perfusion deficits (115). The cross-sectional design of the current study precludes speculation about causality and is unable to detect intra-individual changes in WMH severity or perfusion.

It is also possible that associations with CBF were not observed as non-vascular mechanisms such as inflammation, oedema, vessel wall leakage (132), and increased genetic risk (278) (275) may be more strongly causally related to the development of WMHs and may have obscured weak associations.

6.5.2 Study Strengths and Limitations

This study shares many of the strengths and limitations discussed in Chapters 4 and 5. In brief, strengths include the ethnically diverse and well-defined population cohort. The study was entirely conducted in a single centre, cardiovascular data were robust with few missing data points. Imaging strengths include robust MRI protocol application and advanced automated processing of brain segmentation and WMH volumetry. Analyses of stratified models avoided confounding by ethnicity and sex and revealed potential differences in associations of vascular risk and brain outcomes. The inclusion of participants reflecting ethnically diverse populations is important for future studies to consider in order to confidently generalise results to wider populations and to inform clinical decisions oriented to individualised precision medicine. Such advances in preventative care result in saving health care costs, more timely effective interventions at the most effective stage in an individual's life course to promote the optimum cognitive outcomes in old age. However, this cohort may have been too healthy to detect changes in CBF due to preserved cerebral autoregulatory function.

As discussed previously in this thesis, the use of individually measured Hct in the Buxton equation for calculation of CBF from ASL improved the accuracy of CBF estimation in this elderly ethnically diverse cohort.

Limitations of the study emerge in the stratified analyses which were underpowered to detect the small effect sizes of vascular risk on brain outcomes. This resulted in wide and overlapping confidence margins which made many results uncertain.

The cross-sectional design precludes any conclusions about causal relationships between variables. Longitudinal data would have yielded information regarding the progression of WMHs as there is much inter-individual variation. Furthermore, this study measured brain volume which is a surrogate marker for brain atrophy(56).

Visualisation of WMHs using a FLAIR sequence provides evidence of late stage damage. The rate of WMH expansion may be a more relevant marker of cognitive function. FA from DTI would provide more sensitive evidence at an earlier stage of WM connective deterioration.

6.5.3 Future studies

Further investigation using a larger population cohort to provide more robust results particularly regarding the modifying effects of ethnicity and sex is warranted, as the present study is limited by lack of power. Longitudinal studies would also be able to indicate possible direction of causality and risk factors linked to trajectories of change. It remains unknown whether CBF remains matched to cortical volume in the atrophied brain or whether the brain shrinks due to loss of blood flow. It is also not clear whether the aetiology of WMHs includes a response to restricted blood flow, or if CBF decreases as WMHs alter metabolic demand (112). Use of the FRS to represent composite vascular risk means that age cannot be disentangled from other risk factors. Testing of the individual components of the algorithm would give a better indication whether age was the driving factor between FRS and brain outcomes, but inclusion of the individual risk factors would complicate statistical modelling considerably. Use of more sensitive or dynamic measures such as imaging CBF under hypercapnic challenge to detect vasoreactivity deficiencies and use of increasingly sophisticated DTI sequences to examine FA, MD and tractography enable detection of earlier as well as more subtle localised WM pathology (279). Separation of the components of vascular risk instead of use of a composite metric would reveal those factors most closely related to unhealthy brain ageing and would facilitate clinical decision-making for effective and timely interventions tailored more closely to the individual. The close association of age with brain volume and WMH severity makes it possible the associations of FRS with brain markers found in this study are largely due to the age component of the composite risk algorithm.

6.5.4 Summary

The findings of this chapter support the hypothesis that vascular risk is associated with MR markers of brain ageing. Ethnicity and sex appear to modify these complex relationships. CBF was not associated with any of the brain outcomes tested in this study. Future studies on larger population cohorts could provide further evidence of the extent of ethnic and gender variations on these relationships. More sensitive methods of brain imaging are required to detect earlier and more subtle signs of brain ageing.

7 . Summary of results and future directions

The final chapter reviews the main findings of this thesis. Strengths and limitations of the study are briefly recapped, followed by a discussion of future directions and a final summary.

This thesis investigated the relationships of CBF, estimated using an improved method employing measured as opposed to estimated Hct. This facilitated the investigation of associations between CBF, vascular risk and the MR markers of accelerated brain ageing. Analyses focused on the roles of sex and ethnicity as effect modifiers on these relationships.

7.1 Review of hypotheses and results

7.1.1 Chapter 4

Chapter 4 was an investigation of the effect of variation of Hct on CBF estimation. The impact on sex and ethnic groups of using the population Hct mean rather than individually measured Hct to calculate the T1 of blood was evaluated in a tri-ethnic elderly population cohort.

1. Hypothesis:

- a) *The inclusion of individualised measurements of Hct in the calculation of CBF from ASL improves accuracy when investigating group associations of cerebral perfusion.***

Summary of Findings

Compared to quantification using a fixed Hct of 43.5% as recommended in the ISMRM white paper, use of measured individual Hct decreased CBF estimates from ASL in all ethnic and sex categories except European men. The size of

this effect differed by ethnicity and sex: cortical CBF estimates from ASL in women, non-European ethnicities and individuals with diabetes are overestimated. Individually measured Hct should be used to calculate the longitudinal relaxation time of blood but if this is not practical, a group mean value adjusted for ethnicity and sex would improve accuracy of CBF estimations. Hct corrected ASL could be potentially important both in research for group investigations and in clinical use for CBF threshold decision making in the fields of neurodegenerative disease and neuro-oncology.

7.1.2 Chapter 5

Chapter 5 analysed the association of vascular risk, represented by separate VRFs and a composite vascular risk score (FRS), with CBF estimated using the method described in Chapter 4. Interactions of vascular risk with ethnicity aimed to detect group differences in these relationships. To explore possible effect modification by sex and diabetes, secondary analyses were performed on groups stratified by sex and diabetes status.

1. Hypotheses

- a) Individual components of the FRS are associated with CBF in elderly populations.***
- b) Sex and ethnicity are in some instances effect modifiers of this relationship.***

2. Hypotheses

- a) Elevated combined vascular risk represented by the FRS is associated with decreased cortical CBF in elderly populations.***
- b) Sex and ethnicity are effect modifiers in this relationship.***

Summary of Findings

Systolic BP was inversely associated with CBF and HDL cholesterol was positively associated with CBF in the pooled sample, although effect sizes were small. Diabetes was weakly associated with decreased CBF. In sex stratified samples the relationship of systolic BP with CBF was only seen in men.

Increased combined vascular risk (FRS) was associated with decreased CBF. However, there was no indication of a synergistic effect of multiple VRFs. Ethnicity moderated this result. Europeans with low FRS had higher CBF than other ethnicities with comparable vascular risk scores, but their CBF decreased more with increasing FRS than other ethnicities. The corollary of this result may be that South Asians and African Caribbeans displayed a 'floor' effect: their CBF was low but did not decline further with increase in FRS. Earlier onset and longer duration of vascular disease may explain this result. On inspection of sex stratified samples, the role of ethnicity as an effect modifier was only apparent in women in these analyses. As the association of age with CBF was strongest in European women, age may be the component of the FRS algorithm accounting for this finding. It is possible that South Asian and African Caribbean women experience the effects of vascular risk on CBF earlier in their life course.

Groups stratified by diabetes were under-powered which made evidence from these analyses unconvincing. Additionally, omitted variables including duration of diabetes and glycaemic control may have confounded results. However, there was some evidence that non-European participants in the 'no diabetes' group displayed a phenotype of vascular risk similar to all participants in the 'with diabetes' group. In the 'no diabetes' group, Europeans were differentiated from other ethnicities as they had higher CBF at low FRS, whereas there were no ethnic differences in this relationship in the 'with diabetes' group. This result aligns with the hypothesis that South Asians and African Caribbeans may be more at risk of neurodegenerative disease and cognitive impairment than Europeans in relation to level of vascular risk.

7.1.3 Chapter 6

Chapter 6 investigated associations of FRS and CBF, estimated using the method described in Chapter 4, with cortical tissue volume and WMH volumes. The role of CBF as a potential mediator between vascular disease and the MR markers of brain ageing was evaluated.

1. Hypotheses

- a) *Elevated combined vascular risk represented by the FRS is associated with decreased cortical tissue volume and increased WMH volume in an elderly ethnically diverse population.*
- b) *Sex and ethnicity are in some instances effect modifiers of the association of combined vascular risk and brain outcomes.*

2. Hypotheses

- a) *Hypoperfusion is associated with decreased cortical tissue volume and increased WMH volume in elderly populations.*
- b) *Sex and ethnicity are in some instances effect modifiers of the associations of CBF and brain outcomes.*

3. Hypothesis

- a) *Cortical CBF is a mediator in associations of combined vascular risk with cortical tissue volume and WMH volume in elderly populations.*
- b) *The strength of CBF as a mediator in the association of combined vascular risk with WMH volume will vary with zonal location.*

Summary of findings

Decreased cortical tissue volume and increased WMH volumes were associated with increased FRS. However, the use of the composite FRS did not provide evidence as to which elements of the algorithm were most closely

correlated. The strong association of cortical volume and WMH volumes with age indicates that the relative effect size of vascular risk on these relationships is small. The stronger association of FRS with brain volume and WMHs in South Asians and African Caribbeans may have been due to confounding by diabetes prevalence which has a disproportionate effect on brain ageing not captured by the FRS. South Asian women appeared to experience less decline in cortical volume with FRS but differences in associations by ethnicity in sex stratified models were difficult to interpret with confidence due to lack of power and small effect sizes.

CBF did not mediate the effect of FRS on cortical tissue volume or any WMH volume variable. This finding may be due to the relatively healthy study sample who were mostly in early old age or were brain ageing successfully. They were therefore more likely to be able to maintain perfusion at rest via cerebral autoregulation within a normal range. Alternatively, it cannot be discounted that the mechanisms of vascular risk on the acceleration of brain ageing may be unrelated to hypoperfusion.

7.2 Strengths and Limitations

The main strength of this study was its large sample size relative to previous studies using ASL to measure brain perfusion. However, statistical power was limited when samples were stratified by sex and diabetes. The SABRE study was a community-based population cohort and therefore is more representative of the general population than symptomatic cardiovascular disease cohorts or those drawn from memory clinics. However, it did not include individuals with very severe cognitive symptoms or mobility limitations which may have led to a selection bias towards more healthy individuals than in the general population. This may have impacted the ability of this study to detect hypoperfusion under resting conditions.

A major strength of this study was the use of individually measured Hct for the calculation of CBF from ASL which improved accuracy of CBF estimation in this elderly ethnically diverse cohort.

The cross-sectional design of the study had a number of drawbacks. Brain volume is a surrogate measure of brain atrophy and is difficult to interpret due to inter-individual variation of brain size and the possible non-linear association of atrophy with age (56). Tracking of individual changes in longitudinal studies over a period of years provides a more robust measure. Similarly, rate of progression of WMHs is a more accurate predictor of cognitive function than cross-sectional measurement (280). The detection of WMHs using the FLAIR MR sequence supplies evidence of late stage WM damage. Use of DTI would have provided earlier and more sensitive evidence of deterioration in WM connectivity.

The cross-sectional design also discounted consideration of variables such as duration and pattern of VRFs including variation of BP e.g. periodic hypertension/hypotension, and duration of diabetes or history of glycaemic control. The cross-sectional design also excludes inference of causal direction, so it is not possible to speculate whether CBF is a result of increasing vascular risk, whether it is a concurrent parallel process with vascular risk or whether CBF promotes vascular disease. Many studies (75) have indicated that vascular disease in middle age is an important predictor of cognitive decline in old age. However, this pattern of association can only be captured in longitudinal studies (244) (107) (105).

This study cannot discount unmeasured confounders affecting the relationship between VRFs and CBF. Furthermore, these may be more prevalent in non-European ethnic groups, thus confounding results that indicate effect modification by ethnicity. Although some factors that have been implicated in brain outcomes were omitted, including obesity, vascular stiffness, cardiac index, exercise (281) and genetic factors such as APOE4 (281), the variables

included in the models for this thesis were selected *a priori* according to strong evidence-based research on predictors of cardiovascular events. FRS was selected as a measure of combined vascular risk as it has undergone extensive international validation. However, it has been criticised for failing to perform equally well in all ages, ethnicities and sexes (195) (250) (196).

The measurement of CBF in mL/100g/min neglects the role of brain atrophy in assessing the effects of VRFs on cerebrovascular disease in old age. Severely atrophied brains that are reasonably perfused will not be identified if CBF is considered in isolation. Without longitudinal studies it is not possible to disentangle whether an atrophied brain is the result of decreased blood flow or whether decreased blood flow is the result of the reduction in metabolic demand from smaller rarefied brain tissue. Inclusion of brain volume, adjusted for intracranial volume, in conjunction with CBF might provide more useful biomarkers of brain health in ageing populations.

7.3 Future Directions

ASL in elderly populations is a challenging technique but promises to become a useful biomarker of dementia in advance of symptomatic disease onset. Measurement errors can be introduced due to slow flow and vessel collateralisation leading to delayed bolus arrival. Susceptibility artefacts caused by dental work affect the MR signal, and tortuosity of the neck vessels may affect the efficiency of RF blood labelling. Improvements in ASL sequences such as 4D fast acquisition using multi TIs to visualise arrival of the full bolus (282) (283), improved bolus labelling such as velocity selective ASL (284), correction for off-resonance effects in the labelling plane caused by factors such as dental implants (285), and improvements in SNR (286) (287) may extend robust measurement to perfusion of WM and regional CBF and to the use of ASL at higher field strengths. The present study did not include regional CBF measurements as global cortical measurement was considered to be more reliable using current techniques. However, future studies investigating flow in

brain areas associated with AD such as temporal and parietal lobes, might provide stronger evidence for the role of decreased CBF in brain ageing and cognitive decline. Assessment of vasoreactivity such as the hypercapnic challenge used by Glodzik et al (166), might also be more sensitive to early signs of hypoperfusion, possibly prior to symptoms of cognitive decline.

The literature review in this thesis included examples of the value of longitudinal studies for assessing the MR markers of brain ageing. Progression of WMHs and acceleration of brain atrophy were often strongly associated with vascular risk and CBF when cross-sectional data did not show correlations (112) (117) (115) (130). Longitudinal studies also provide valuable information regarding the effects of VRFs throughout the life-course. Confidence in some of the results in this thesis, particularly those in highly stratified models, are hampered by relatively small sample sizes in relation to effect sizes. If possible, future investigations would benefit from a focus on very large prospective studies such as UK Biobank (288) or meta-analyses of cohorts from multiple studies which are able to produce comprehensive stratified phenotyping including genetic, metabolic and environmental data.

References

1. Toth P, Tarantini S, Csiszar A, Ungvari Z. Functional vascular contributions to cognitive impairment and dementia: mechanisms and consequences of cerebral autoregulatory dysfunction, endothelial impairment, and neurovascular uncoupling in aging. *American Journal of Physiology - Heart and Circulatory Physiology*. 2017;312(1):H1-H20.
2. Cipolla M.J. *The Cerebral Circulation, Ch 2 Anatomy and Ultrastructure*, . San Rafael (CA): Morgan and Claypool Life Sciences; 2009. Available from: <https://www.ncbi.nlm.nih.gov/books/NBK53086/>.
3. Moody DM, Brown WR, Challa VR, Ghazi-Birry HS, Reboussin DM. Cerebral microvascular alterations in aging, leukoaraiosis, and Alzheimer's disease. *Ann N Y Acad Sci*. 1997;826:103-16.
4. Brown WR, Thore CR. Review: cerebral microvascular pathology in ageing and neurodegeneration. *Neuropathol Appl Neurobiol*. 2011;37(1):56-74.
5. Suter OC, Sunthorn T, Kraftsik R, Straubel J, Darekar P, Khalili K, et al. Cerebral Hypoperfusion Generates Cortical Watershed Microinfarcts in Alzheimer Disease. *Stroke*. 2002;33(8):1986-92.
6. Thomas DL, Lythgoe MF. The measurement of diffusion and perfusion in biological systems using magnetic resonance imaging. *Phys Med Biol* 1999;45.
7. Zlokovic BV. Neurovascular pathways to neurodegeneration in Alzheimer's disease and other disorders. *Nat Rev Neurosci*. 2011;12(12):723-38.
8. Nelson AR, Sweeney MD, Sagare AP, Zlokovic BV. Neurovascular dysfunction and neurodegeneration in dementia and Alzheimer's disease. *Biochim Biophys Acta*. 2015.
9. Muoio V, Persson PB, Sendeski MM. The neurovascular unit – concept review. *Acta Physiologica*. 2014;210(4):790-8.
10. Morris AWJ, Carare RO, Schreiber S, Hawkes CA. The Cerebrovascular Basement Membrane: Role in the Clearance of β -amyloid and Cerebral Amyloid Angiopathy. *Frontiers in aging neuroscience*. 2014;6(251).
11. Hamilton N, Attwell D, Hall C. Pericyte-mediated regulation of capillary diameter: a component of neurovascular coupling in health and disease. *Frontiers in Neuroenergetics*. 2010;2(5).
12. De Silva TM, Faraci FM. Microvascular Dysfunction and Cognitive Impairment. *Cell Mol Neurobiol*. 2016;36(2):241-58.
13. Ostergaard L, Engedal TS, Moreton F, Hansen MB, Wardlaw JM, Dalkara T, et al. Cerebral small vessel disease: Capillary pathways to stroke and cognitive decline. *J Cereb Blood Flow Metab*. 2016;36(2):302-25.
14. Lassen NA. Control of cerebral circulation in health and disease. *Circ Res*. 1974;34(6):749-60.

15. Markus HS. Cerebral perfusion and stroke. *Journal of Neurology, Neurosurgery & Psychiatry*. 2004;75(3):353.
16. Strandgaard S, Paulson OB. Cerebral autoregulation. *Stroke*. 1984;15(3):413-6.
17. Iadecola C. Neurovascular regulation in the normal brain and in Alzheimer's disease. *Nat Rev Neurosci*. 2004;5(5):347-60.
18. Panza JA, Quyyumi AA, Brush JE, Epstein SE. Abnormal Endothelium-Dependent Vascular Relaxation in Patients with Essential Hypertension. *New England Journal of Medicine*. 1990;323(1):22-7.
19. Pires PW, Dams Ramos CM, Matin N, Dorrance AM. The effects of hypertension on the cerebral circulation. *Am J Physiol Heart Circ Physiol*. 2013;304(12):H1598-614.
20. Iadecola C. The Neurovascular Unit Coming of Age: A Journey through Neurovascular Coupling in Health and Disease. *Neuron*. 2017;96(1):17-42.
21. Abbott NJ, Patabendige AA, Dolman DE, Yusof SR, Begley DJ. Structure and function of the blood-brain barrier. *Neurobiol Dis*. 2010;37(1):13-25.
22. Grammas P. Neurovascular dysfunction, inflammation and endothelial activation: implications for the pathogenesis of Alzheimer's disease. *Journal of neuroinflammation*. 2011;8:26.
23. Montagne A, Barnes SR, Sweeney MD, Halliday MR, Sagare AP, Zhao Z, et al. Blood-brain barrier breakdown in the aging human hippocampus. *Neuron*. 2015;85(2):296-302.
24. Attwell D, Mishra A, Hall CN, O'Farrell FM, Dalkara T. What is a pericyte? *J Cereb Blood Flow Metab*. 2016;36(2):451-5.
25. Jack CR, Jr., Knopman DS, Jagust WJ, Shaw LM, Aisen PS, Weiner MW, et al. Hypothetical model of dynamic biomarkers of the Alzheimer's pathological cascade. *Lancet Neurol*. 2010;9(1):119-28.
26. Mosconi L, Berti V, Glodzik L, Pupi A, De Santi S, de Leon MJ. Pre-clinical detection of Alzheimer's disease using FDG-PET, with or without amyloid imaging. *Journal of Alzheimer's disease : JAD*. 2010;20(3):843-54.
27. Johnson KA, Sperling RA, Gidicsin CM, Carmasin JS, Maye JE, Coleman RE, et al. Florbetapir (F18-AV-45) PET to assess amyloid burden in Alzheimer's disease dementia, mild cognitive impairment, and normal aging. *Alzheimer's & Dementia*. 2013;9(5):S72-S83.
28. Mosconi L, Tsui WH, Herholz K, Pupi A, Drzezga A, Lucignani G, et al. Multicenter standardized 18F-FDG PET diagnosis of mild cognitive impairment, Alzheimer's disease, and other dementias. *J Nucl Med*. 2008;49(3):390-8.
29. Del Sole A, Clerici F, Chiti A, Lecchi M, Mariani C, Maggiore L, et al. Individual cerebral metabolic deficits in Alzheimer's disease and amnesic mild cognitive impairment: an FDG PET study. *Eur J Nucl Med Mol Imaging*. 2008;35(7):1357-66.

30. Chen Y, Wolk DA, Reddin JS, Korczykowski M, Martinez PM, Musiek ES, et al. Voxel-level comparison of arterial spin-labeled perfusion MRI and FDG-PET in Alzheimer disease. *Neurology*. 2011;77(22):1977-85.
31. Verfaillie SC, Adriaanse SM, Binnewijzend MA, Benedictus MR, Ossenkoppele R, Wattjes MP, et al. Cerebral perfusion and glucose metabolism in Alzheimer's disease and frontotemporal dementia: two sides of the same coin? *European radiology*. 2015;25(10):3050-9.
32. Musiek ES, Chen Y, Korczykowski M, Saboury B, Martinez PM, Reddin JS, et al. Direct comparison of fluorodeoxyglucose positron emission tomography and arterial spin labeling magnetic resonance imaging in Alzheimer's disease. *Alzheimer's & dementia : the journal of the Alzheimer's Association*. 2012;8(1):51-9.
33. Iturria-Medina Y, Sotero RC, Toussaint PJ, Mateos-Perez JM, Evans AC, Alzheimer's Disease Neuroimaging I. Early role of vascular dysregulation on late-onset Alzheimer's disease based on multifactorial data-driven analysis. *Nat Commun*. 2016;7:11934.
34. Thies B, Truschke E, Morrison-Bogorad M, Hodes RJ. Consensus report of the Working Group on: molecular and biochemical markers of Alzheimer's disease. *Neurobiology of aging*. 1999;20(2):247.
35. Kety SS, Schmidt CF. The Nitrous Oxide Method for the Quantitative Determination of Cerebral Blood Flow in Man: Theory, Procedure and Normal Values. *J Clin Invest*. 1948;27(4):476-83.
36. Golay X. Arterial spin labeling-MRI: acquisition and analysis techniques. In: Zaharchuk G, Barker PB, Golay X, editors. *Clinical Perfusion MRI: Techniques and Applications*. Cambridge: Cambridge University Press; 2013. p. 38-57.
37. Buxton RB, Frank LR, C. WE, Siewert B, Warach S, Edelman RR. A General Kinetic Model for Quantitative Perfusion Imaging with Arterial Spin Labeling. *MRM*. 1998;40:383-96.
38. Detre JA, Leigh JS, Williams DS, Koretsky AP. Perfusion Imaging. *Magnetic Resonance in Medicine*. 1992;23:37-45.
39. Williams DS, Detre JA, Leigh JS, Koretsky AP. Magnetic resonance imaging of perfusion using spin inversion of arterial water. *Proc Natl Acad Sci U S A*. 1992;89(1):212-6.
40. Detre JA, Alsop DC. Perfusion magnetic resonance imaging with continuous arterial spin labeling: methods and clinical applications in the central nervous system. *European journal of radiology*. 1999;30(2):115-24.
41. Edelman RR, al. e. Qualitative Mapping of Cerebral Blood Flow and Functional Localization with Echo-planar MR Imaging and Signal Targeting with Alternating Radio Frequency. *Neuroradiology*. 1994;192:513-20.
42. Alsop DC, Detre JA, Golay X, Gunther M, Hendrikse J, Hernandez-Garcia L, et al. Recommended implementation of arterial spin-labeled perfusion MRI for clinical applications: A consensus of the ISMRM perfusion study group and the European consortium for ASL in dementia. *Magn Reson Med*. 2014.

43. Kim SG. Quantification of relative cerebral blood flow change by flow-sensitive alternating inversion recovery (FAIR) technique: Application to functional mapping. *Magnetic Resonance in Medicine*. 1995;34(3):293-301.
44. Luh W-M, Wong EC, Bandettini PA, Hyde JS. QUIPSS II with thin-slice TI 1 periodic saturation: a method for improving accuracy of quantitative perfusion imaging using pulsed arterial spin labeling. *Magnetic resonance in medicine*. 1999;41(6):1246-54.
45. Dai W, Garcia D, de Bazelaire C, Alsop DC. Continuous flow-driven inversion for arterial spin labeling using pulsed radio frequency and gradient fields. *Magn Reson Med*. 2008;60(6):1488-97.
46. Wu WC, Fernandez-Seara M, Detre JA, Wehrli FW, Wang J. A theoretical and experimental investigation of the tagging efficiency of pseudocontinuous arterial spin labeling. *Magn Reson Med*. 2007;58(5):1020-7.
47. Ballester MAG, Zisserman AP, Brady M. Estimation of the partial volume effect in MRI. *Medical image analysis*. 2002;6(4):389-405.
48. Asllani I, Borogovac A, Brown TR. Regression algorithm correcting for partial volume effects in arterial spin labeling MRI. *Magn Reson Med*. 2008;60(6):1362-71.
49. Wyss-Coray T. Ageing, neurodegeneration and brain rejuvenation. *Nature*. 2016;539(7628):180-6.
50. Mugler III JP, Brookeman JR. Rapid three-dimensional T1-weighted MR imaging with the MP-RAGE sequence. *Journal of Magnetic Resonance Imaging*. 1991;1(5):561-7.
51. Brant-Zawadzki M, Gillan GD, Nitz WR. MP RAGE: a three-dimensional, T1-weighted, gradient-echo sequence--initial experience in the brain. *Radiology*. 1992;182(3):769-75.
52. Resnick SM, Pham DL, Kraut MA, Zonderman AB, Davatzikos C. Longitudinal Magnetic Resonance Imaging Studies of Older Adults: A Shrinking Brain. *The Journal of Neuroscience*. 2003;23(8):3295.
53. Fox NC, Schott JM. Imaging cerebral atrophy: normal ageing to Alzheimer's disease. *The Lancet*. 2004;363(9406):392-4.
54. Sigurdsson S, Aspelund T, Forsberg L, Fredriksson J, Kjartansson O, Oskarsdottir B, et al. Brain tissue volumes in the general population of the elderly: the AGES-Reykjavik study. *NeuroImage*. 2012;59(4):3862-70.
55. Jernigan TL, Archibald SL, Fennema-Notestine C, Gamst AC, Stout JC, Bonner J, et al. Effects of age on tissues and regions of the cerebrum and cerebellum. *Neurobiology of aging*. 2001;22(4):581-94.
56. Fox NC, Scahill RI, Crum WR, Rossor MN. Correlation between rates of brain atrophy and cognitive decline in AD. *Neurology*. 1999;52(8):1687-9.
57. Raz N, Ghisletta P, Rodrigue KM, Kennedy KM, Lindenberger U. Trajectories of brain aging in middle-aged and older adults: Regional and individual differences. *NeuroImage*. 2010;51(2):501-11.
58. Peters R. Ageing and the brain. *Postgrad Med J*. 2006;82(964):84-8.

59. Ball M, Hachinski V, Fox A, Kirshen A, Fisman M, Blume W, et al. A new definition of Alzheimer's disease: a hippocampal dementia. *The Lancet*. 1985;325(8419):14-6.
60. Olszewski J. Subcortical arteriosclerotic encephalopathy: review of the literature on the so-called Binswanger's disease and presentation of two cases. *World Neurol*. 1965;3:359-73.
61. Caplan LR. Binswanger's disease--revisited. *Neurology*. 1995;45(4):626-33.
62. De Leeuw F, de Groot JC, Achten E, Oudkerk M, Ramos L, Heijboer R, et al. Prevalence of cerebral white matter lesions in elderly people: a population based magnetic resonance imaging study. The Rotterdam Scan Study. *Journal of Neurology, Neurosurgery & Psychiatry*. 2001;70(1):9-14.
63. Wardlaw JM, Valdes Hernandez MC, Munoz-Maniega S. What are white matter hyperintensities made of? Relevance to vascular cognitive impairment. *J Am Heart Assoc*. 2015;4(6):001140.
64. Wharton SB, Simpson JE, Brayne C, Ince PG. Age-Associated White Matter Lesions: The MRC Cognitive Function and Aging Study. *Brain pathology*. 2015;25(1):35-43.
65. Fernando MS, Simpson JE, Matthews F, Brayne C, Lewis CE, Barber R, et al. White matter lesions in an unselected cohort of the elderly: molecular pathology suggests origin from chronic hypoperfusion injury. *Stroke*. 2006;37(6):1391-8.
66. Pantoni L. Pathophysiology of Age-Related Cerebral White Matter Changes. *Cerebrovasc Dis*. 2002;13:7-10.
67. Schmidt R, Schmidt H, Haybaeck J, Loitfelder M, Weis S, Cavalieri M, et al. Heterogeneity in age-related white matter changes. *Acta neuropathologica*. 2011;122(2):171-85.
68. Schmidt R, Petrovic K, Ropele S, Enzinger C, Fazekas F. Progression of leukoaraiosis and cognition. *Stroke*. 2007;38(9):2619-25.
69. de Groot M, Verhaaren BF, de Boer R, Klein S, Hofman A, van der Lugt A, et al. Changes in normal-appearing white matter precede development of white matter lesions. *Stroke*. 2013;44(4):1037-42.
70. Prince M, Knapp M, Guerchet M, McCrone P, et al. *Dementia UK: Update, 2nd Edition*. 2014.
71. Smith GE, Bondi MW. *Mild Cognitive Impairment and Dementia: Definitions, Diagnosis and Treatment*. McPherson S, et al, editors. U.S.A.: Oxford University Press; 2013.
72. Association AP. *Diagnostic and statistical manual of mental disorders (DSM-5®)*: American Psychiatric Pub; 2013.
73. Gorelick PB, Scuteri A, Black SE, Decarli C, Greenberg SM, Iadecola C, et al. Vascular contributions to cognitive impairment and dementia: a statement for healthcare professionals from the American Heart Association/American Stroke Association. *Stroke*. 2011;42(9):2672-713.

74. Pham TM, Petersen I, Walters K, Raine R, Manthorpe J, Mukadam N, et al. Trends in dementia diagnosis rates in UK ethnic groups: analysis of UK primary care data. *Clinical epidemiology*. 2018;10:949.
75. Livingston G, Sommerlad A, Orgeta V, Costafreda SG, Huntley J, Ames D, et al. Dementia prevention, intervention, and care. *The Lancet*. 2017;390(10113):2673-734.
76. Hardy JA, Higgins GA. Alzheimer's disease: the amyloid cascade hypothesis. *Science*. 1992;256(5054):184.
77. Snowdon DA, Greiner LH, Mortimer JA, Riley KP, Greiner PA, Markesbery WR. Brain infarction and the clinical expression of Alzheimer disease. *JAMA*. 1997;277(10):813 - 7.
78. Binnewijzend MA, Kuijter JP, Benedictus MR, van der Flier WM, Wink AM, Wattjes MP, et al. Cerebral blood flow measured with 3D pseudocontinuous arterial spin-labeling MR imaging in Alzheimer disease and mild cognitive impairment: a marker for disease severity. *Radiology*. 2013;267(1):221-30.
79. Binnewijzend MA, Benedictus MR, Kuijter JP, van der Flier WM, Teunissen CE, Prins ND, et al. Cerebral perfusion in the prodementia stages of Alzheimer's disease. *European radiology*. 2015.
80. Schuff N, Matsumoto S, Kmieciak J, Studholme C, Du A, Ezekiel F, et al. Cerebral blood flow in ischemic vascular dementia and Alzheimer's disease, measured by arterial spin-labeling magnetic resonance imaging. *Alzheimer's & dementia : the journal of the Alzheimer's Association*. 2009;5(6):454-62.
81. Alexopoulos P, Sorg C, Forschler A, Grimmer T, Skokou M, Wohlschlagel A, et al. Perfusion abnormalities in mild cognitive impairment and mild dementia in Alzheimer's disease measured by pulsed arterial spin labeling MRI. *Eur Arch Psychiatry Clin Neurosci*. 2012;262(1):69-77.
82. Leeuwis AE, Benedictus MR, Kuijter JP, Binnewijzend MA, Hooghiemstra AM, Verfaillie SC, et al. Lower cerebral blood flow is associated with impairment in multiple cognitive domains in Alzheimer's disease. *Alzheimer's & dementia : the journal of the Alzheimer's Association*. 2016:531-40.
83. Dai W, Lopez OL, et al. Mild Cognitive Impairment and Alzheimer Disease: Patterns of Altered Cerebral Blood Flow at MR Imaging. *Radiology*. 2009;250(3).
84. Chao LL, Buckley ST, Kornak J, Schuff N, Madison C, Yaffe K, et al. ASL perfusion MRI predicts cognitive decline and conversion from MCI to dementia. *Alzheimer disease and associated disorders*. 2010;24(1):19-27.
85. Benedictus MR, Leeuwis AE, Binnewijzend MA, Kuijter JP, Scheltens P, Barkhof F, et al. Lower cerebral blood flow is associated with faster cognitive decline in Alzheimer's disease. *European radiology*. 2017;27(3):1169-75.
86. NICE. *Clinical Knowledge Summaries, Diabetes - type 2*. 2017.
87. Public Health England. *Hypertension prevalence estimates for local populations*: Public Health England; 2016 [Available from:

<https://www.gov.uk/government/publications/hypertension-prevalence-estimates-for-local-populations>.

88. Mitchell GF, van Buchem MA, Sigurdsson S, Gotal JD, Jonsdottir MK, Kjartansson O, et al. Arterial stiffness, pressure and flow pulsatility and brain structure and function: the Age, Gene/Environment Susceptibility--Reykjavik study. *Brain*. 2011;134(Pt 11):3398-407.
89. Diabetes UK. Diabetes Prevalence 2018 2018 [Available from: <https://www.diabetes.org.uk/professionals/position-statements-reports/statistics/diabetes-prevalence-2018>].
90. NHS Digital. Health Survey for England - 2004: Health of ethnic minorities 2004 [Available from: <https://digital.nhs.uk/data-and-information/publications/statistical/health-survey-for-england/health-survey-for-england-2004-health-of-ethnic-minorities-headline-results>].
91. Chaturvedi N, McKeigue PM, Marmot MG. Resting and ambulatory blood pressure differences in Afro-Caribbeans and Europeans. *Hypertension*. 1993;22(1):90-6.
92. Volpe CMO, Villar-Delfino PH, Dos Anjos PMF, Nogueira-Machado JA. Cellular death, reactive oxygen species (ROS) and diabetic complications. *Cell Death Dis*. 2018;9(2):119.
93. Grundy SM, Stone NJ, Bailey AL, Beam C, Birtcher KK, Blumenthal RS, et al. 2018
AHA/ACC/AACVPR/AAPA/ABC/ACPM/ADA/AGS/APhA/ASPC/NLA/PCNA guideline on the management of blood cholesterol: a report of the American College of Cardiology/American Heart Association Task Force on Clinical Practice Guidelines. *Journal of the American College of Cardiology*. 2018:25709.
94. Holmes MV, Asselbergs FW, Palmer TM, Drenos F, Lanktree MB, Nelson CP, et al. Mendelian randomization of blood lipids for coronary heart disease. *European heart journal*. 2014;36(9):539-50.
95. Steinberg D, Parthasarathy S, Carew TE, Khoo JC, Witztum JL. Beyond cholesterol. *New England Journal of Medicine*. 1989;320(14):915-24.
96. Félix-Redondo FJ, Grau M, Fernández-Bergés D. Cholesterol and cardiovascular disease in the elderly. Facts and gaps. *Aging and disease*. 2013;4(3):154.
97. Ward MA, Bendlin BB, McLaren DG, Hess TM, Gallagher CL, Kastman EK, et al. Low HDL Cholesterol is Associated with Lower Gray Matter Volume in Cognitively Healthy Adults. *Frontiers in aging neuroscience*. 2010;2.
98. Doll R, Peto R. Mortality in relation to smoking: 20 years' observations on male British doctors. *Br med J*. 1976;2(6051):1525-36.
99. Doll R, Gray R, Hafner B, Peto R. Mortality in relation to smoking: 22 years' observations on female British doctors. *Br Med J*. 1980;280(6219):967-71.

100. Messner B, Bernhard D. Smoking and cardiovascular disease: mechanisms of endothelial dysfunction and early atherogenesis. *Arteriosclerosis, thrombosis, and vascular biology*. 2014;34(3):509-15.
101. Townsend N, Wickramasinghe K, Bhatnagar P, Smolina K, Nichols M, Leal J, et al. *Coronary heart disease statistics 2012*. 2012.
102. Alberti KG, Eckel RH, Grundy SM, Zimmet PZ, Cleeman JI, Donato KA, et al. Harmonizing the metabolic syndrome: a joint interim statement of the International Diabetes Federation Task Force on Epidemiology and Prevention; National Heart, Lung, and Blood Institute; American Heart Association; World Heart Federation; International Atherosclerosis Society; and International Association for the Study of Obesity. *Circulation*. 2009;120(16):1640-5.
103. Bangen KJ, Nation DA, Clark LR, Harmell AL, Wierenga CE, Dev SI, et al. Interactive effects of vascular risk burden and advanced age on cerebral blood flow. *Frontiers in aging neuroscience*. 2014;6:159.
104. Luchsinger JA, Reitz C, Honig LS, Tang MX, Shea S, Mayeux R. Aggregation of vascular risk factors and risk of incident Alzheimer disease. *Neurology*. 2005;65(4):545-51.
105. Whitmer RA, Sidney S, Selby J, Johnston SC, Yaffe K. Midlife cardiovascular risk factors and risk of dementia in late life. *Neurology*. 2005;64(2):277.
106. van den Berg E, Kloppenborg RP, Kessels RP, Kappelle LJ, Biessels GJ. Type 2 diabetes mellitus, hypertension, dyslipidemia and obesity: A systematic comparison of their impact on cognition. *Biochim Biophys Acta*. 2009;1792(5):470-81.
107. Kloppenborg RP, van den Berg E, Kappelle LJ, Biessels GJ. Diabetes and other vascular risk factors for dementia: which factor matters most? A systematic review. *Eur J Pharmacol*. 2008;585(1):97-108.
108. Verghese J, Lipton RB, Hall CB, Kuslansky G, Katz MJ. Low blood pressure and the risk of dementia in very old individuals. *Neurology*. 2003;61(12):1667.
109. Mielke MM, Zandi PP, Sjögren M, Gustafson D, Östling S, Steen B, et al. High total cholesterol levels in late life associated with a reduced risk of dementia. *Neurology*. 2005;64(10):1689.
110. Alsop DC, Casement M, de Bazelaire C, Fong T, Press DZ. Hippocampal hyperperfusion in Alzheimer's disease. *NeuroImage*. 2008;42(4):1267-74.
111. Appelman AP, van der Graaf Y, Vincken KL, Tiehuis AM, Witkamp TD, Mali WP, et al. Total cerebral blood flow, white matter lesions and brain atrophy: the SMART-MR study. *J Cereb Blood Flow Metab*. 2008;28(3):633-9.
112. van der Veen PH, Muller M, Vincken KL, Hendrikse J, Mali WP, van der Graaf Y, et al. Longitudinal relationship between cerebral small-vessel disease and cerebral blood flow: the second manifestations of arterial disease-magnetic resonance study. *Stroke*. 2015;46(5):1233-8.

113. Muller M, van der Graaf Y, Visseren FL, Vlek AL, Mali WP, Geerlings MI, et al. Blood pressure, cerebral blood flow, and brain volumes. The SMART-MR study. *J Hypertens*. 2010;28(7):1498-505.
114. van Es AC, van der Grond J, ten Dam VH, de Craen AJ, Blauw GJ, Westendorp RG, et al. Associations between total cerebral blood flow and age related changes of the brain. *PloS one*. 2010;5(3):e9825.
115. ten Dam VH, van den Heuvel DM, de Craen AJ, Bollen EL, Murray HM, Westendorp RG, et al. Decline in total cerebral blood flow is linked with increase in periventricular but not deep white matter hyperintensities. *Radiology*. 2007;243(1):198-203.
116. Vernooij MW, van der Lugt A, Ikram MA, Wielopolski PA, Vrooman HA, Hofman A, et al. Total cerebral blood flow and total brain perfusion in the general population: the Rotterdam Scan Study. *J Cereb Blood Flow Metab*. 2008;28(2):412-9.
117. Zonneveld HI, Loehrer EA, Hofman A, Niessen WJ, van der Lugt A, Krestin GP, et al. The bidirectional association between reduced cerebral blood flow and brain atrophy in the general population. *J Cereb Blood Flow Metab*. 2015;35(11):1882-7.
118. Alosco ML, Gunstad J, Xu X, Clark US, Labbe DR, Riskin-Jones HH, et al. The impact of hypertension on cerebral perfusion and cortical thickness in older adults. *Journal of the American Society of Hypertension : JASH*. 2014;8(8):561-70.
119. Muller M, van der Graaf Y, Visseren FL, Mali WP, Geerlings MI, Group SS. Hypertension and longitudinal changes in cerebral blood flow: the SMART-MR study. *Ann Neurol*. 2012;71(6):825-33.
120. Nobili F, Rodriguez G, Marengo S, De Carli F, Gambaro M, Castello C, et al. Regional cerebral blood flow in chronic hypertension. A correlative study. *Stroke*. 1993;24(8):1148-53.
121. Beason-Held LL, Moghekar A, Zonderman AB, Kraut MA, Resnick SM. Longitudinal changes in cerebral blood flow in the older hypertensive brain. *Stroke*. 2007;38(6):1766-73.
122. Tryambake D, He J, Firbank MJ, O'Brien JT, Blamire AM, Ford GA. Intensive blood pressure lowering increases cerebral blood flow in older subjects with hypertension. *Hypertension*. 2013;61(6):1309-15.
123. Kjeldsen SE, Narkiewicz K, Burnier M, Oparil S. Intensive blood pressure lowering prevents mild cognitive impairment and possible dementia and slows development of white matter lesions in brain: the SPRINT Memory and Cognition IN Decreased Hypertension (SPRINT MIND) study. *Blood Pressure*. 2018;27(5):247-8.
124. Sprint Mind Investigators for the SPRINT Research Group, Williamson JD, Pajewski NM, Auchus AP, Bryan RN, Chelune G, et al. Effect of Intensive vs Standard Blood Pressure Control on Probable Dementia: A Randomized Clinical Trial. *JAMA*. 2019;321(6):553-61.

125. Foster-Dingley JC, Moonen JE, de Craen AJ, de Ruijter W, van der Mast RC, van der Grond J. Blood Pressure Is Not Associated With Cerebral Blood Flow in Older Persons. *Hypertension*. 2015;66(5):954-60.
126. Waldstein SR, Lefkowitz DM, Siegel EL, Rosenberger WF, Spencer RJ, Tankard CF, et al. Reduced cerebral blood flow in older men with higher levels of blood pressure. *Journal of hypertension*. 2010;28(5):993-8.
127. Deverdun J, Akbaraly TN, Charroud C, Abdenmour M, Brickman AM, Chemouny S, et al. Mean arterial pressure change associated with cerebral blood flow in healthy older adults. *Neurobiology of aging*. 2016;46:49-57.
128. Friedman JI, Tang CY, de Haas HJ, Changchien L, Goliash G, Dabas P, et al. Brain imaging changes associated with risk factors for cardiovascular and cerebrovascular disease in asymptomatic patients. *JACC Cardiovascular imaging*. 2014;7(10):1039-53.
129. Beauchet O, Celle S, Roche F, Bartha R, Montero-Odasso M, Allali G, et al. Blood pressure levels and brain volume reduction: a systematic review and meta-analysis. *J Hypertens*. 2013;31(8):1502-16.
130. Knopman DS, Penman AD, Catellier DJ, Coker LH, Shibata DK, Sharrett AR, et al. Vascular risk factors and longitudinal changes on brain MRI: the ARIC study. *Neurology*. 2011;76(22):1879-85.
131. Breteler MMB, van Swieten JC, Bots ML, Grobbee DE, Claus JJ, van den Hout JHW, et al. Cerebral white matter lesions, vascular risk factors, and cognitive function in a population-based study. The Rotterdam Study. 1994;44(7):1246-.
132. Wardlaw JM, Allerhand M, Doubal FN, Valdes Hernandez M, Morris Z, Gow AJ, et al. Vascular risk factors, large-artery atheroma, and brain white matter hyperintensities. *Neurology*. 2014;82(15):1331-8.
133. Tiehuis AM, Vincken KL, van den Berg E, Hendrikse J, Manschot SM, Mali WP, et al. Cerebral perfusion in relation to cognitive function and type 2 diabetes. *Diabetologia*. 2008;51(7):1321-6.
134. Jansen JFA, van Bussel FCG, van de Haar HJ, van Osch MJP, Hofman PAM, van Boxtel MPJ, et al. Cerebral blood flow, blood supply, and cognition in Type 2 Diabetes Mellitus. *Scientific Reports*. 2016;6(1).
135. Hoscheidt SM, Kellawan JM, Berman SE, Rivera-Rivera LA, Krause RA, Oh JM, et al. Insulin resistance is associated with lower arterial blood flow and reduced cortical perfusion in cognitively asymptomatic middle-aged adults. *Journal of Cerebral Blood Flow and Metabolism*. 2017;37(6):2249-61.
136. Bangen KJ, Werhane ML, Weigand AJ, Edmonds EC, Delano-Wood L, Thomas KR, et al. Reduced Regional Cerebral Blood Flow Relates to Poorer Cognition in Older Adults With Type 2 Diabetes. *Frontiers in aging neuroscience*. 2018;10:270.
137. Biessels GJ, Deary IJ, Ryan CM. Cognition and diabetes: a lifespan perspective. *The Lancet Neurology*. 2008;7(2):184-90.

138. Awad N, Gagnon M, Messier C. The relationship between impaired glucose tolerance, type 2 diabetes, and cognitive function. *Journal of clinical and experimental neuropsychology*. 2004;26(8):1044-80.
139. Rusinek H, Ha J, Yau PL, Storey P, Tirsi A, Tsui WH, et al. Cerebral perfusion in insulin resistance and type 2 diabetes. *J Cereb Blood Flow Metab*. 2015;35(1):95-102.
140. Brundel M, Kappelle LJ, Biessels GJ. Brain imaging in type 2 diabetes. *Eur Neuropsychopharmacol*. 2014;24(12):1967-81.
141. Rosenberg J, Lechea N, Pentang GN, Shah NJ. What magnetic resonance imaging reveals - A systematic review of the relationship between type II diabetes and associated brain distortions of structure and cognitive functioning. *Front Neuroendocrinol*. 2018.
142. Last D, Alsop DC, Abduljalil AM, Marquis RP, de Bazelaire C, Hu K, et al. Global and Regional Effects of Type 2 Diabetes on Brain Tissue Volumes and Cerebral Vasoreactivity. *Diabetes care*. 2007;30(5):1193.
143. Jongen C, van der Grond J, Kappelle LJ, Biessels GJ, Viergever MA, Pluim JP, et al. Automated measurement of brain and white matter lesion volume in type 2 diabetes mellitus. *Diabetologia*. 2007;50(7):1509-16.
144. Tiehuis AM, van der Graaf Y, Visseren FL, Vincken KL, Biessels GJ, Appelman AP, et al. Diabetes increases atrophy and vascular lesions on brain MRI in patients with symptomatic arterial disease. *Stroke*. 2008;39(5):1600-3.
145. Launer LJ, Lewis CE, Schreiner PJ, Sidney S, Battapady H, Jacobs DR, et al. Vascular factors and multiple measures of early brain health: CARDIA brain MRI study. *PloS one*. 2015;10(3):e0122138.
146. Launer LJ, Miller ME, Williamson JD, Lazar RM, Gerstein HC, Murray AM, et al. Effects of intensive glucose lowering on brain structure and function in people with type 2 diabetes (ACCORD MIND): a randomised open-label substudy. *The Lancet Neurology*. 2011;10(11):969-77.
147. van Harten B, Oosterman JM, Potter van Loon BJ, Scheltens P, Weinstein HC. Brain lesions on MRI in elderly patients with type 2 diabetes mellitus. *Eur Neurol*. 2007;57(2):70-4.
148. Jeerakathil T, Wolf PA, Beiser A, Massaro J, Seshadri S, D'Agostino RB, et al. Stroke risk profile predicts white matter hyperintensity volume: the Framingham Study. *Stroke*. 2004;35(8):1857-61.
149. Kooistra M, Geerlings MI, van der Graaf Y, Mali WP, Vincken KL, Kappelle LJ, et al. Vascular brain lesions, brain atrophy, and cognitive decline. The Second Manifestations of ARTERial disease--Magnetic Resonance (SMART-MR) study. *Neurobiology of aging*. 2014;35(1):35-41.
150. Reitz C, Tang M-X, Luchsinger J, Mayeux R. Relation of plasma lipids to Alzheimer disease and vascular dementia. *Archives of neurology*. 2004;61(5):705-14.
151. Meyer JS, Rogers RL, Mortel KF, Judd BW. Hyperlipidemia Is a Risk Factor for Decreased Cerebral Perfusion and Stroke. *Archives of Neurology*. 1987;44(4):418-22.

152. Shobab LA, Hsiung G-YR, Feldman HH. Cholesterol in Alzheimer's disease. *The Lancet Neurology*. 2005;4(12):841-52.
153. Wolf H, Hensel A, Arendt T, Kivipelto M, Winblad B, Gertz HJ. Serum lipids and hippocampal volume: the link to Alzheimer's disease? *Annals of Neurology: Official Journal of the American Neurological Association and the Child Neurology Society*. 2004;56(5):745-9.
154. Murray AD, Staff RT, Shenkin SD, Deary IJ, Starr JM, Whalley LJ. Brain white matter hyperintensities: relative importance of vascular risk factors in nondemented elderly people. *Radiology*. 2005;237(1):251-7.
155. Toda N, Okamura T. Cigarette smoking impairs nitric oxide-mediated cerebral blood flow increase: Implications for Alzheimer's disease. *J Pharmacol Sci*. 2016;131(4):223-32.
156. Rogers RL, Meyer JS, Judd BW, Mortel KF. Abstinence from cigarette smoking improves cerebral perfusion among elderly chronic smokers. *JAMA*. 1985;253(20):2970-4.
157. Yamashita K, Kobayashi S, Yamaguchi S, Kitani M, Tsunematsu T. Effect of smoking on regional cerebral blood flow in the normal aged volunteers. *Gerontology*. 1988;34(4):199-204.
158. Elbejjani M, Auer R, Dolui S, Jacobs DR, Jr., Haight T, Goff DC, Jr., et al. Cigarette smoking and cerebral blood flow in a cohort of middle-aged adults. *J Cereb Blood Flow Metab*. 2018:271678X18754973.
159. Rogers RL, Meyer JS, Shaw TG, Mortel KF, Hardenberg JP, Zaid RR. Cigarette Smoking Decreases Cerebral Blood Flow Suggesting Increased Risk for Stroke. *JAMA*. 1983;250(20):2796-800.
160. Pan P, Shi H, Zhong J, Xiao P, Shen Y, Wu L, et al. Chronic smoking and brain gray matter changes: evidence from meta-analysis of voxel-based morphometry studies. *Neurological Sciences*. 2013;34(6):813-7.
161. Liao D, Cooper L, Cai J, Toole J, Bryan N, Burke G, et al. The Prevalence and Severity of White Matter Lesions, Their Relationship with Age, Ethnicity, Gender, and Cardiovascular Disease Risk Factors: The ARIC Study. *Neuroepidemiology*. 1997;16(3):149-62.
162. Kivipelto M, Ngandu T, Fratiglioni L, Viitanen M, Kareholt I, Winblad B, et al. Obesity and vascular risk factors at midlife and the risk of dementia and Alzheimer disease. *Arch Neurol*. 2005;62(10):1556-60.
163. Birdsill AC, Carlsson CM, Willette AA, Okonkwo OC, Johnson SC, Xu G, et al. Low cerebral blood flow is associated with lower memory function in metabolic syndrome. *Obesity (Silver Spring)*. 2013;21(7):1313-20.
164. Yaffe K. Metabolic syndrome and cognitive disorders: is the sum greater than its parts? *Alzheimer Disease & Associated Disorders*. 2007;21(2):167-71.
165. Luchsinger JA. A Work in Progress: The Metabolic Syndrome. *Science of Aging Knowledge Environment*. 2006;2006(10):pe19.
166. Glodzik L, Rusinek H, Brys M, Tsui WH, Switalski R, Mosconi L, et al. Framingham cardiovascular risk profile correlates with impaired hippocampal

and cortical vasoreactivity to hypercapnia. *J Cereb Blood Flow Metab.* 2011;31(2):671-9.

167. Jennings JR, Heim AF, Kuan DC, Gianaros PJ, Muldoon MF, Manuck SB. Use of total cerebral blood flow as an imaging biomarker of known cardiovascular risks. *Stroke.* 2013;44(9):2480-5.

168. Bastos-Leite AJ, Kuijter JP, Rombouts SA, Sanz-Arigita E, van Straaten EC, Gouw AA, et al. Cerebral blood flow by using pulsed arterial spin-labeling in elderly subjects with white matter hyperintensities. *AJNR American journal of neuroradiology.* 2008;29(7):1296-301.

169. Benedictus MR, Binnewijzend MA, Kuijter JP, Steenwijk MD, Versteeg A, Vrenken H, et al. Brain volume and white matter hyperintensities as determinants of cerebral blood flow in Alzheimer's disease. *Neurobiology of aging.* 2014;35(12):2665-70.

170. Appelman AP, van der Graaf Y, Vincken KL, Tiehuis AM, Witkamp TD, Mali WP, et al. Total Cerebral Blood Flow, White Matter Lesions and Brain Atrophy: The SMART-MR Study. *Journal of Cerebral Blood Flow & Metabolism.* 2008;28(3):633-9.

171. Shi Y, Thrippleton MJ, Makin SD, Marshall I, Geerlings MI, de Craen AJ, et al. Cerebral blood flow in small vessel disease: A systematic review and meta-analysis. *J Cereb Blood Flow Metab.* 2016;36(10):1653-67.

172. Spilt A, Box FM, van der Geest RJ, Reiber JH, Kunz P, Kamper AM, et al. Reproducibility of total cerebral blood flow measurements using phase contrast magnetic resonance imaging. *J Magn Reson Imaging.* 2002;16(1):1-5.

173. Tillin T, Forouhi NG, McKeigue PM, Chaturvedi N. Southall And Brent REvisited: Cohort profile of SABRE, a UK population-based comparison of cardiovascular disease and diabetes in people of European, Indian Asian and African Caribbean origins. *International journal of epidemiology.* 2012;41(1):33-42.

174. Leeuwis AE, Smith LA, Melbourne A, Hughes AD, Richards M, Prins ND, et al. Cerebral Blood Flow and Cognitive Functioning in a Community-Based, Multi-Ethnic Cohort: The SABRE Study. *Frontiers in aging neuroscience.* 2018;10:279-.

175. Cardoso MJ, Modat M, Wolz R, Melbourne A, Cash D, Rueckert D, et al. Geodesic Information Flows: Spatially-Variant Graphs and Their Application to Segmentation and Fusion. *IEEE Trans Med Imaging.* 2015;34(9):1976-88.

176. Aljabar P, Heckemann RA, Hammers A, Hajnal JV, Rueckert D. Multi-atlas based segmentation of brain images: atlas selection and its effect on accuracy. *NeuroImage.* 2009;46(3):726-38.

177. Rohlfing T, Russakoff DB, Maurer CR. Performance-based classifier combination in atlas-based image segmentation using expectation-maximization parameter estimation. *IEEE transactions on medical imaging.* 2004;23(8):983-94.

178. Wolz R, Aljabar P, Hajnal JV, Hammers A, Rueckert D, Alzheimer's Disease Neuroimaging I. LEAP: learning embeddings for atlas propagation. *NeuroImage*. 2010;49(2):1316-25.
179. Cardoso MJ, Ourselin S, Wolz R, Rueckert D. System and Method for Annotating Images by Propagating Information. 2015;US20150262372A1.
180. Fazekas F, Chawluk JB, Alavi A, Hurtig HI, Zimmerman RA. MR signal abnormalities at 1.5 T in Alzheimer's dementia and normal aging. *AJR Am J Roentgenol*. 1987;149(2):351-6.
181. Scheltens P, Barkhof F, Leys D, Pruvo JP, Nauta JJ, Vermersch P, et al. A semiquantitative rating scale for the assessment of signal hyperintensities on magnetic resonance imaging. *J Neurol Sci*. 1993;114(1):7-12.
182. Manolio TA, Kronmal RA, Burke GL, et al. Magnetic Resonance Abnormalities and Cardiovascular Disease in Older Adults. The Cardiovascular Health Study. *Stroke*. 1994;25 (2):318-27.
183. Sudre CH, Cardoso MJ, Bouvy WH, Biessels GJ, Barnes J, Ourselin S. Bayesian Model Selection for Pathological Neuroimaging Data Applied to White Matter Lesion Segmentation. *IEEE Trans Med Imaging*. 2015;34(10):2079-102.
184. Admiraal-Behloul F, Van Den Heuvel D, Olofsen H, van Osch MJ, van der Grond J, Van Buchem M, et al. Fully automatic segmentation of white matter hyperintensities in MR images of the elderly. *NeuroImage*. 2005;28(3):607-17.
185. Sudre CH, Anson BG, Davagnanam I, Schmitt A, Mendelson AF, Prados F, et al. Bullseye's representation of cerebral white matter hyperintensities. *J Neuroradiol*. 2017.
186. Melbourne A, Toussaint N, Owen D, Simpson I, Anthopoulos T, De Vita E, et al. NiftyFit: a Software Package for Multi-parametric Model-Fitting of 4D Magnetic Resonance Imaging Data. *Neuroinformatics*. 2016;14(3):319-37.
187. Lu H, Clingman C, Golay X, van Zijl PC. Determining the longitudinal relaxation time (T1) of blood at 3.0 Tesla. *Magn Reson Med*. 2004;52(3):679-82.
188. Donahue MJ, Lu H, Jones CK, Pekar JJ, van Zijl PC. An account of the discrepancy between MRI and PET cerebral blood flow measures. A high-field MRI investigation. *NMR Biomed*. 2006;19(8):1043-54.
189. Mancia G, Fagard R, Narkiewicz K, Redon J, Zanchetti A, Böhm M, et al. ESH/ESC Guidelines for the management of arterial hypertension: The Task Force for the management of arterial hypertension of the European Society of Hypertension (ESH) and of the European Society of Cardiology (ESC). *European Heart Journal*. 2013;34(28):2159-219.
190. Geddes L, Newberg D. Cuff pressure oscillations in the measurement of relative blood pressure. *Psychophysiology*. 1977;14(2):198-202.
191. Friedewald WT, Levy RI, Fredrickson DS. Estimation of the concentration of low-density lipoprotein cholesterol in plasma, without use of the preparative ultracentrifuge. *Clinical chemistry*. 1972;18(6):499-502.

192. World Health Organisation. Definition, diagnosis and classification of diabetes mellitus and its complications: report of a WHO consultation. Part 1, Diagnosis and classification of diabetes mellitus. 1999.
193. International Expert Committee. International Expert Committee report on the role of the A1C assay in the diagnosis of diabetes. *Diabetes Care*. 2009;32(7):1327-34.
194. D'Agostino RB, Sr, Grundy S, Sullivan LM, Wilson P, for the CHDRPG. Validation of the framingham coronary heart disease prediction scores: Results of a multiple ethnic groups investigation. *JAMA*. 2001;286(2):180-7.
195. Chia YC, Gray SY, Ching SM, Lim HM, Chinna K. Validation of the Framingham general cardiovascular risk score in a multiethnic Asian population: a retrospective cohort study. *BMJ Open*. 2015;5(5):e007324.
196. Tillin T, Hughes AD, Whincup P, Mayet J, Sattar N, McKeigue PM, et al. Ethnicity and prediction of cardiovascular disease: performance of QRISK2 and Framingham scores in a U.K. tri-ethnic prospective cohort study (SABRE--Southall And Brent REvisited). *Heart*. 2014;100(1):60-7.
197. Woodward M, Brindle P, Tunstall-Pedoe H. Adding social deprivation and family history to cardiovascular risk assessment: the ASSIGN score from the Scottish Heart Health Extended Cohort (SHHEC). *Heart*. 2007;93(2):172-6.
198. D'Agostino RB, Sr., Vasan RS, Pencina MJ, Wolf PA, Cobain M, Massaro JM, et al. General cardiovascular risk profile for use in primary care: the Framingham Heart Study. *Circulation*. 2008;117(6):743-53.
199. Amrhein V, Greenland S, McShane B. Scientists rise up against statistical significance. *Nature Publishing Group*; 2019.
200. Kou S, Cao JY, Yeo S, Holmes-Walker DJ, Lau SL, Gunton JE. Ethnicity influences cardiovascular outcomes and complications in patients with type 2 diabetes. *J Diabetes Complications*. 2018;32(2):144-9.
201. Strain WD, Chaturvedi N, Nihoyannopoulos P, Bulpitt CJ, Rajkumar C, Shore AC. Differences in the association between type 2 diabetes and impaired microvascular function among Europeans and African Caribbeans. *Diabetologia*. 2005;48(11):2269-77.
202. Legato MJ, Johnson PA, Manson JE. Consideration of Sex Differences in Medicine to Improve Health Care and Patient Outcomes. *JAMA*. 2016;316(18):1865-6.
203. Leening MJ, Ferket BS, Steyerberg EW, Kavousi M, Deckers JW, Nieboer D, et al. Sex differences in lifetime risk and first manifestation of cardiovascular disease: prospective population based cohort study. *BMJ*. 2014;349:g5992.
204. Ferretti MT, Iulita MF, Cavedo E, Chiesa PA, Schumacher Dimech A, Santuccione Chadha A, et al. Sex differences in Alzheimer disease - the gateway to precision medicine. *Nat Rev Neurol*. 2018;14(8):457-69.
205. Haller S, Zaharchuk G, Thomas DL, Lovblad KO, Barkhof F, Golay X. Arterial Spin Labeling Perfusion of the Brain: Emerging Clinical Applications. *Radiology*. 2016;281(2):337-56.

206. Binnewijzend MA, Benedictus MR, Kuijter JP, van der Flier WM, Teunissen CE, Prins ND, et al. Cerebral perfusion in the predementia stages of Alzheimer's disease. *European radiology*. 2016;26(2):506-14.
207. Binnewijzend MA, Kuijter JP, van der Flier WM, Benedictus MR, Moller CM, Pijnenburg YA, et al. Distinct perfusion patterns in Alzheimer's disease, frontotemporal dementia and dementia with Lewy bodies. *European radiology*. 2014;24(9):2326-33.
208. Henriksen OM, Kruuse C, Olesen J, Jensen LT, Larsson HB, Birk S, et al. Sources of variability of resting cerebral blood flow in healthy subjects: a study using (1)(3)(3)Xe SPECT measurements. *J Cereb Blood Flow Metab*. 2013;33(5):787-92.
209. Clement P, Mutsaerts HJ, Vaclavu L, Ghariq E, Pizzini FB, Smits M, et al. Variability of physiological brain perfusion in healthy subjects - A systematic review of modifiers. Considerations for multi-center ASL studies. *J Cereb Blood Flow Metab*. 2017:271678X17702156.
210. Buxton RB. Quantifying CBF with arterial spin labeling. *J Magn Reson Imaging*. 2005;22(6):723-6.
211. de Simone G, Devereux RB, Chien S, Alderman MH, Atlas SA, Laragh JH. Relation of blood viscosity to demographic and physiologic variables and to cardiovascular risk factors in apparently normal adults. *Circulation*. 1990;81(1):107-17.
212. Cheng CK, Chan J, Cembrowski GS, van Assendelft OW. Complete blood count reference interval diagrams derived from NHANES III: stratification by age, sex, and race. *Lab Hematol*. 2004;10(1):42-53.
213. Lim E, Miyamura J, Chen JJ. Racial/ethnic-specific reference intervals for common laboratory tests: a comparison among Asians, Blacks, Hispanics, and White. *Hawai'i Journal of Medicine & Public Health*. 2015;74(9):302.
214. McDonough J, Garrison G, Hames C. Blood pressure and hypertensive disease among negroes and whites: a study in Evans County, Georgia. *Annals of Internal Medicine*. 1964;61(2):208-28.
215. Tamariz LJ, Young JH, Pankow JS, Yeh HC, Schmidt MI, Astor B, et al. Blood viscosity and hematocrit as risk factors for type 2 diabetes mellitus: the atherosclerosis risk in communities (ARIC) study. *Am J Epidemiol*. 2008;168(10):1153-60.
216. Vlagopoulos PT, Tighiouart H, Weiner DE, Griffith J, Pettitt D, Salem DN, et al. Anemia as a risk factor for cardiovascular disease and all-cause mortality in diabetes: the impact of chronic kidney disease. *J Am Soc Nephrol*. 2005;16(11):3403-10.
217. de Jager J, Kooy A, Lehert P, Wulffelé MG, van der Kolk J, Bets D, et al. Long term treatment with metformin in patients with type 2 diabetes and risk of vitamin B-12 deficiency: randomised placebo controlled trial. *BMJ*. 2010;340:c2181.
218. Vaclavu L, van der Land V, Heijtel DF, van Osch MJ, Cnossen MH, Majoie CB, et al. In Vivo T1 of Blood Measurements in Children with Sickle Cell

- Disease Improve Cerebral Blood Flow Quantification from Arterial Spin-Labeling MRI. *AJNR American journal of neuroradiology*. 2016;37(9):1727-32.
219. De Vis JB, Hendrikse J, Groenendaal F, de Vries LS, Kersbergen KJ, Benders MJ, et al. Impact of neonate haematocrit variability on the longitudinal relaxation time of blood: Implications for arterial spin labelling MRI. *NeuroImage Clinical*. 2014;4:517-25.
220. Parkes LM, Rashid W, Chard DT, Tofts PS. Normal cerebral perfusion measurements using arterial spin labeling: reproducibility, stability, and age and gender effects. *Magn Reson Med*. 2004;51(4):736-43.
221. Aanerud J, Borghammer P, Rodell A, Jonsdottir KY, Gjedde A. Sex differences of human cortical blood flow and energy metabolism. *J Cereb Blood Flow Metab*. 2017;37(7):2433-40.
222. Baxter LR, Mazziotta JC, Phelps ME, Selin CE, Guze BH, Fairbanks L. Cerebral glucose metabolic rates in normal human females versus normal males. *Psychiatry Research*. 1987;21(3):237-45.
223. Ibaraki M, Shinohara Y, Nakamura K, Miura S, Kinoshita F, Kinoshita T. Interindividual variations of cerebral blood flow, oxygen delivery, and metabolism in relation to hemoglobin concentration measured by positron emission tomography in humans. *J Cereb Blood Flow Metab*. 2010;30(7):1296-305.
224. Grotta J, Ackerman R, Correia J, Fallick G, Chang J. Whole blood viscosity parameters and cerebral blood flow. *Stroke*. 1982;13(3):296-301.
225. Parkes LM, Detre JA. ASL: Blood Perfusion Measurements Using Arterial Spin Labelling. In: Tofts PS, editor. *Quantitative MRI of the Brain: Measuring Changes Caused by Disease*. Chichester, West Sussex: John Wiley and Sons Ltd.; 2003. p. 455-73.
226. Chen JJ, Rosas HD, Salat DH. Age-associated reductions in cerebral blood flow are independent from regional atrophy. *NeuroImage*. 2011;55(2):468-78.
227. Dolui S, Vidorreta M, Wang Z, Nasrallah IM, Alavi A, Wolk DA, et al. Comparison of Pasi, Pcasl, and background-suppressed 3d Pcasl in mild cognitive impairment. *Human brain mapping*. 2017;38(10):5260-73.
228. Rosmini S, Bulluck H, Treibel TA, Bhuvana AN, Abdel-Gadir A, Culotta V, et al. Hematocrit, iron and HDL-cholesterol explain 90% of variation in native blood T1. *Journal of Cardiovascular Magnetic Resonance*. 2016;18(Suppl 1):O86.
229. Mokken FC, van der Waart FJ, Henny CP, Goedhart PT, Gelb AW. Differences in peripheral arterial and venous hemorheologic parameters. *Ann Hematol*. 1996;73(3):135-7.
230. Treibel TA, Fontana M, Maestrini V, Castelletti S, Rosmini S, Simpson J, et al. Automatic Measurement of the Myocardial Interstitium: Synthetic Extracellular Volume Quantification Without Hematocrit Sampling. *JACC Cardiovascular imaging*. 2016;9(1):54-63.

231. Li W, Liu P, Lu H, Strouse JJ, van Zijl PCM, Qin Q. Fast measurement of blood T1 in the human carotid artery at 3T: Accuracy, precision, and reproducibility. *Magn Reson Med*. 2017;77(6):2296-302.
232. Kim H, Kim S. A prospective study on the added value of pulsed arterial spin-labeling and apparent diffusion coefficients in the grading of gliomas. *American Journal of Neuroradiology*. 2007;28(9):1693-9.
233. Pollock JM, Tan H, Kraft RA, Whitlow CT, Burdette JH, Maldjian JA. Arterial spin-labeled MR perfusion imaging: clinical applications. *Magn Reson Imaging Clin N Am*. 2009;17(2):315-38.
234. Tiehuis AM, van der Graaf Y, Mali WP, Vincken K, Muller M, Geerlings MI. Metabolic syndrome, prediabetes, and brain abnormalities on mri in patients with manifest arterial disease: the SMART-MR study. *Diabetes care*. 2014;37(9):2515-21.
235. Bryan RN, Bilello M, Davatzikos C, Lazar RM, Murray A, Horowitz K, et al. Effect of diabetes on brain structure: the action to control cardiovascular risk in diabetes MR imaging baseline data. *Radiology*. 2014;272(1):210-6.
236. Kooistra M, Geerlings MI, Mali WP, Vincken KL, van der Graaf Y, Biessels GJ, et al. Diabetes mellitus and progression of vascular brain lesions and brain atrophy in patients with symptomatic atherosclerotic disease. The SMART-MR study. *J Neurol Sci*. 2013;332(1-2):69-74.
237. Nyquist PA, Bilgel MS, Gottesman R, Yanek LR, Moy TF, Becker LC, et al. Extreme deep white matter hyperintensity volumes are associated with African American race. *Cerebrovasc Dis*. 2014;37(4):244-50.
238. Tillin T, Hughes AD, Mayet J, Whincup P, Sattar N, Forouhi NG, et al. The relationship between metabolic risk factors and incident cardiovascular disease in Europeans, South Asians, and African Caribbeans: SABRE (Southall and Brent Revisited) -- a prospective population-based study. *Journal of the American College of Cardiology*. 2013;61(17):1777-86.
239. Asllani I, Habeck C, Borogovac A, Brown TR, Brickman AM, Stern Y. Separating function from structure in perfusion imaging of the aging brain. *Hum Brain Mapp*. 2009;30(9):2927-35.
240. Bathula R, Hughes AD, Panerai RB, Potter JF, Mc GTSA, Tillin T, et al. South Asians have adverse cerebrovascular haemodynamics, despite equivalent blood pressure, compared with Europeans. This is due to their greater hyperglycaemia. *International journal of epidemiology*. 2011;40(6):1490-8.
241. Cosentino F, Volpe M. Hypertension, stroke, and endothelium. *Current hypertension reports*. 2005;7(1):68-71.
242. van Laar PJ, van der Graaf Y, Mali WP, van der Grond J, Hendrikse J. Effect of cerebrovascular risk factors on regional cerebral blood flow. *Radiology*. 2008;246(1):198-204.
243. Novak V, Zhao P, Manor B, Sejdic E, Alsop D, Abduljalil A, et al. Adhesion molecules, altered vasoreactivity, and brain atrophy in type 2 diabetes. *Diabetes care*. 2011;34(11):2438-41.

244. Gottesman RF, Coresh J, Catellier DJ, Sharrett AR, Rose KM, Coker LH, et al. Blood pressure and white-matter disease progression in a biethnic cohort: Atherosclerosis Risk in Communities (ARIC) study. *Stroke*. 2010;41(1):3-8.
245. Tillin T, Forouhi NG, McKeigue PM, Chaturvedi N. The role of diabetes and components of the metabolic syndrome in stroke and coronary heart disease mortality in U.K. white and African-Caribbean populations. *Diabetes care*. 2006;29(9):2127-9.
246. Forouhi NG, Sattar N, Tillin T, McKeigue PM, Chaturvedi N. Do known risk factors explain the higher coronary heart disease mortality in South Asian compared with European men? Prospective follow-up of the Southall and Brent studies, UK. *Diabetologia*. 2006;49(11):2580-8.
247. Sarwar N, Aspelund T, Eiriksdottir G, Gobin R, Seshasai SR, Forouhi NG, et al. Markers of dysglycaemia and risk of coronary heart disease in people without diabetes: Reykjavik prospective study and systematic review. *PLoS Med*. 2010;7(5):e1000278.
248. Gujral UP, Pradeepa R, Weber MB, Narayan KM, Mohan V. Type 2 diabetes in South Asians: similarities and differences with white Caucasian and other populations. *Ann N Y Acad Sci*. 2013;1281:51-63.
249. Cavagnoli G, Pimentel AL, Freitas PA, Gross JL, Camargo JL. Effect of ethnicity on HbA1c levels in individuals without diabetes: Systematic review and meta-analysis. *PloS one*. 2017;12(2):e0171315.
250. Koller MT, Steyerberg EW, Wolbers M, Stijnen T, Bucher HC, Hunink MG, et al. Validity of the Framingham point scores in the elderly: results from the Rotterdam study. *Am Heart J*. 2007;154(1):87-93.
251. Selvarajah S, Kaur G, Haniff J, Cheong KC, Hiong TG, van der Graaf Y, et al. Comparison of the Framingham Risk Score, SCORE and WHO/ISH cardiovascular risk prediction models in an Asian population. *Int J Cardiol*. 2014;176(1):211-8.
252. Bozorgmanesh M, Hadaegh F, Azizi F. Predictive accuracy of the 'Framingham's general CVD algorithm' in a Middle Eastern population: Tehran Lipid and Glucose Study. *International Journal of Clinical Practice*. 2011;65(3):264-73.
253. Kim M, Tan I, Butlin M, Avolio A. Effect Of Pulsatility In Central Aorta On Cerebral Blood Flow With Advancing Age And Hypertension. *Journal of Hypertension*. 2018;36:e128.
254. Jefferson AL, Liu D, Gupta DK, Pechman KR, Watchmaker JM, Gordon EA, et al. Lower cardiac index levels relate to lower cerebral blood flow in older adults. *Neurology*. 2017;89(23):2327-34.
255. Thomas BP, Yezhuvath US, Tseng BY, Liu P, Levine BD, Zhang R, et al. Life-long aerobic exercise preserved baseline cerebral blood flow but reduced vascular reactivity to CO₂. *J Magn Reson Imaging*. 2013;38(5):1177-83.
256. Wierenga CE, Clark LR, Dev SI, Shin DD, Jurick SM, Rissman RA, et al. Interaction of age and APOE genotype on cerebral blood flow at rest. *Journal of Alzheimer's disease : JAD*. 2013;34(4):921-35.

257. VanderWeele TJ, Robins JM. Four types of effect modification: a classification based on directed acyclic graphs. *Epidemiology*. 2007;18(5):561-8.
258. Gouw AA, Seewann A, van der Flier WM, Barkhof F, Rozemuller AM, Scheltens P, et al. Heterogeneity of small vessel disease: a systematic review of MRI and histopathology correlations. *J Neurol Neurosurg Psychiatry*. 2011;82(2):126-35.
259. Tang Y, Whitman GT, Lopez I, Baloh RW. Brain volume changes on longitudinal magnetic resonance imaging in normal older people. *Journal of Neuroimaging*. 2001;11(4):393-400.
260. Scheltens P, Barkhof F, Leys D, Wolters EC, Ravid R, Kamphorst W. Histopathologic correlates of white matter changes on MRI in Alzheimer's disease and normal aging. *Neurology*. 1995;45(5):883-8.
261. Rusinek H, De Santi S, Frid D, Tsui W-H, Tarshish CY, Convit A, et al. Regional brain atrophy rate predicts future cognitive decline: 6-year longitudinal MR imaging study of normal aging. *Radiology*. 2003;229(3):691.
262. Raz N, Yang Y, Dahle CL, Land S. Volume of white matter hyperintensities in healthy adults: contribution of age, vascular risk factors, and inflammation-related genetic variants. *Biochim Biophys Acta*. 2012;1822(3):361-9.
263. Mathalon DH, Sullivan EV, Rawles JM, Pfefferbaum A. Correction for head size in brain-imaging measurements. *Psychiatry Research: Neuroimaging*. 1993;50(2):121-39.
264. Gunzler D, Chen T, Wu P, Zhang H. Introduction to mediation analysis with structural equation modeling. *Shanghai Arch Psychiatry*. 2013;25(6):390-4.
265. Tomarken AJ, Waller NG. Structural equation modeling: strengths, limitations, and misconceptions. *Annu Rev Clin Psychol*. 2005;1:31-65.
266. Walhovd KB, Fjell AM, Reinvang I, Lundervold A, Dale AM, Eilertsen DE, et al. Effects of age on volumes of cortex, white matter and subcortical structures. *Neurobiology of aging*. 2005;26(9):1261-70; discussion 75-8.
267. Giorgio A, Santelli L, Tomassini V, Bosnell R, Smith S, De Stefano N, et al. Age-related changes in grey and white matter structure throughout adulthood. *NeuroImage*. 2010;51(3):943-51.
268. Vinke EJ, de Groot M, Venkatraghavan V, Klein S, Niessen WJ, Ikram MA, et al. Trajectories of imaging markers in brain aging: the Rotterdam Study. *Neurobiology of aging*. 2018;71:32-40.
269. Ikram MA, Vrooman HA, Vernooij MW, van der Lijn F, Hofman A, van der Lugt A, et al. Brain tissue volumes in the general elderly population. The Rotterdam Scan Study. *Neurobiology of aging*. 2008;29(6):882-90.
270. Enzinger C, Fazekas F, Matthews P, Ropele S, Schmidt H, Smith S, et al. Risk factors for progression of brain atrophy in aging Six-year follow-up of normal subjects. *Neurology*. 2005;64(10):1704-11.

271. Van Harten B, de Leeuw F-E, Weinstein HC, Scheltens P, Biessels GJ. Brain imaging in patients with diabetes: a systematic review. *Diabetes care*. 2006;29(11):2539-48.
272. Manolio TA, Kronmal RA, Burke GL, Poirier V, O'leary DH, Gardin JM, et al. Magnetic resonance abnormalities and cardiovascular disease in older adults. The Cardiovascular Health Study. *Stroke*. 1994;25(2):318-27.
273. Kennedy KM, Raz N. Pattern of normal age-related regional differences in white matter microstructure is modified by vascular risk. *Brain Res*. 2009;1297:41-56.
274. Armstrong NJ, Mather KA, Sargurupremraj M, Knol MJ, Malik R, Satizabal CL, et al. Common genetic variation indicates separate etiologies for periventricular and deep white matter hyperintensities. 2019.
275. Verhaaren BF, Debette S, Bis JC, Smith JA, Ikram MK, Adams HH, et al. Multiethnic genome-wide association study of cerebral white matter hyperintensities on MRI. *Circ Cardiovasc Genet*. 2015;8(2):398-409.
276. Crane DE, Black SE, Ganda A, Mikulis DJ, Nestor SM, Donahue MJ, et al. Gray matter blood flow and volume are reduced in association with white matter hyperintensity lesion burden: a cross-sectional MRI study. *Frontiers in aging neuroscience*. 2015;7:131.
277. Wagner M, Helfrich M, Volz S, Magerkurth J, Blasel S, Porto L, et al. Quantitative T₂, T₂^{*}, and T₂' MR imaging in patients with ischemic leukoaraiosis might detect microstructural changes and cortical hypoxia. *Neuroradiology*. 2015;57(10):1023-30.
278. Persson J, Lind J, Larsson A, Ingvar M, Cruts M, Van Broeckhoven C, et al. Altered brain white matter integrity in healthy carriers of the *APOE* ε4 allele. A risk for AD? 2006;66(7):1029-33.
279. Cox SR, Ritchie SJ, Tucker-Drob EM, Liewald DC, Hagenaars SP, Davies G, et al. Ageing and brain white matter structure in 3,513 UK Biobank participants. *Nat Commun*. 2016;7:13629.
280. Debette S, Markus H. The clinical importance of white matter hyperintensities on brain magnetic resonance imaging: systematic review and meta-analysis. *Bmj*. 2010;341:c3666.
281. Hamer M, Sharma N, Batty GD. Association of objectively measured physical activity with brain structure: UK Biobank study. *J Intern Med*. 2018;284(4):439-43.
282. Nakamura M, Yoneyama M, Tabuchi T, Takemura A, Obara M, Tatsuno S, et al. Vessel-selective, non-contrast enhanced, time-resolved MR angiography with vessel-selective arterial spin labeling technique (CINEMA-SELECT) in intracranial arteries. *Radiological physics and technology*. 2013;6(2):327-34.
283. Okell TW, Chappell MA, Schulz UG, Jezzard P. A kinetic model for vessel-encoded dynamic angiography with arterial spin labeling. *Magn Reson Med*. 2012;68(3):969-79.

284. Wong EC, Cronin M, Wu WC, Inglis B, Frank LR, Liu TT. Velocity-selective arterial spin labeling. *Magnetic Resonance in Medicine: An Official Journal of the International Society for Magnetic Resonance in Medicine*. 2006;55(6):1334-41.
285. Berry ESK, Jezzard P, Okell TW. Off-resonance correction for pseudo-continuous arterial spin labeling using the optimized encoding scheme. *NeuroImage*. 2019.
286. Luh WM, Talagala SL, Li TQ, Bandettini PA. Pseudo-continuous arterial spin labeling at 7 T for human brain: estimation and correction for off-resonance effects using a Prescan. *Magn Reson Med*. 2013;69(2):402-10.
287. Gardener AG, Jezzard P. Investigating white matter perfusion using optimal sampling strategy arterial spin labeling at 7 Tesla. *Magn Reson Med*. 2015;73(6):2243-8.
288. Sudlow C, Gallacher J, Allen N, Beral V, Burton P, Danesh J, et al. UK biobank: an open access resource for identifying the causes of a wide range of complex diseases of middle and old age. *PLoS medicine*. 2015;12(3):e1001779.

8 . Appendices

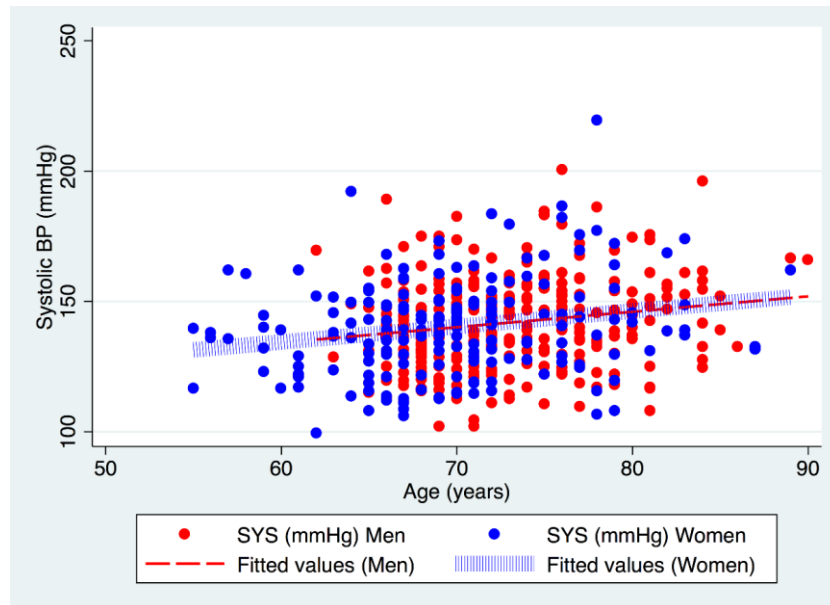


Figure 8-1. Scatter plots showing the correlation of systolic BP and age.

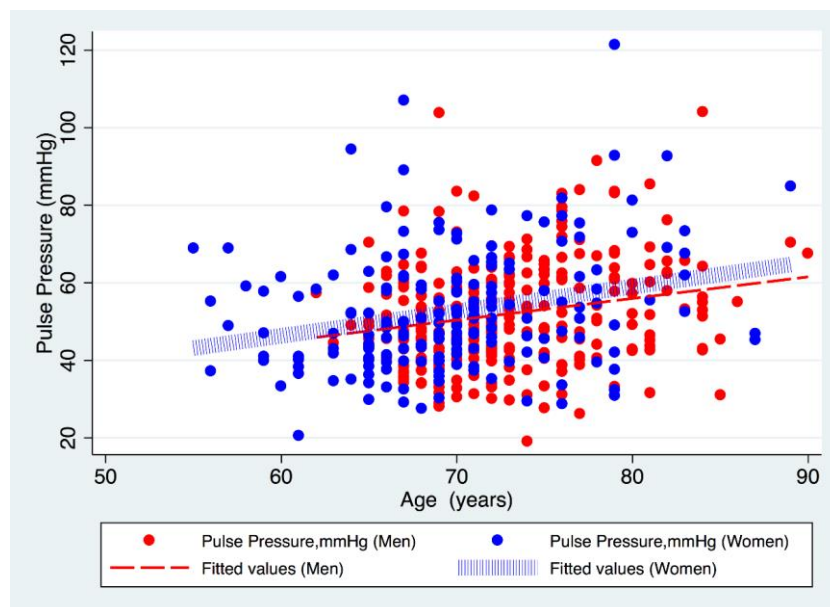


Figure 8-2. Scatter plots showing the correlation of pulse pressure and age.

Dependent variable: total WMH volume (mm³) (all participants)

	<i>Model 1d (n=482)</i>				<i>Model 2d (n=482)</i>				<i>Interaction model (n=482)</i>			
<i>AIC</i>	19.49				19.49				19.49			
	exp B	(95%CI)		<i>P</i>	exp B	(95%CI)		<i>P</i>	exp B	(95%CI)		<i>P</i>
<i>Age, years</i>	1.05	1.03	1.07	<.001	1.05	1.03	1.07	<.001	1.03	1.00	1.06	.025
<i>Sex, female</i>	1.23	0.93	1.63	.141	1.27	0.95	1.71	.108	1.30	0.96	1.75	.085
<i>South Asian</i>	1.10	0.83	1.45	.524	0.04	0.00	1.06	.054
<i>African Caribbean</i>	1.15	0.82	1.60	.419	0.43	0.01	16.82	.654
<i>South Asian*age, years</i>	1.05	1.00	1.09	.047
<i>African Caribbean*age, years</i>	1.01	0.96	1.07	.595

Table 8-1. Dependent variable: total white matter hyperintensities volume (all participants). Models are adjusted for TIV exponentiated beta coefficients, *P* <.05 shown in bold.